Supporting Information

Ethanol as a Hydrogen Carrier with a Value-Added Co-Product

Andrew R. Rander,[a] Shayna R. Kohl,[a] Valeriy Cherepakhin,[a] Long Zhang,[a] Van K. Do,[a] Hanna Breunig,[b] and Travis J. Williams*[,a]

[a] Donald P. and Katherine B. Loker Hydrocarbon Research Institute, Wrigley Institute for Environment and Sustainability, and the Department of Chemistry, University of Southern California, Los Angeles, California 90089-1661, USA

[b] Sustainable Energy Systems Group, Energy Analysis and Environmental Impacts Division Lawrence Berkeley National Lab, 1 Cyclotron Road, 90-2012, Berkeley, California, 94720, USA

*travisw@usc.edu

Contents

General Procedures

I. NMR Analysis Methods

All NMRs spectra were obtained on a Varian Mercury 400, Varian VNMRS 500, or VNMRS 600 using MestreLab MestReNOVA software for analysis. Chemical shifts are reported as ppm in reference to a residual ^{1}H solvent peak.

II. Titration Methods

To determine the quantity of potassium hydroxide remaining in each sample, back titrations using dilute hydrochloric acid (HCl) and dilute sodium hydroxide (NaOH). Samples were diluted in 50 mL of deionized water where 10 mL aliquots were portioned out and neutralized with additions of HCl in 5 mL increments. The resulting solution was then titrated with a dilute solution of NaOH where methyl orange and phenolphthalein were used as indicators. All volumes are recorded in milliliters and the following equation was used to determine the molar percentage of potassium hydroxide and acetate.

$$mol\ \%(OH^-) = \frac{[HCl]*V_{added} - [NaOH]*V_{equivalence\ point\ 2}}{[HCl]*V_{added} - [NaOH]*V_{equivalence\ point\ 1}} \qquad \textbf{Equation 1}$$

$$mol\ \%(KAc) = 1 - mol\%(OH^-) \qquad \textbf{Equation 2}$$

III. General Chemical Preparation

Ethanol (200 proof) was acquired from Koptec Chemicals and both sodium and potassium hydroxide were purchased from VWR. Potassium hydroxide used in reactions was ground to a fine powder in a nitrogen filled glovebox to avoid water absorption. Potassium hydroxide was determined to be KOH•1/2 H_2O by acid-base titration. ACS grade toluene was purchased from VWR chemicals and was distilled from benzophenone ketyl and stored in a nitrogen filled box over sodium metal; sodium and benzophenone were purchased from Sigma Aldrich chemicals. Quantitative NMR was taken using dimethyl formamide (VWR chemicals) as an internal standard with a recycle delay of 30 seconds. All deuterated solvents (toluene, deuterium oxide, methanol, etc.) were obtained from Cambridge Isotope Laboratories. Complexes **7**, **8**, **10**, **11**, **12**, and **16** were obtained from Strem Chemicals. Complexes **6**, **9**, **13**, and **17** were provided by Los Alamos National Laboratory. Complexes **1**, **3**, **14**, **15**, and **18-23** were synthesized using previously reported methods. Complexes **2**, **4**, and **5** are introduced here with preparative procedures. The (pyridyl)carbene ligand for complex **5** was purchased as a silver chloride dimer from Catapower Inc. For titration analysis, methyl orange was obtained from Fischer chemicals while phenolphthalein was obtained from Sigma Aldrich.

IV. PN-Ligand Synthesis

For complexes **2**, **4**, and **5** the (pyridyl)phosphine ligand (**L**) was synthesized using previously reported synthetic methods from Cejale et al.[1] Di-tertbutylchlorophosphine, 1-methyl pyridine, and the iridium-1,5-cyclooctadiene chloride dimer were all purchased from STREM chemicals, or the later was generated by recycling iridium waste.

V. Gas Evolution and Pressure Calculations

In ambient reactions, the amount of hydrogen evolved was calculated using the ideal gas law assuming 100% conversion of ethanol to acetate and hydrogen. When run under self-pressurizing conditions, the volume of the Parr reactor was taken as 125 mL. Values of constants are listed below.

Ambient Reactions

$P * V = n * R * T$

$R = 0.082\ L*atm/mol*K$

$T = 298\ K$

$P = 1\ atm$

Self-Pressurizing Reactions

$P * V = n * R * T$

$R = 0.082\ L*atm/mol*K$

$T = 393\ K\ or\ 353\ K$

$V = .125\ L$

Initial Reaction Screening Experiments

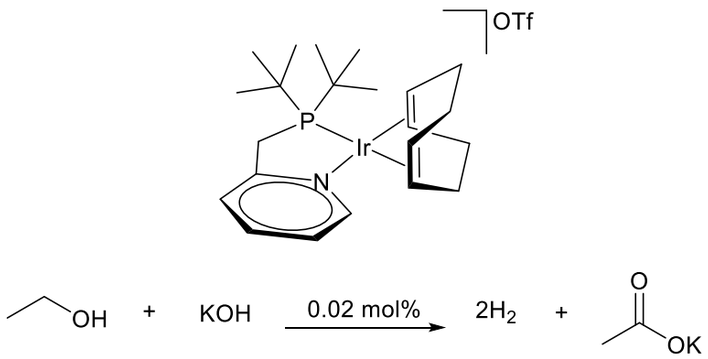

In a nitrogen filled glovebox, IrPN (**1**, 5 mg, 7.28 μmol) and potassium hydroxide (271 mg, 4.17 mmol) were weighed out into a 5 mL round bottom flask. To this, ethanol (200 prof, 250 μL) was added along with a stir bar. The resulting solution was refluxed at 90 °C for thirty minutes after which deuterium oxide (1 mL) was added to the flask and the contents were analyzed by ^{1}H NMR. A small peak at a chemical shift of 1.90 ppm verified the presence of potassium acetate.

Initial Reaction Screening Spectra

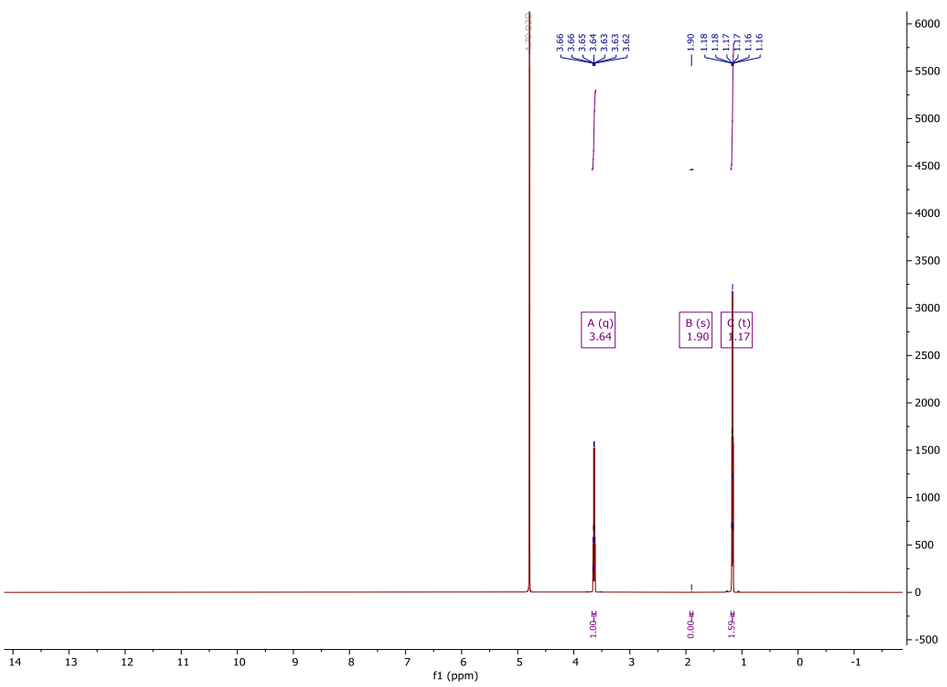

Figure S1: ^{1}H Spectrum of reaction mixture in D_2O.

Initial Reaction Screening Experiments cont.

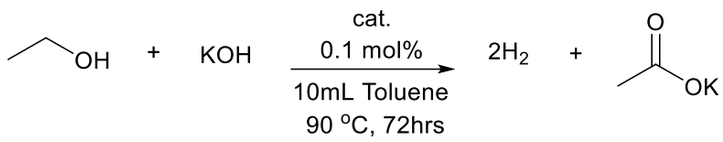

In a nitrogen filled glovebox, ground potassium hydroxide (561 mg, 8.60 mmol) was weighed out in a 25 mL round bottom flask. Next, catalyst (0.1 mol%, with respect to ethanol) was weighed out and added to the flask with dry toluene (10 mL). Finally, ethanol (200 prof, 0.60 mL, 10 mmol) was weighed in a vial and quantitatively transferred to the round bottom flask. The same procedure was duplicated for each reaction, corresponding to entries in table 1 & 2. Each reaction was refluxed under inert conditions and hydrogen evolution was quantified using a water eudiometer to determine the progress of each reaction.

Table S1: Initial Reaction Screening Experiments

Entry	Catalyst	NMR Yield (AcO^-)
1	**1**	25
2	**3**	34

Initial Reaction Screening Spectra Cont.

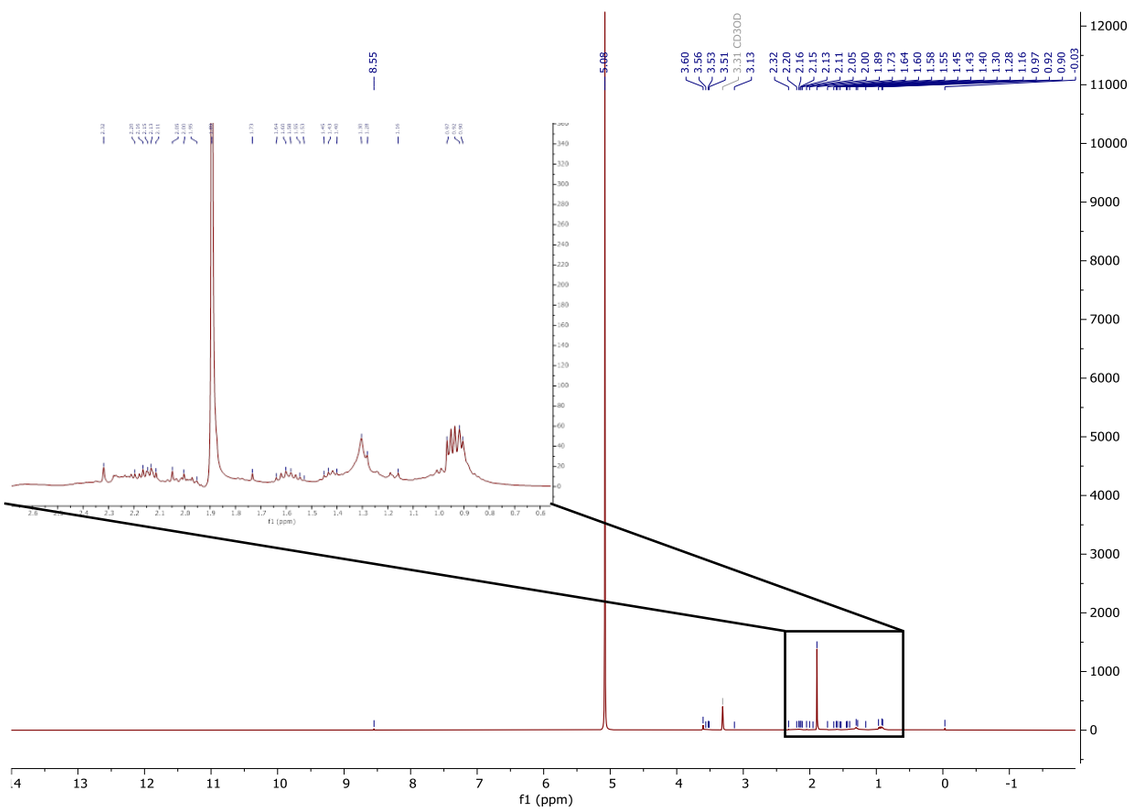

Figure S2: ^{1}H Spectrum of the crude reaction mixture from table S1, entry 1 in CD_3OD.

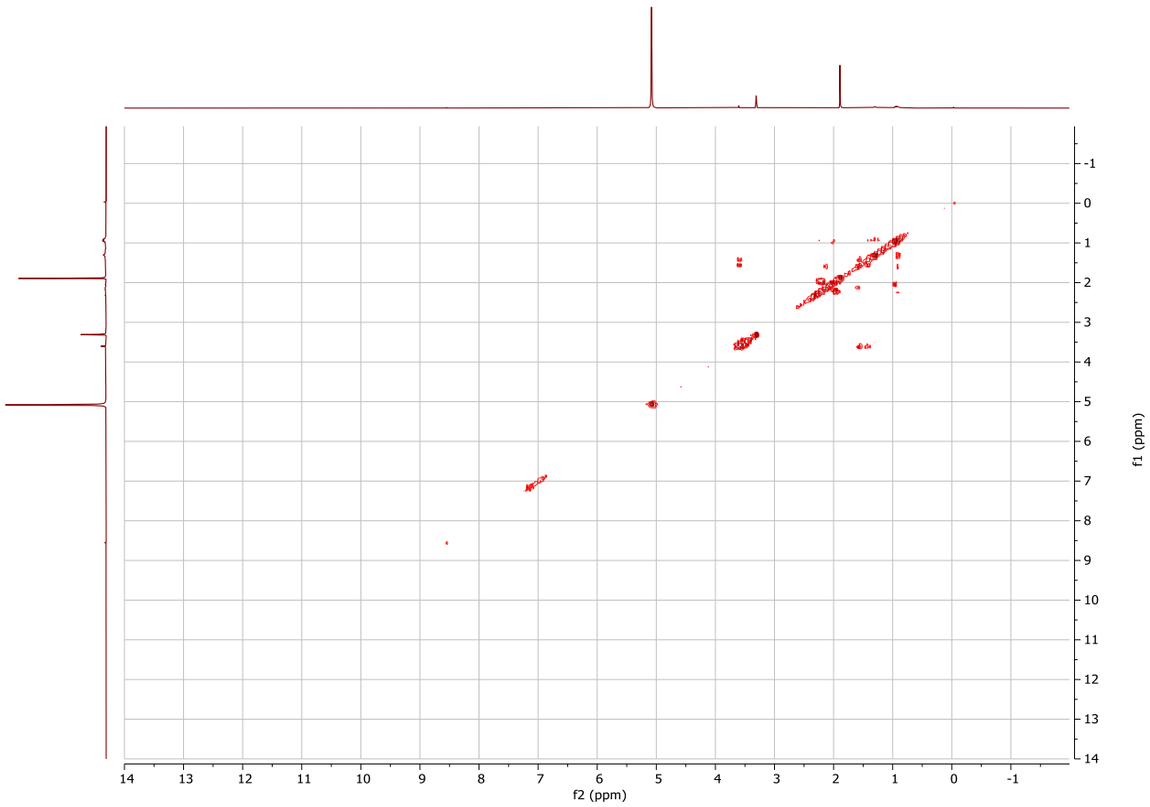

Figure S3: ^{1}H-^{1}H COSY Spectrum of the crude reaction mixture from table S1 entry 1 in CD_3OD.

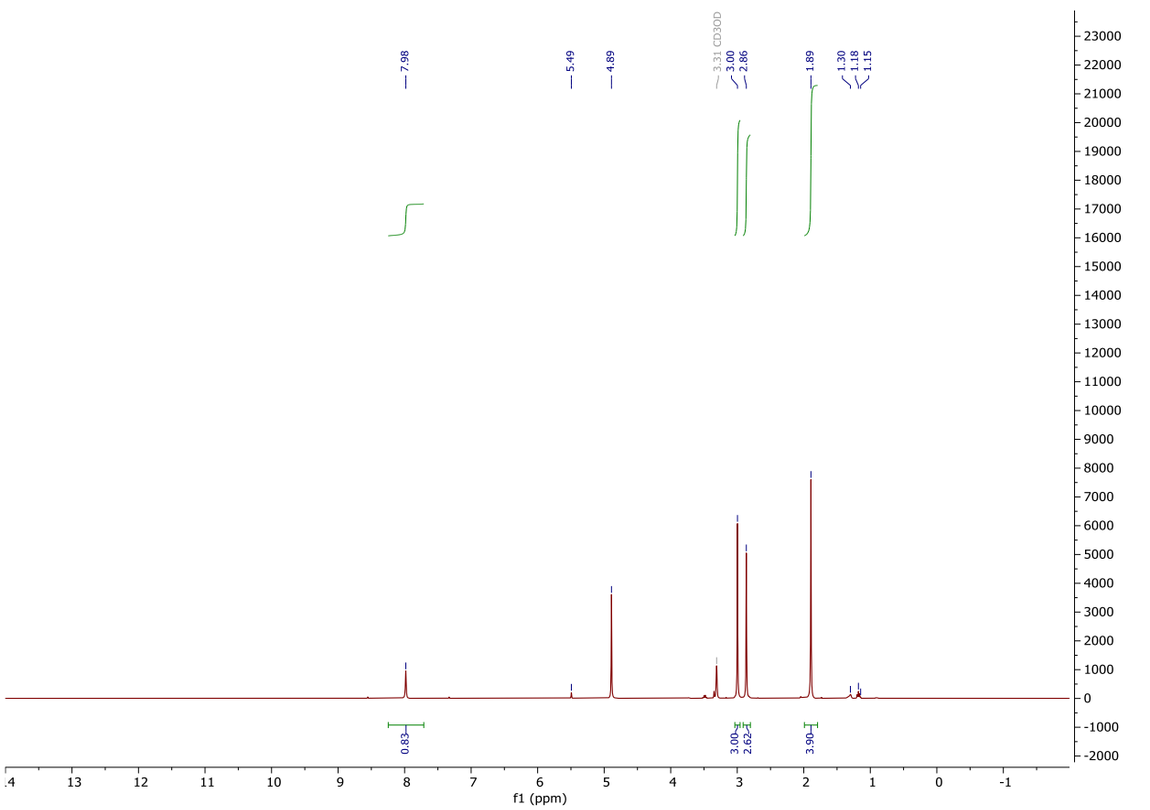

Figure S4: Quantitative ^{1}H Spectrum of the crude reaction mixture from table S1, entry 1 in CD_3OD.

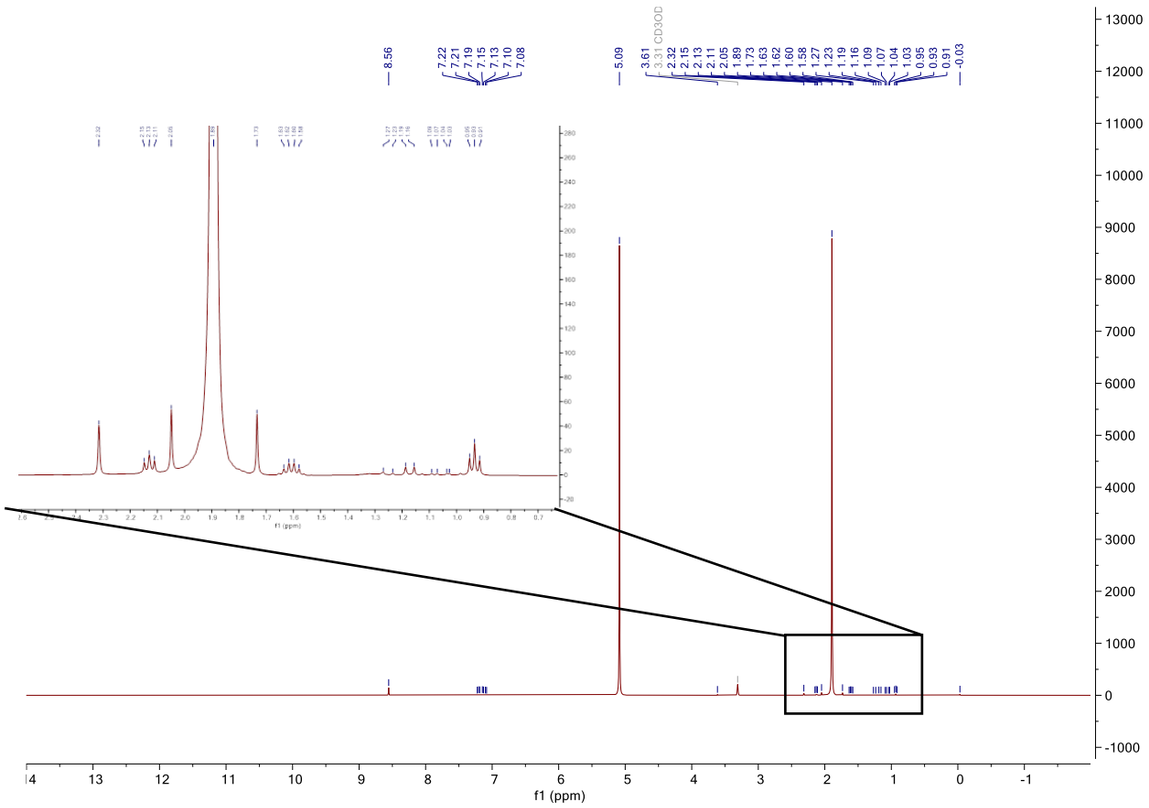

Figure S5: ^{1}H Spectrum of the crude reaction mixture from table S1, entry 2 in CD_3OD.

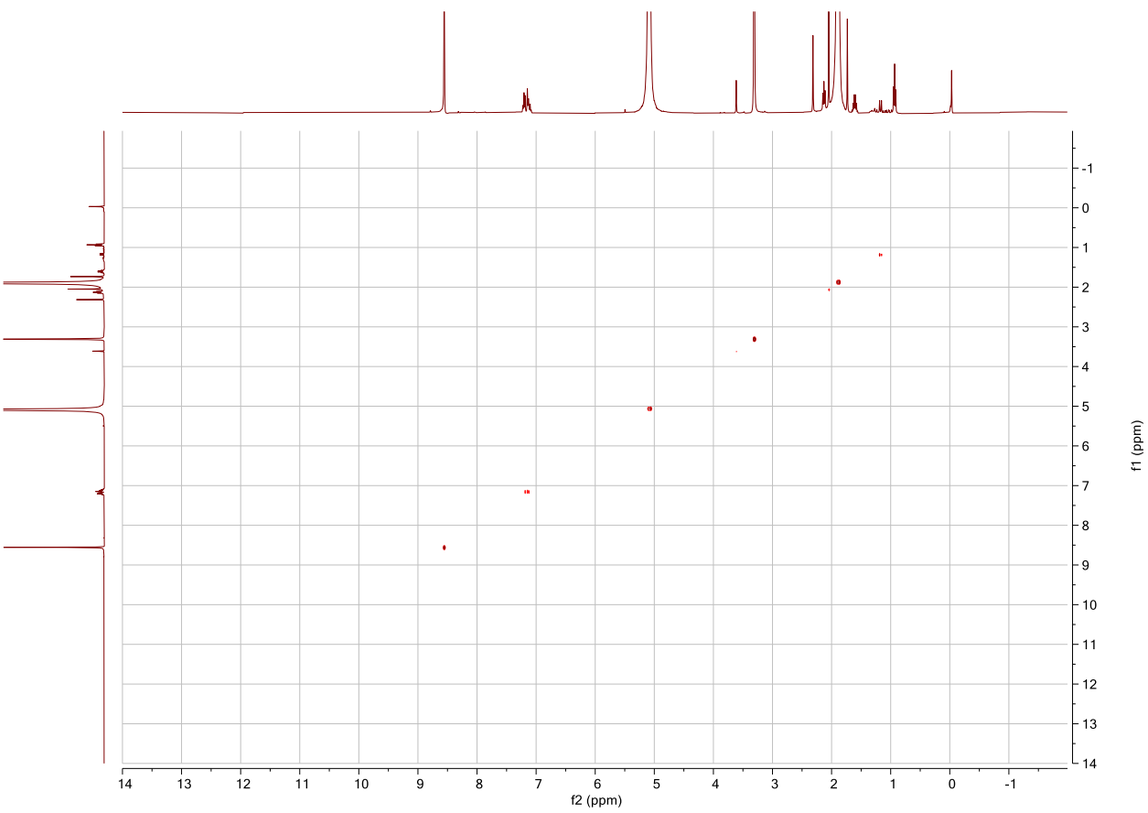

Figure S6: ^{1}H-^{1}H COSY Spectrum of the crude reaction mixture from table S1, entry 2 in CD_3OD.

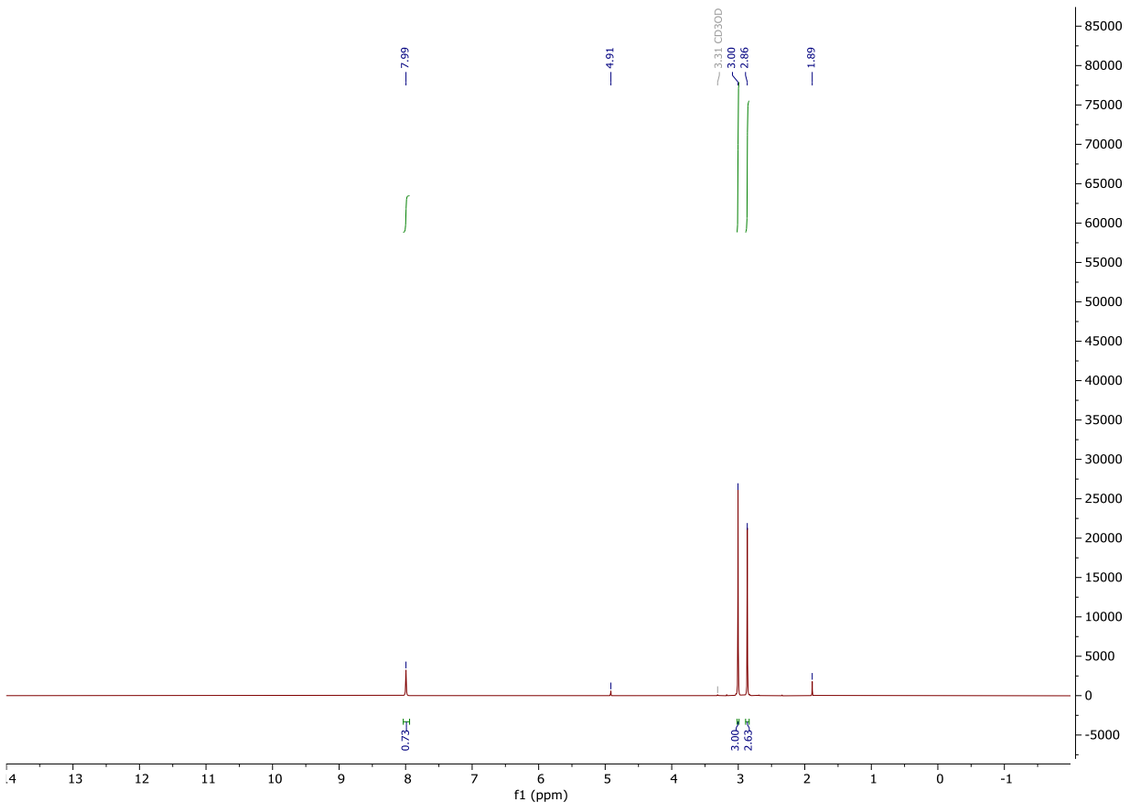

Figure S7: Quantitative ^{1}H Spectrum of the crude reaction mixture from table S1, entry 2 in CD_3OD.

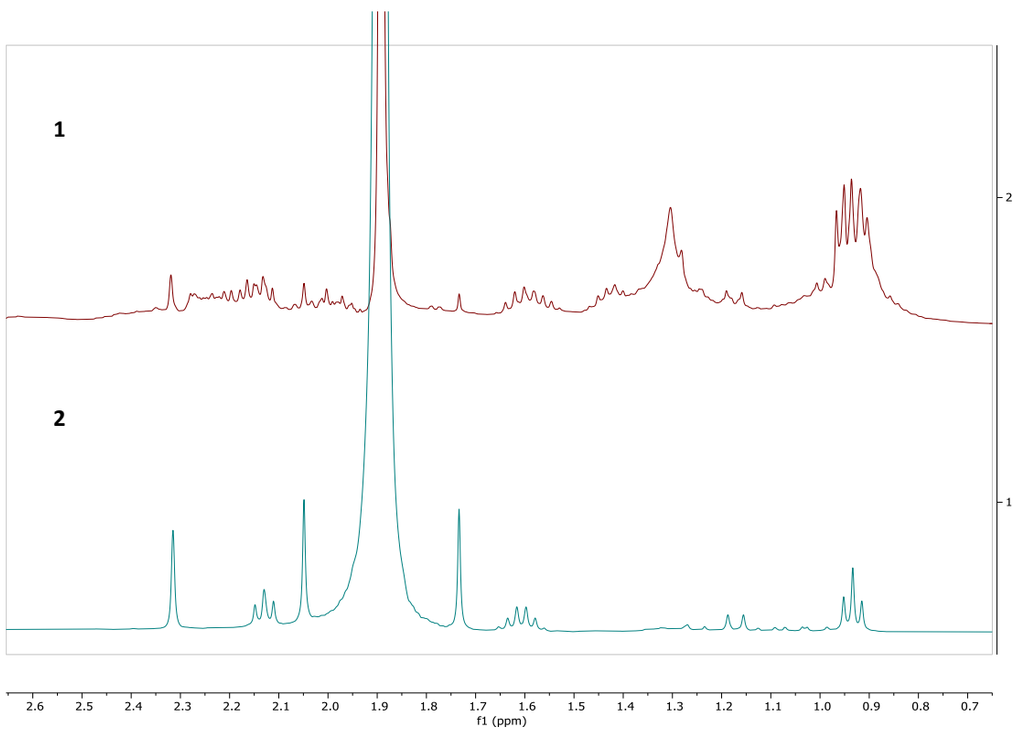

Figure S8: NMR analysis of initial screening of reactions involving **1** and **2**. Both spectra suggest the presence of butyrate (2.29 (t, 2H), 1.61 (tq, 2H). 0.93 (t, 3H)); however, in spectrum 1 (**1**) we see peaks at corresponding to 2-ethyl-1-butanol (3.31 (d, 2H), 1.63-1.4 (m, 5H), 0.84 (t, 6H)) the Guerbet product, as well as peaks corresponding to higher order alcohols from iterative Guerbet reactions.

Catalyst Screening Experiments

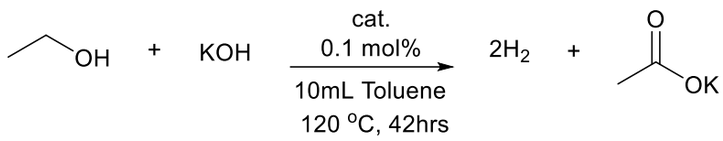

All catalyst screening reactions were run with 0.1 mol% catalyst loading with respect to ethanol. In a nitrogen filled glovebox, one equivalent of ethanol (200 proof, 0.92 g, 20 mmol) and one equivalent of potassium hydroxide (0.56 g, 23 mmol) in toluene (10 mL, distilled from benzophenone ketyl) were combined with a catalyst (0.1 mol% relative to EtOH) in a 25 mL round bottom flask. The flask was removed from the glovebox, and a condenser was attached and capped with a septum. The reaction was then heated and stirred in an oil bath. Reaction progress was monitored by water eudiometry via needle and tubing. After 42 hours, volatiles removed using a rotary evaporator under reduced pressure and quantitative NMR was recorded using dimethyl formamide as an internal standard. The remaining product was diluted in water (deionized, 50 mL) and subsequently back-titrated with hydrochloric acid (0.2657 M) and dilute sodium hydroxide (0.2556 M) solutions.

Table S2. Results of Catalyst Screening

			Anions (mol %)[b]			
Entry	**Cat.**	**Acetate (%)[a]**	**OH^-**	**Formate**	**Acetate**	**Butyrate**
1	1	10	76	2	22	0
2	2	29	63	22	15	0
3	3	26	60	12	27	1
4	4	37	71	0	28	< 1
5	5	87	18	3	79	0
6	6	18	58	1	40	< 1
7	7	7	80	1	19	0
8	8	19	71	1	28	0
9	9	1	63	2	35	0
10	10	80	5	3	90	1
11	11	75	21	7	71	1
12	12	68	14	3	83	0
13	13	14	66	0	32	2
14	14	17	73	1	26	0
15	15	12	87	1	11	< 1
16	16	7	64	32	4	0
17	17	24	56	25	19	0
18	18	41	51	4	49	1
19	19	7	61	4	39	2
20	20	66	37	2	63	< 1
21	21	8	70	4	30	< 1
22	22	2	83	3	17	< 1
23	23	9	69	3	31	5

[a] Determined by ^{1}H NMR using DMF as an internal standard. [b] Determined by acid-base back titration and ^{1}H NMR.

Catalyst Screening Spectra

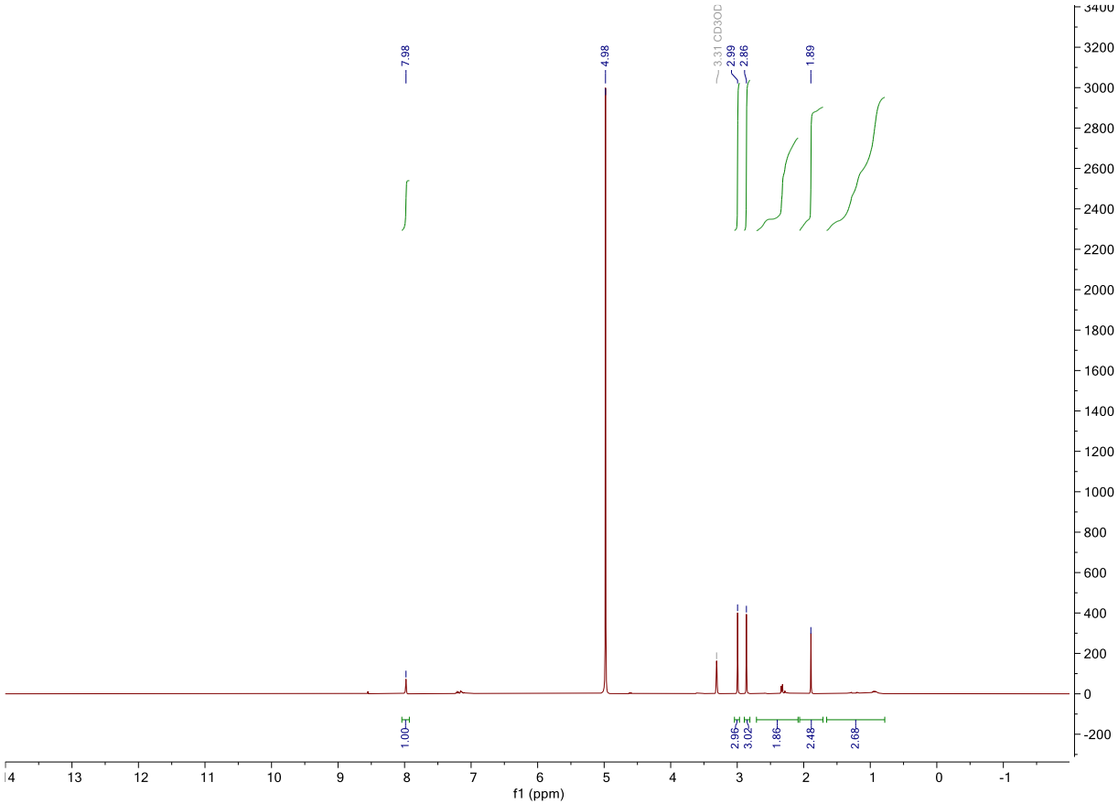

Figure S9: Quantitative ^{1}H Spectrum of product mixture for table S2, entry 1 (catalyst **1**) in CD_3OD.

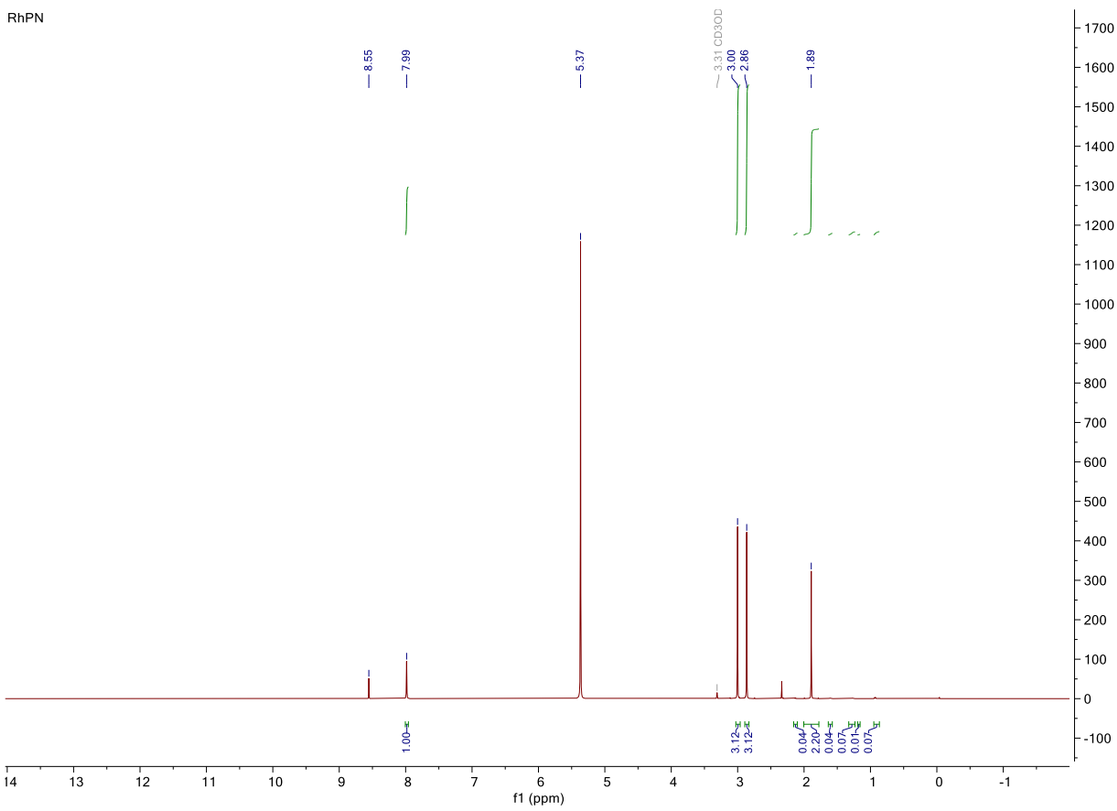

Figure S10: Quantitative ^{1}H Spectrum of product mixture for table S2, entry 2 (catalyst **2**) in CD_3OD.

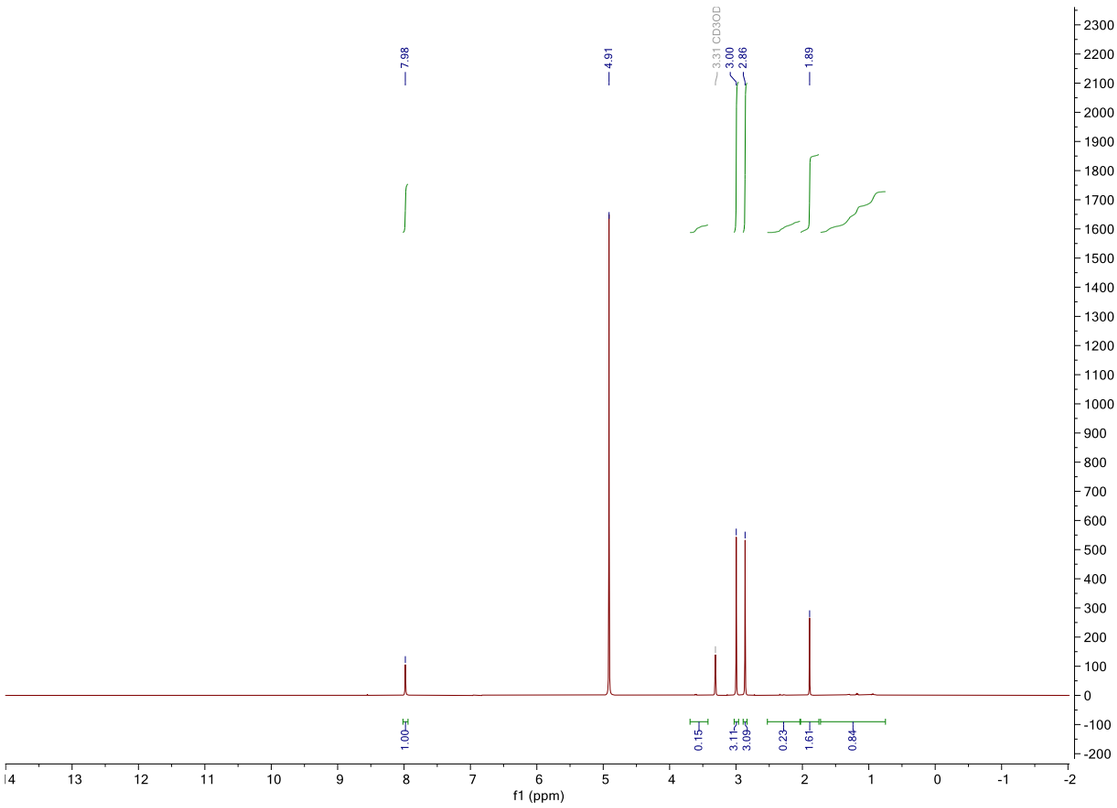

Figure S11: Quantitative ^{1}H Spectrum of product mixture for table S2, entry 3 (catalyst **3**) in CD_3OD.

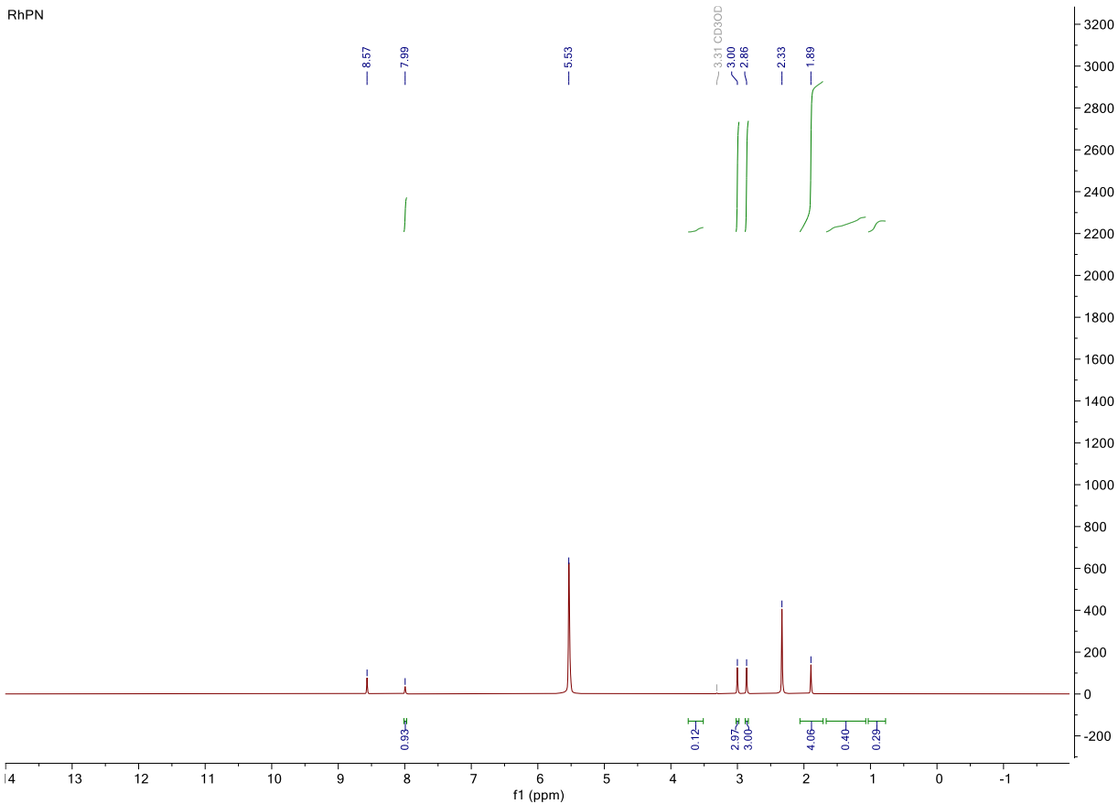

Figure S12: Quantitative ^{1}H Spectrum of product mixture for table S2, entry 4 (catalyst **4**) in CD_3OD.

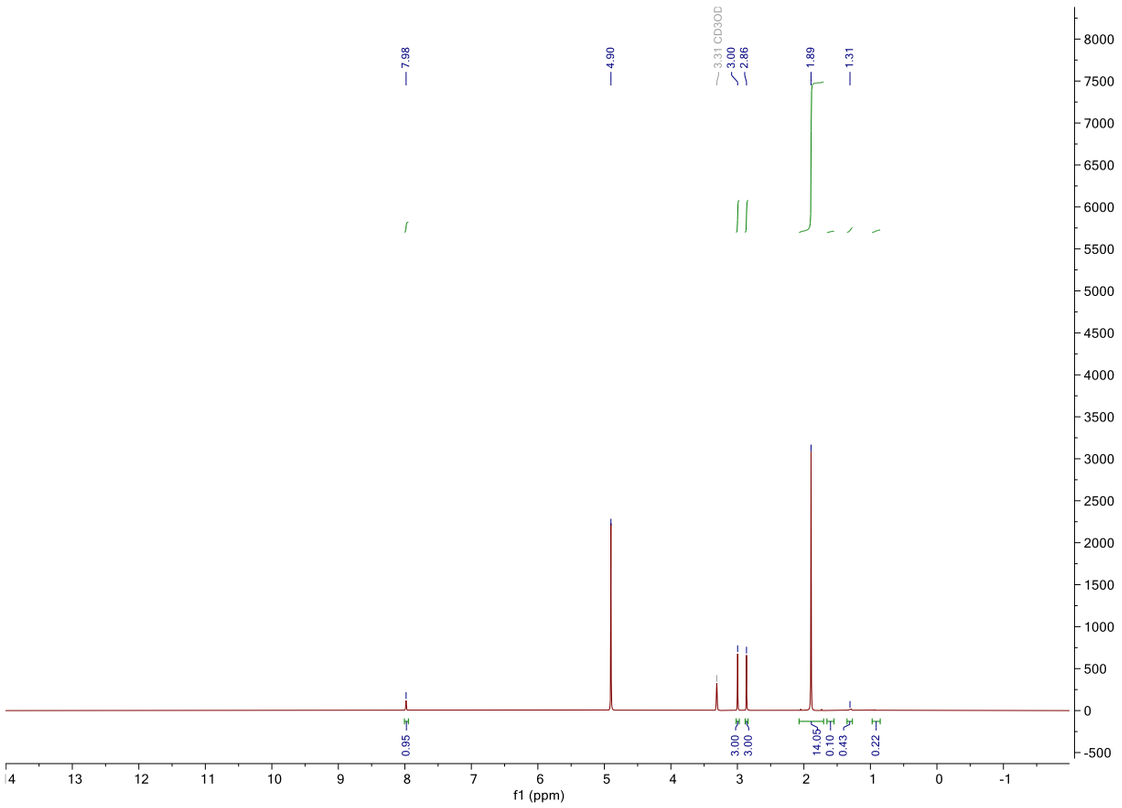

Figure S13: Quantitative ^{1}H Spectrum of product mixture for table S2, entry 5 (catalyst **5**) in CD_3OD.

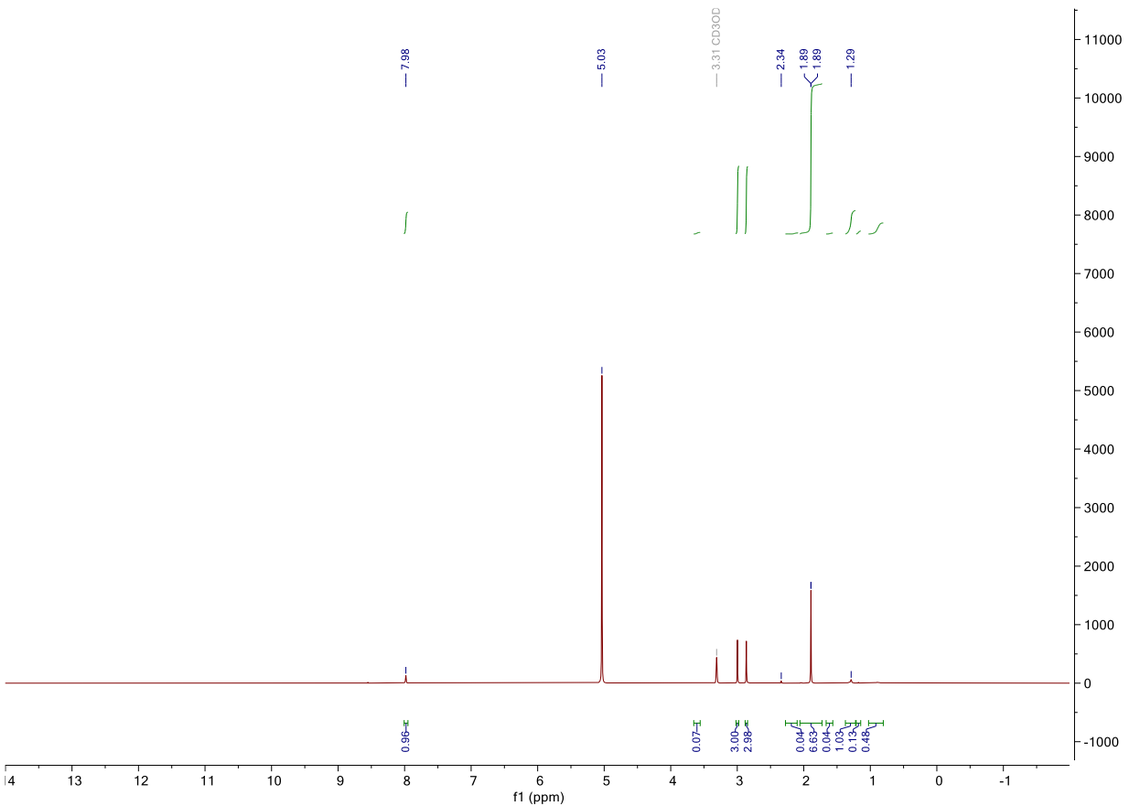

Figure S14: Quantitative ^{1}H Spectrum of product mixture for table S2, entry 6 (catalyst **6**) in CD_3OD.

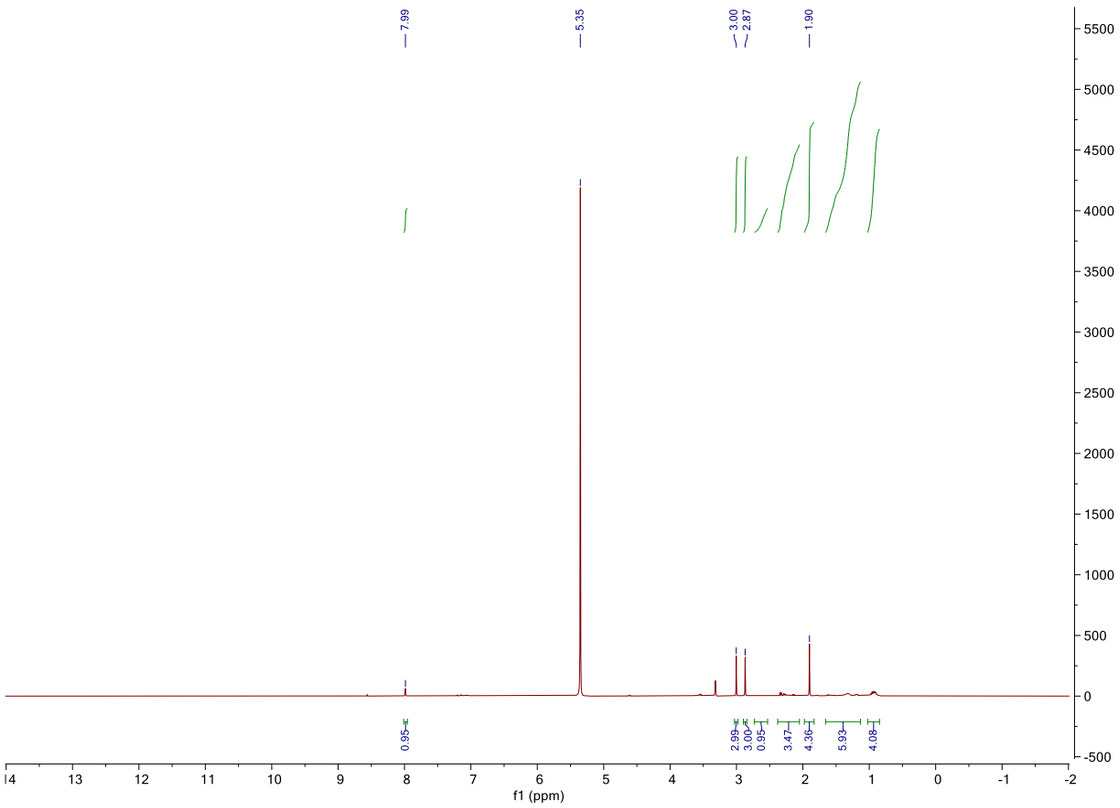

Figure S15: Quantitative ^{1}H Spectrum of product mixture for table S2, entry 7 (catalyst **7**) in CD_3OD.

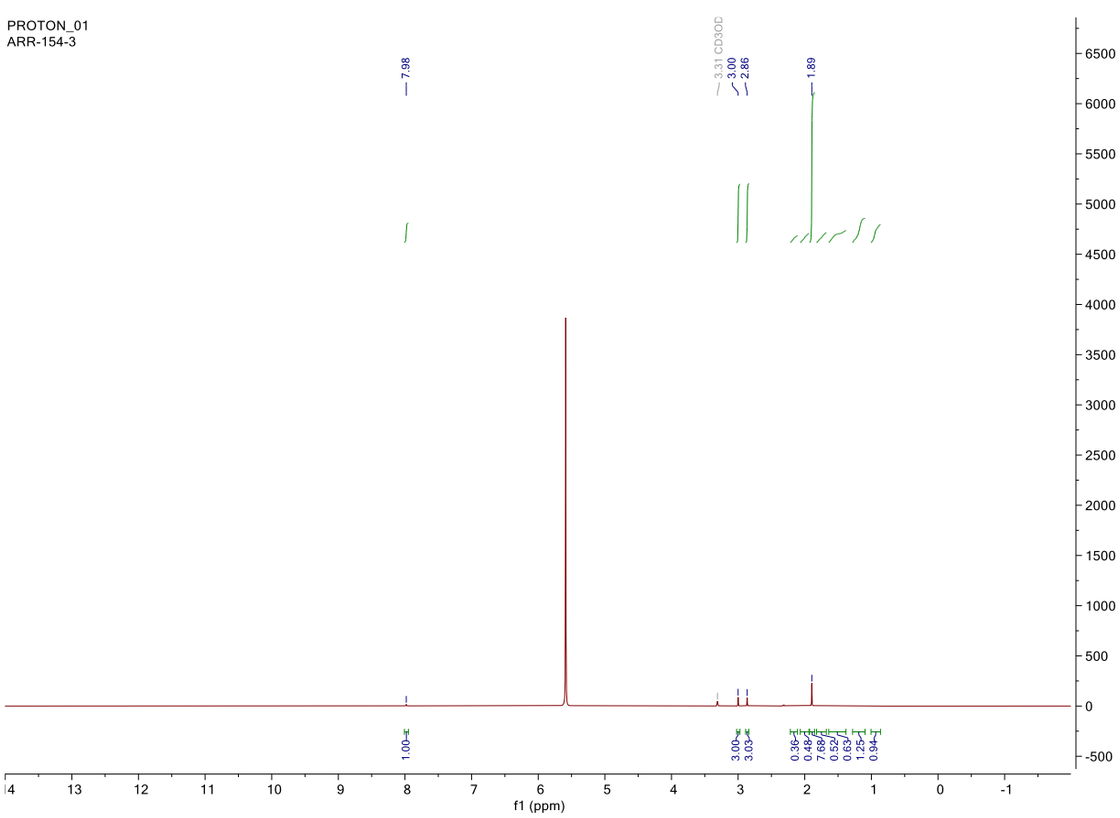

Figure S16: Quantitative ^{1}H Spectrum of product mixture for table S2, entry 8 (catalyst **8**) in CD_3OD.

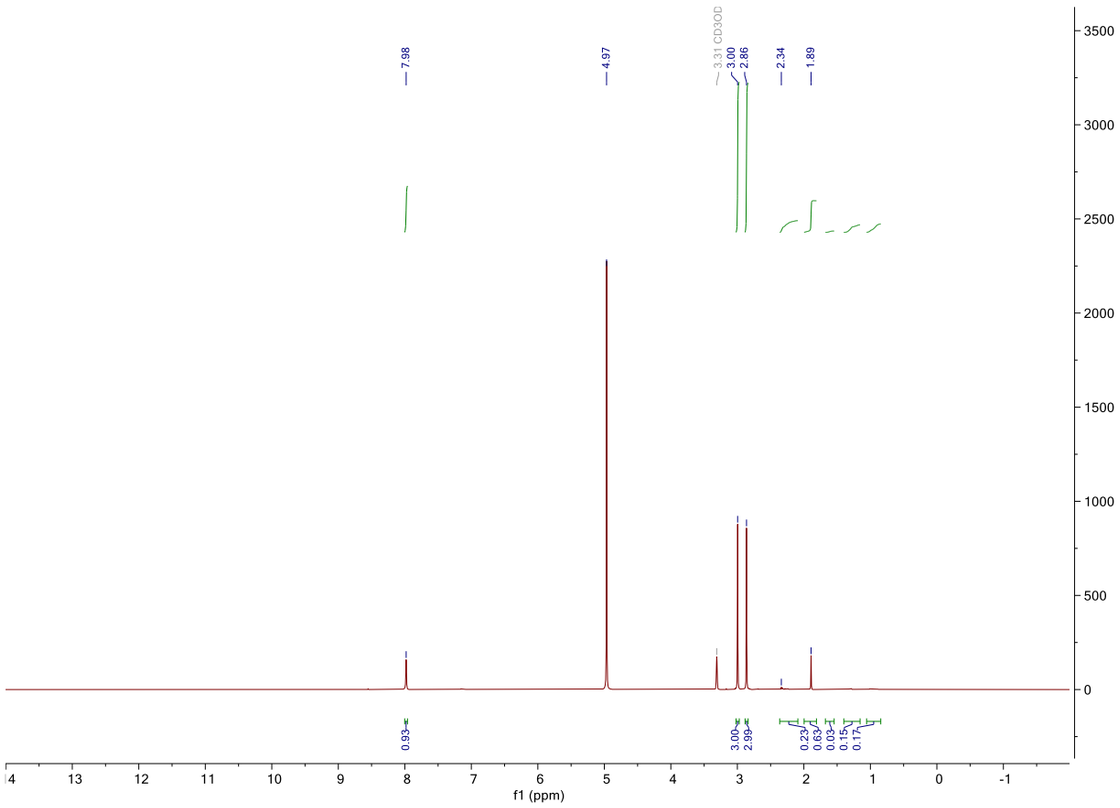

Figure S17: Quantitative ^{1}H Spectrum of product mixture for table S2, entry 9 (catalyst **9**) in CD_3OD.

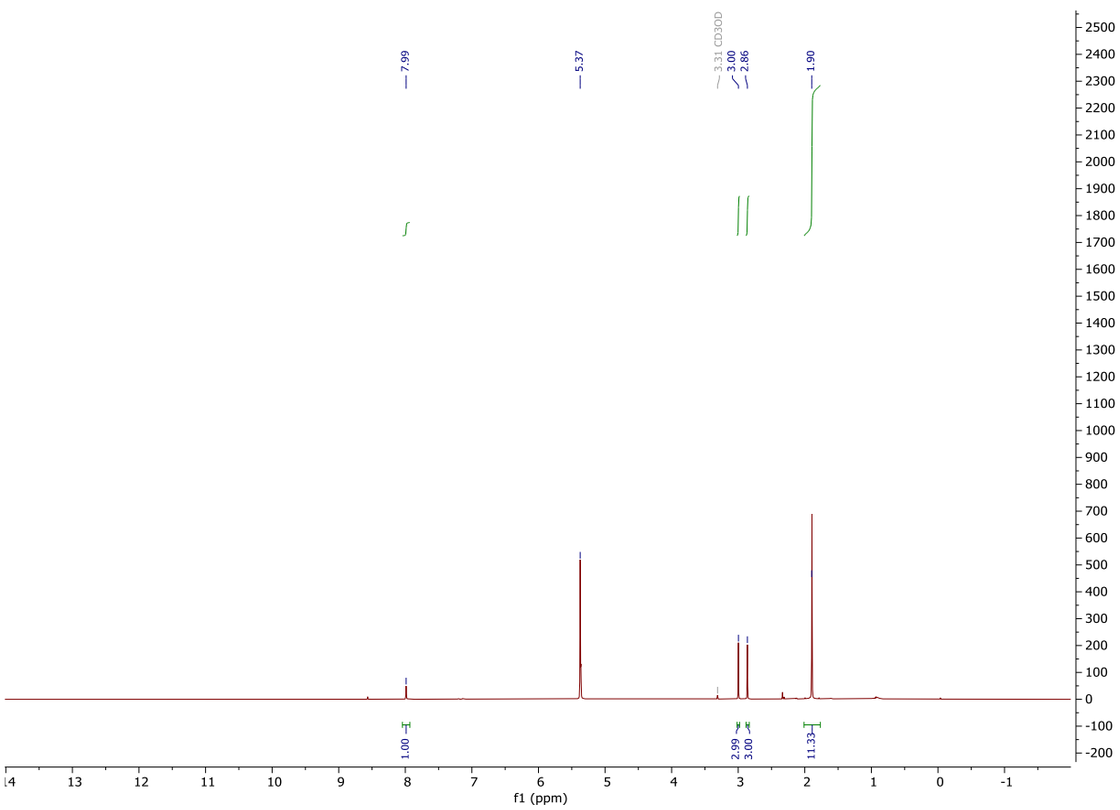

Figure S18: Quantitative ^{1}H Spectrum of product mixture for table S2, entry 10 (catalyst **10**) in CD_3OD.

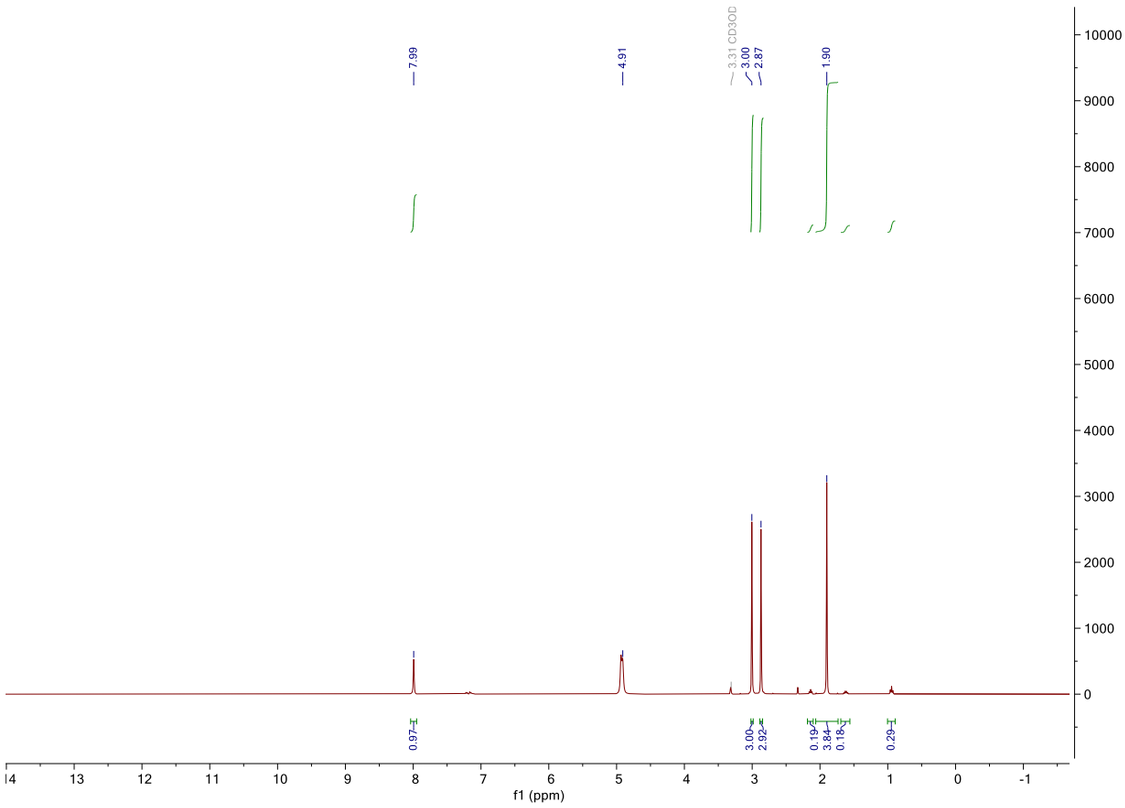

Figure S19: Quantitative ^{1}H Spectrum of product mixture for table S2, entry 11 (catalyst **11**) in CD_3OD.

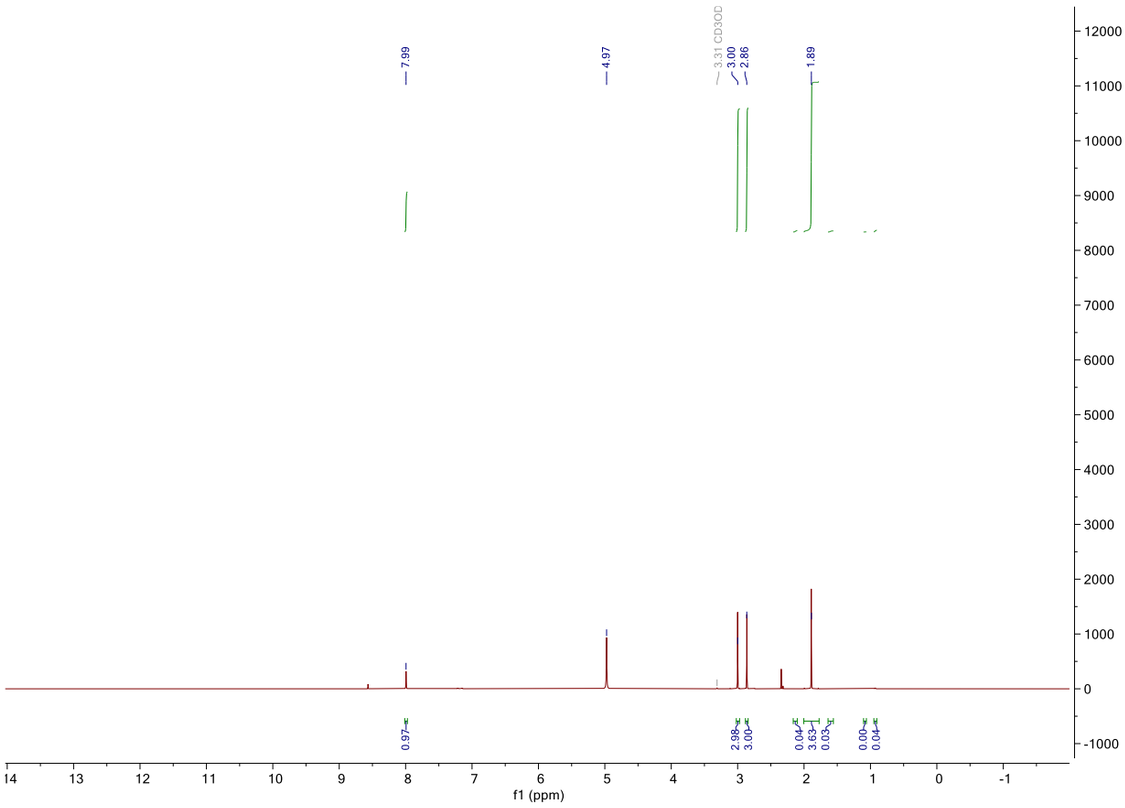

Figure S20: Quantitative ^{1}H Spectrum of product mixture for table S2, entry 12 (catalyst **12**) in CD_3OD.

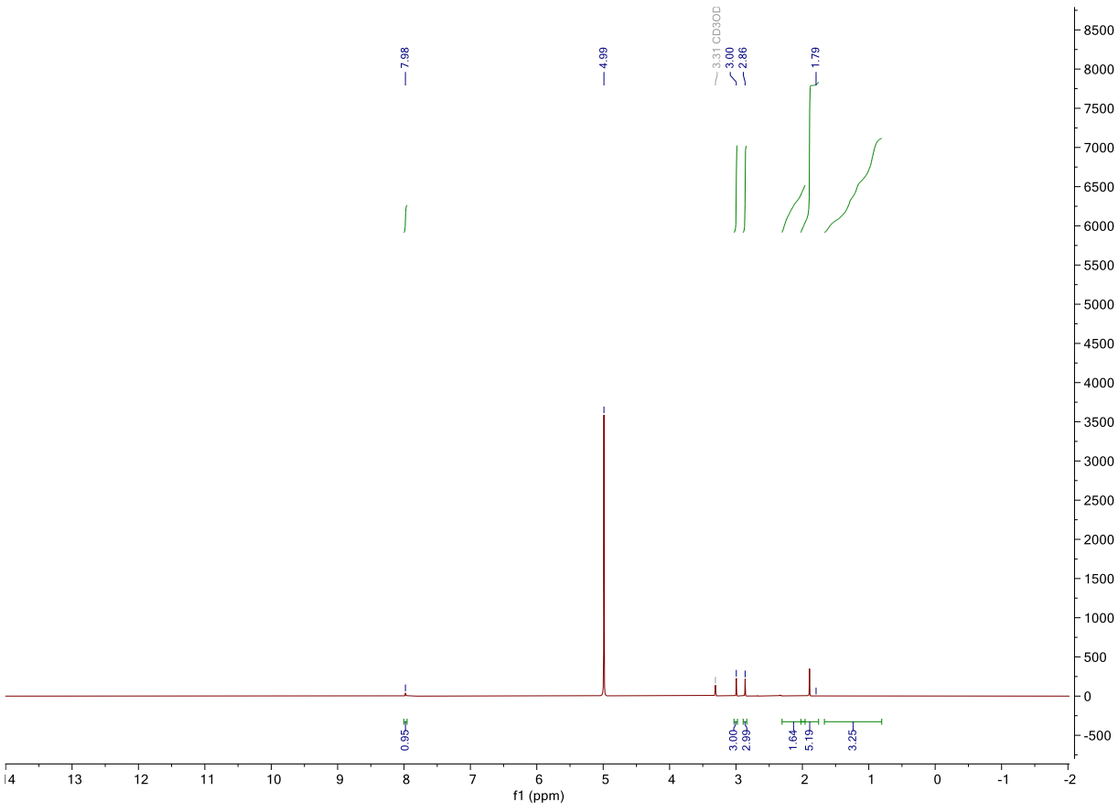

Figure S21: Quantitative ^{1}H Spectrum of product mixture for table S2, entry 13 (catalyst **13**) in CD_3OD.

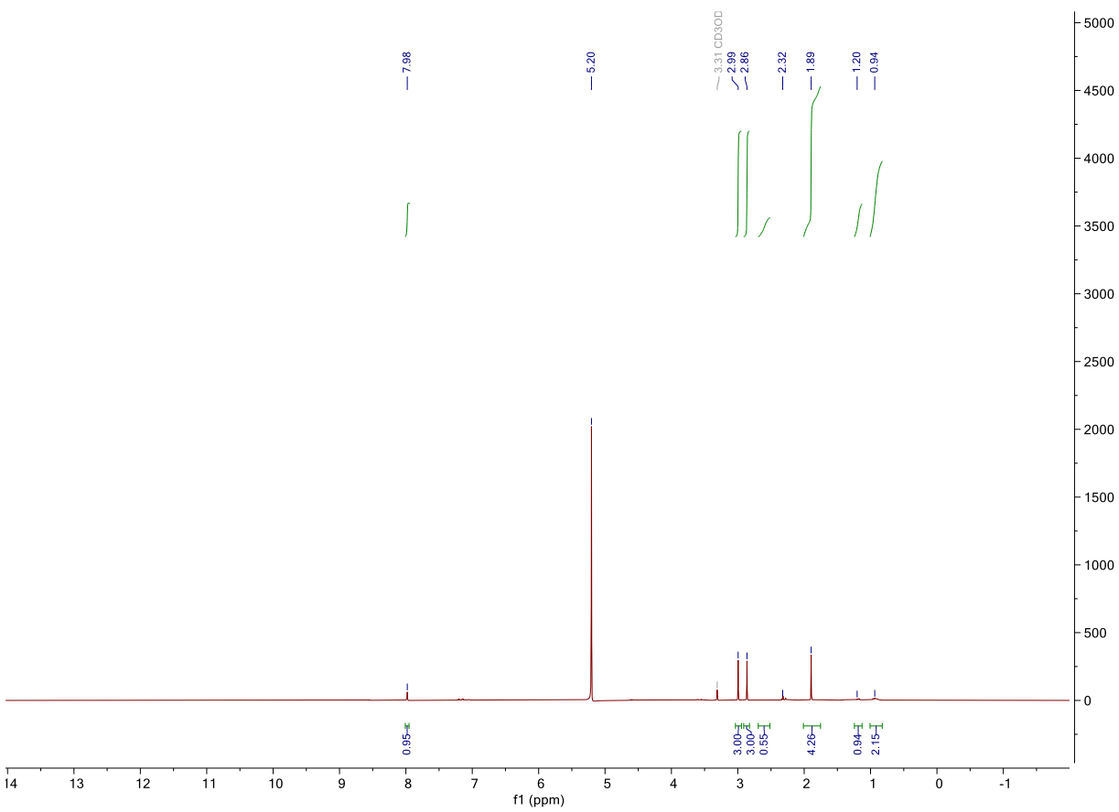

Figure S22: Quantitative ^{1}H Spectrum of product mixture for table S2, entry 14 (catalyst **14**) in CD_3OD.

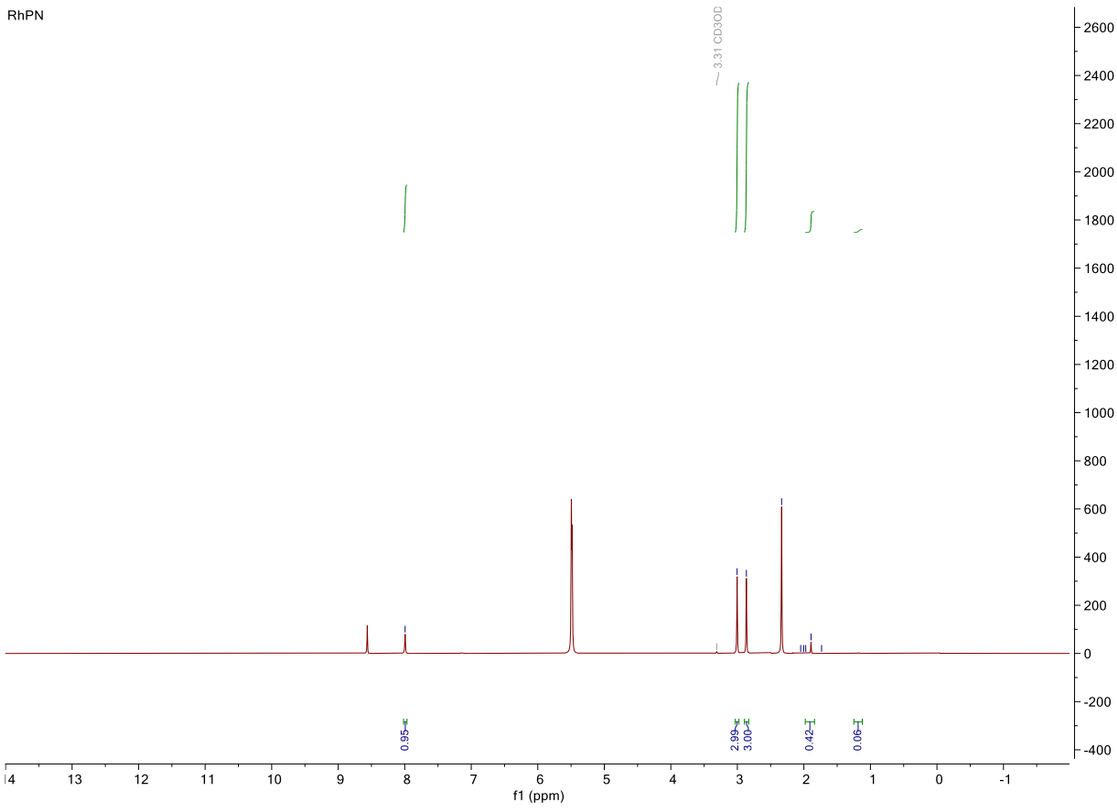

Figure S23: Quantitative ^{1}H Spectrum of product mixture for table S2, entry 15 (catalyst **15**) in CD_3OD.

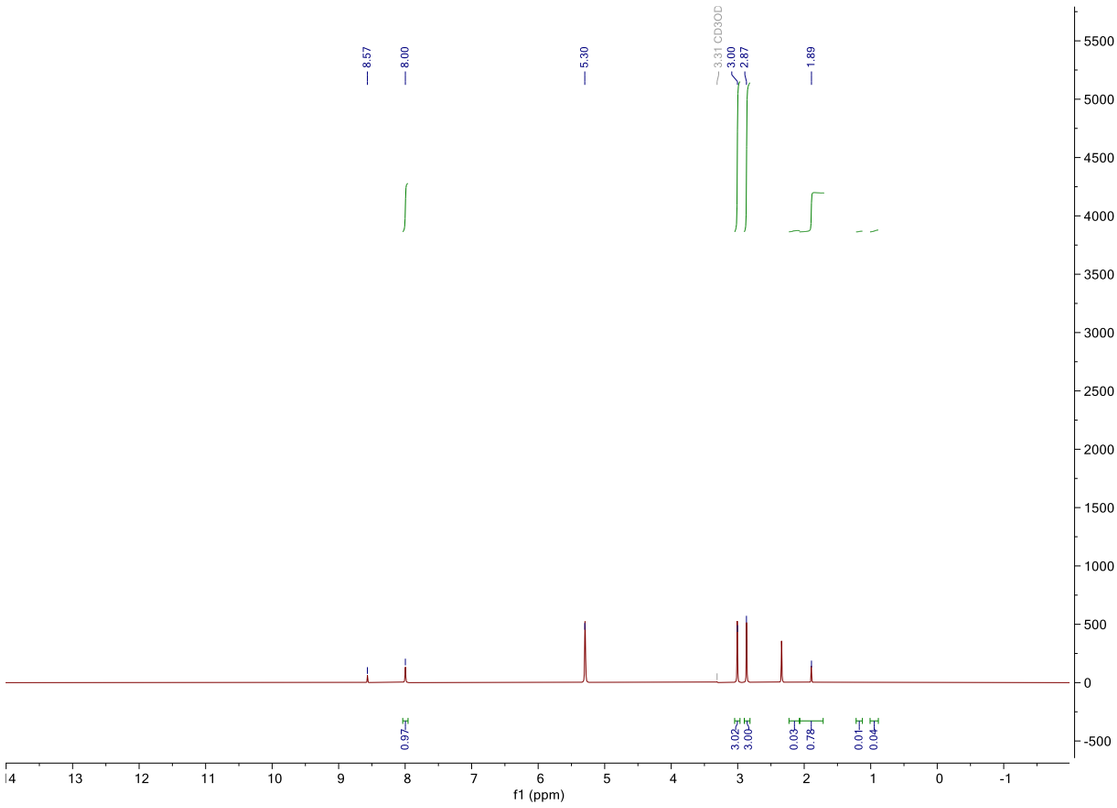

Figure S24: Quantitative ^{1}H Spectrum of product mixture for table S2, entry 16 (catalyst **16**) in CD_3OD.

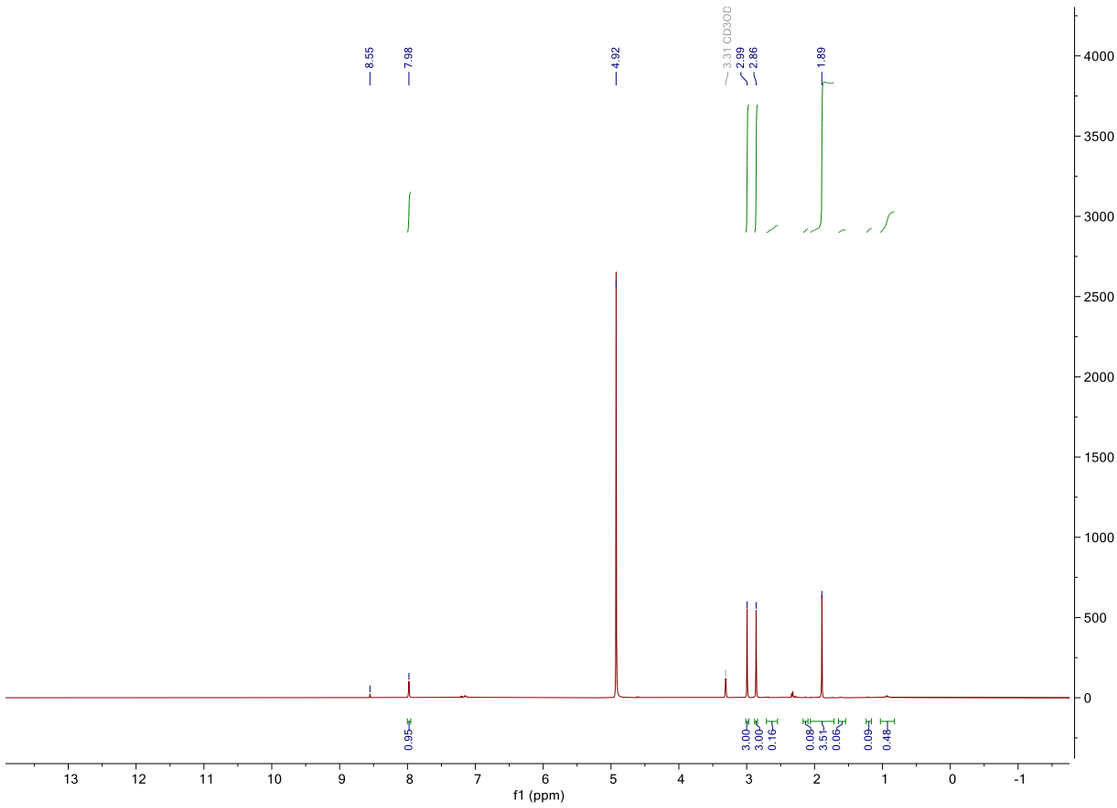

Figure S25: Quantitative ^{1}H Spectrum of product mixture for table S2, entry 17 (catalyst **17**) in CD_3OD.

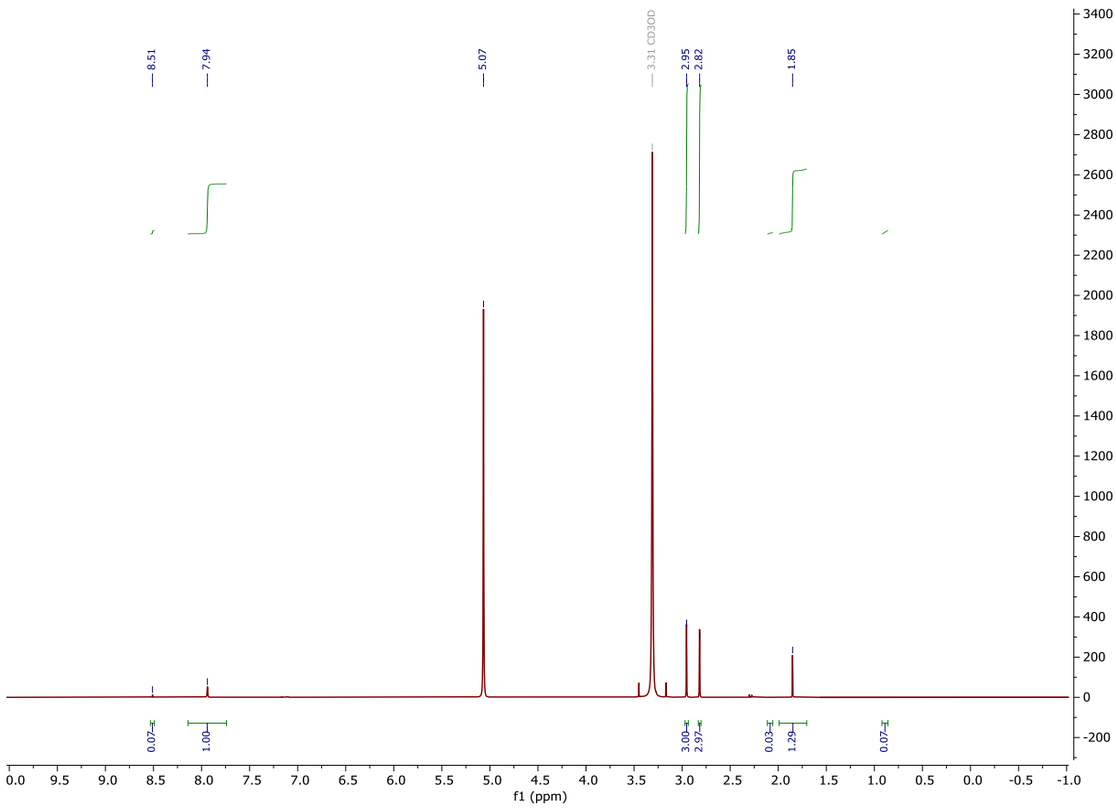

Figure S26: Quantitative ^{1}H Spectrum of product mixture for table S2, entry 18 (catalyst **18**) in CD_3OD.

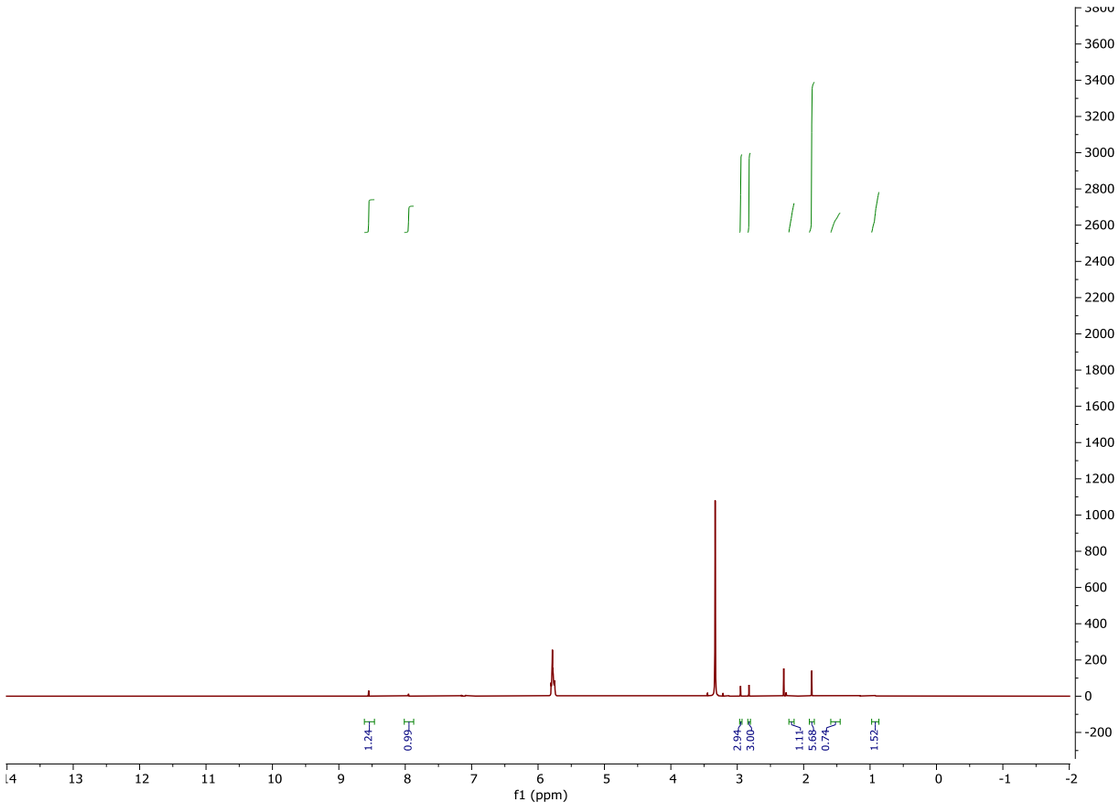

Figure S27: Quantitative ^{1}H Spectrum of product mixture for table S2, entry 19 (catalyst **19**) in CD_3OD.

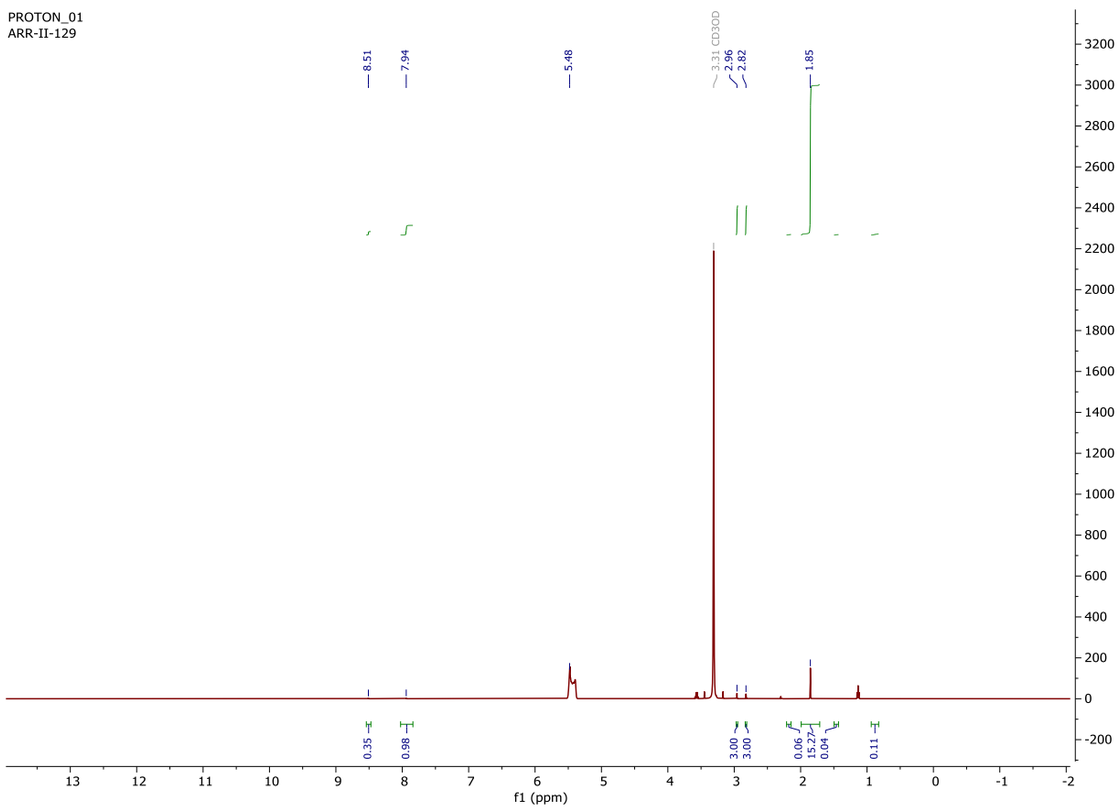

Figure S28: Quantitative ^{1}H Spectrum of product mixture for table S2, entry 20 (catalyst **20**) in CD_3OD.

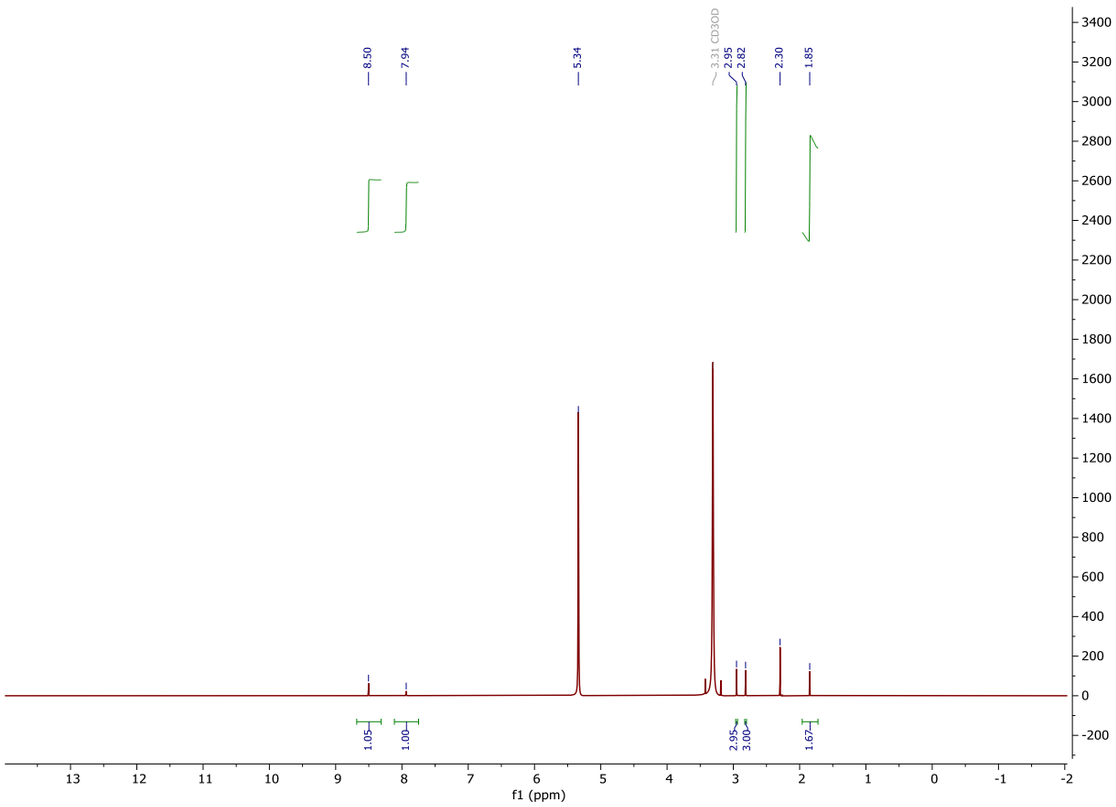

Figure S29: Quantitative ^{1}H Spectrum of product mixture for table S2, entry 21 (catalyst **21**) in CD_3OD.

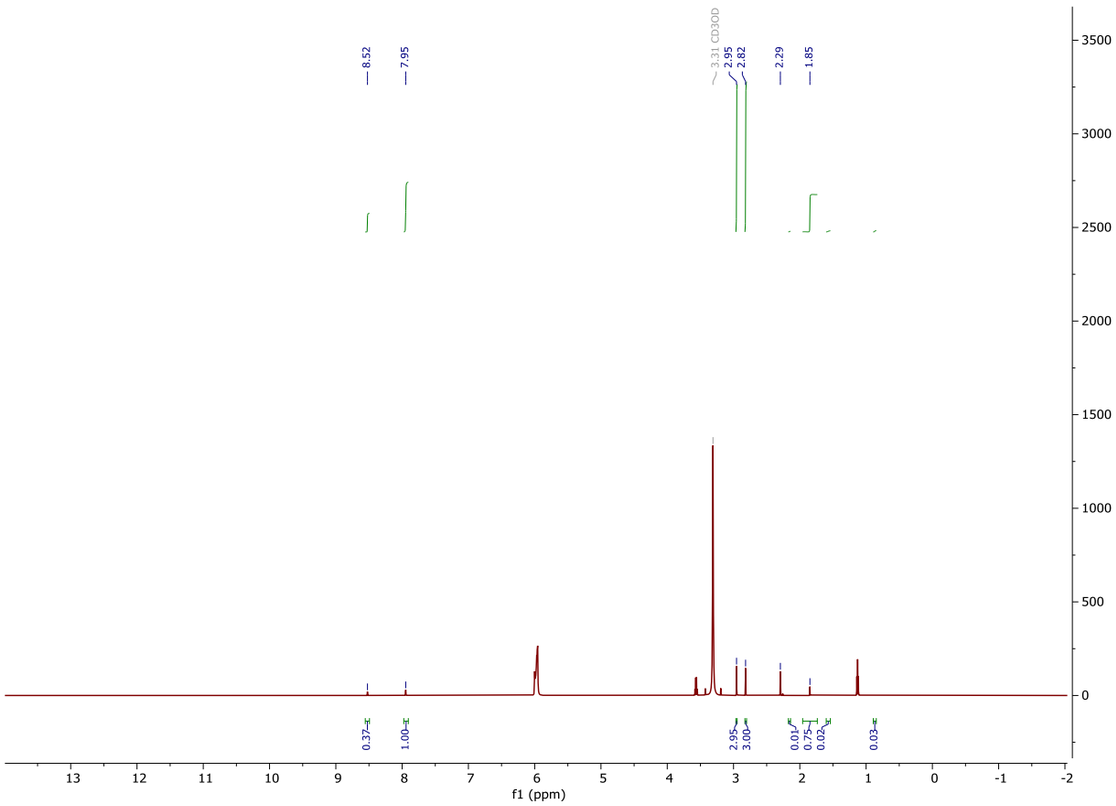

Figure S30: Quantitative ^{1}H Spectrum of product mixture for table S2, entry 22 (catalyst **22**) in CD_3OD.

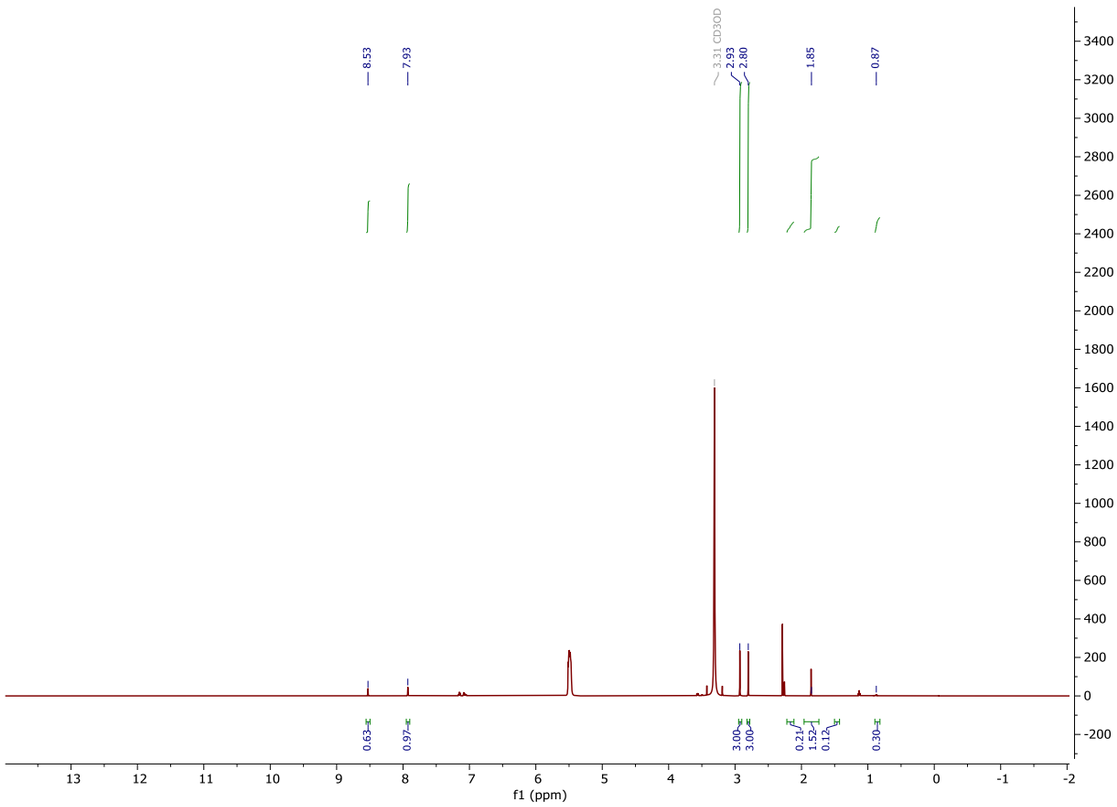

Figure S31: Quantitative ^{1}H Spectrum of product mixture for table S2, entry 23 (catalyst **23**) in CD_3OD.

Ambient Condition Optimization Reactions

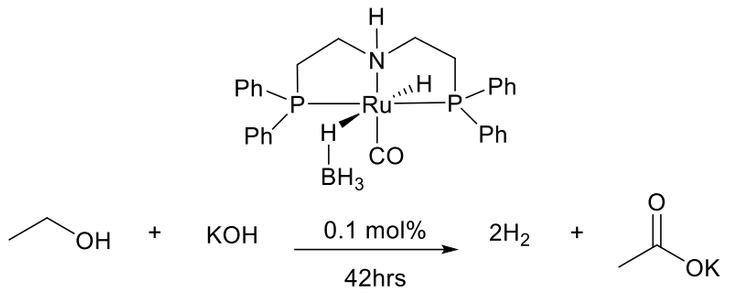

Each reaction was done with varying amounts of reagents, solvent, or additives as summarized in table S3. In a representative procedure, in a nitrogen filled glovebox, potassium hydroxide (0.5 equiv = 0.64 g, 9.8 mmol) was weighed out and added to a 25 mL round bottom flask. Next, Ru-MACHO-BH (catalyst **10**, 0.1 mol %, 11.7mg, 20 μmol relative to reactant in excess) and toluene (10 mL, distilled from benzophenone ketyl, or 0 mL if described as "neat") was weighed out and added. Finally, an amount of ethanol (200 proof, 1 equiv = 0.92 g, 20 mmol) was weighed in a vial and quantitatively transferred to the round bottom flask. Each reaction flask was added a reflux condenser outfitted with a septum, and each was refluxed for a minimum of 42 hours at 120 °C. Gas production was measured by water eudiometry, attached through a needle. After 42 hours, volatiles removed using a rotary evaporator under reduced pressure. Quantitative NMR samples were prepared by adding methanol-d_4 (700 mL) and dimethylformamide (DMF, 0.10 g, 1.37 mmol) and subsequently analyzed by ^{1}H NMR. After NMR analysis, volatiles were again removed using a rotary evaporator under reduced pressure and the resulting solid was diluted in 50 mL of deionized water and titrated to determine the molar percentage of acetate in the sample.

Table S3: Results of Reaction Optimization

Entry	EtOH (eq)	KOH (eq)	Solvent	Temperature (˚C)	Solvent (mL)	Acetate (%)	Carboxylates (mol%)[b]
1	1	0.75	Toluene	120	10	73.2	98
2	1	0.5	Toluene	120	10	94	99
3	0.75	1	Toluene	120	10	18	47
4	0.5	1	Toluene	120	10	27	48
5	1	0.5	Toluene	80	10	77	94
6	1	0.5	Neat	80	Neat	3	14
7	1	0.17	Neat	80	Neat	87	96

[a] Catalyst loading based on moles of ethanol entries 1-4. Based on moles of KOH entries 5-7. [b] Molar percent carboxylates determined by titration. [c] Run at 80 ˚C.

Ambient Condition Optimization NMR Spectra

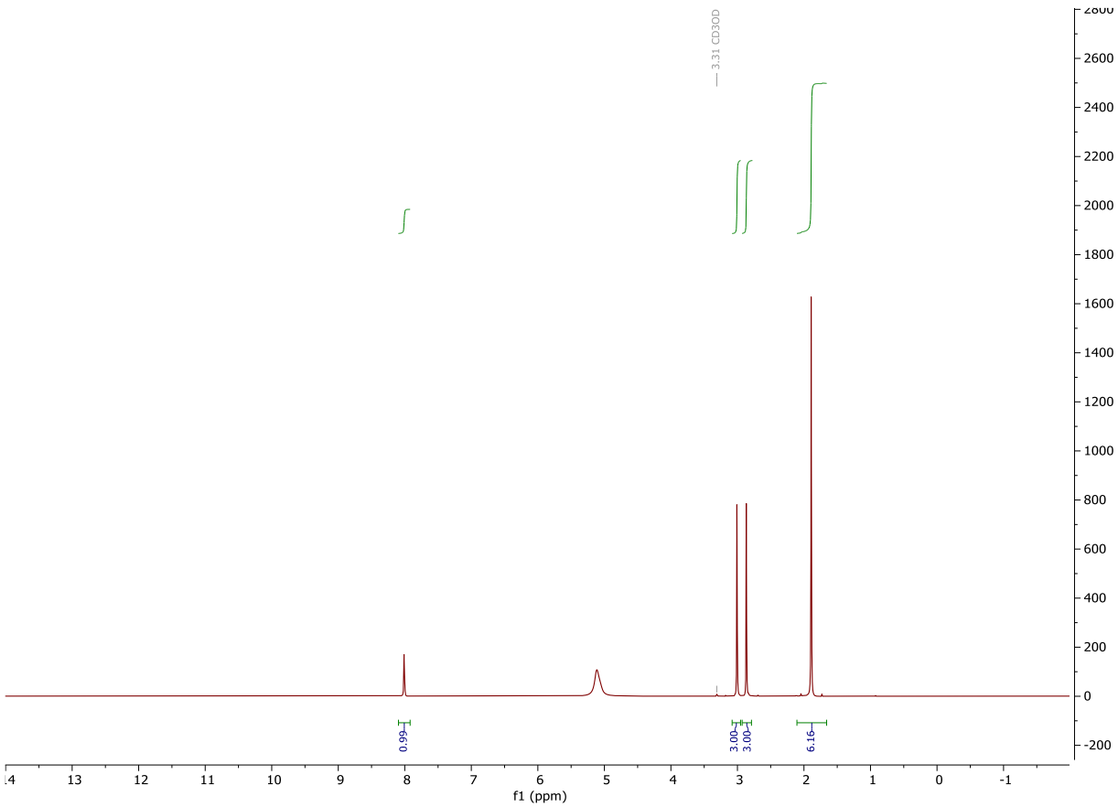

Figure S32: Quantitative ^{1}H Spectrum of product mixture for table S3, entry 1 in CD_3OD.

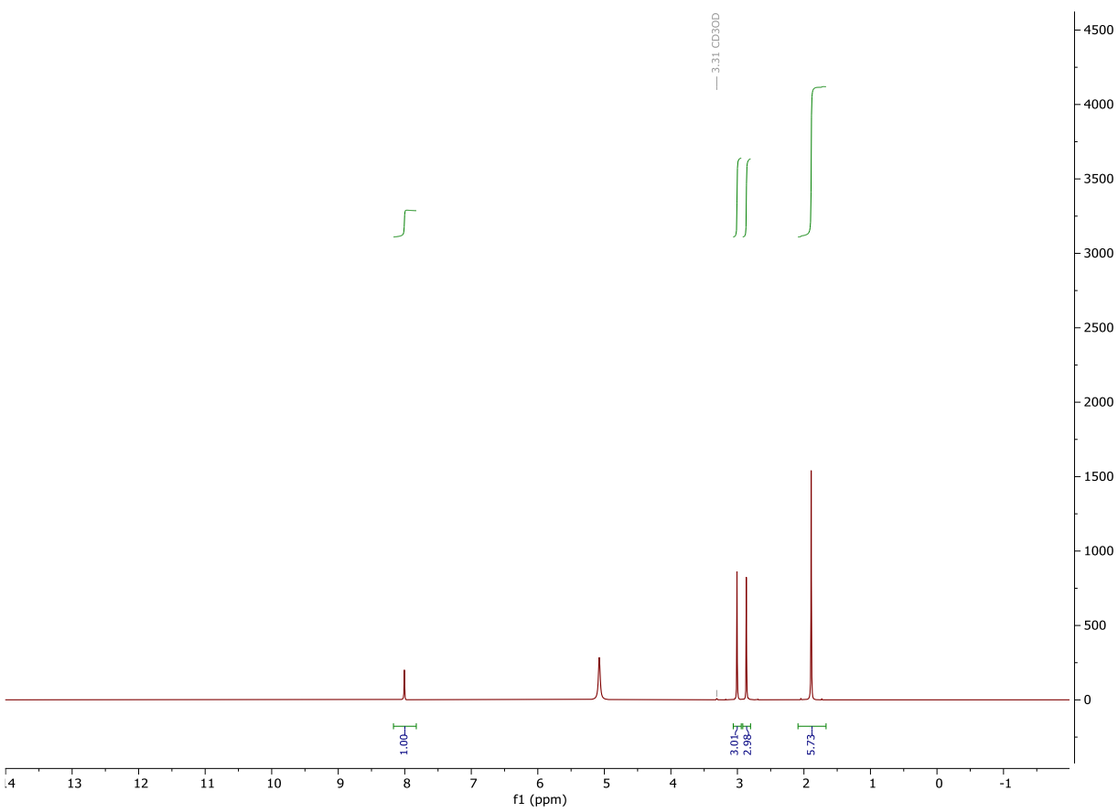

Figure S33: Quantitative ^{1}H Spectrum of product mixture for table S3, entry 2 in CD_3OD.

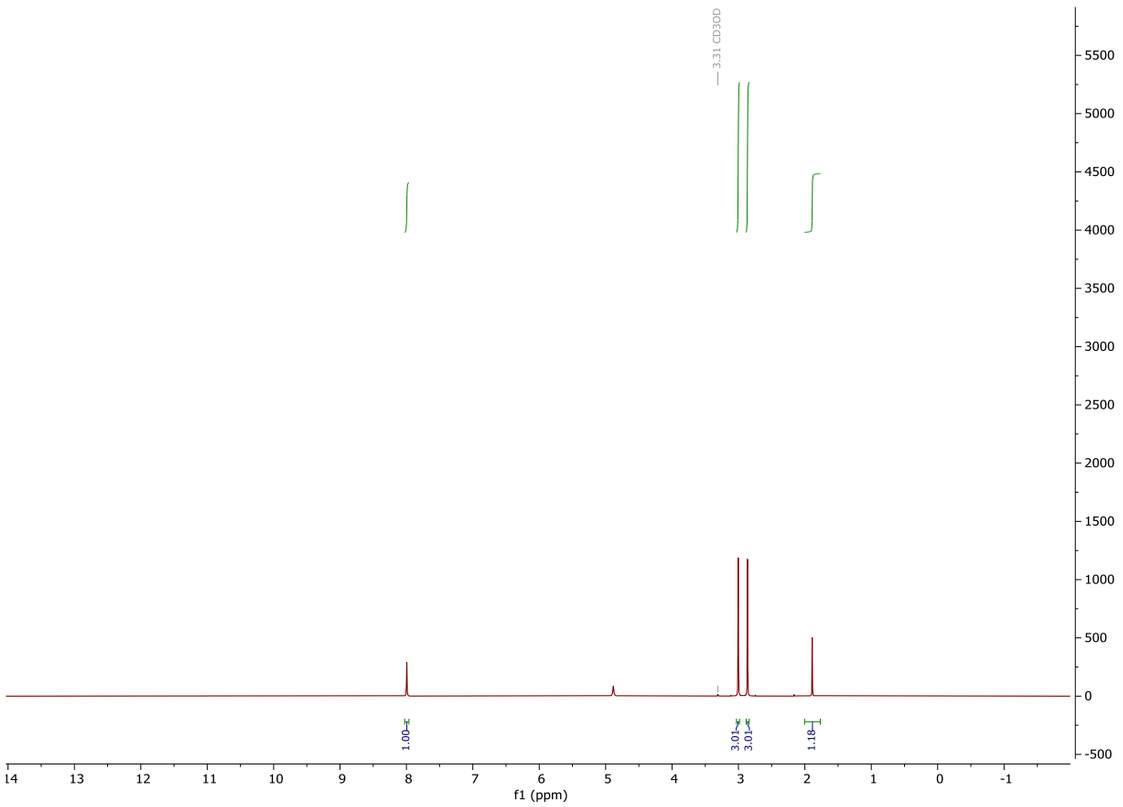

Figure S34: Quantitative ^{1}H Spectrum of product mixture for table S3, entry 3 in CD_3OD.

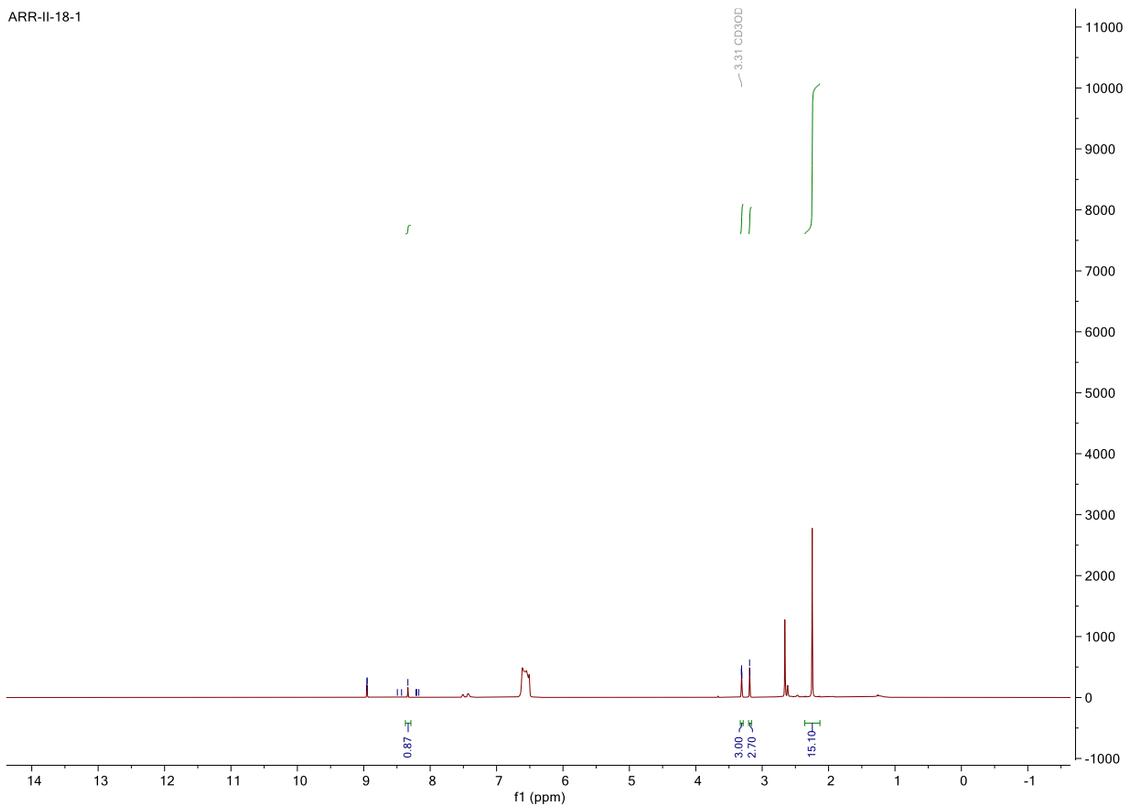

Figure S35: Quantitative ^{1}H Spectrum of product mixture for table S3, entry 4 in CD_3OD.

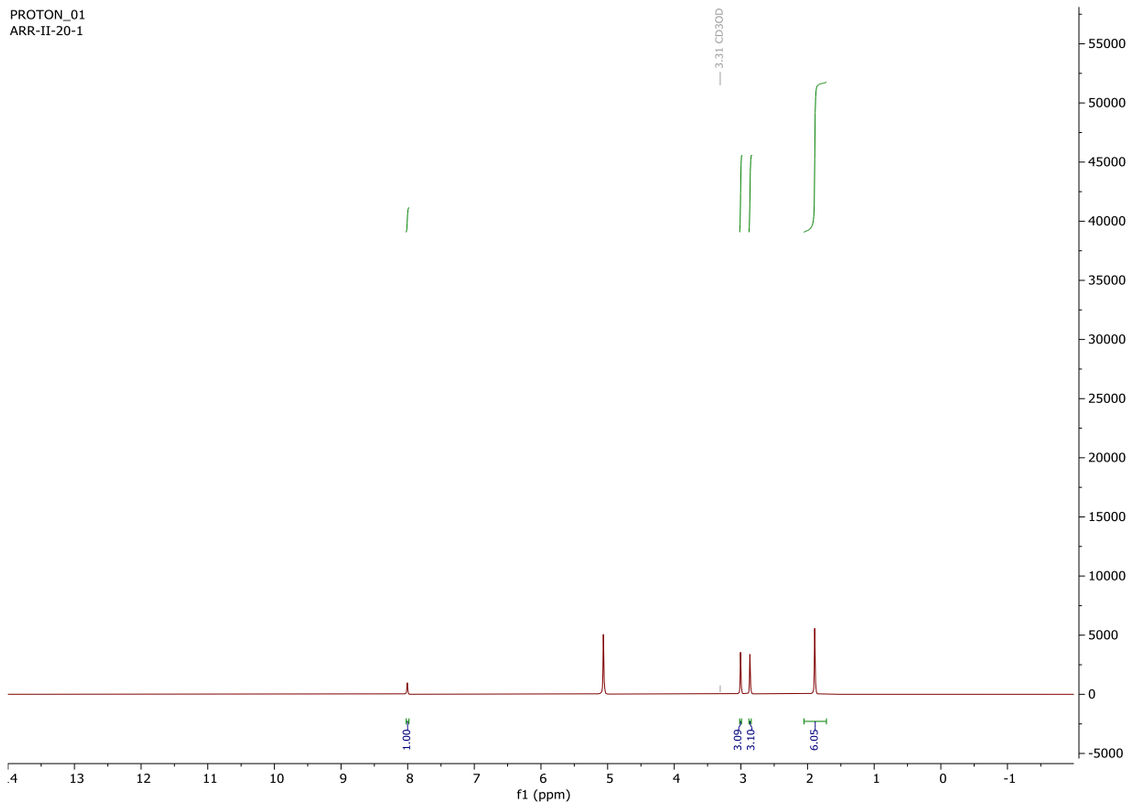

Figure S36: Quantitative ^{1}H Spectrum of product mixture for table S3, entry 5 in CD_3OD.

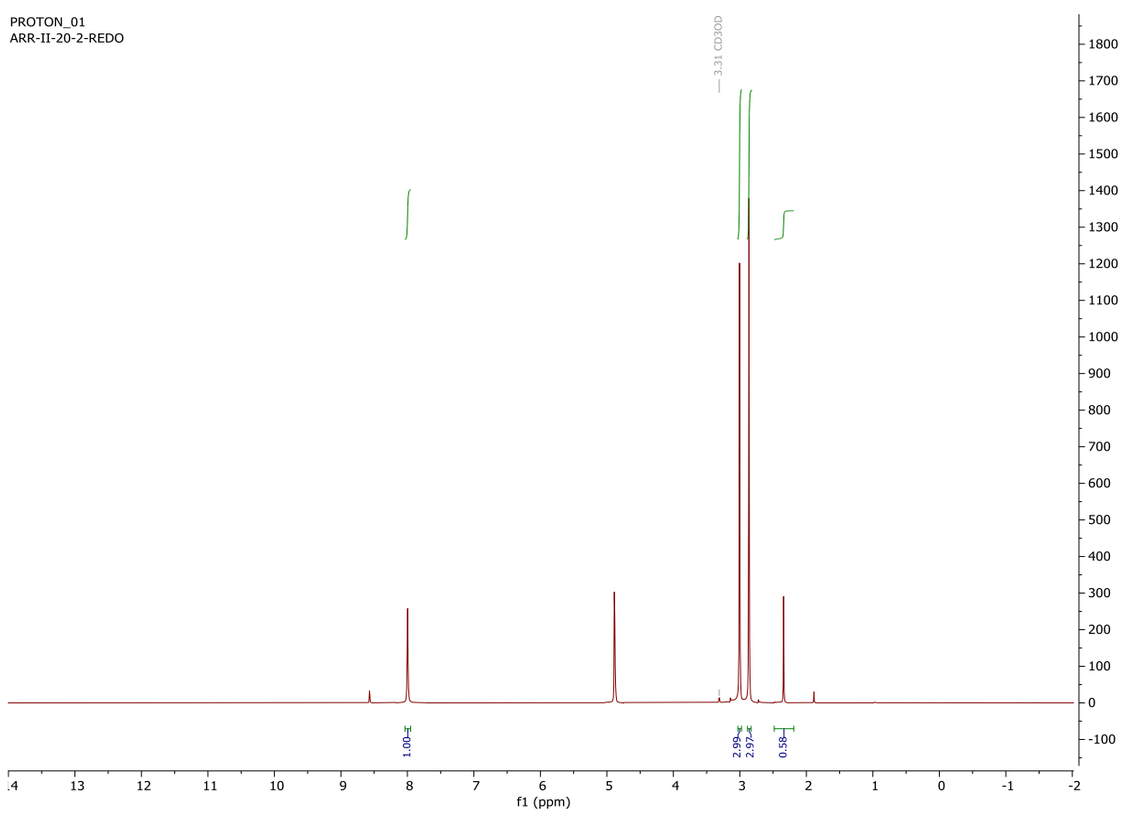

Figure S37: Quantitative ^{1}H Spectrum of product mixture for table S3, entry 6 in CD_3OD.

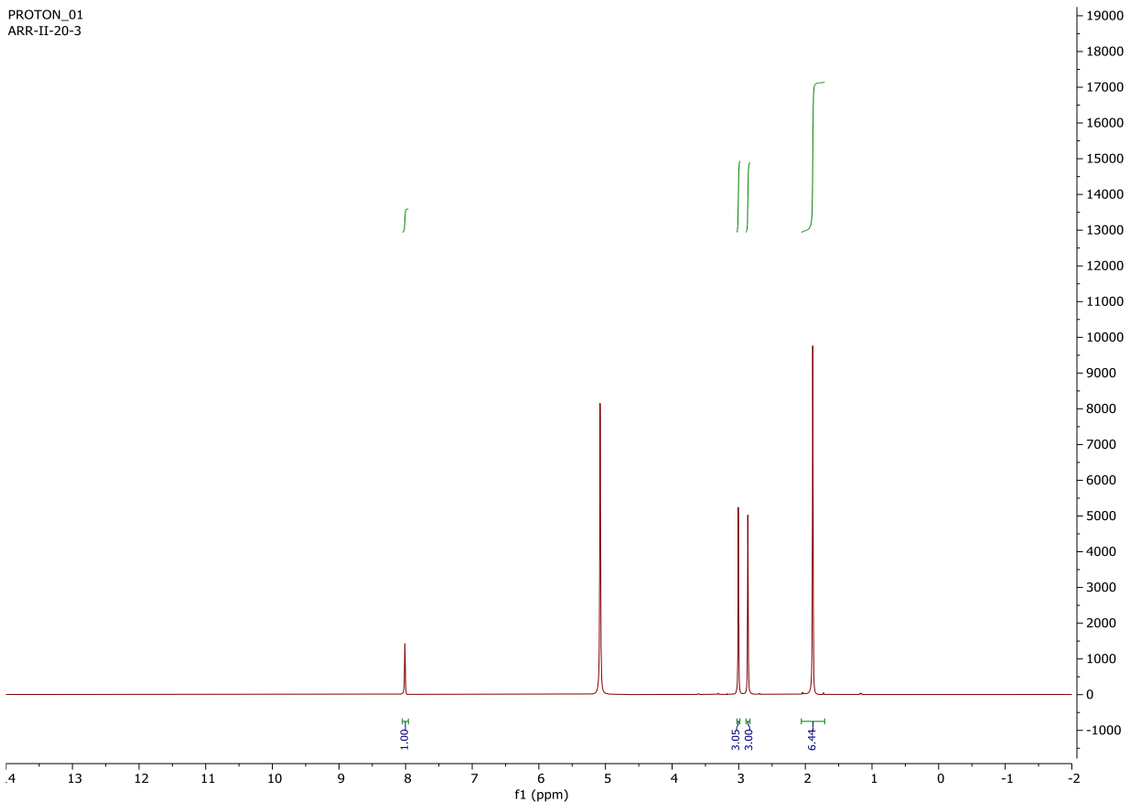

Figure S38: Quantitative ^{1}H Spectrum of product mixture for table S3, entry 7 in CD_3OD.

Large Scale Reaction Utilizing Catalyst 10

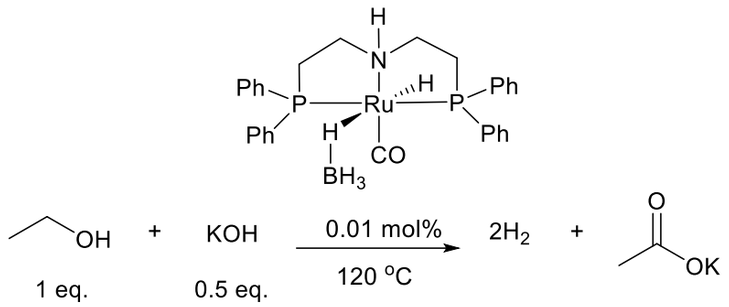

In a nitrogen filled glovebox, of potassium hydroxide (6.40 g, 98 mmol) was weighed out in a 250 mL round bottom flask with **10** (11.3 mg, 0.01 mol%, 19.3 μmol) and a stir bar. To this were added toluene (100 mL, distilled from benzophenone ketyl) and ethanol (200 proof, 9.2 g, 11.66 mL, 200 mol). The resulting solution was brought out of the glovebox, attached to a condenser, sealed with a septum, and brought to reflux in a 120 ˚C oil bath. Gas production was monitored by water eudiometry. Once gas evolution ceased (ca. 155 hrs), the flask was removed from the condenser under inert gas flow, sealed, and returned to the glovebox, where the solids were filtered and washed with minimal toluene. The solid was added back to the round bottom flask and dried under vacuum after which a quantitative NMR was prepared using CD_3OD (1 mL) and DMF (82 mg, 1.12 mmol) as an internal standard (Table S4, entry 1). After NMR, the product was dried on a rotary evaporator under reduced pressure and diluted in deionized water (50 mL); this was back titrated with dilute hydrochloric acid (0.1996 M) and sodium hydroxide (0.2005 M) solutions. The resulting toluene solution from filtration was added to a clean, dry 250 mL round bottom flask, recharged with more potassium hydroxide (6.40 g, 98.0 mmol) and ethanol (200 proof, 9.20 g, 11.7 mL, 200 mmol) and was rerun (entry 2). This was repeated a third time (entry 3).

Table S4: Results of Large-Scale Reactions of 10

Entry	Scale (g)	EtOH (eq)	KOH (eq)	Temp (°C)	Acetate (%)	Carboxylates (mol%)[b]	Total TON
1	10	1	0.5	120	30	30	4646
2	10	1	0.5	120	20	43	8187
3	10	1	0.5	120	ND[a]	36	55,000

[a] Not determined. [b] Molar percent carboxylates determined by titration.

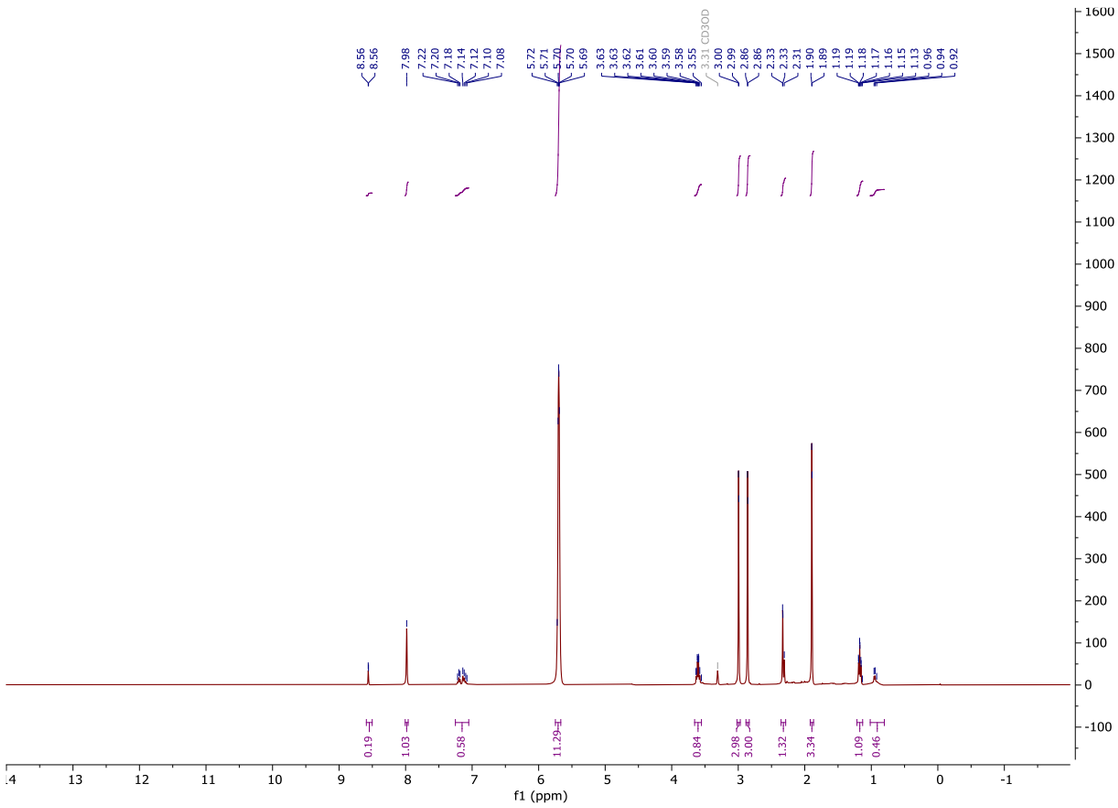

Figure S39: Quantitative ^{1}H spectrum of table S4, entry 1 product mixture in CD_3OD.

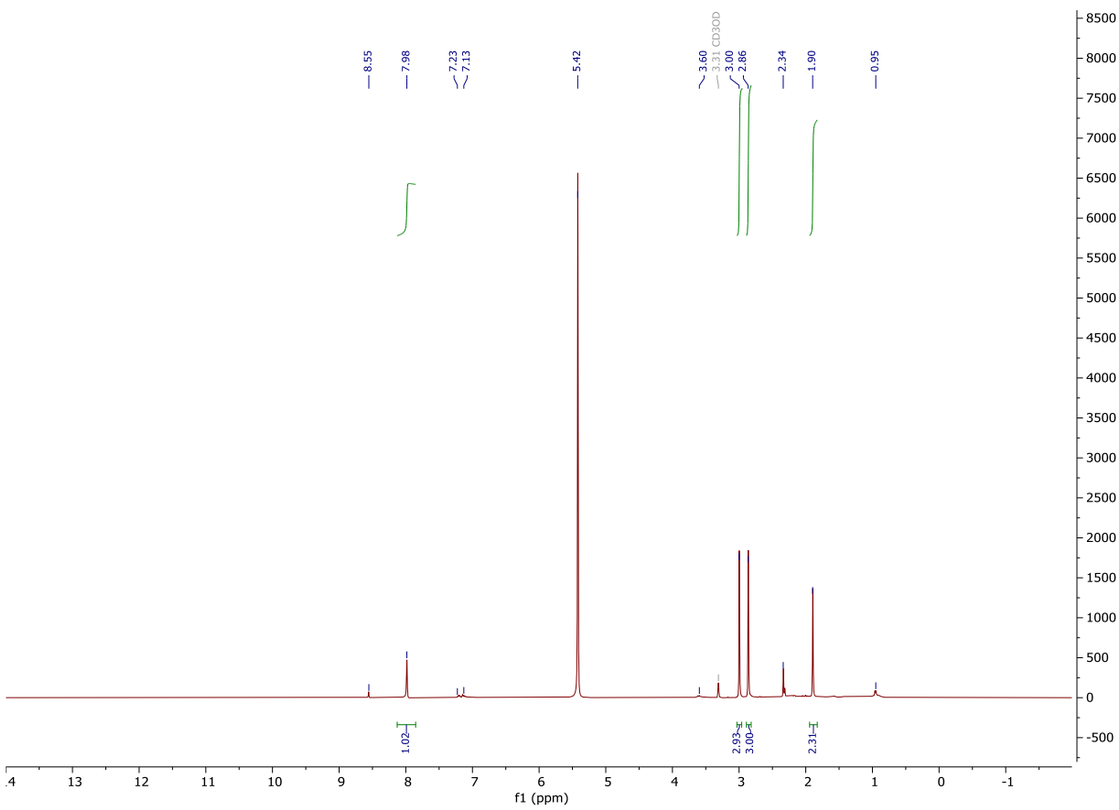

Figure S40: Quantitative ^{1}H spectrum of table S4, entry 2 product mixture in CD_3OD.

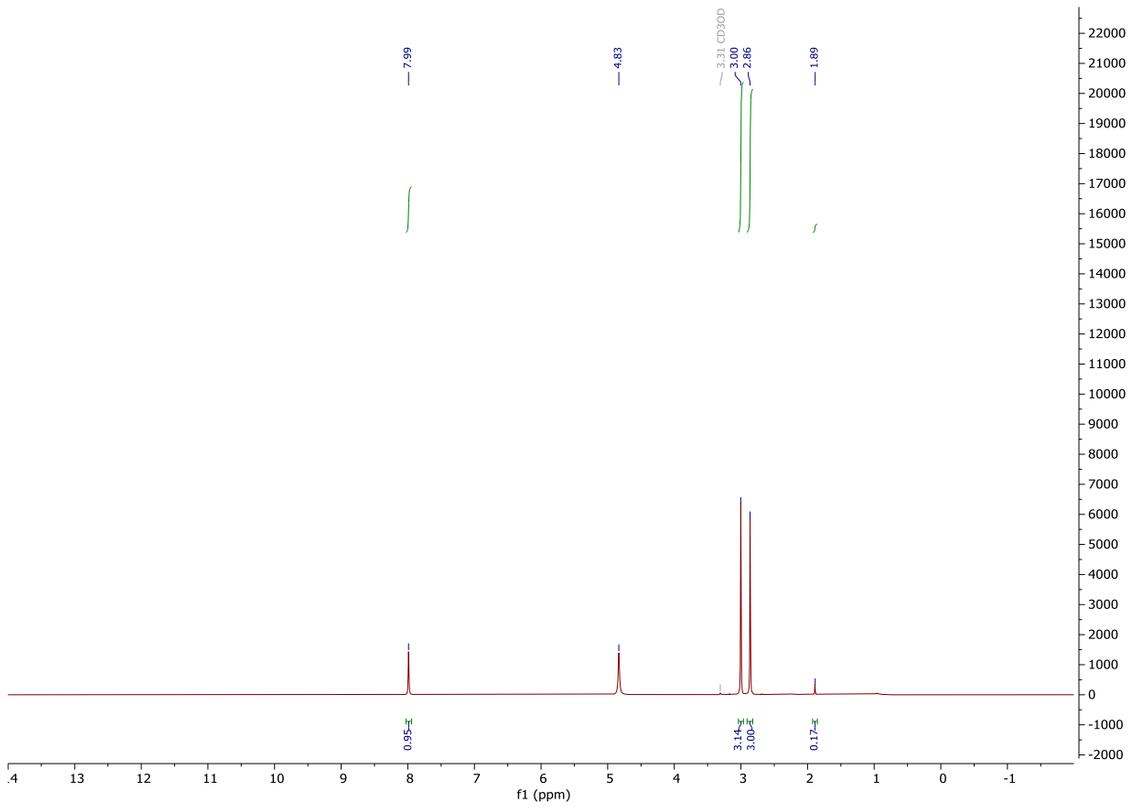

Figure S41: Quantitative ^{1}H spectrum of table S4, entry 3 product mixture in CD_3OD.

TON During Table S4, Entry 3 Utilizing Catalyst 10

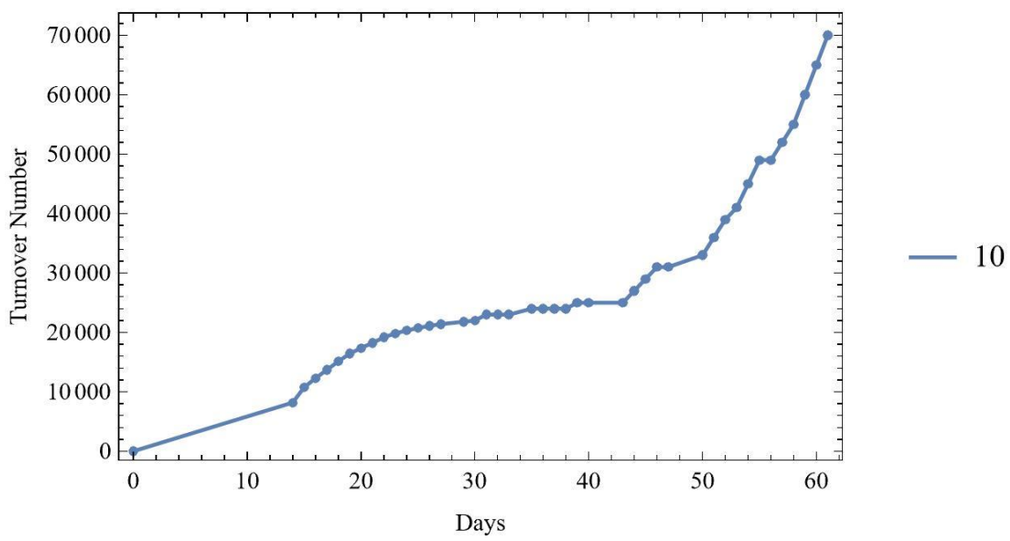

Figure S42: TON of table S4, entry 3 over 60 days.

Large Scale Reaction Utilizing Catalyst 1

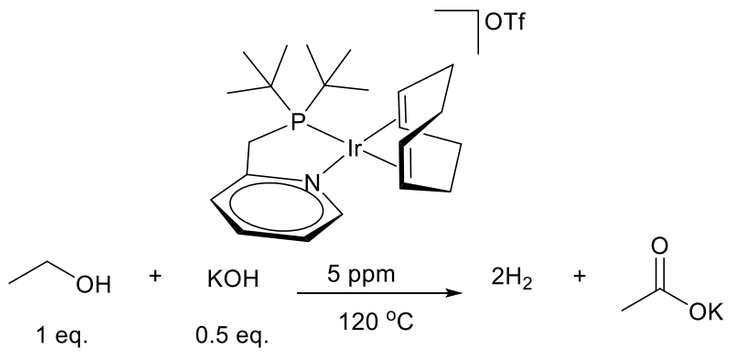

In a nitrogen filled glovebox, of potassium hydroxide (6.40 g, 98.0 mmol) was weighed out in a 250 mL round bottom flask with **1** (0.657 mg, 5 ppm, 0.96 μmol) and a stir bar. To this were added toluene (100 mL, distilled from benzophenone ketyl) and ethanol (200 proof, 9.20 g, 11.7 mL, 200 mmol). The resulting solution was brought out of the glovebox, attached to a condenser, sealed with a septum, and brought to reflux in a 120 ˚C oil bath. Gas production was monitored by water eudiometry. Once gas evolution ceased (ca. 88 days), the flask was removed from the condenser under inert gas flow, sealed, and returned to the glovebox, where the solids were filtered and washed with minimal toluene. The solid was added back to the round bottom flask and removed from the glovebox where it was diluted in deionized water and extracted with dichloromethane. Both phases were dried on a rotary evaporator under reduced pressure; the organic layer was diluted in $CDCl_3$ (0.7 mL), and NMR was taken. The resulting solid after drying from the aqueous phases was diluted in deionized water (50 mL) and subsequently back titrated with dilute hydrochloric acid (0.1885 M) and sodium hydroxide (0.192 M) solutions.

Table S5: Result of Large-Scale Reaction Utilizing 1

Entry	Scale (g)	EtOH (eq)	KOH (eq)	Temp (°C)	Acetate (%)	Carboxylates (mol%)[b]	Total TON
1	10	1	0.5	120	ND	84	168,000

[a] Not determined. [b] Molar percent carboxylates determined by titration.

^{1}H NMR Spectrum of a Large-Scale Reaction Using Catalyst 1

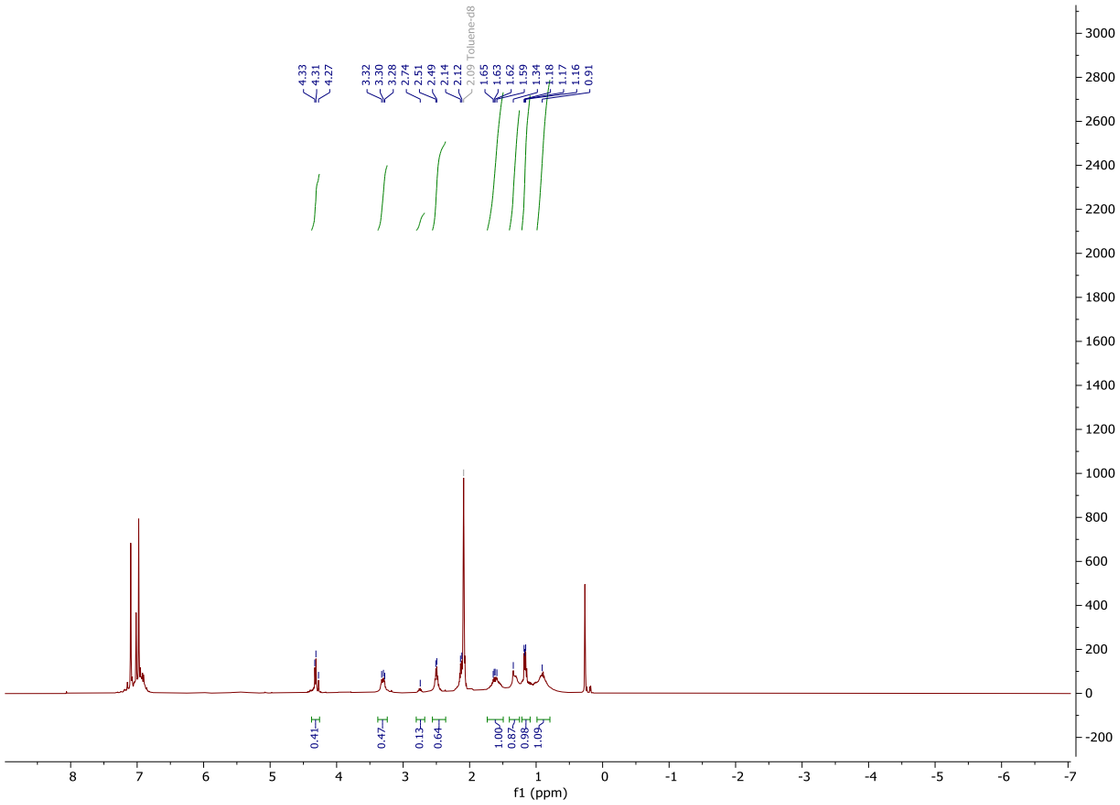

Figure S43: ^{1}H spectrum of organics from table S5, entry 1 in toluene-d_8.

TON During Large Scale Reaction Using Catalyst 1

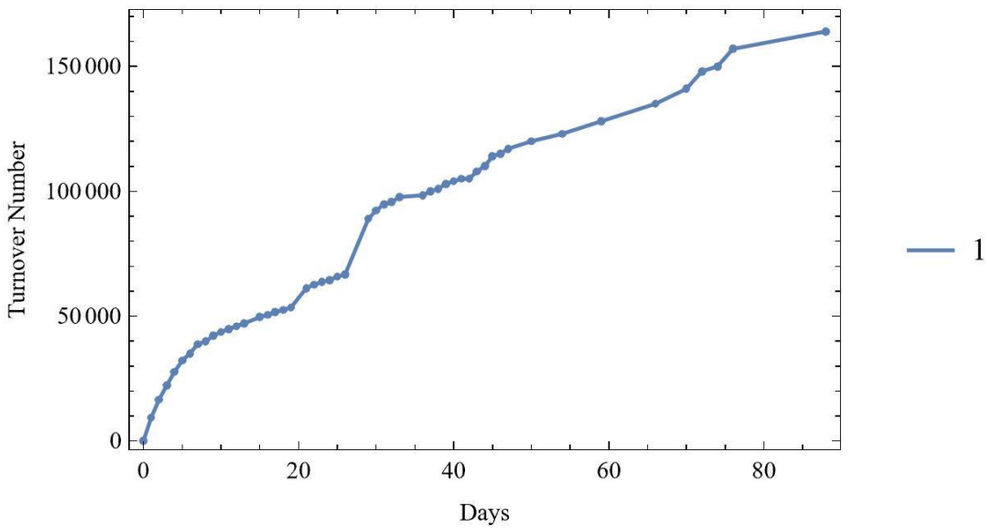

Figure S44: TON over 88 days.

Large Scale Reaction Utilizing Catalyst 5

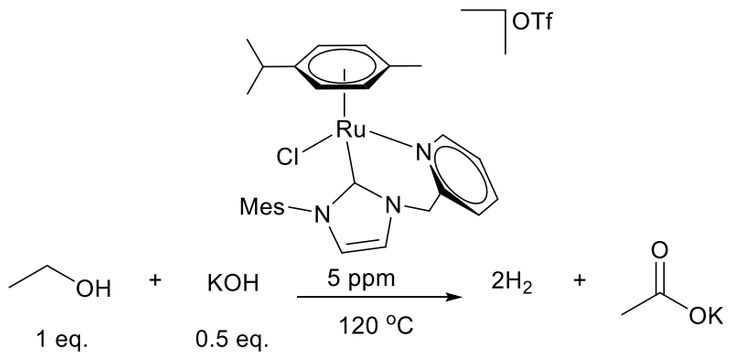

In a nitrogen filled glovebox, of potassium hydroxide (4.70 g, 72.0 mmol) was weighed out in a 100 mL round bottom flask with **5** (0.03 mg, 5 ppm, 0.07 μmol) and a stir bar. To this were added toluene (30 mL, distilled from benzophenone ketyl) and ethanol (200 proof, 4.70 g, 1.17 mL, 100 mmol). The resulting solution was brought out of the glovebox, attached to a condenser, sealed with a septum, and brought to reflux in a 120 ˚C oil bath. Gas production was monitored by water eudiometry. Once gas evolution ceased (ca. 21 days), the flask was removed from the condenser under inert gas flow, sealed, and returned to the glovebox, where the solids were filtered and washed with minimal toluene. The solid was added back to the round bottom flask, removed from the glovebox, dried on a rotary evaporator under reduced pressure after which a quantitative NMR was prepared using CD_3OD (1 mL) and DMF (237 mg, 3.24 mmol) as an internal standard (Table S6, entry 1). After NMR, the product was dried on a rotary evaporator under reduced pressure and the resulting solid was diluted in deionized water (50 mL); this was back titrated with dilute hydrochloric acid (0.1885 M) and sodium hydroxide (0.192 M) solutions.

Table S6: Results of Large-Scale Reaction of 5

Entry	Scale (g)	EtOH (eq)	KOH (eq)	Temp (°C)	Acetate (%)	Carboxylates (mol%)[b]	Total TON
1	10	1	0.5	120	ND	55%	168,000

[a] Not determined. [b] Molar percent carboxylates determined by titration.

^{1}H NMR Spectrum of a Large-Scale Reaction Utilizing Catalyst 5

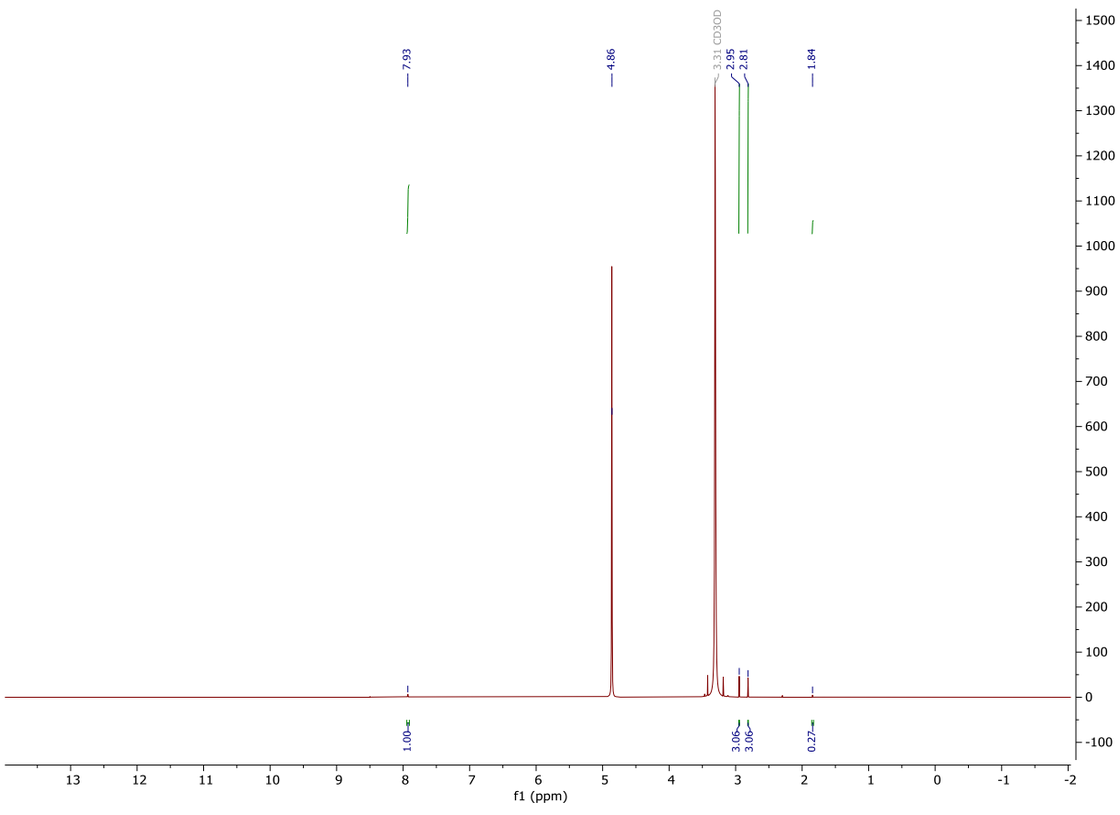

Figure S45: ^{1}H Spectrum of product mixture in CD_3OD.

TON During Large Scale Reaction Using Catalyst 5

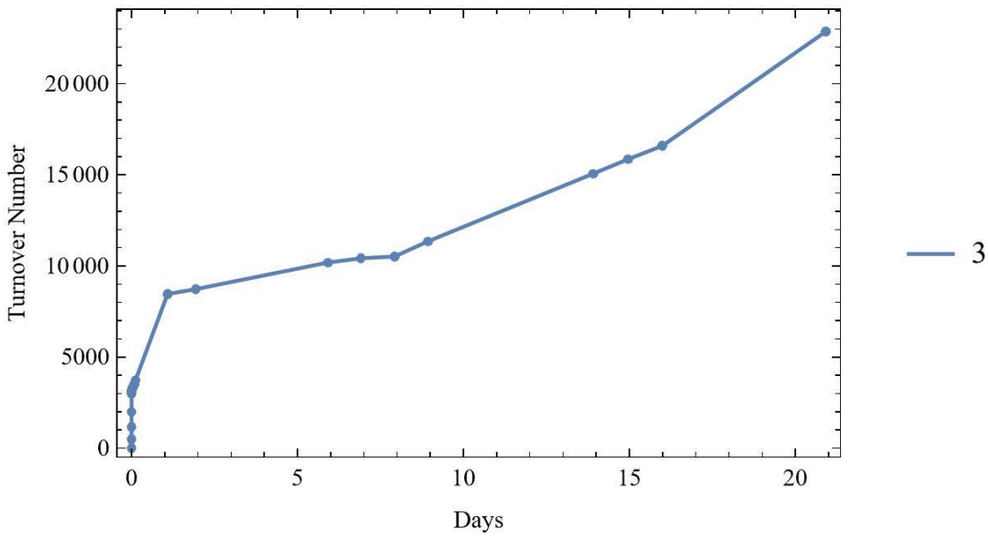

Figure S46: TON over 21 days.

Self-Pressurizing Optimization Reactions

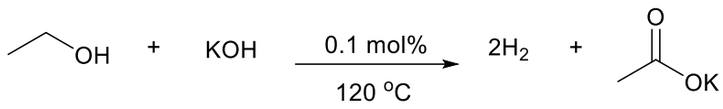

Several reactions (Table S7) were done with varying amounts of reagents, solvent, or additives. In a representative procedure, in a nitrogen filled glovebox, potassium hydroxide (0.5 equiv = 1.84 g, 28.3 mmol), catalyst (**1**, 0.1 mol%, 60 μmol, with respect to ethanol unless otherwise noted), toluene (10 mL, distilled from benzophenone ketyl), and ethanol (200 proof, 2.64 g, 3.34 mL, 57.0 mmol) were added to a 125 mL Parr high pressure reactor with an analog pressure gauge. Each reaction was sealed in the Parr reactor and heated to a bath temperature of 120 °C. Gas production was measured by monitoring pressure readings from the reactor. After 42 hours, each reaction was quantitatively transferred to a 50 mL round bottom flask (rinsing with deionized water) and dried on a rotary evaporator under reduced pressure. Quantitative NMR samples were prepared with methanol-d_4 (1 mL) and dimethylformamide (DMF 96.2 mg, 1.32 mmol) and subsequently analyzed by ^{1}H NMR. The remainder of each sample was diluted in 50 mL of deionized water and titrated to determine the molar percentage of acetate in the sample. After NMR, the product was dried on a rotary evaporator under reduced pressure and the resulting residue was diluted in deionized water (50 mL); this was back titrated with dilute hydrochloric acid (0.1967 M) and sodium hydroxide (0.1928 M) solutions.

Table S7: Results of Self-Pressurizing Reaction Optimization

Entry	Cat.	EtOH (eq)	KOH (eq)	Solvent	Time (hrs)	Solvent (mL)	Final Pressure (Bar)	Acetate (%)	Carboxylates (mol%)[b]
1	**1**	1	1	Toluene	45	10	8	64	67
2	**1**	1	0.5	Toluene	25	10	6	28	50
3	**5**	1	1	Toluene	47.1	10	9	66	70
4	**10**	1	1	Toluene	45	10	9	82	74
5	**10**	1	0.5	Toluene	45	10	14	95	98
6	**10**	0.5	1	Toluene	48	10	10	57	47
7	**10**	1	0.17	Neat	68	Neat	26	100	97

[a] Catalyst loading based on moles of ethanol. [b] Molar percent acetate determined by titration. Calculated to pressurize to 30 bar.

^{1}H NMR Spectra of Self-Pressurizing Optimization

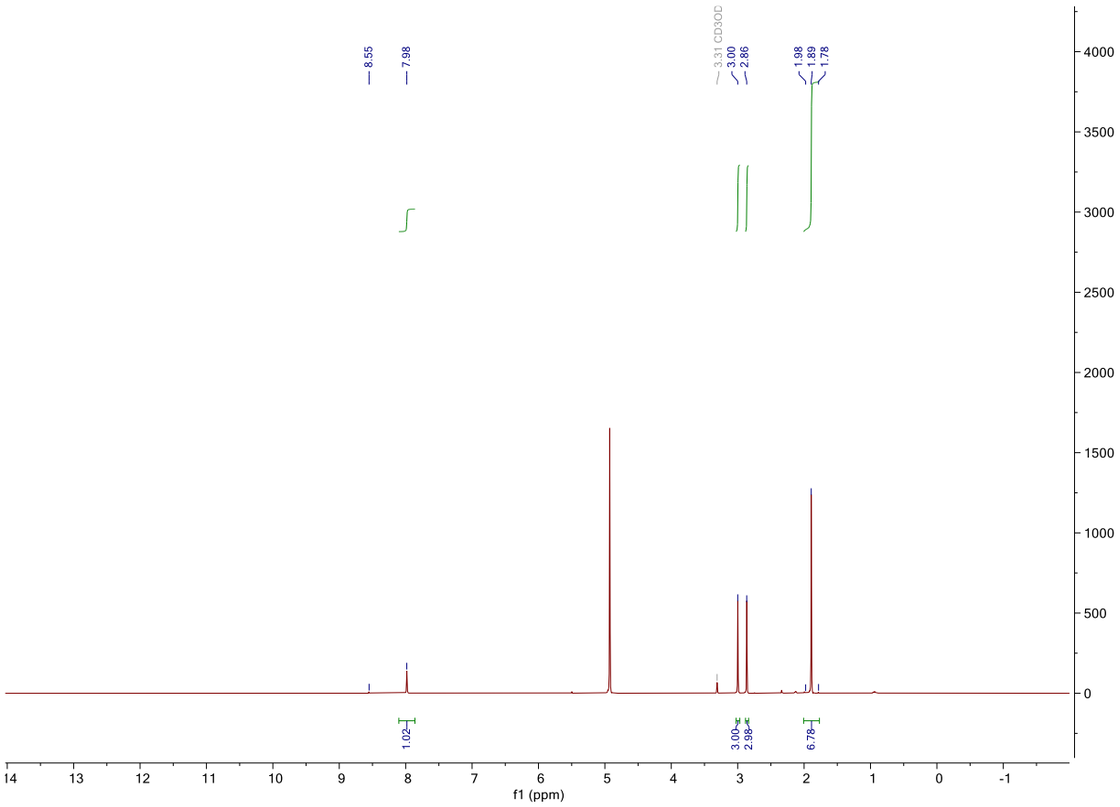

Figure S47: Quantitative ^{1}H spectrum of the table S7, entry 1 reaction mixture in CD_3OD.

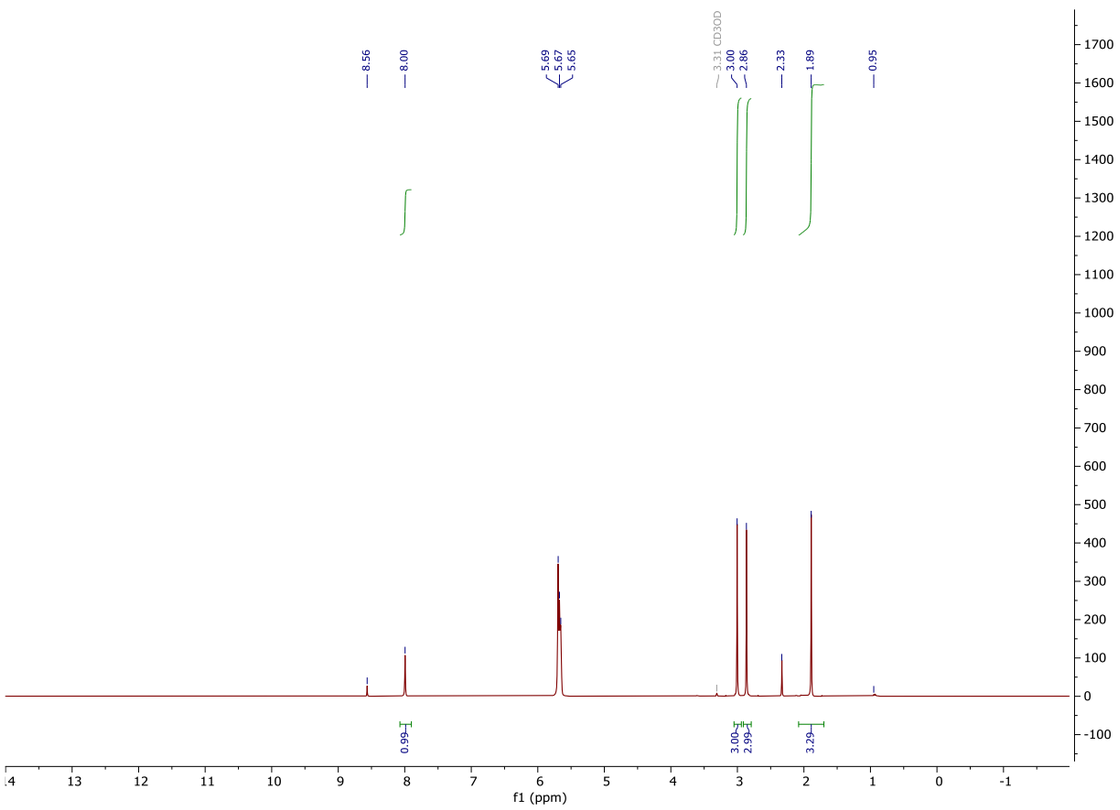

Figure S48: Quantitative ^{1}H spectrum of the table S7, entry 2 reaction mixture in CD_3OD.

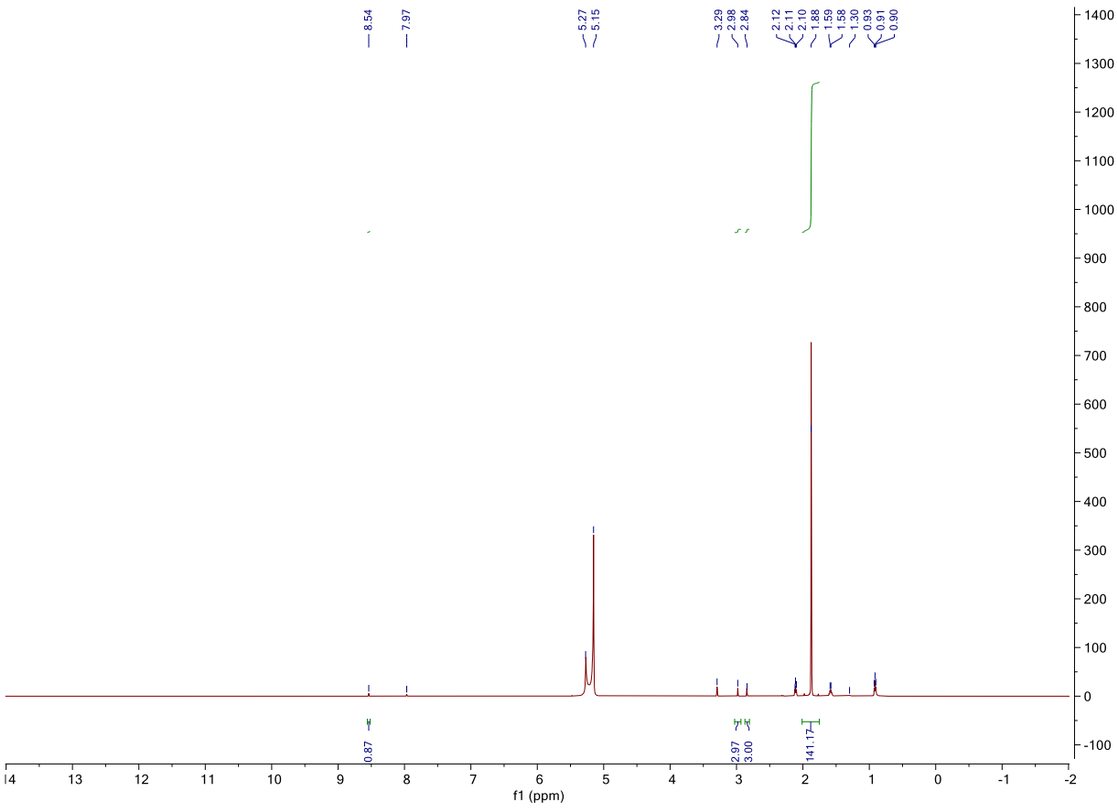

Figure S49: Quantitative ^{1}H spectrum of the table S7, entry 4 reaction mixture in CD_3OD.

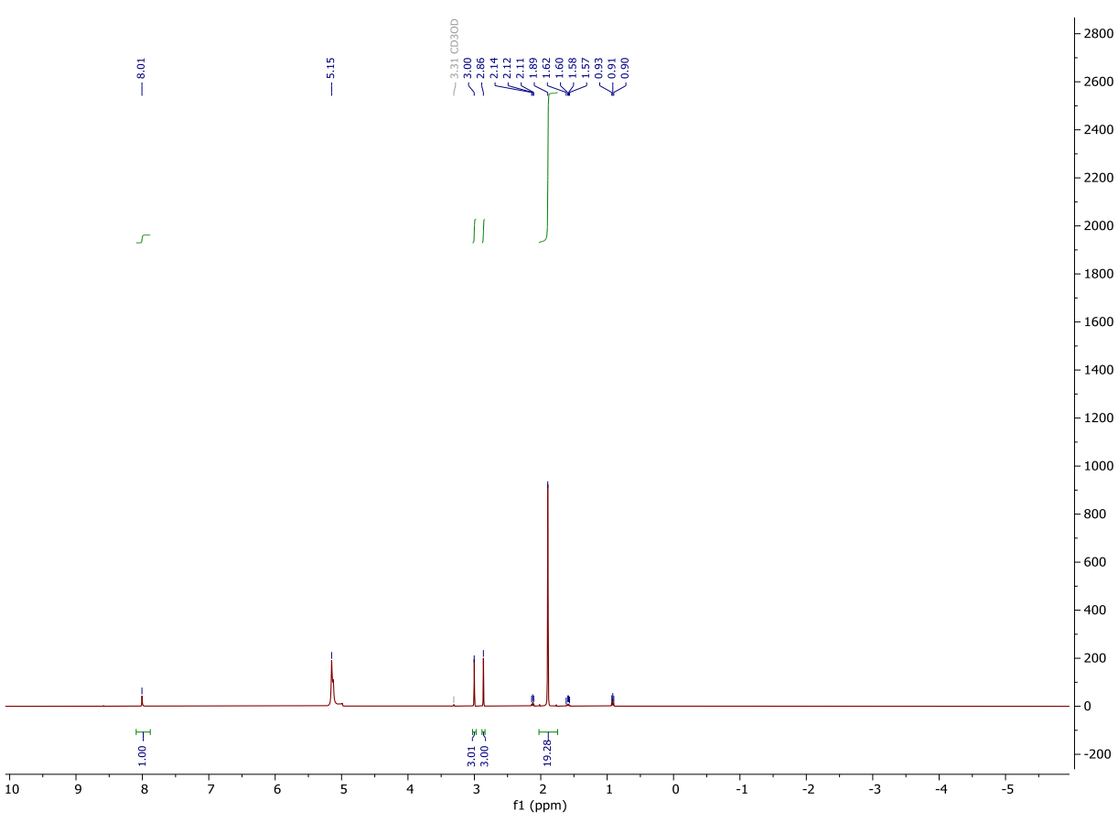

Figure S50: Quantitative ^{1}H spectrum of the table S7, entry 5 reaction mixture in CD_3OD.

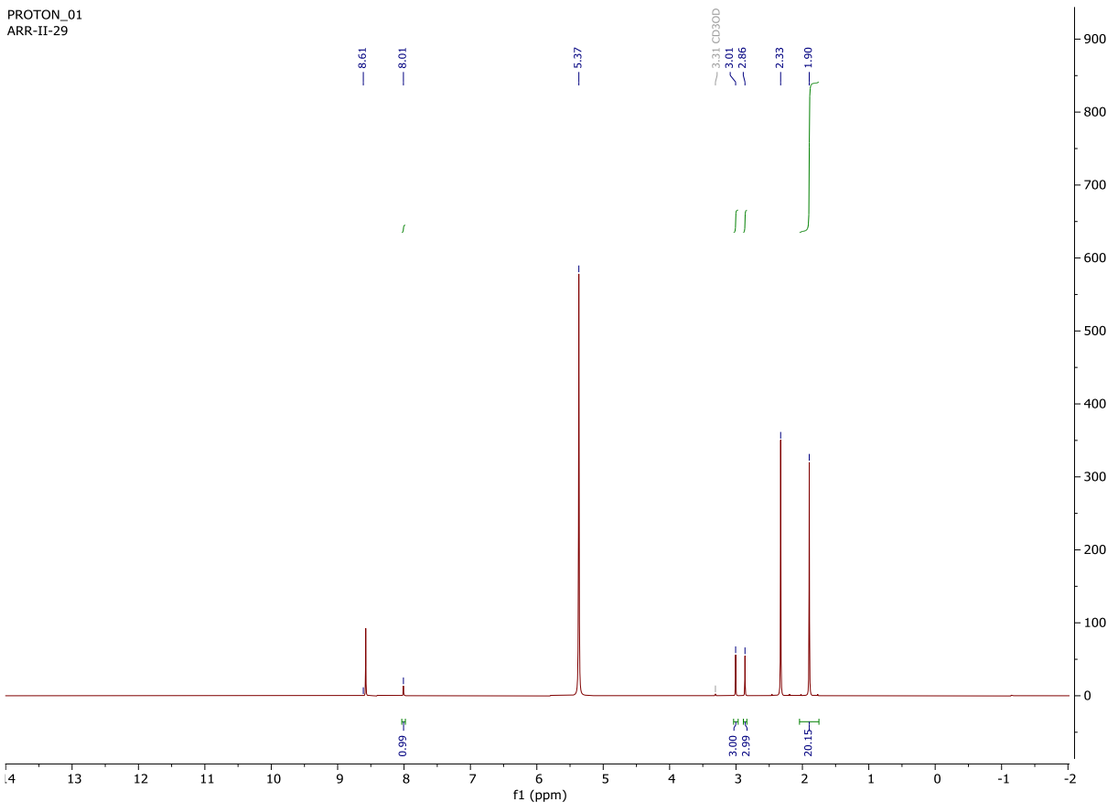

Figure S51: Quantitative ^{1}H spectrum of the table S7, entry 6 reaction mixture in CD_3OD.

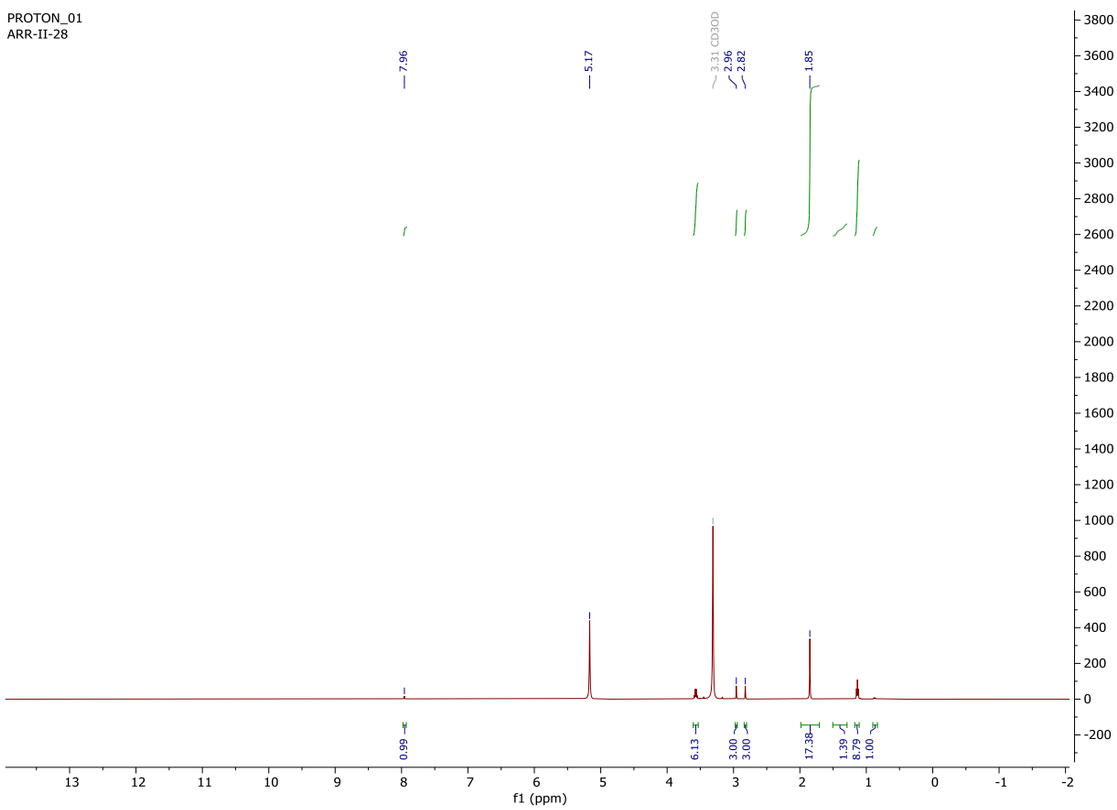

Figure S52: Quantitative ^{1}H spectrum of the table S7, entry 7 reaction mixture in CD_3OD.

Other Additives Reactions

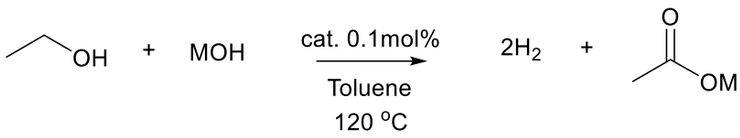

In a nitrogen filled glovebox, ethanol (0.92 g, 20 mmol), base (10 mmol hydroxide equivalents), and toluene (10 mL, distilled from benzophenone ketyl) were combined with **10** (11.7 mg, 20.0 μmol) in a 25 mL round bottom flask. Outside the glovebox, each flask was added a reflux condenser outfitted with a septum, refluxed for 42 hours at 120 °C. Gas production was measured by water eudiometry, attached through a needle. After 42 hours, volatiles removed using a rotary evaporator and quantitative NMR was taken using dimethyl formamide (67.1 mg, 0.918 mmol) as an internal standard in CD_3OD (1 mL). After NMR analysis, volatiles were again removed using a rotary evaporator under reduced pressure and the resulting solid was diluted in water (50 mL, deionized) and titrated using dilute hydrochloric acid (0.1967 M) and sodium hydroxide (0.1928 M) solutions.

Table S8: Results of Other Additive Reactions

Entry	Cat.	EtOH (eq)	MOH (eq)	Base	Solvent (mL)	Acetate (%)	Carboxylates (mol%)[b]
1	**10**	1	1	$Ca(OH)_2$	10	2	12
2	**10**	1	0.5	NaOH	10	83	98

[a] Catalyst loading based on moles of ethanol. [b] Molar percent acetate determined by titration. All at ambient pressure.

NMR Spectra of Other Additive Reactions

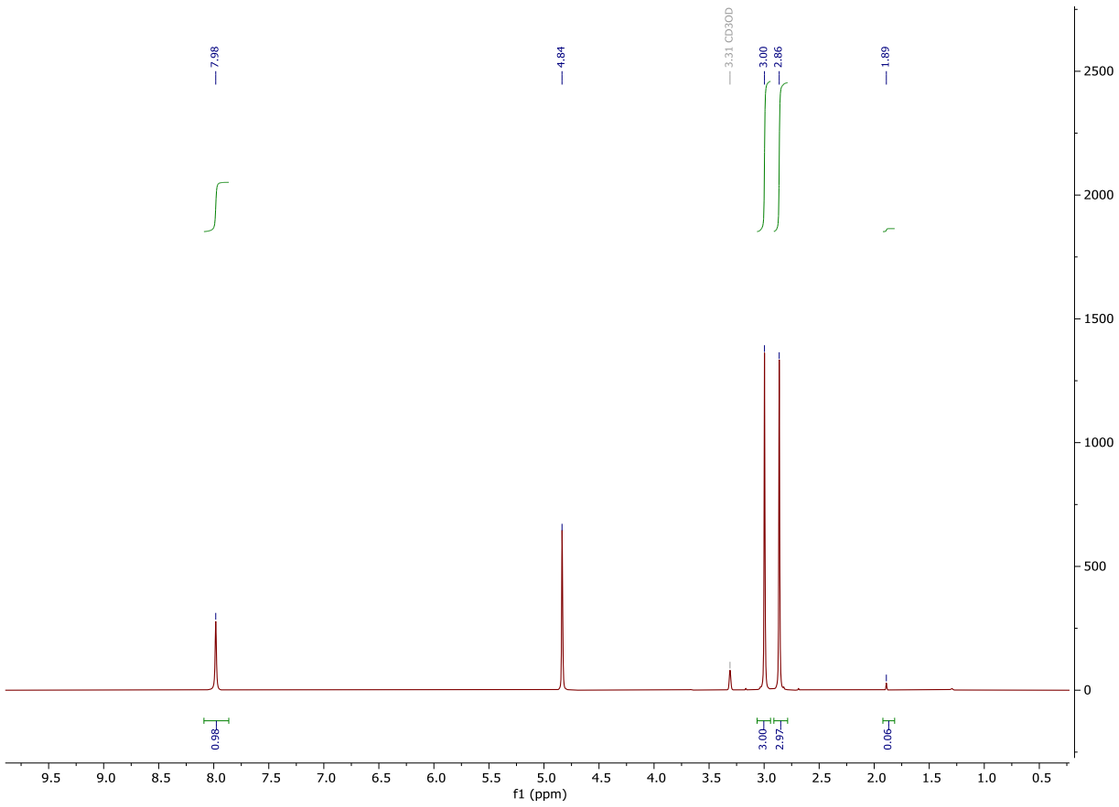

Figure S53: Quantitative ^{1}H spectrum of the table S8, entry 1 reaction mixture in CD_3OD.

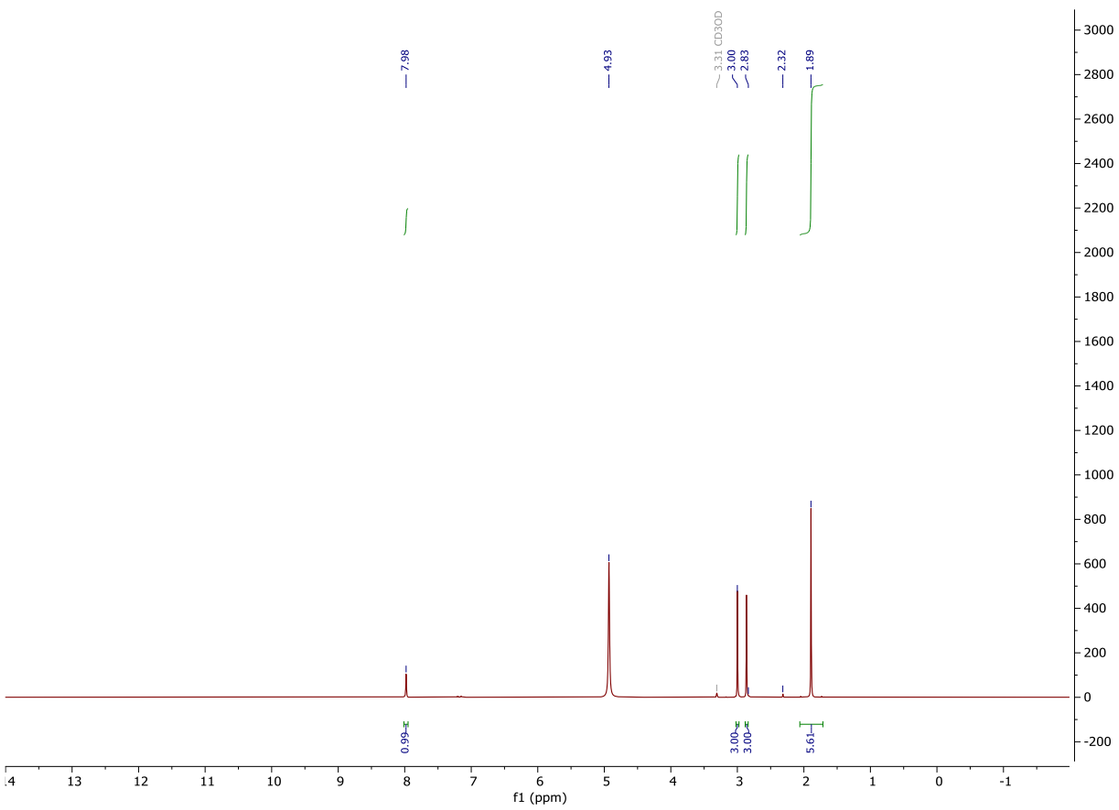

Figure S54: Quantitative ^{1}H spectrum of the table S8, entry 2 reaction mixture in CD_3OD.

Acetate Hydrogenation Reactions

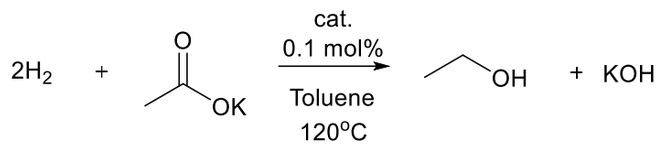

In a nitrogen filled glovebox, potassium acetate (2.94 g, 30.0 mmol), catalyst (**8** or **10**, 0.1 mol% with respect to acetate, entry 1: 17.6 mg, 30.0 μmol), and toluene (10 mL, distilled from benzophenone ketyl) were added to a 125 mL Parr high pressure reactor with an analog pressure gauge. Each reaction was sealed in the Parr reactor and charged with 17 bar of hydrogen pressure. The reactor was then placed in an oil bath temperature at 120 °C. Gas production was measured by monitoring pressure readings from the reactor. After 42 hours, an aliquot of the head space was taken in a gas chromatography sampling bag and run through GCMS. The pH was tested of each reaction, and then each reaction was quantitatively transferred to a 50 mL round bottom flask (rinsing with deionized water) and dried on a rotary evaporator under reduced pressure. Quantitative NMR samples were prepared with methanol-d_6 (1 mL) and dimethylformamide (135 mg, 1.84 mmol) and subsequently analyzed by ^{1}H NMR. After NMR, solvent was removed on a rotary evaporator and resulting residue was diluted in deionized water (50 mL); this was back titrated with dilute hydrochloric acid (0.2239 M) and sodium hydroxide (0.3454 M) solutions.

Table S9: Results of Acetate Hydrogenation Reactions

Entry	Cat.	H_2 Pressure (Bar)	Final Pressure (Bar)[a]	Cat. Loading (mol%)	Acetate (%)[b]	Carboxylates (mol%)[c]
1	**10**	17	10	0.1	100	99
2	**8**	17	17	0.1	100	99

[a] Pressure taken at 25 °C. [b] With respect to acetate with DMF as an internal standard. [c] Determined by titration.

Acetate Hydrogenation NMR Spectra

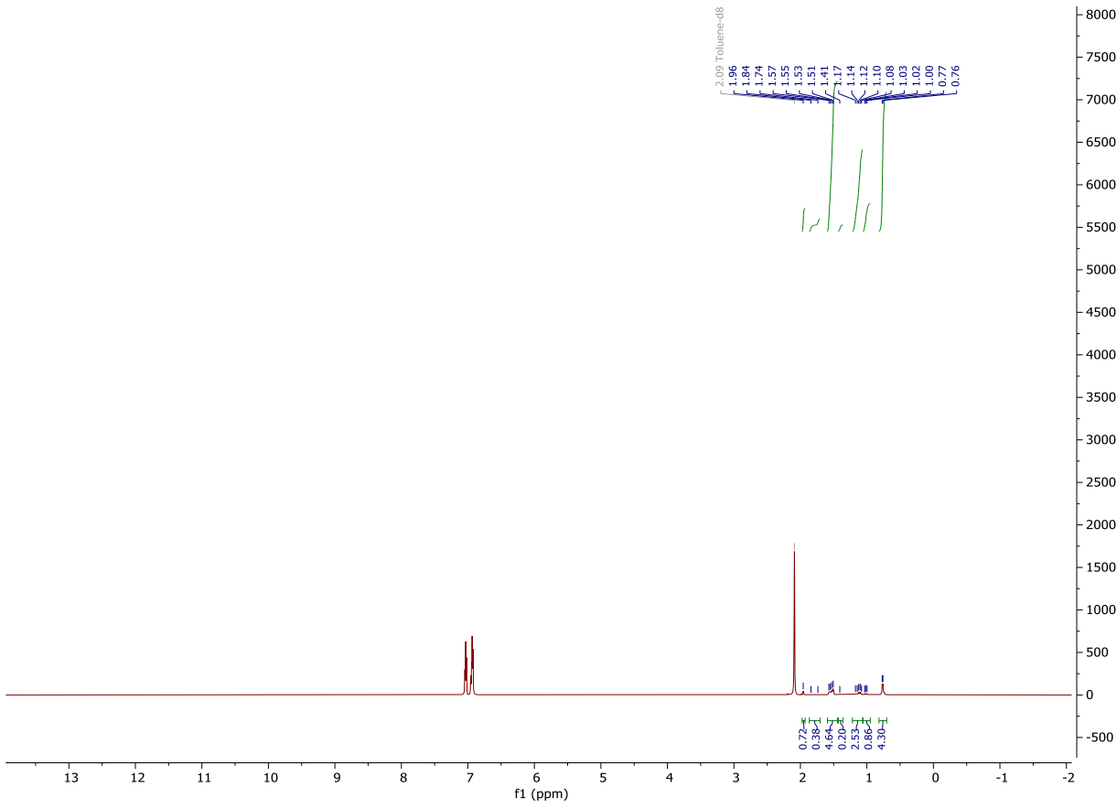

Figure S55: ^{1}H Spectrum of table S9 entry 1 reaction mixture in d_8-toluene. This suggests the hydrogenation of the solvent to methyl cyclohexane. No ethanol is observed.

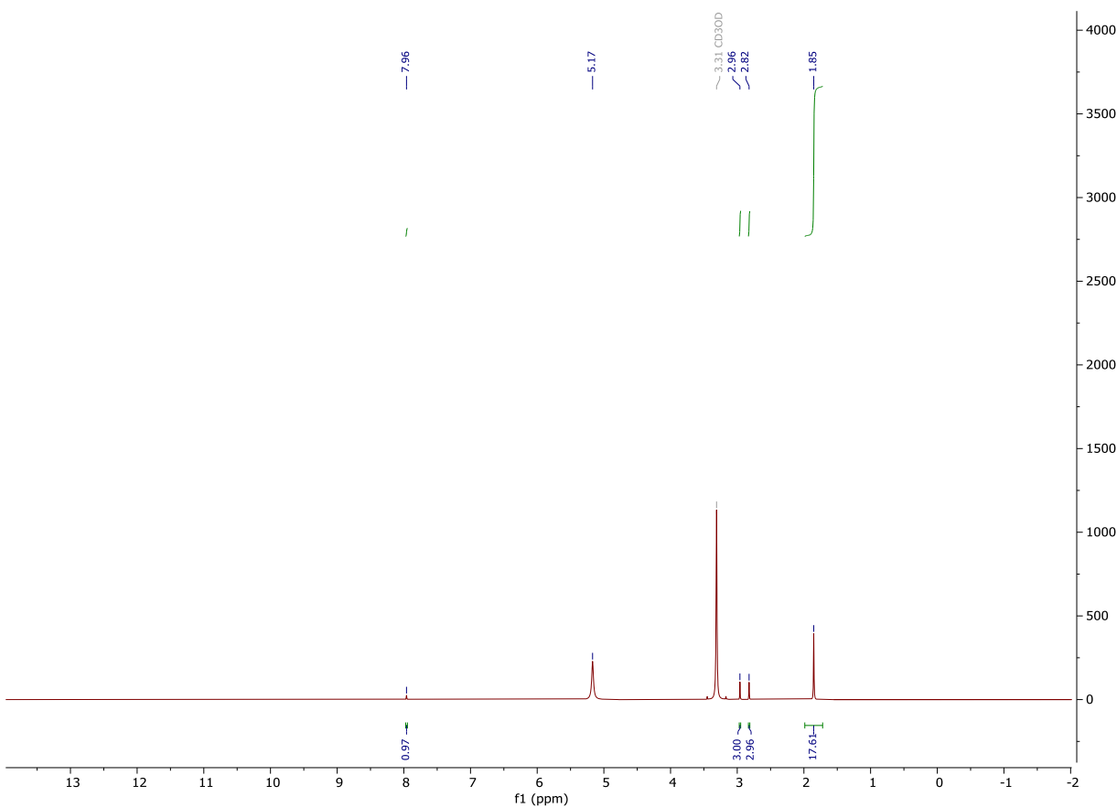

Figure S56: Quantitative ^{1}H Spectrum of table S9 entry 1 product mixture in CD_3OD.

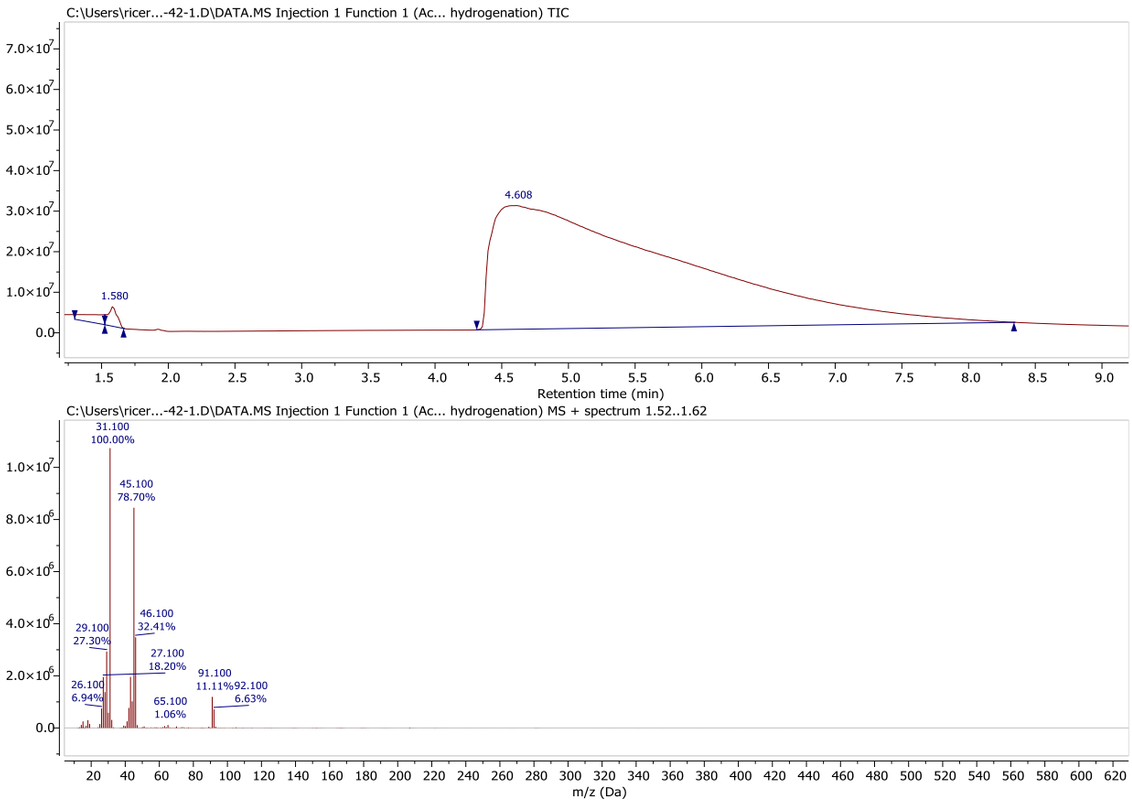

Figure S57: Gas chromatography trace and mass spectrum from GCMS on table S9 entry 1 headspace after reaction. These data suggest some ethanol and some methyl cyclohexane. pH was not strongly alkaline suggesting no KOH.

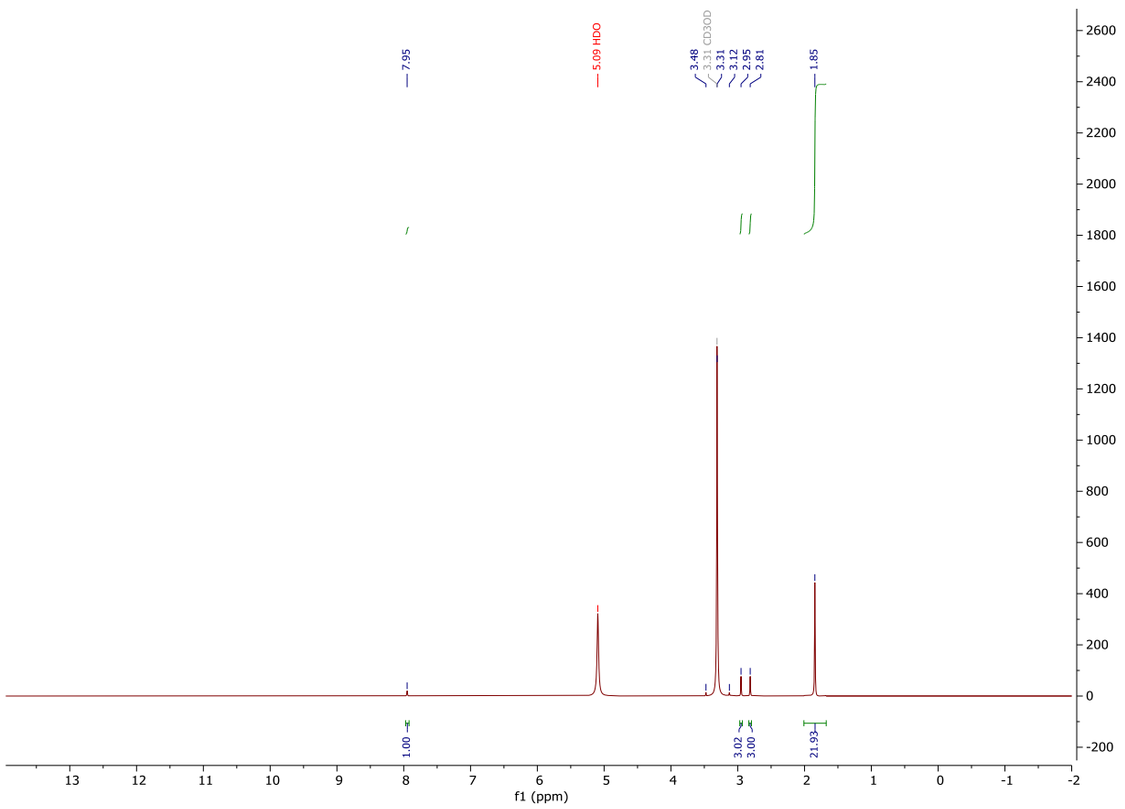

Figure S58: Quantitative ^{1}H Spectrum of table S9 entry 2 reaction mixture in CD_3OD.

Kinetics Experiments

Several reactions (Table S7) were done with varying amounts of reagents, solvent, or additives. In a representative procedure, in a nitrogen filled glovebox, potassium hydroxide (0.50 equiv = 0.64 g, 9.8 mmol), catalyst (**1**, 0.10 mol %, 19 μmol, with respect to ethanol unless otherwise noted), toluene (10 mL, distilled from benzophenone ketyl), and ethanol (200 proof, 1.0 equiv = 0.92 g, 20 mmol) were added to a 25 mL round bottom flask. Each reaction flask was added a reflux condenser outfitted with a septum and each reaction was refluxed at 120 °C (unless otherwise noted) with reaction progress monitored by water eudiometry. After gas production stopped, volatiles removed using a rotary evaporator under reduced pressure. Quantitative NMR samples were prepared by adding methanol-d_4 (700 mL) and dimethylformamide (DMF, 0.100 g, 1.37 mmol) and subsequently analyzed by ^{1}H NMR. After NMR analysis, volatiles were again removed using a rotary evaporator under reduced pressure and the resulting solid was diluted in 50 mL of deionized water and titrated to determine the molar percentage of acetate in the sample.

Table S10: Reaction Conditions for Kinetics Studies

Entry	Cat.	EtOH (eq)	KOH (eq)	Solvent (mL)	Reaction Time (hr)
1	**1**	1	0.5	10	42.8
2	**3**	1	0.5	10	19.25
3	**2**	1	0.5	10	19.25
4	**4**	1	0.5	10	42.8
5	**10**	1	0.5	10	2.5
6 [a]	**10**	1	0.17	Neat	93.9
7	**13**	1	0.5	10	57.55
8	**18**	1	1	10	44.1
9	**19**	1	1	10	45.1
10	**20**	1	1	10	56.2
11	**21**	1	1	10	46
12	**22**	1	1	10	46
13	**23**	1	1	10	57.92

[a] Catalyst loading based on moles of KOH; run at 80 °C.

Kinetics Graphs

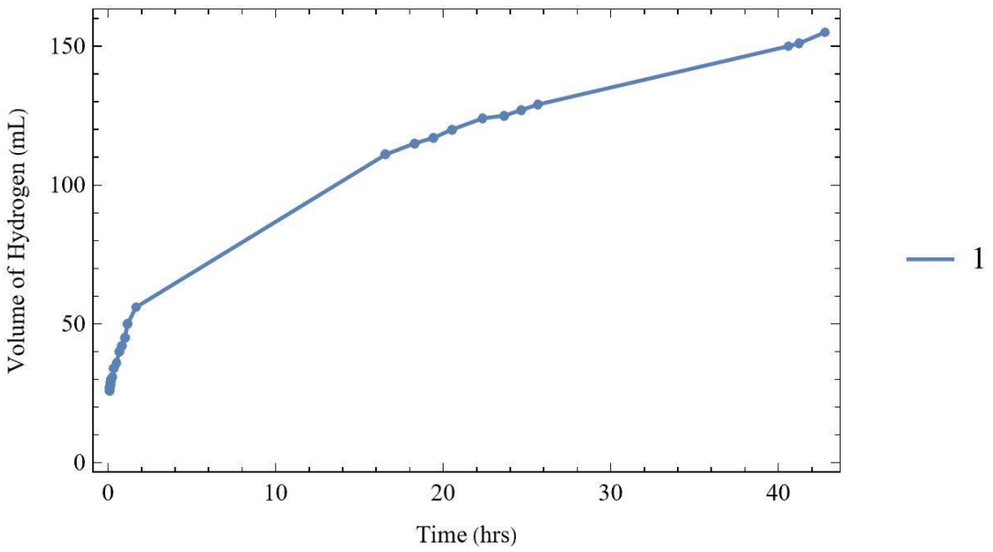

Figure S59: Kinetics for **1** (entry 1)

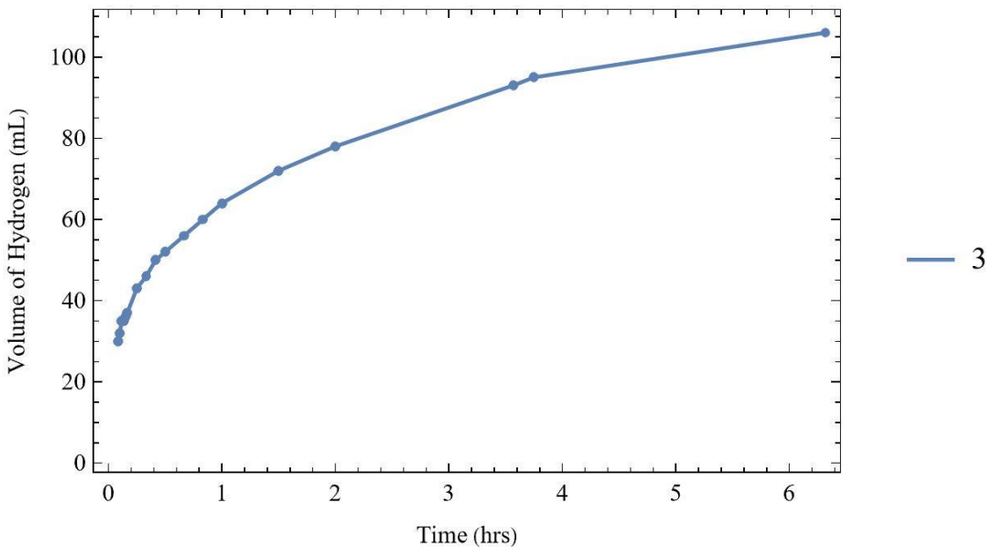

Figure S60: Kinetics for **3** (entry 2)

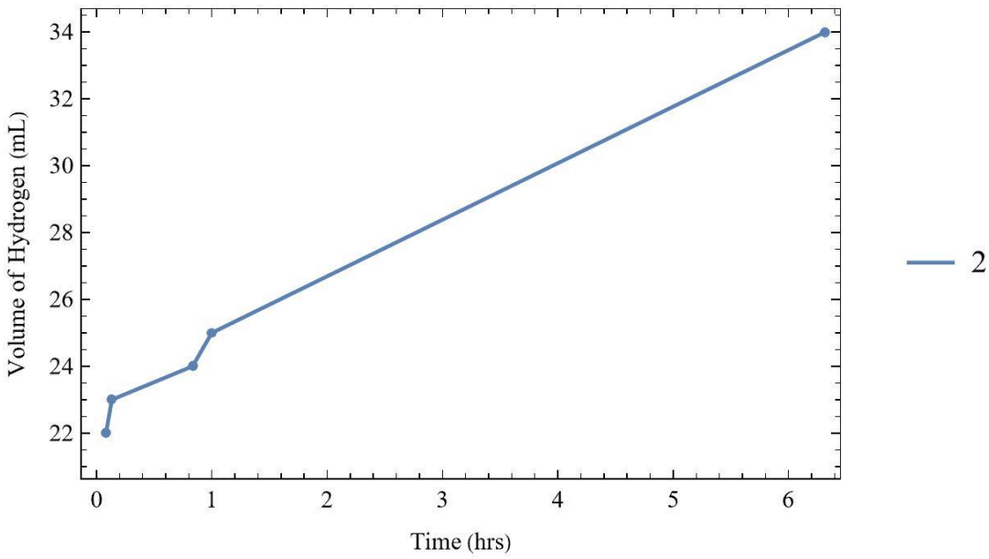

Figure S61: Kinetics for **2** (entry 4)

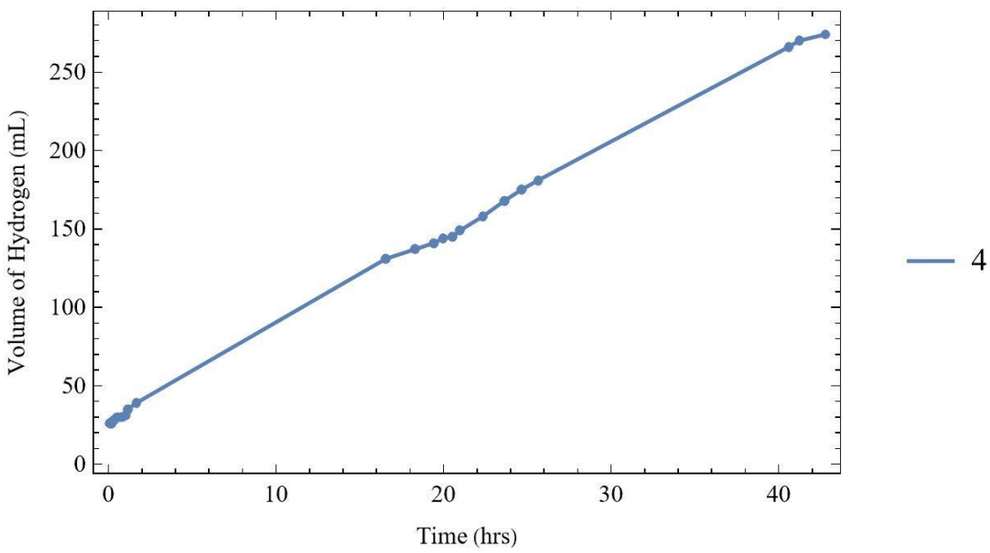

Figure S62: Kinetics for **4** (entry 4)

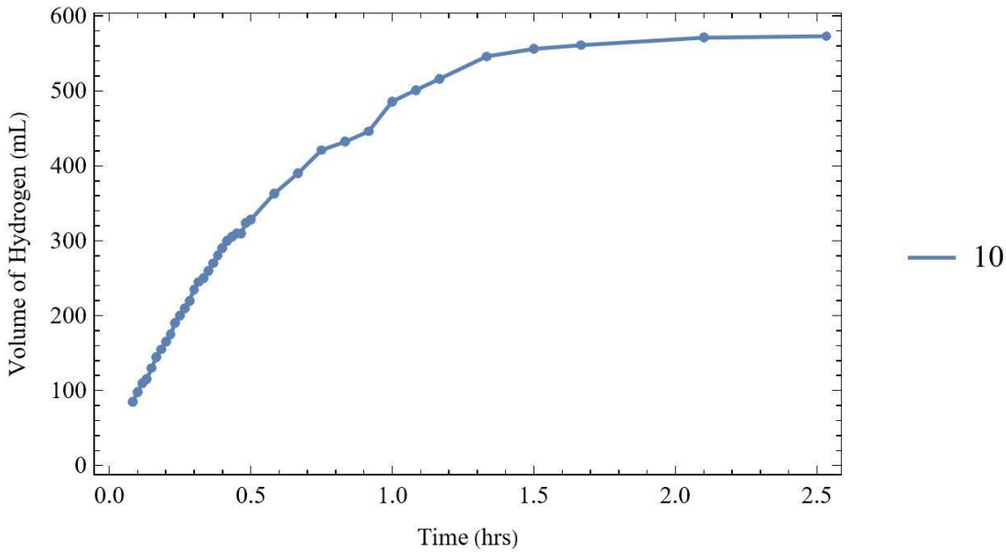

Figure S63: Kinetics for **10** (entry 5) TOF = 1.34 s^{-1}

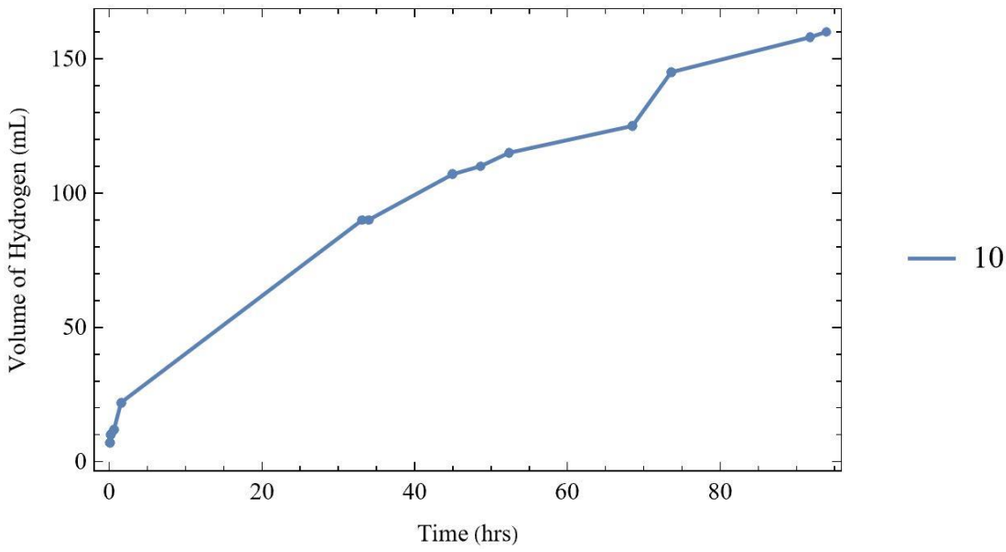

Figure S64: Kinetics for **10** (entry 6)

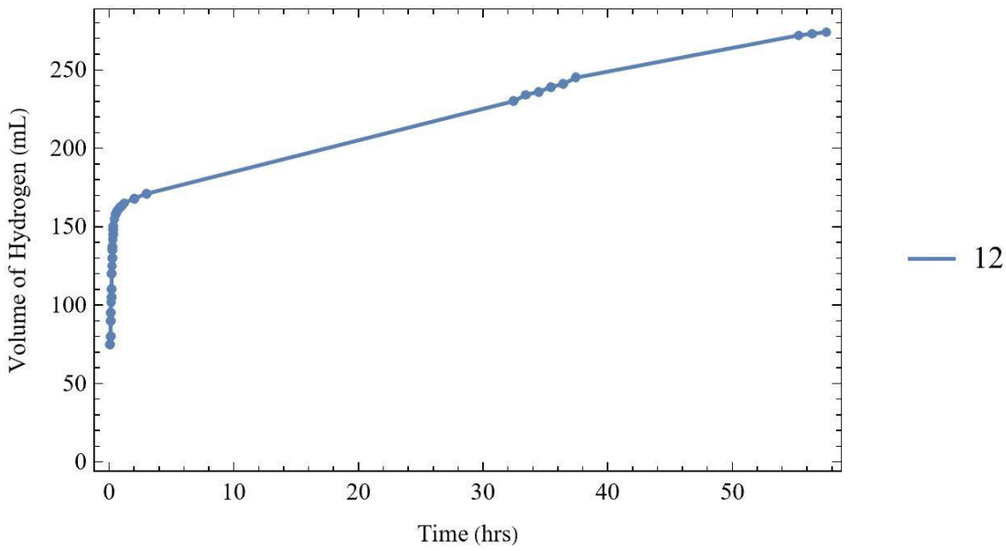

Figure S65: Kinetics for **12** (entry 7)

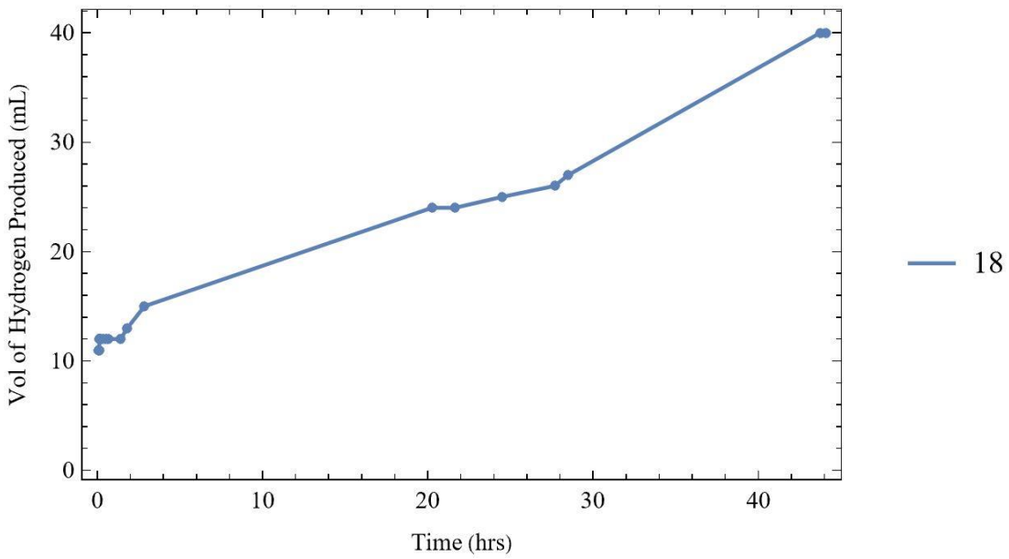

Figure S66: Kinetics for **18** (entry 8). TOF = 5.32 x 10^{-3} s^{-1}

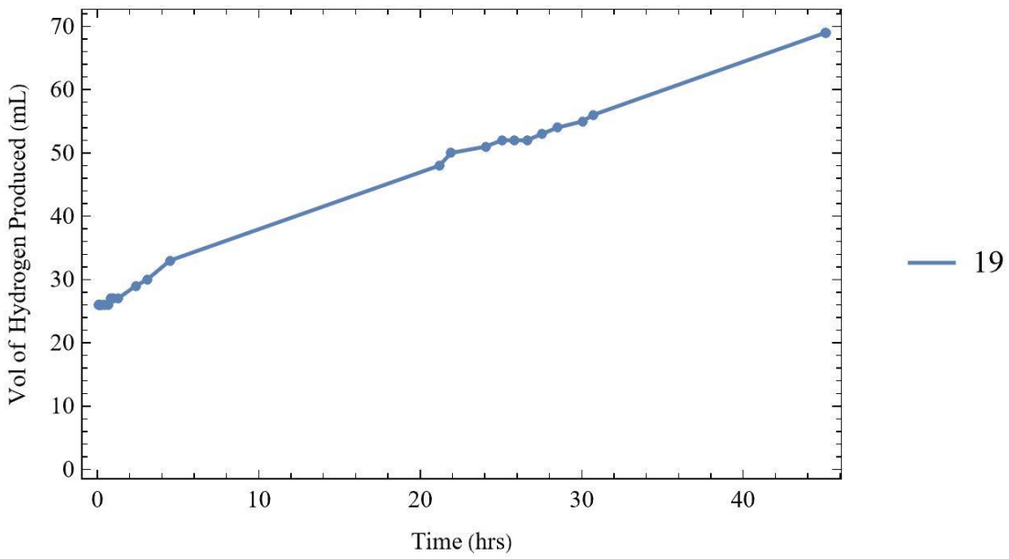

Figure S67: Kinetics for **19** (entry 9). TOF = 2.55 x 10^{-2} s^{-1}

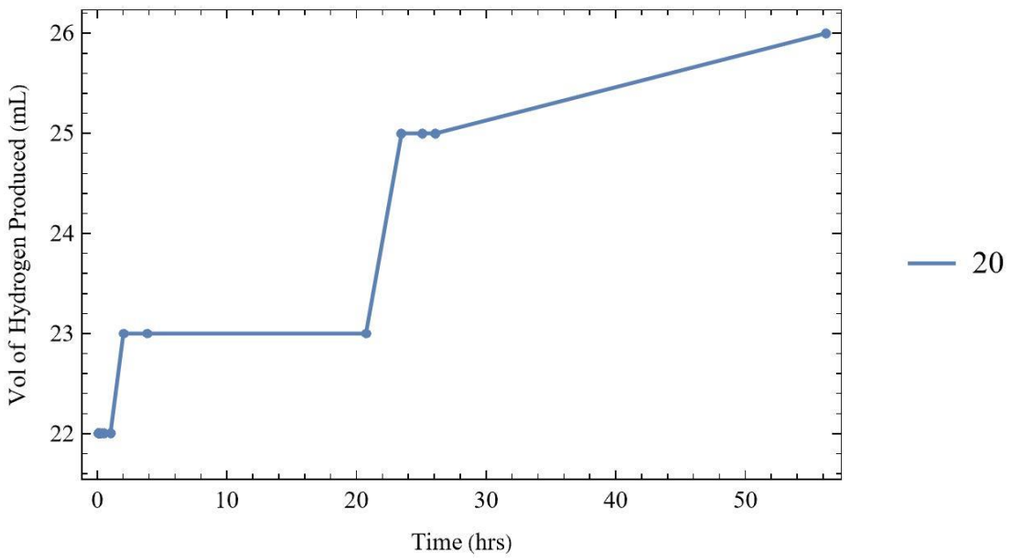

Figure S68: Kinetics for **20** (entry 10). TOF = 5 x 10^{-3} s^{-1}

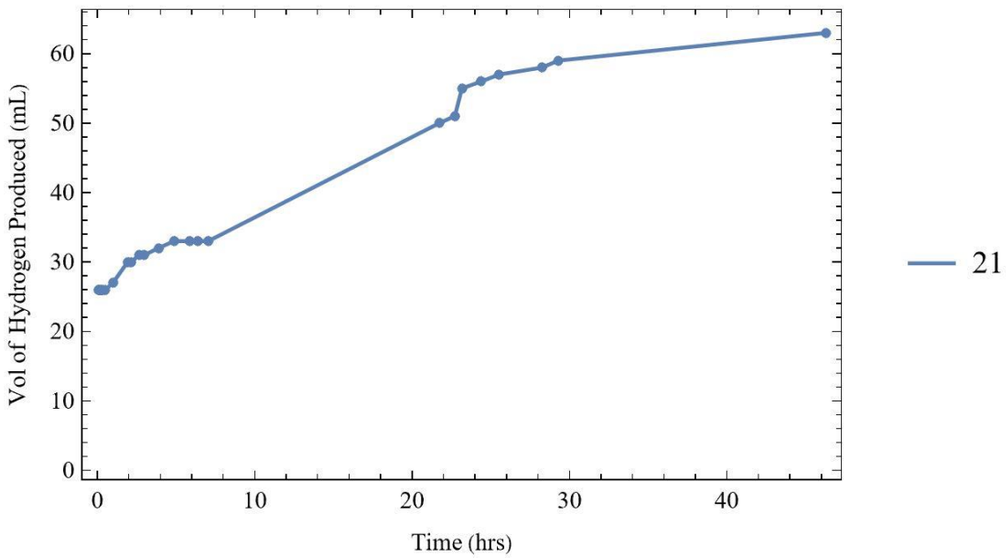

Figure S69: Kinetics for **21** (entry 11). TOF = 38 x 10^{-2} s^{-1}

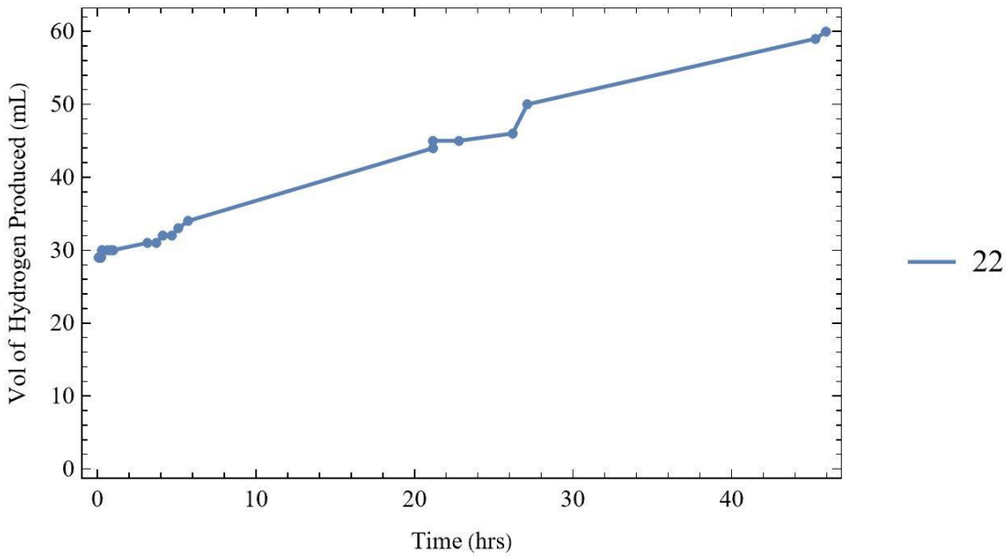

Figure S70: Kinetics for **22** (entry 12). TOF = 1.37 x 10^{-2} s^{-1}

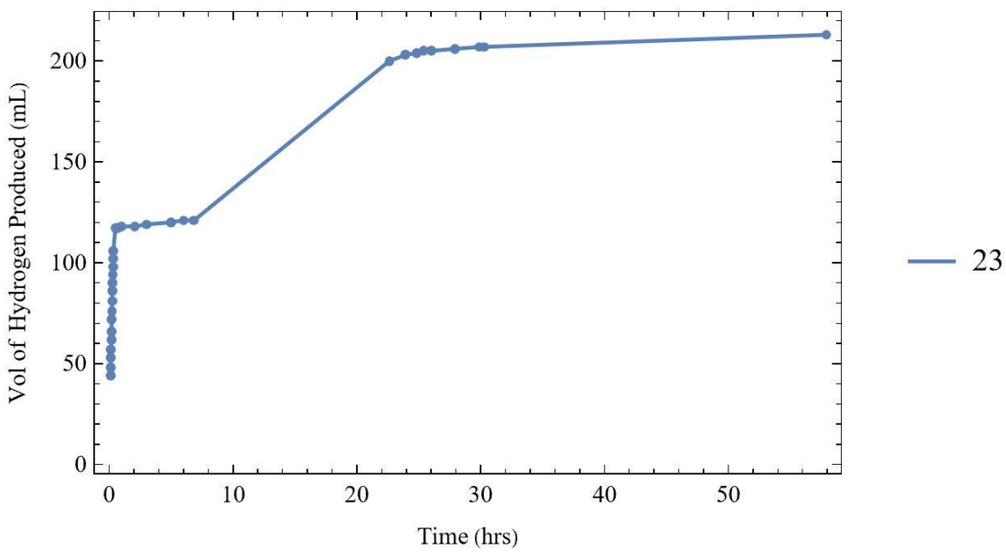

Figure S71: Kinetics for **23** (entry 13). TOF = 37 x 10^{-2} s^{-1}

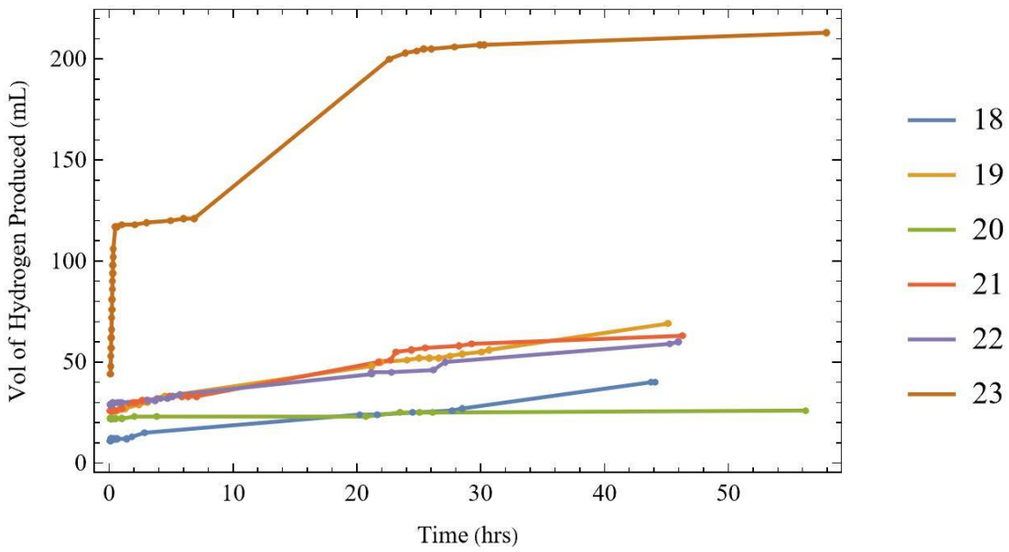

Figure S72: Kinetics for **18-23**

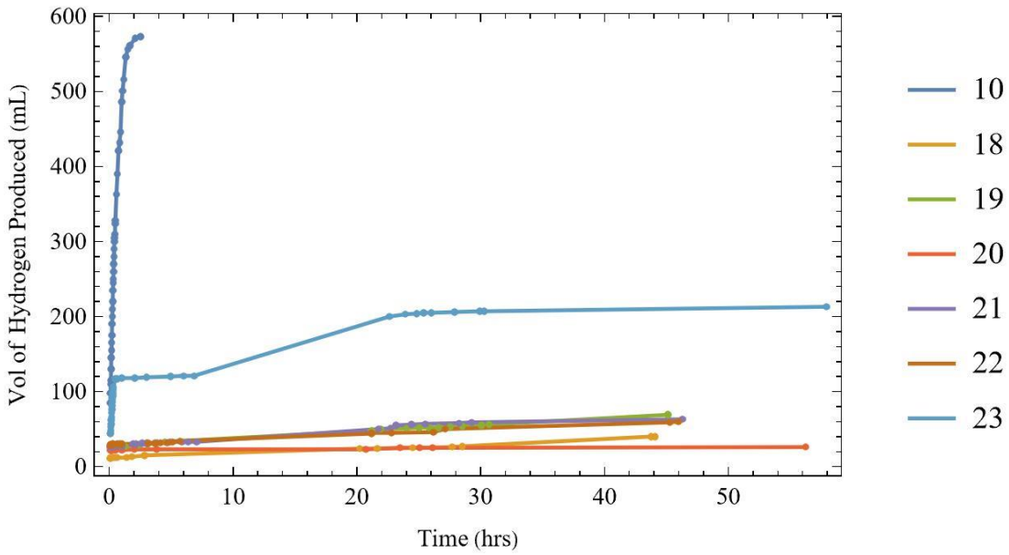

Figure S73: Kinetics for **10** and **18-23**

RuMACHO-BH Mechanistic Study

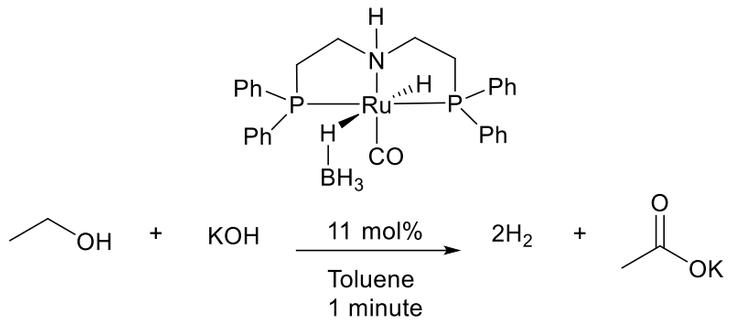

In a nitrogen filled glovebox, potassium hydroxide (0.146 g, 2.24 mmol), **10** (30 mg, 51 µmol), and ethanol (200 proof, 0.21 g, 4.5 mmol) were combined with toluene (5 mL, distilled from benzophenone ketyl) in a Schlenk flask. The flask was sealed with a septum and brought out of the glovebox where it was attached to a water eudiometer. The flask was then lowered into an oil bath at 120 °C for 1 minute during which the color changed from milky white to bright, clear yellow. After 1 minute, the reaction dried under reduced pressure giving an orange solid. The flask was returned to the glovebox where toluene-d_8 (1.5 mL) was added directly to the flask. This was filtered and an NMR was taken. After the NMR, the solution was diluted with benzene, filtered, and evaporated to dryness.

The above procedure was repeated, and the orange solid residue was dissolved in a minimal volume of benzene (Millipore Sigma, dried on a JC Meyer solvent purification system) To this was slowly added hexanes (VWR, dried on a JC Meyer solvent purification system) which induced the formation of crystalline solids that were assigned as **10b** & **10c**.

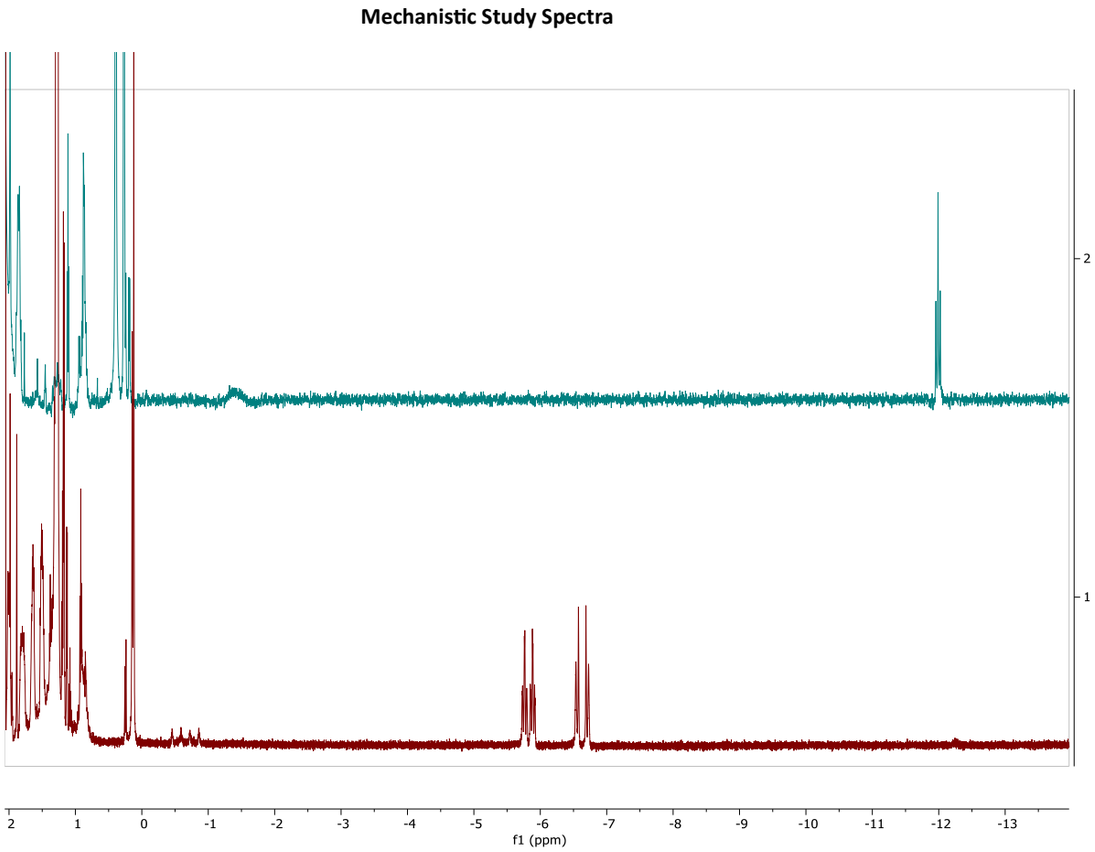

Figure S74: ^{1}H spectra of **10** (top) and the reaction mixture after 1 minute at 120 °C (Bottom) in toluene-d_8.

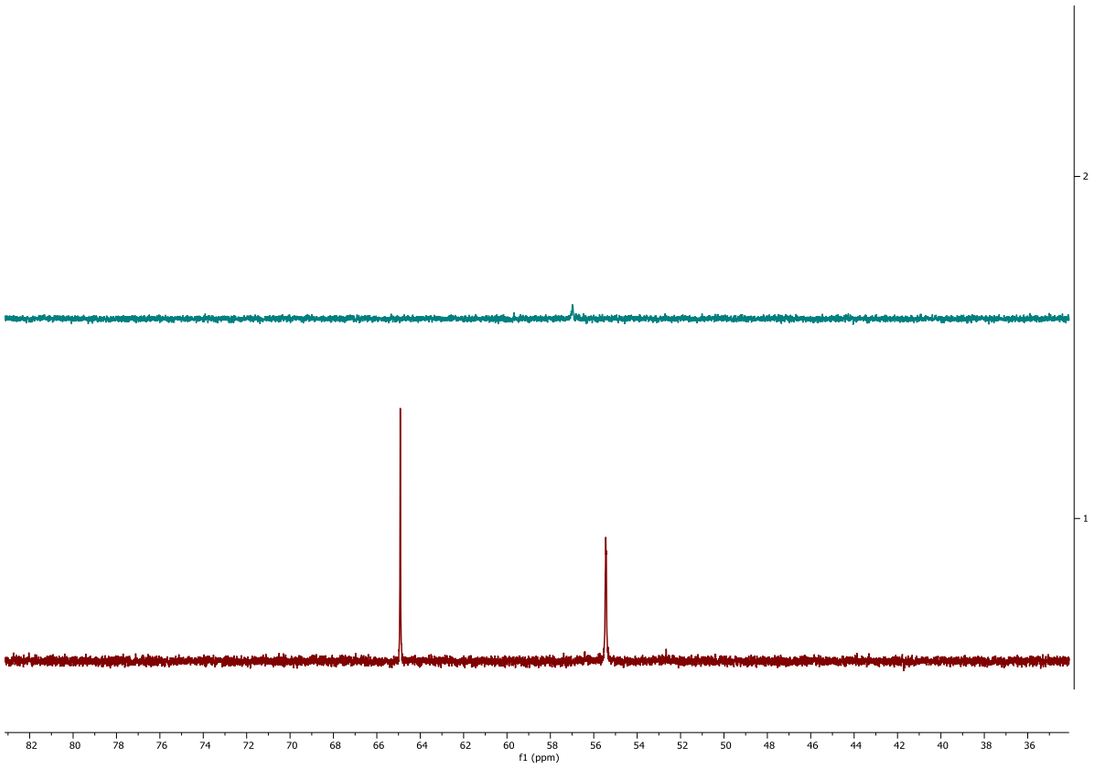

Figure S75: ^{31}P spectra of **10** (top) and the reaction mixture after 1 minute at 120 °C (Bottom) in toluene-d_8.

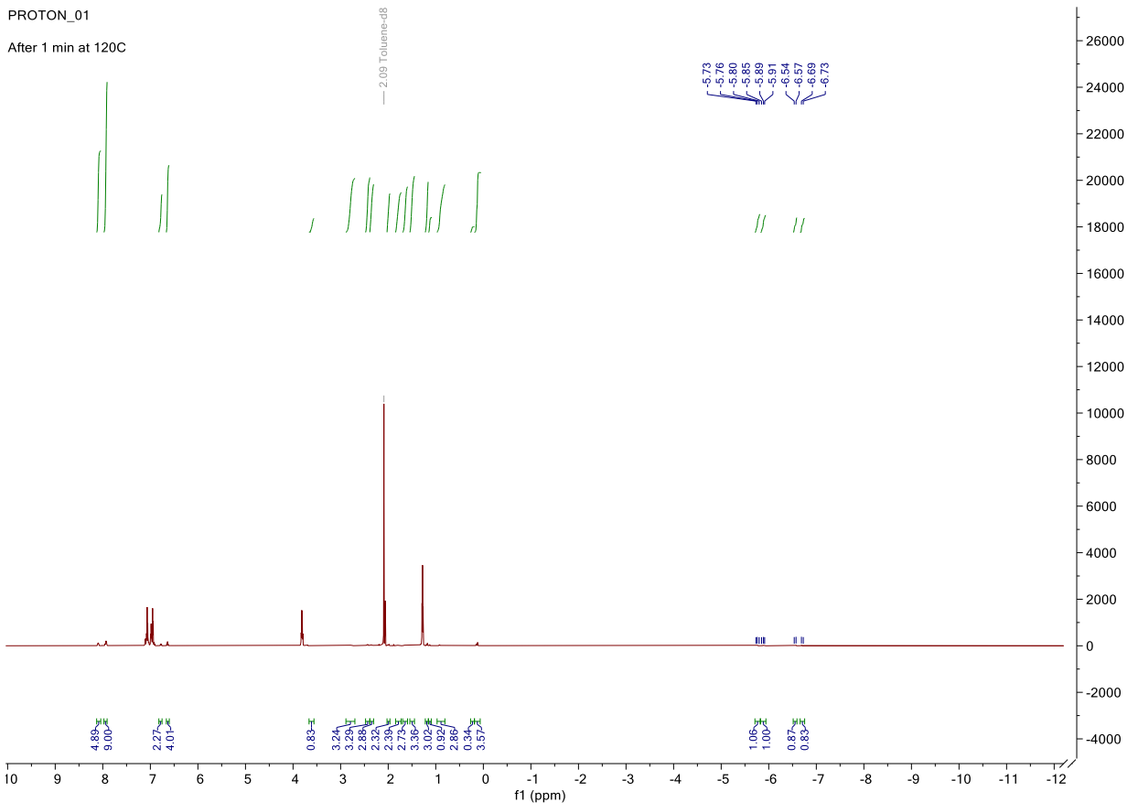

Figure S76: Full ^{1}H spectra of reaction mixture after 1 minute at 120 °C in toluene-d_8.

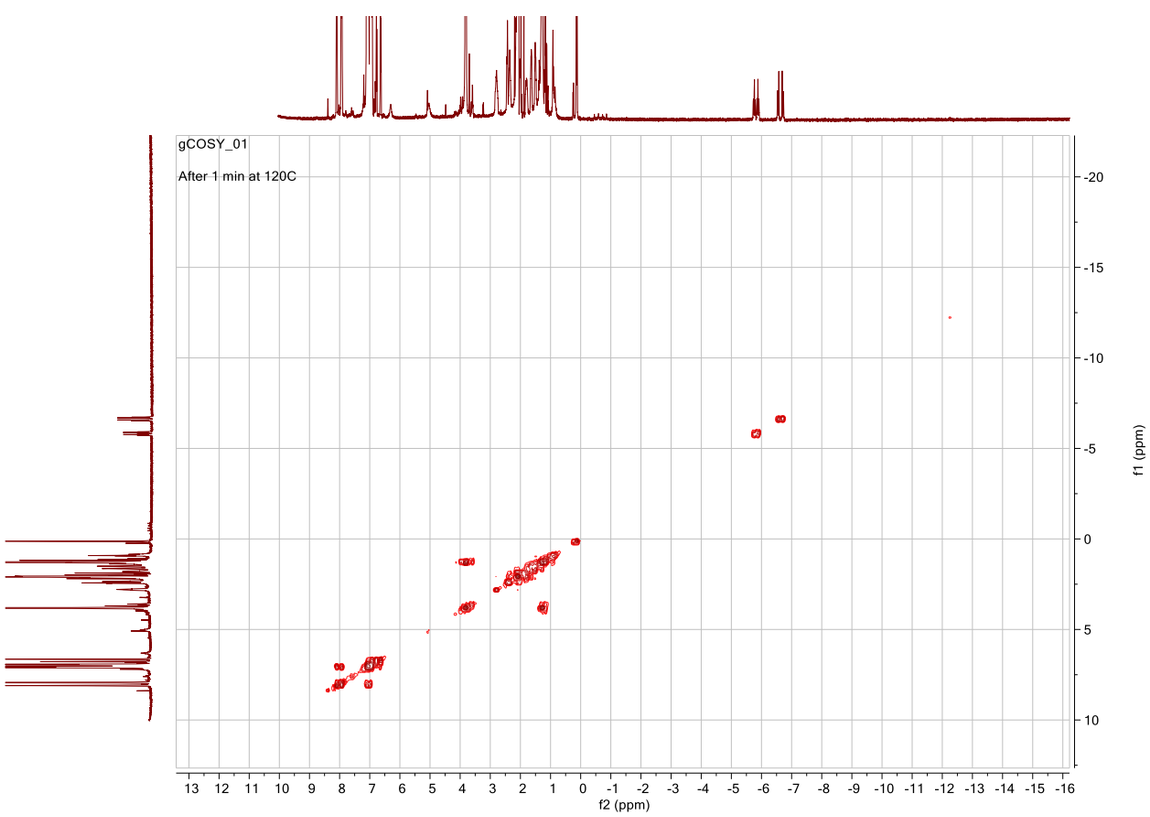

Figure S77: ^{1}H-^{1}H COSY spectra of reaction mixture after 1 minute at 120 °C in toluene-d_8.

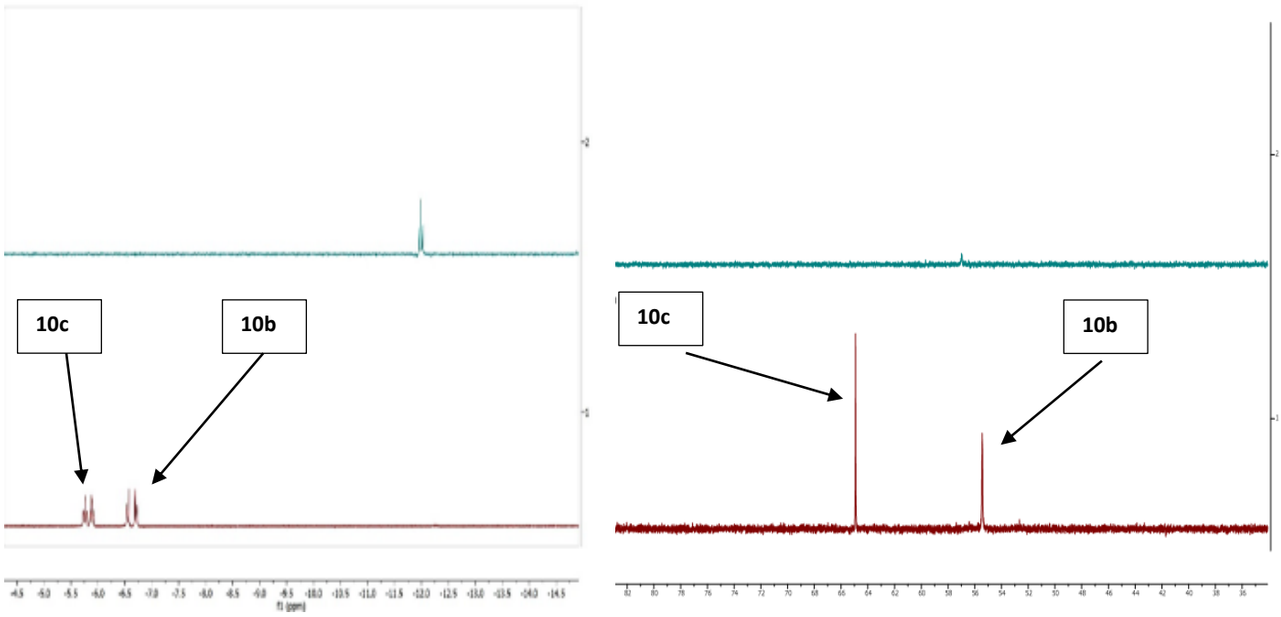

Figure S78: Left: RuMACHO-BH (top) before the reaction and (bottom) the isomers formed after initiation and removal of ethanol. Right: ^{31}P spectrum of RuMACHO-BH (top) and isomers (bottom). **10b** (*fac* isomer, ^{1}H -6.62 ppm, ^{31}P 55.39), **10c** (*mer* isomer, ^{1}H -5.87 ppm, ^{31}P 64.72).

Isomers 10c and 10b

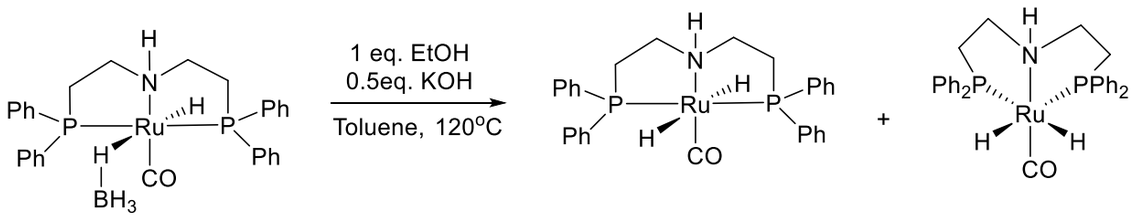

10 **10c** **10b**

In a nitrogen filled glovebox, **10** (103 mg, 175 µmol) was combined with ethanol (0.157 g, 0.200 mL, 3.41 mmol) and potassium hydroxide (0.1 g, 1.54 mmol) in a round bottom flask with toluene (2 mL, distilled from benzophenone ketyl). This was attached to a condenser capped with a septum outside of the glovebox under inert conditions. The round bottom was lowered into an oil bath at 120 °C. After 7 minutes, the H_2 evolution stopped, and the round bottom was returned to the glovebox where the solid was diluted with benzene, filtered, and evaporated to dryness. This filtration procedure was repeated once more, then residual solids were recrystallized by slow addition of hexanes to a minimal volume of benzene giving **10b** & **10c**. Recrystallization gave 70.6 mg of the isomers (89 % yield).

m. p. 148.7-151.1 °C (decomposition).

^{1}H NMR (500 MHz, C_6D_6) δ 8.21 (q, *J* = 6.3 Hz, 3H), 7.99 (at, *J* = 9.2, 8.5 Hz, 4H), 7.95 – 7.88 (m, 3H), 7.15 – 7.04 (m, 9H), 7.03 – 6.89 (m, 11H), 6.81 (at, *J* = 7.4 Hz, 2H), 6.67 (at, *J* = 7.1, 6.6 Hz, 4H), 6.54 (at, *J* = 11.28, 10.09 Hz, 1H), 3.23 – 3.08 (m, 2H), 2.81 (at, *J* = 15.6, 13.2 Hz, 2H), 2.49 (ad, *J* = 14.6 Hz, 2H), 2.36 – 2.12 (m, 4H), 1.95 – 1.80 (m, 2H), 1.61 (dtd, *J* = 23.4, 15.4, 9.2 Hz, 4H), -5.87 (dt, *J* = 117.40, 19.81, 19.45 2H), -6.62 (dd, *J* = 88.1, 23.68 Hz, 2H).

^{13}C NMR (500 MHz, C_6D_6) δ 133.58 (4C), 133.06 (4C), 132.76 (4C), 130.50 (6C), 128.78 (12C), 127.96 (10C), 127.77 (4C), 127.57 (2C), 53.13 (4C), 50.33 (2C), 50.24 (2C), 31.57 (2C), 30.40 (2C).

^{31}P NMR (202 MHz, C_6D_6) δ 64.72, 55.39.

Elemental Analysis: calc'd: C 60.83%, H 5.46%, N 2.45%; found: C 60.83%, H 5.435%, N 2.355%.

IR (KBr, cm^{-1}): 3051, 1894, 1572, 1433, 1097, 831, 694, 601, 505.

MALDI MS for $C_{29}H_{31}P_2Ru$: calc'd 573.09 g/mol; found m/z = 570.28 $[M-3H]^+$, 1114.69 g/mol.

Spectra of Complexes 10b and 10c

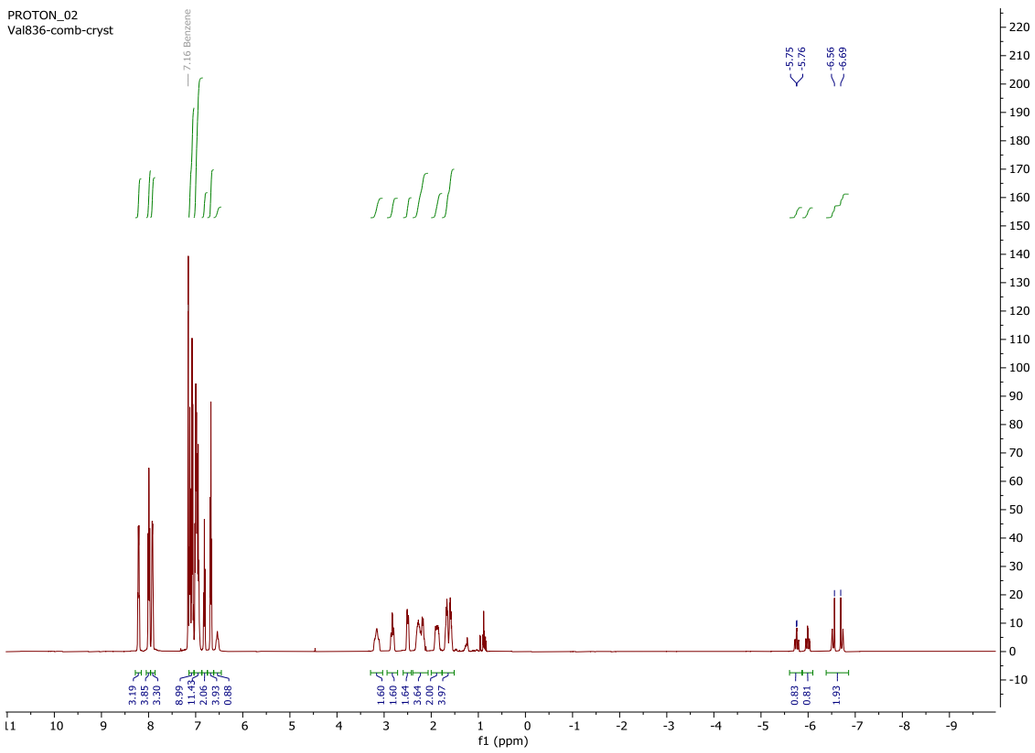

Figure S79: Full ^{1}H spectrum of complexes **10b** & **10c** in C_6D_6.

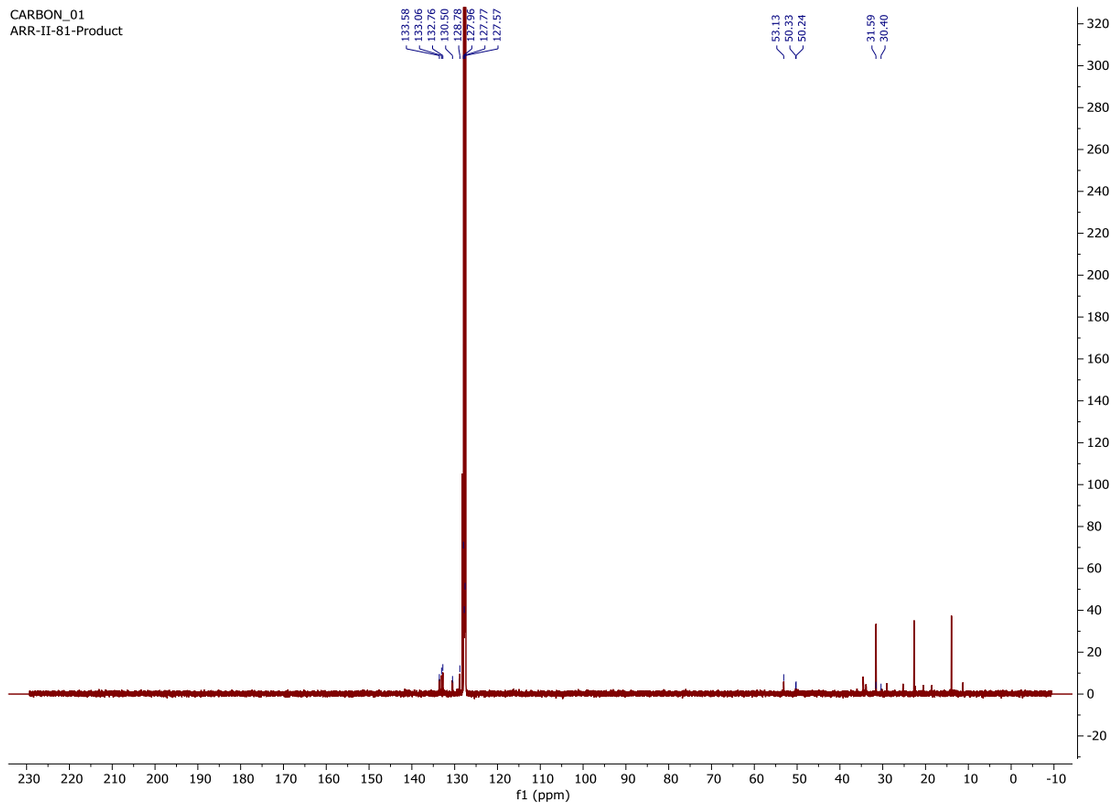

Figure S80: Full ^{13}C spectrum of complexes **10b** & **10c** in C_6D_6.

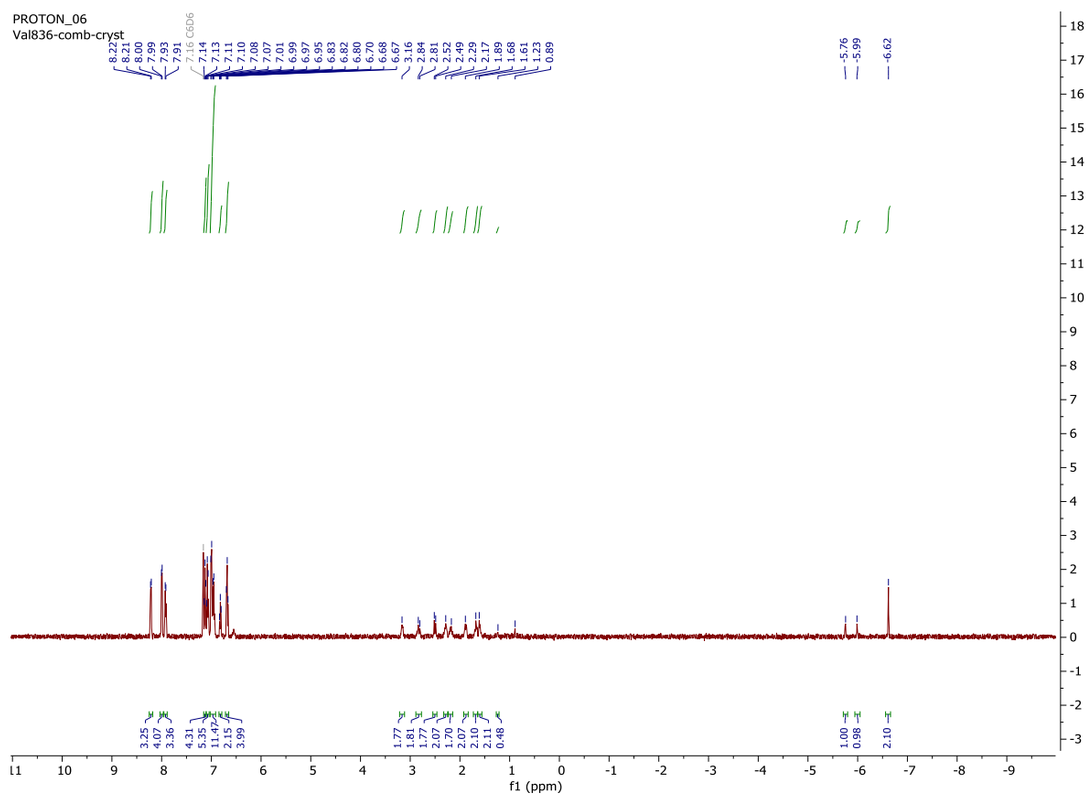

Figure S81: Full $^{1}H\{^{31}P\}$ spectrum of complexes **10b** & **10c** in C_6D_6.

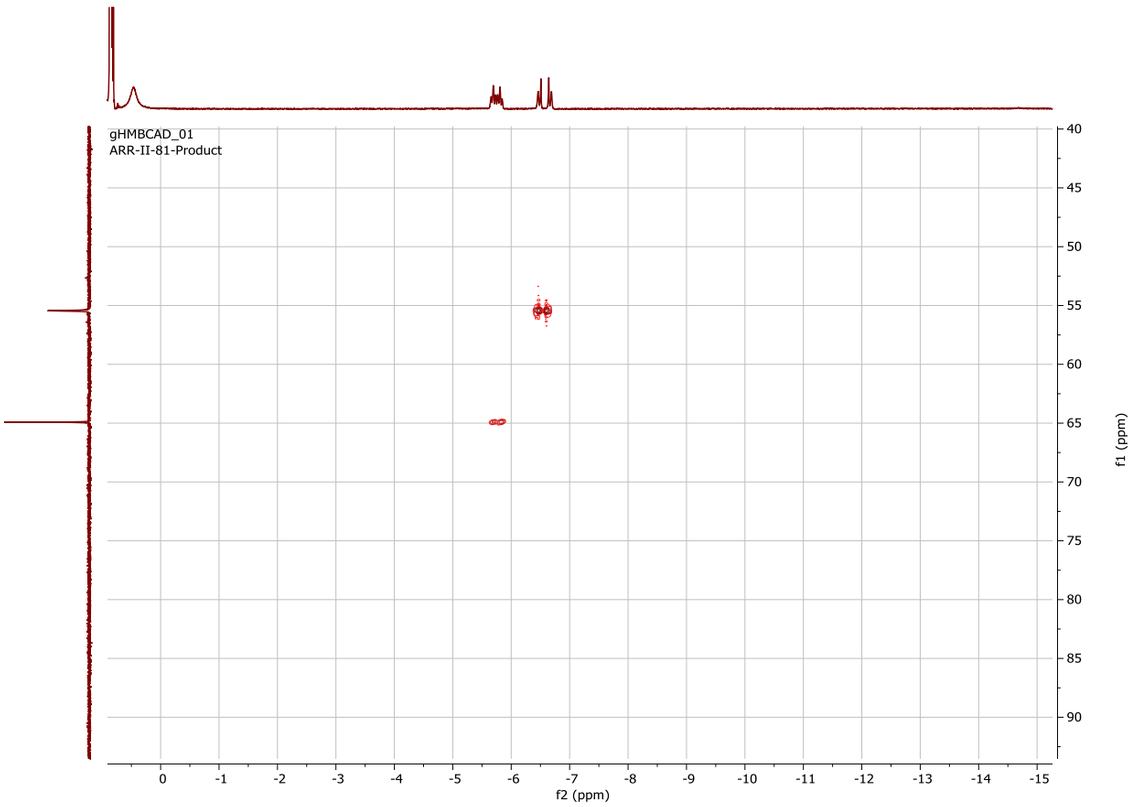

Figure S82: ^{1}H-^{31}P HMBC of **10b** & **10c** demonstrating hydride-phosphorus coupling in C_6D_6.

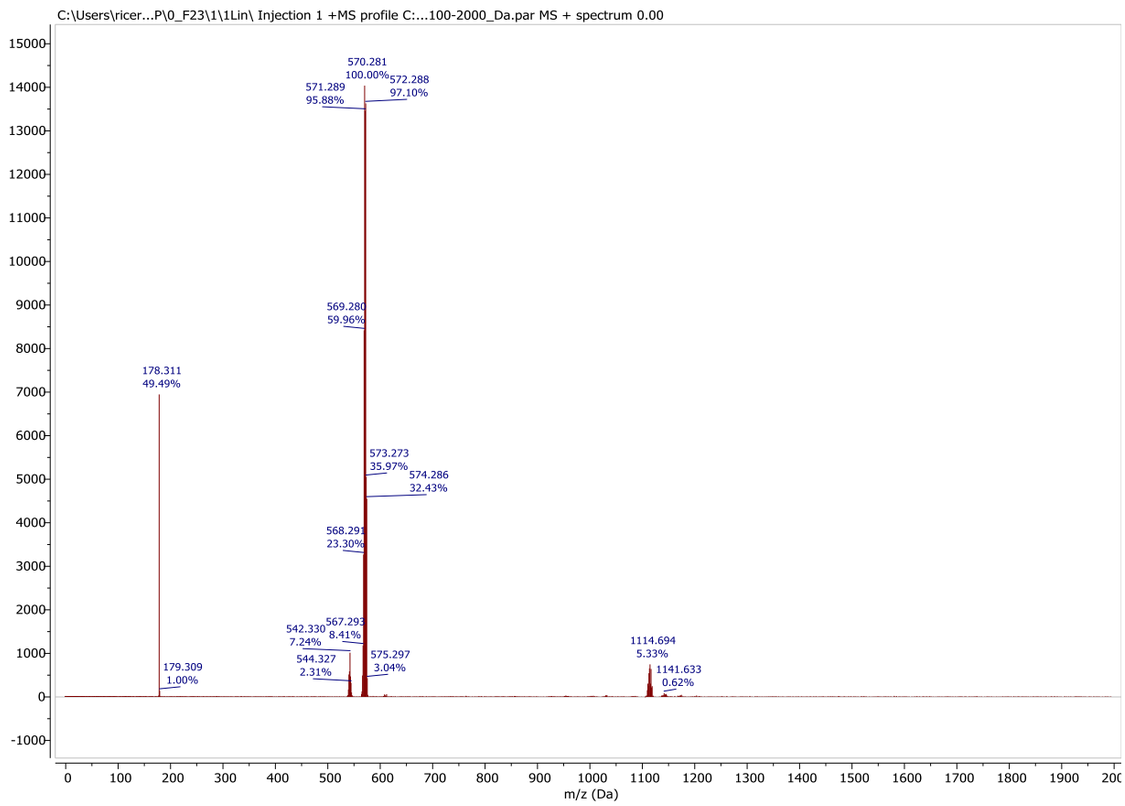

Figure S83: MALDI [M^+] spectra of **10b** & **10c**. Anthracene was used as the matrix.

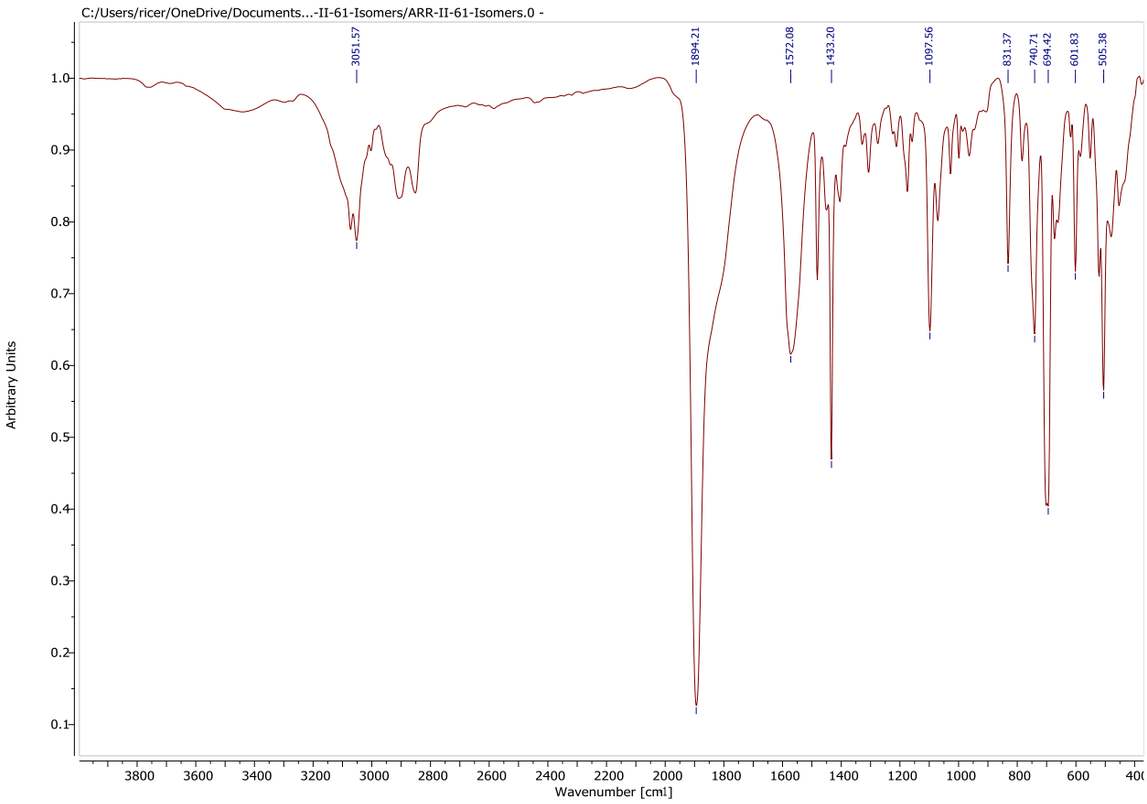

Figure S84: IR spectrum of complexes **10b** & **10c**.

Kinetic Competence Testing of 10b and 10c

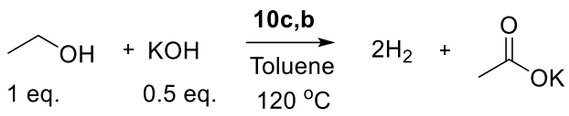

In a nitrogen filled glovebox, potassium hydroxide (0.561 g, 8.80 mmol) was weighed out and added to a 25 mL round bottom flask. Next, a mixture of **10b** and **10c** (0.1 mol % with respect to ethanol, 11.4 mg, 20 μmol), toluene (10 mL, distilled from benzophenone ketyl), ethanol (200 proof, 0.92 g, 1.2 mL, 20 mmol) were added. Outside the glovebox, the flask was attached to a condenser and immersed in a 120 °C oil bath for 3 hours. Gas production was measured by water eudiometry, attached through a needle. After 3 hours, volatiles removed from the resulting solution using a rotary evaporator under reduced pressure. Quantitative NMR samples were prepared by adding methanol-d_4 (700 mL) and dimethylformamide (DMF, 111 mg, 1.52 μmol) and subsequently analyzed by ^{1}H NMR. After NMR analysis, volatiles were again removed using a rotary evaporator under reduced pressure and the resulting solid was diluted in water (50 mL, deionized) and titrated with dilute hydrochloric acid (0.3454 M) and sodium hydroxide (0.3407 M) solutions. This gave 80% acetate by NMR and 98% carboxylates by titration.

Rate During Reaction Using 10b and 10c

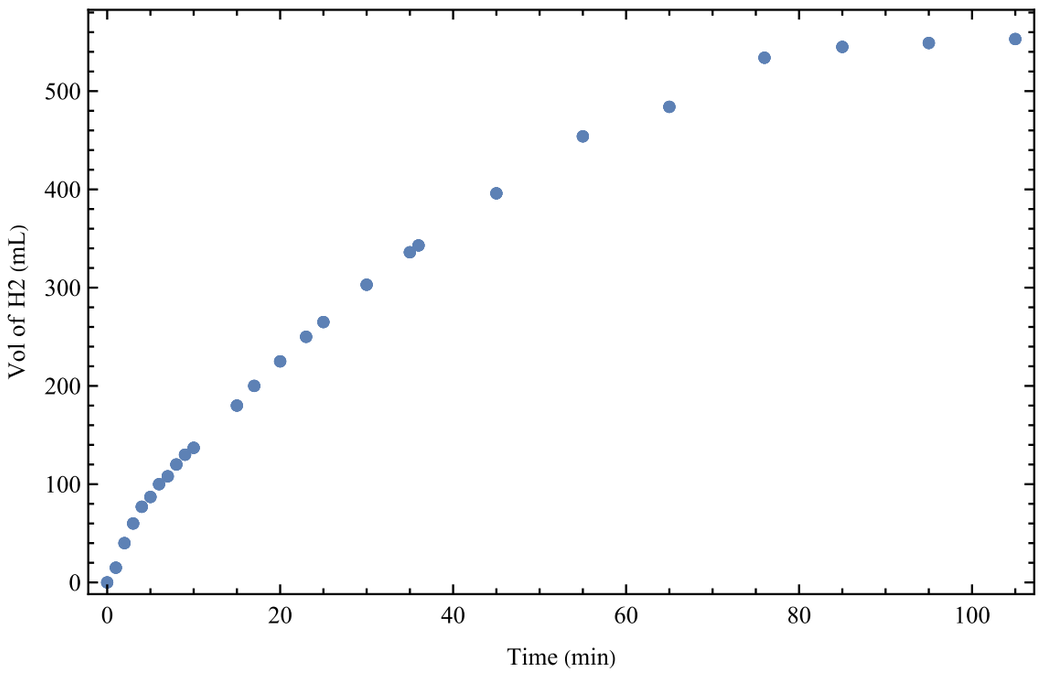

Figure S85: H_2 production from a reaction involving catalysts **10b** and **10c** over 3 hours.

Kinetic Competence of 10b and 10c NMR Spectrum

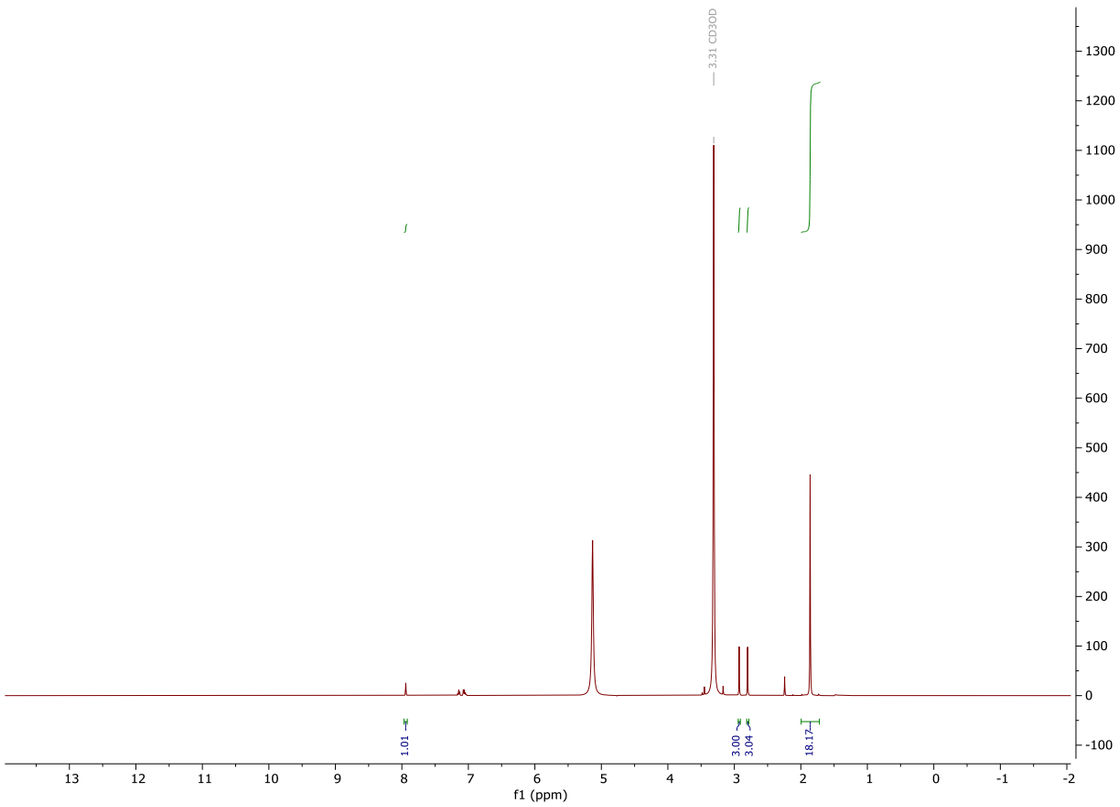

Figure S86: ^{1}H Spectrum of product mixture in CD_3OD.

Chlorination of Isomers

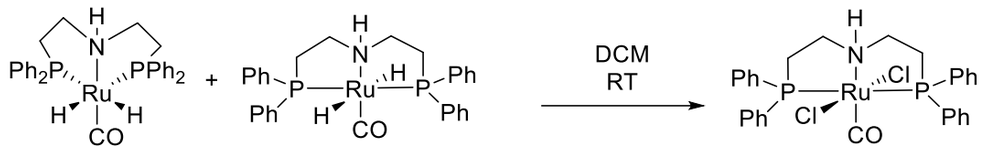

10b **10c** **10d**

In a nitrogen filled glovebox, a mixture of **10b** and **10c** (15 mg, 26 μmol) were diluted in dichlormethane-d_2 (0.5 mL) and added to a J. Young NMR tube. Initially the solution was colorless, but after 5 minutes the solution was tan. After an hour the solution was yellow.

Isomer Chlorination Spectra

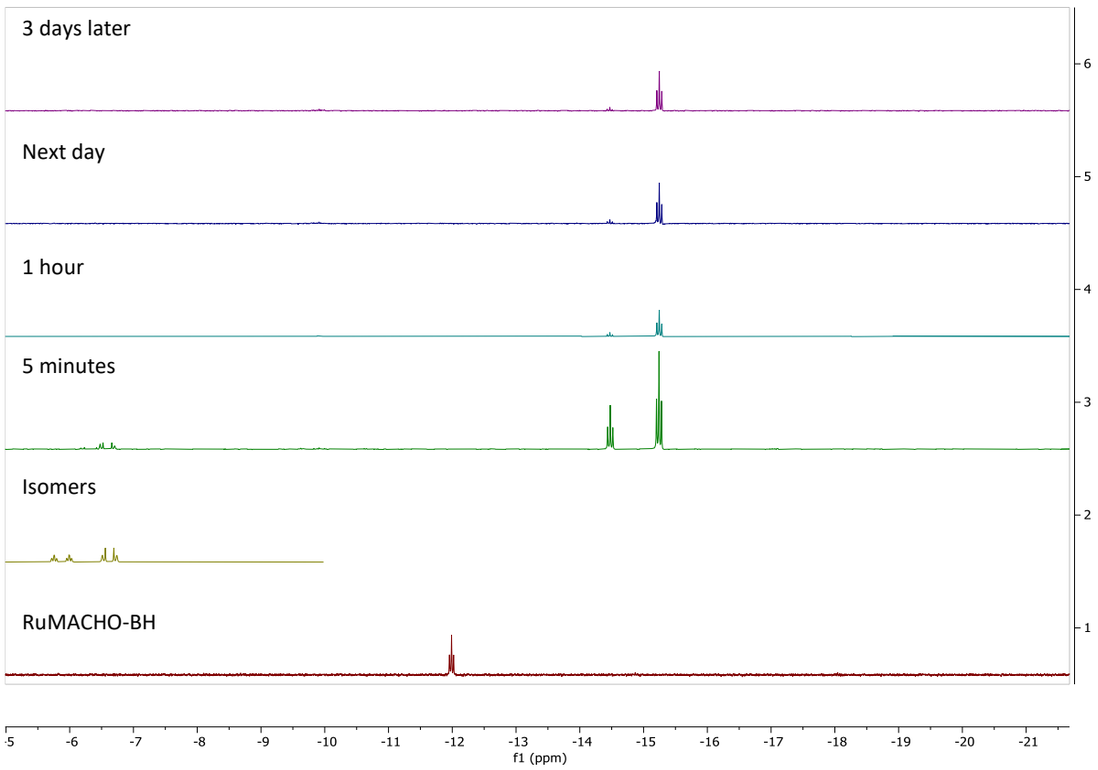

Figure S87: ^{1}H spectra over time of **10c** & **10b** in deuterated dichlormethane-d_2.

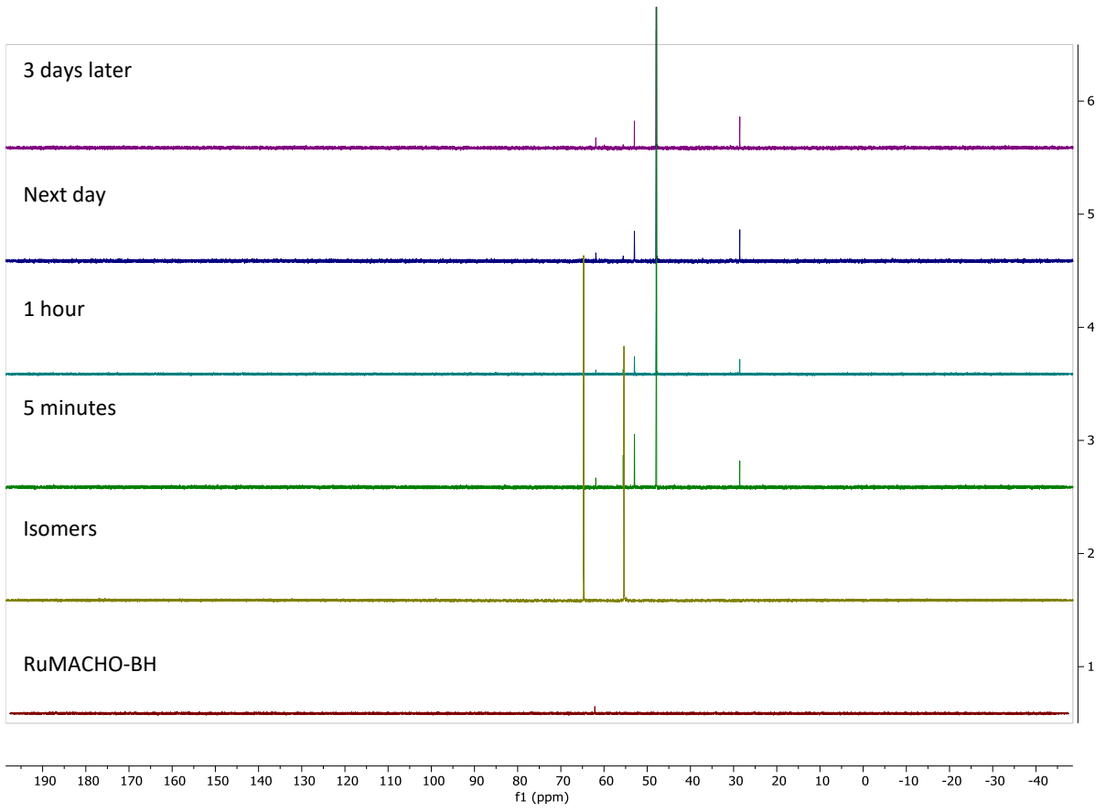

Figure S88: ^{31}P spectra over time of **10b** & **10c** in dichlormethane-d_2.

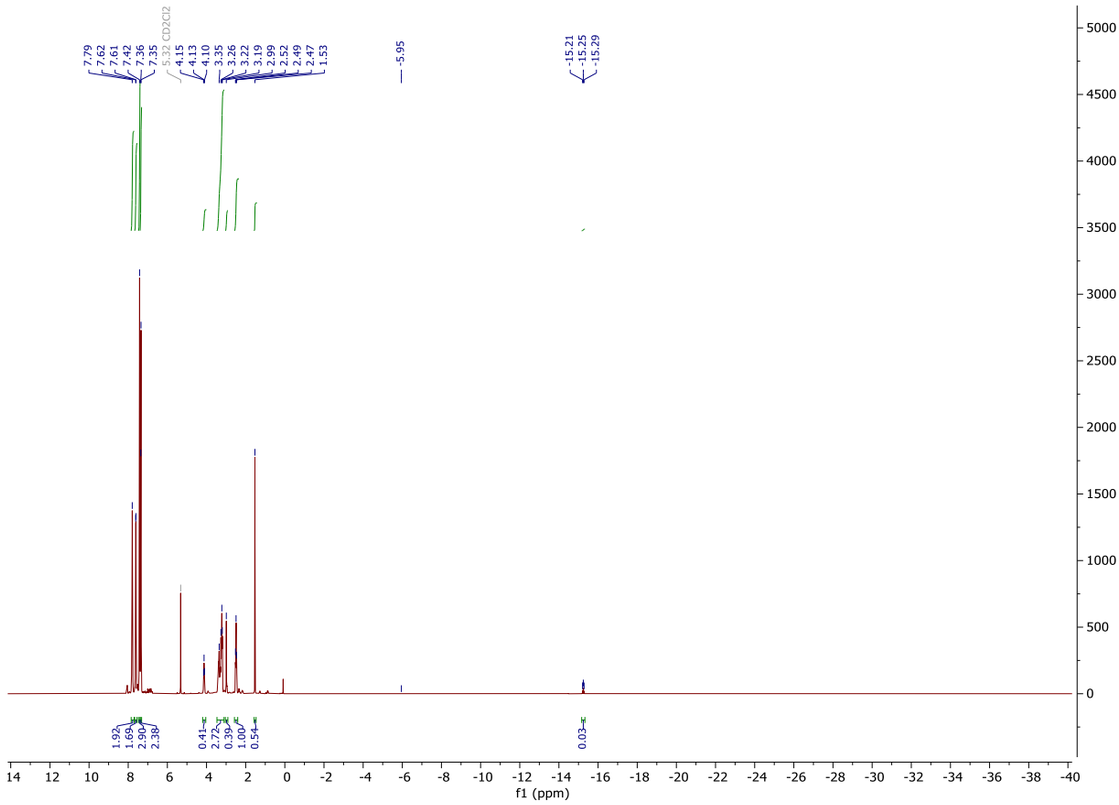

Figure S89: ^{1}H spectra over time of **10b** & **10c** after 3 days in dichlormethane-d_2.

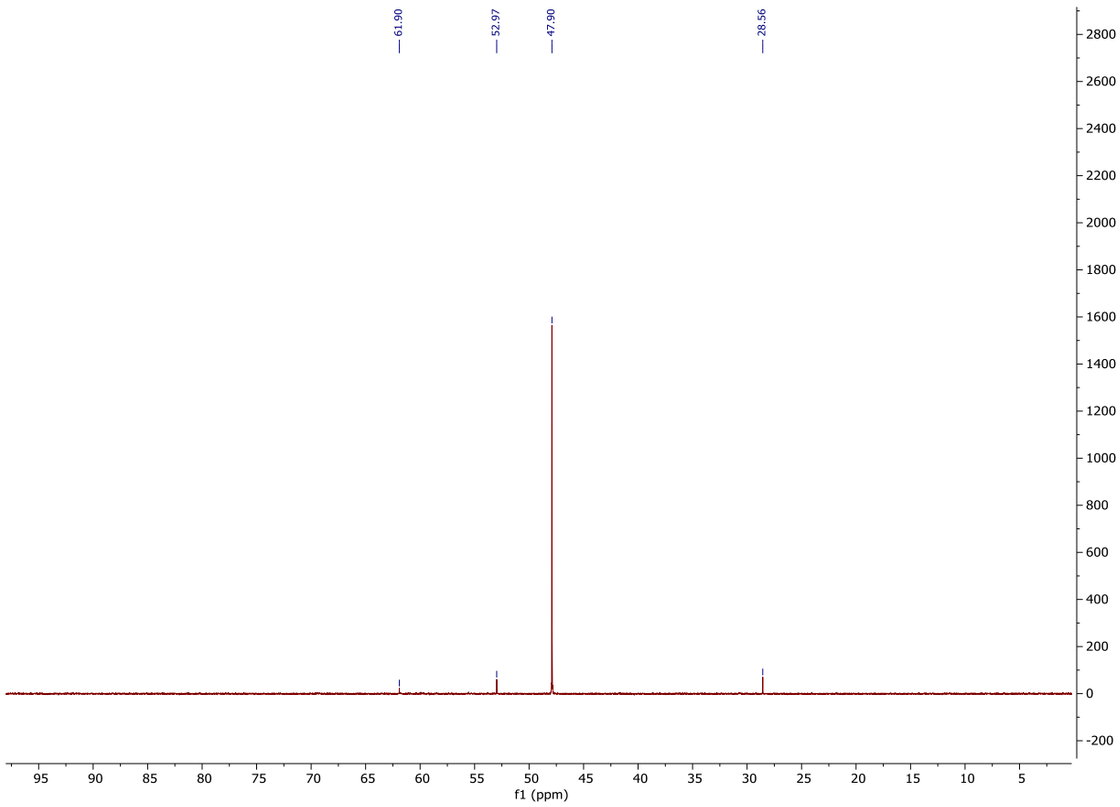

Figure S90: ^{31}P spectra over time of **10b** & **10c** after 3 days in dichlormethane-d_2.

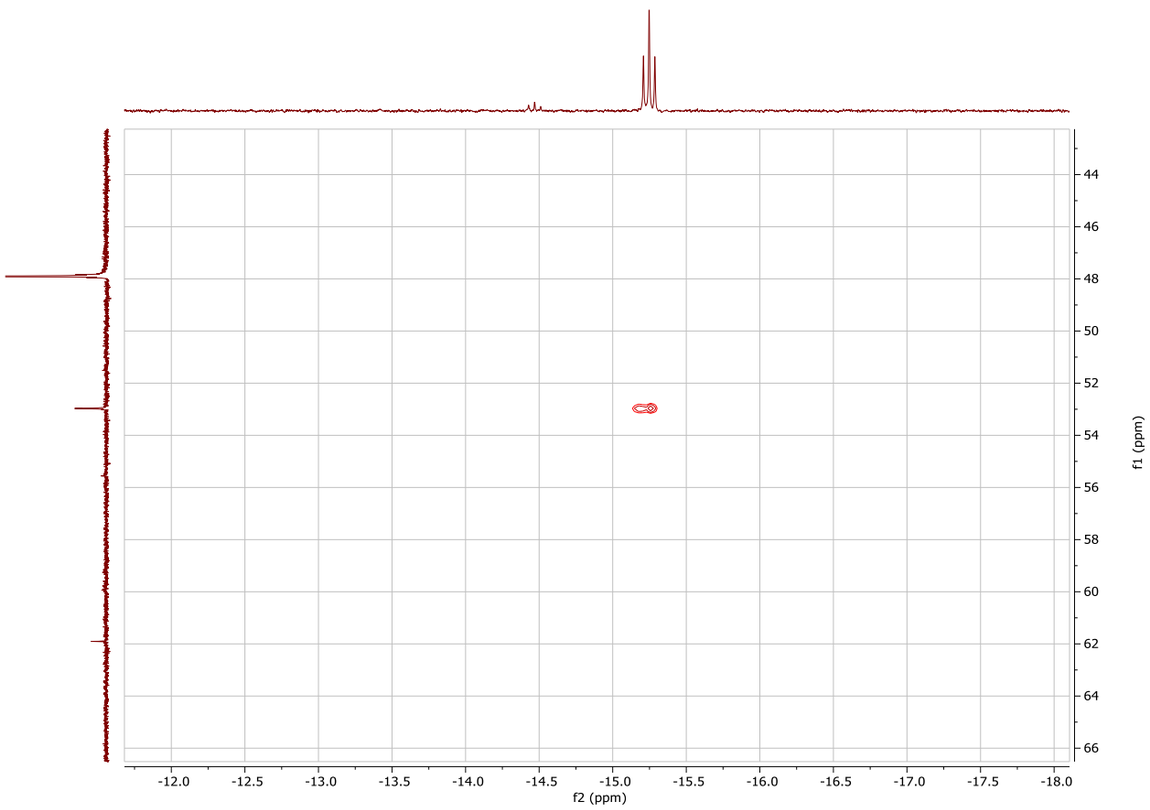

Figure S91: ^{1}H-^{31}P HMBC of chlorination reaction after 3 days in dichlormethane-d_2. Major species in phosphorous spectra is not associated with hydride in proton spectrum.

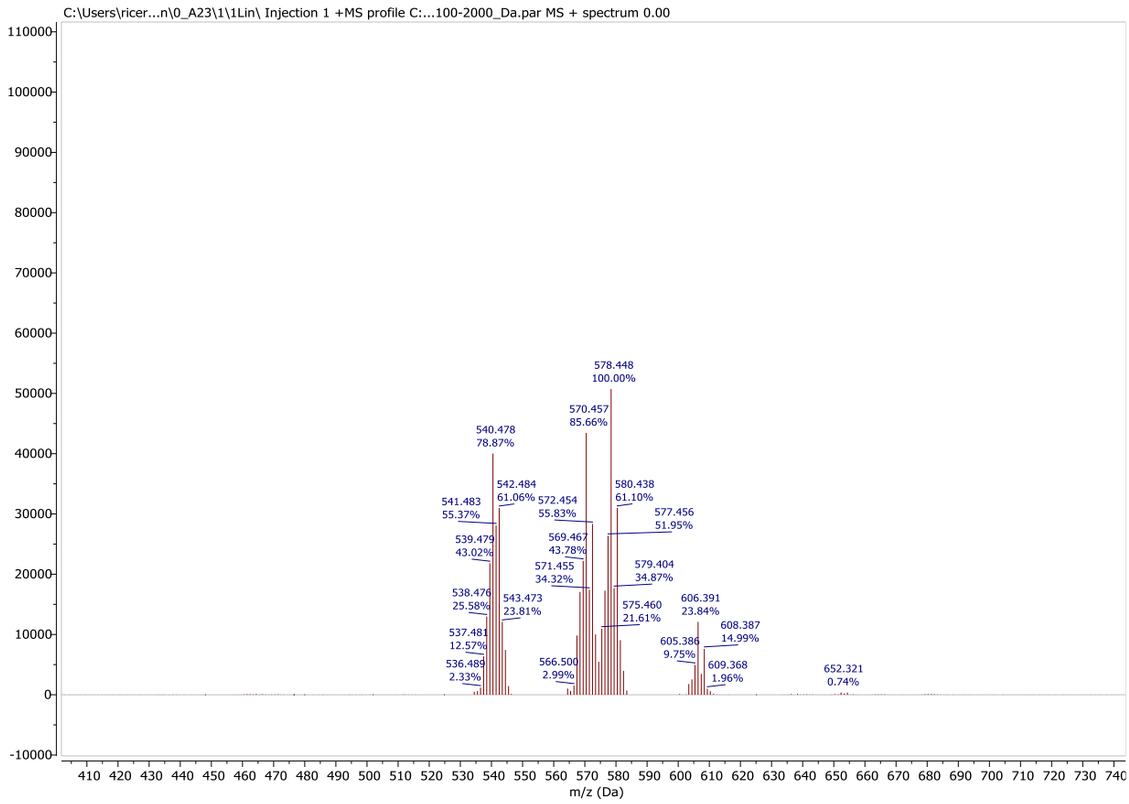

Figure S92: MALDI [M⁺] of chlorinated products. Calculated *m/z* = 641.0145; Found *m/z* = 606.391, corresponding to single chloride loss.

Excess KOH Reaction

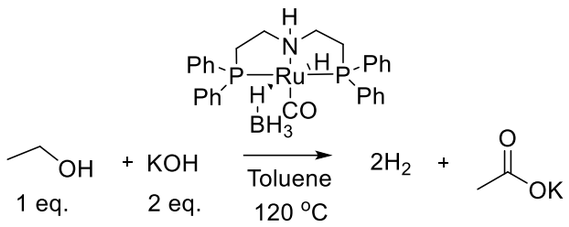

In a nitrogen filled glovebox, potassium hydroxide (1.28 g, 19.7 mmol), ethanol (200 proof, 0.46 g, 10 mmol), and **10** (46 mg, 78 μmol) were combined with toluene (10 mL, distilled from benzophenone ketyl) in a Schlenk flask. The flask was sealed with a septum and brought out of the glovebox where it was attached to a water eudiometer via a needle and tubing. The flask was then lowered into an oil bath at 120 °C and allowed to stir until no more gas was produced (4 hours, 22 minutes). The flask was returned to the glovebox where an NMR sample was prepared in toluene-d_8 (0.7 mL). After NMR, the sample was combined back into the flask which was filtered and concentrated to dryness. Another NMR sample was prepared in C_6D_6 (700 μL); again, afterwards it was added back the mixture, which was dissolved in benzene, filtered, and evaporated to dryness. The remaining solid was dissolved in benzene and recrystallized from slow addition of hexanes.

Excess KOH Reaction Spectra

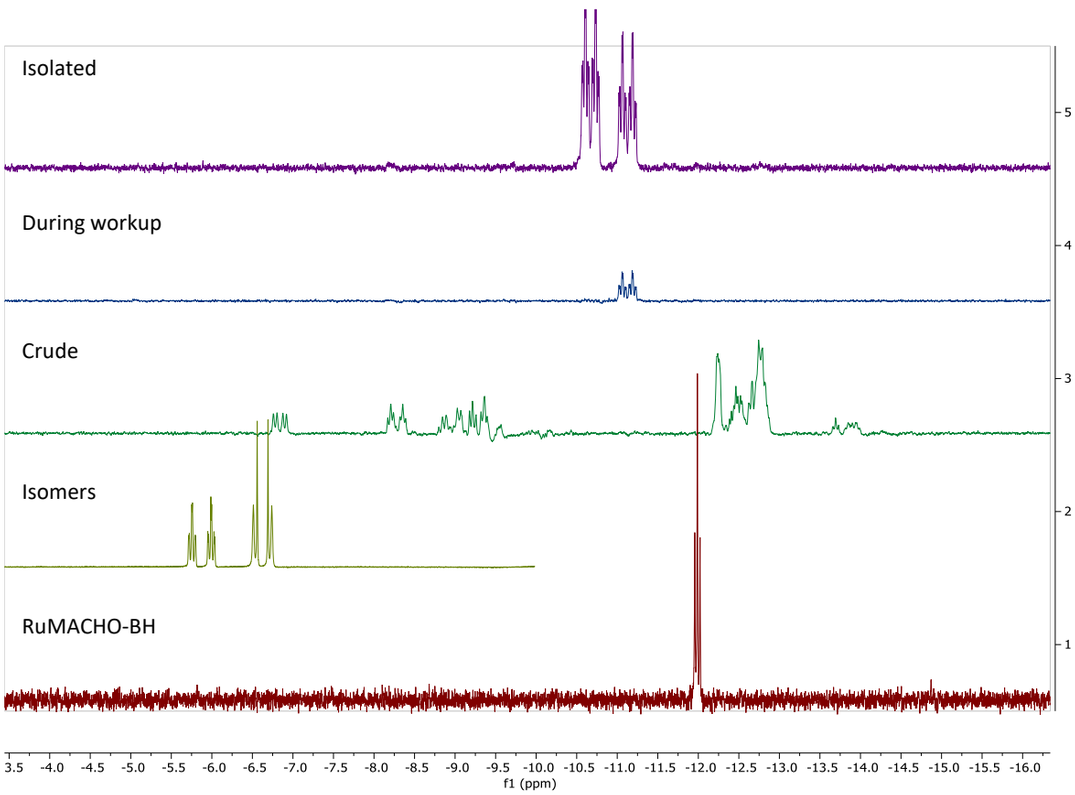

Figure S93: ^{1}H spectra of the reaction mixture over time compared to isomers and complex **10**.

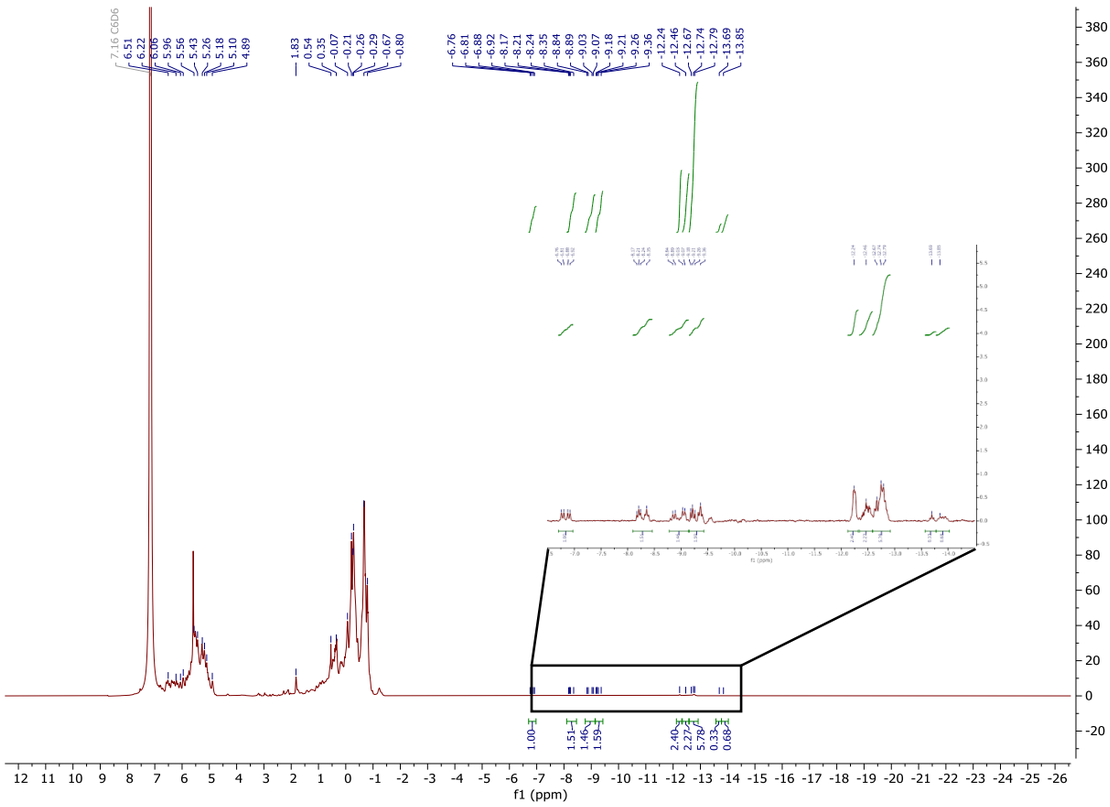

Figure S94: ^{1}H spectrum of crude reaction mixture in d_8-toluene.

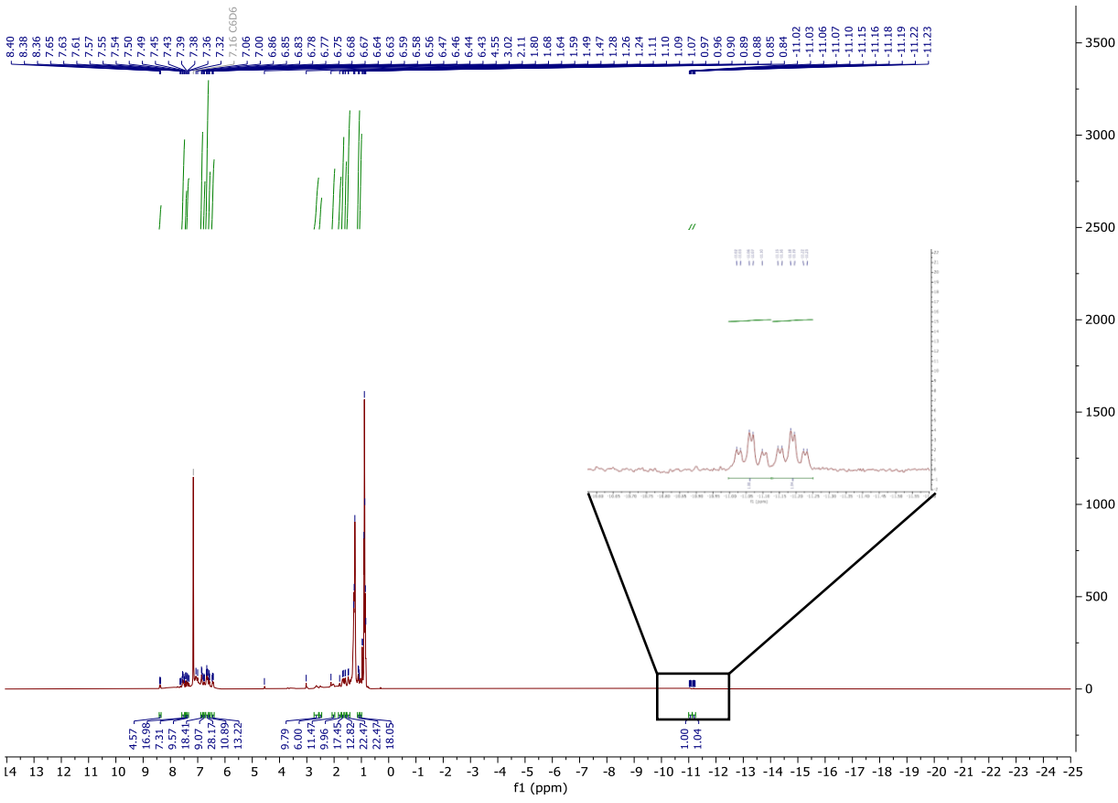

Figure S95: ^{1}H spectrum of reaction mixture during work up in C_6D_6.

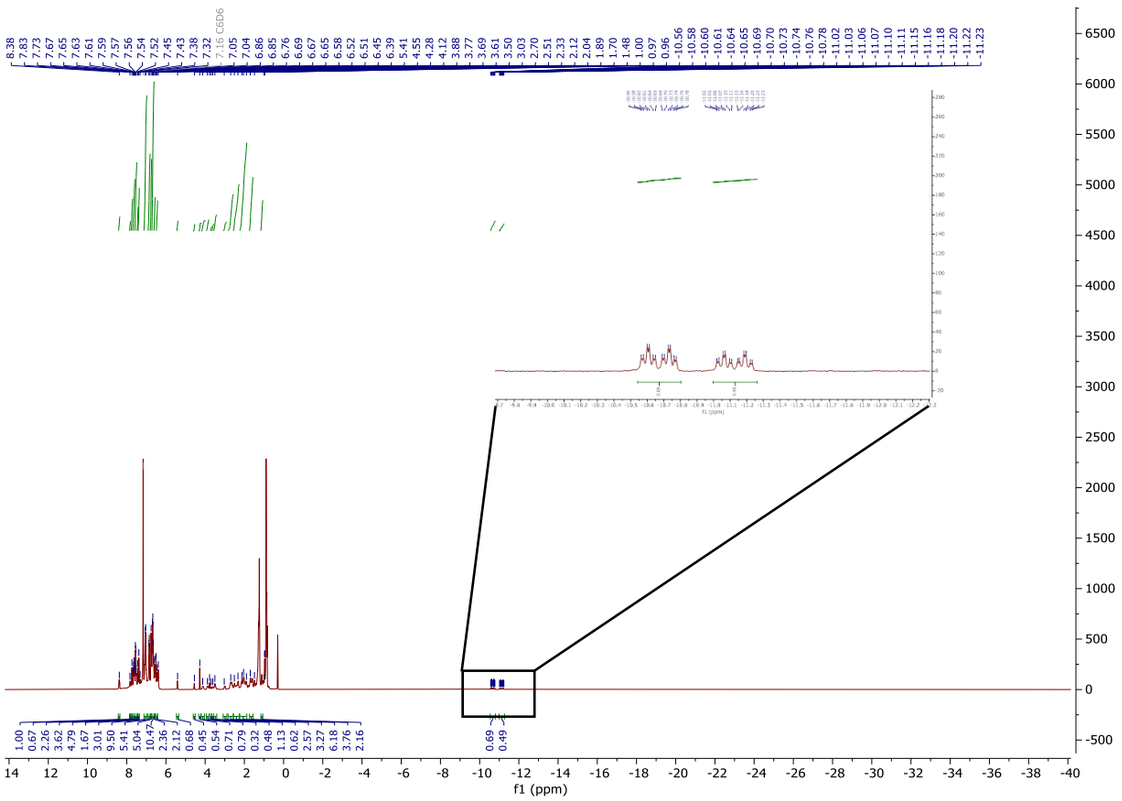

Figure S96: ^{1}H spectrum of isolated species after recrystallization in C_6D_6.

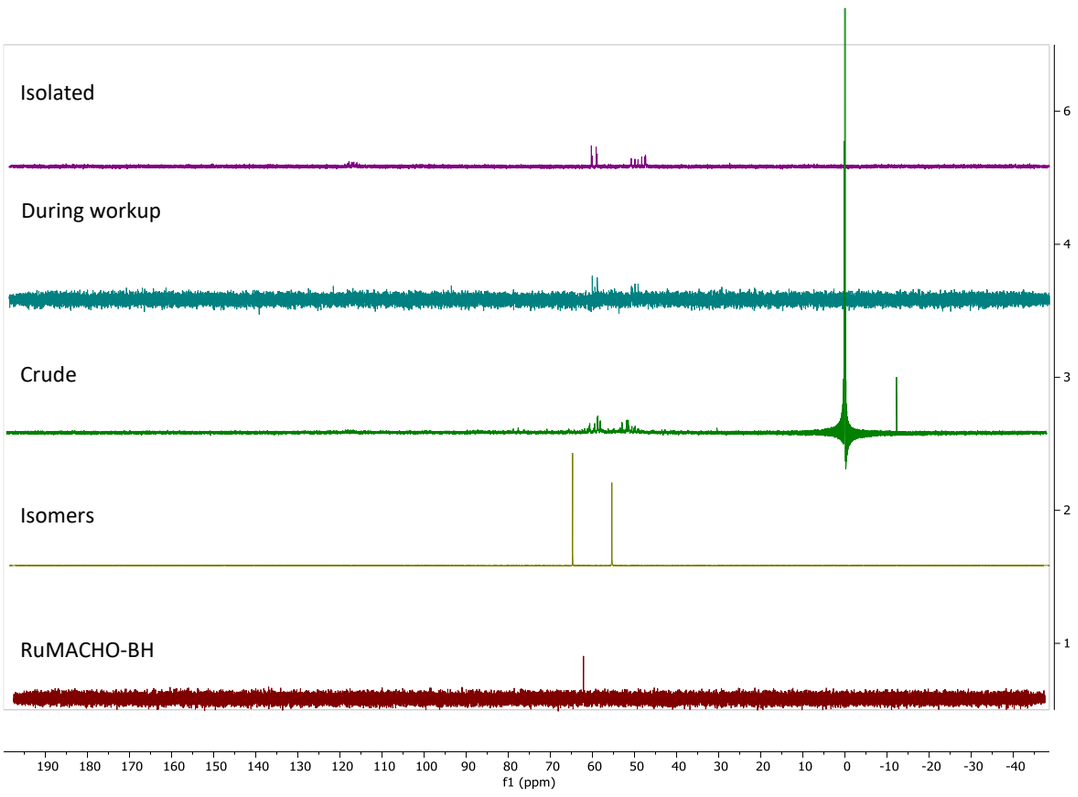

Figure S97: ^{31}P spectra of the reaction mixture over time compared to isomers and complex **10**.

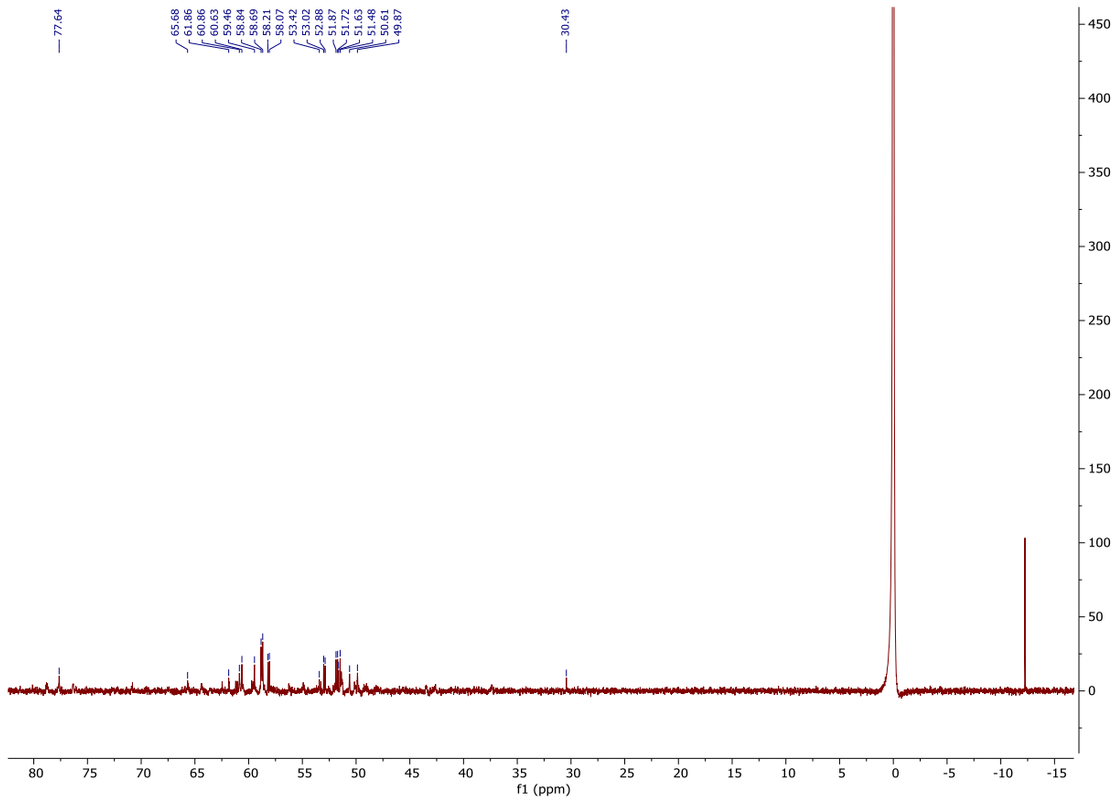

Figure S98: ^{31}P spectrum of crude reaction mixture.

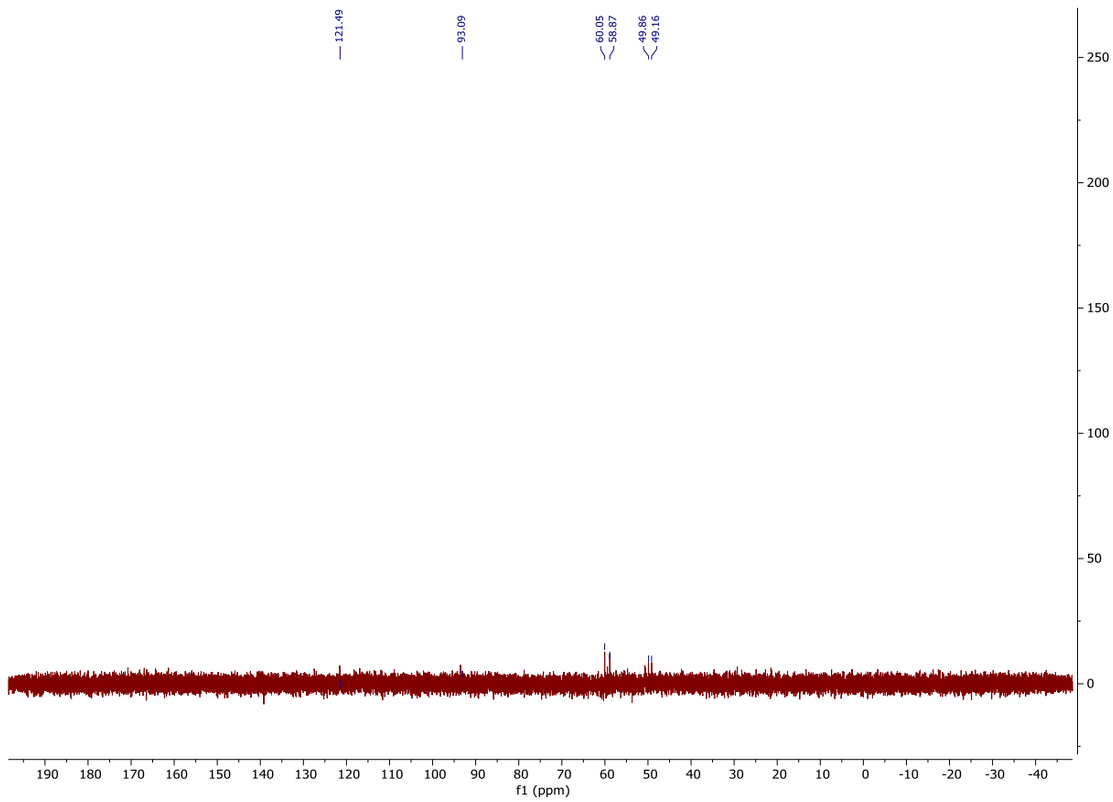

Figure S99: ^{31}P spectra of reaction mixture during workup.

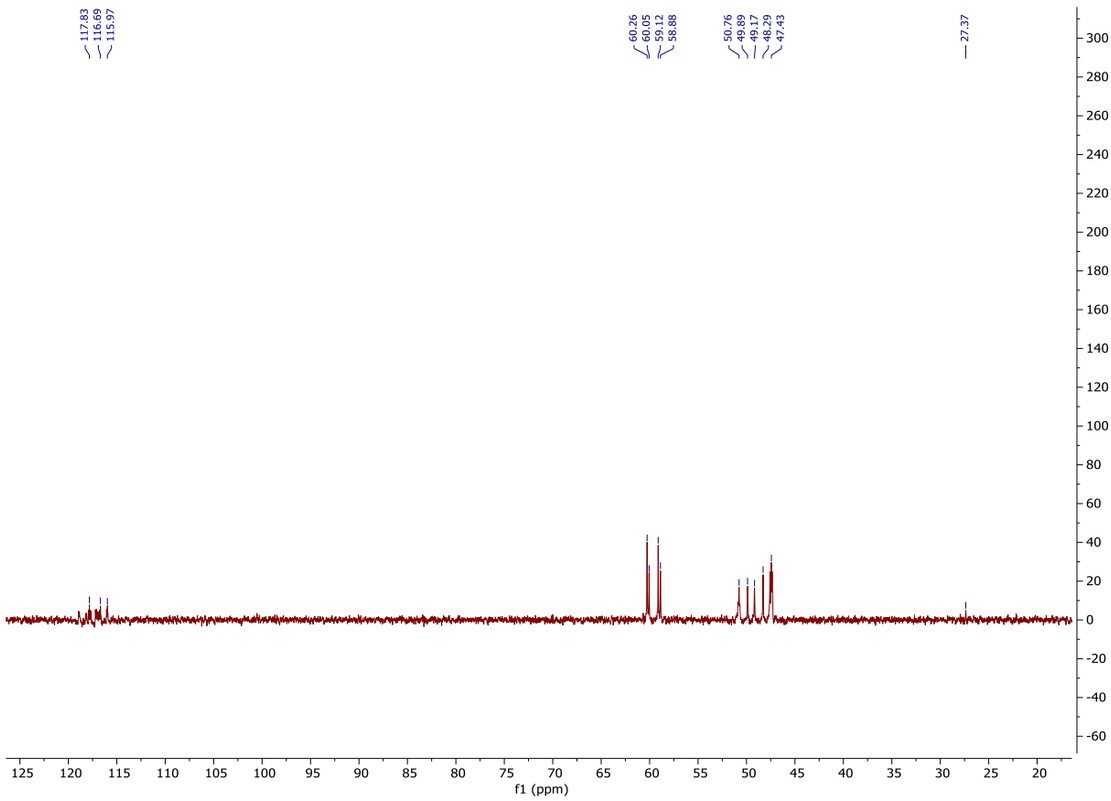

Figure S100: ^{31}P spectrum of isolated complex compound.

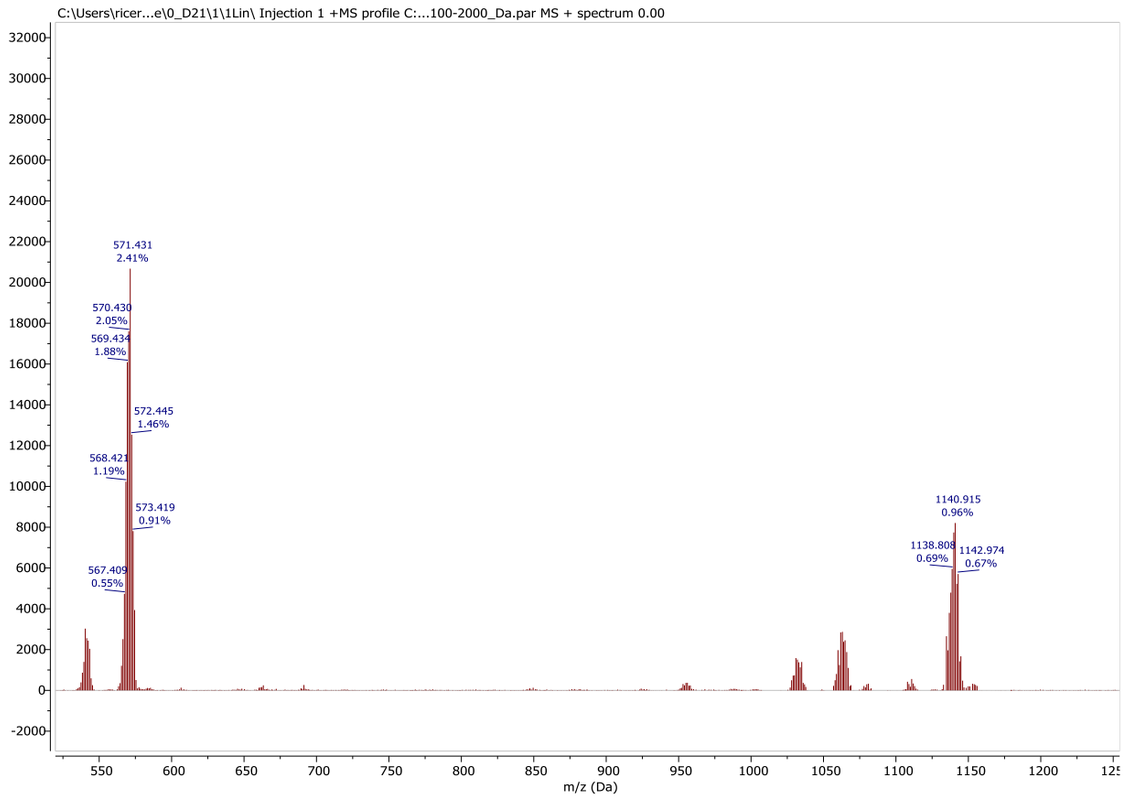

Figure S101: MALDI [M⁺] spectrum of pure product with anthracene matrix. Proposed structures below.[2]

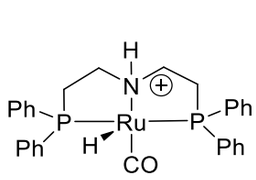

m/z = 572.08

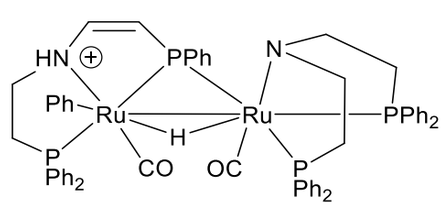

m/z = 1141.15

Treatment of RuMACHO-BH with t-BuOK

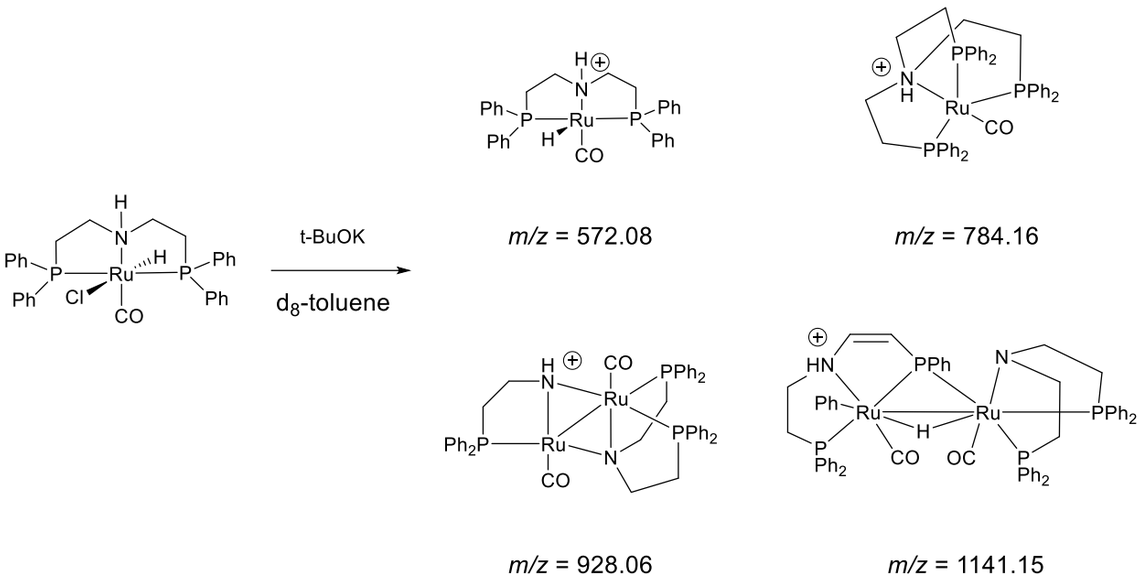

In a J. Young NMR tube, RuMACHO (**10**) was combined with potassium *tert*-butoxide in deuterated toluene and allowed to react for one week taking the solution from milky white to orange. Resulting peaks did not match those observed through our NMR experiments, MALDI peaks correspond to those observed by Anaby et al.[2]

Treatment of RuMACHO with t-BuOK Spectra

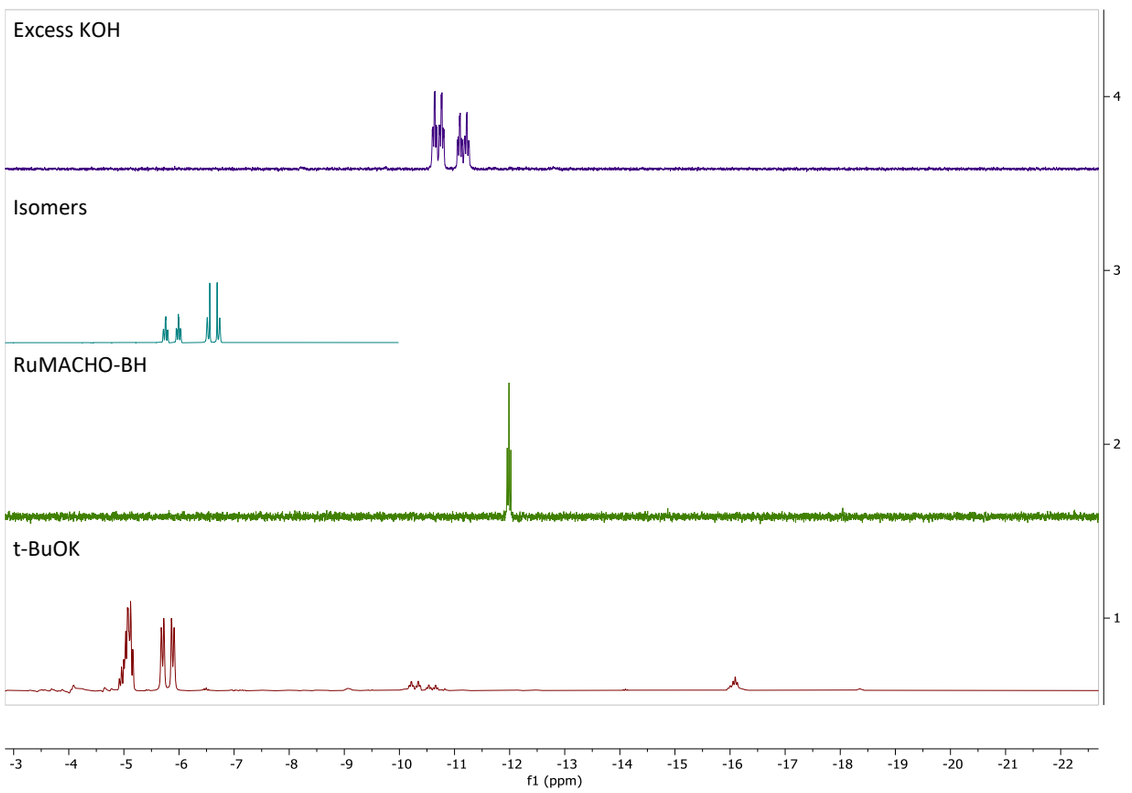

Figure S102: ^{1}H spectra of the reaction mixture compared to isomers, complex **10**, and excess potassium hydroxide reaction.

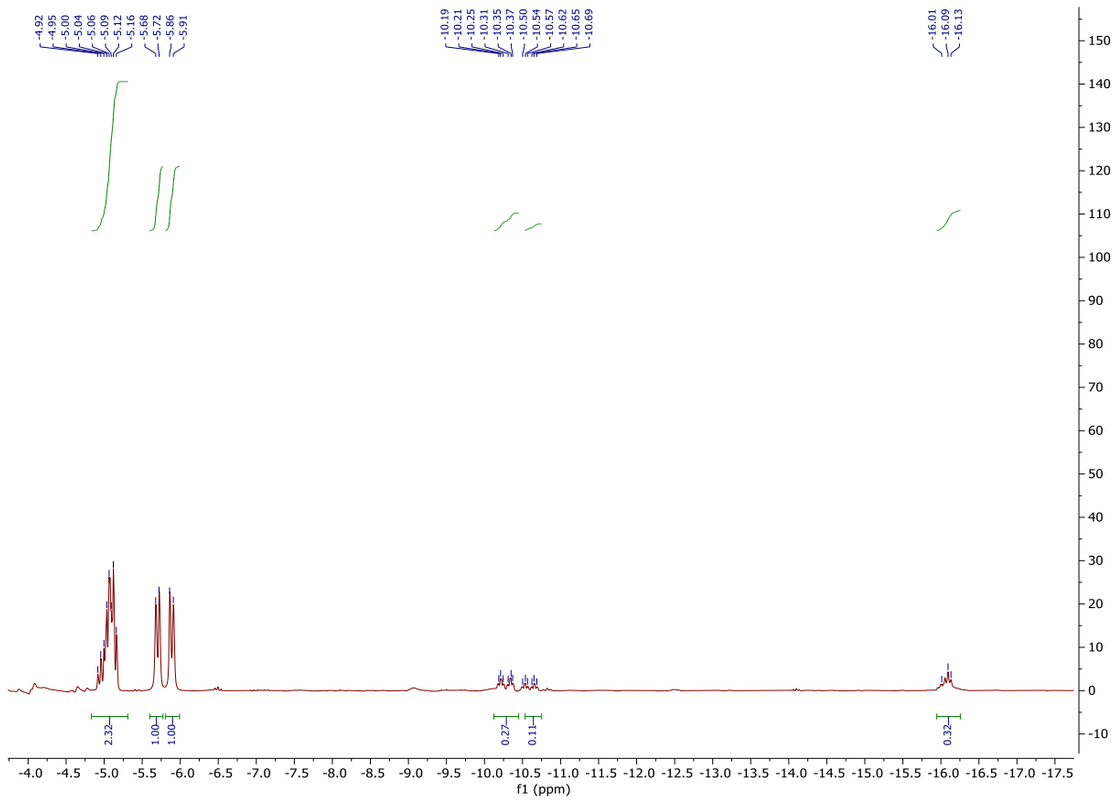

Figure S103: ^{1}H spectra of the reaction mixture in toluene-d_8.

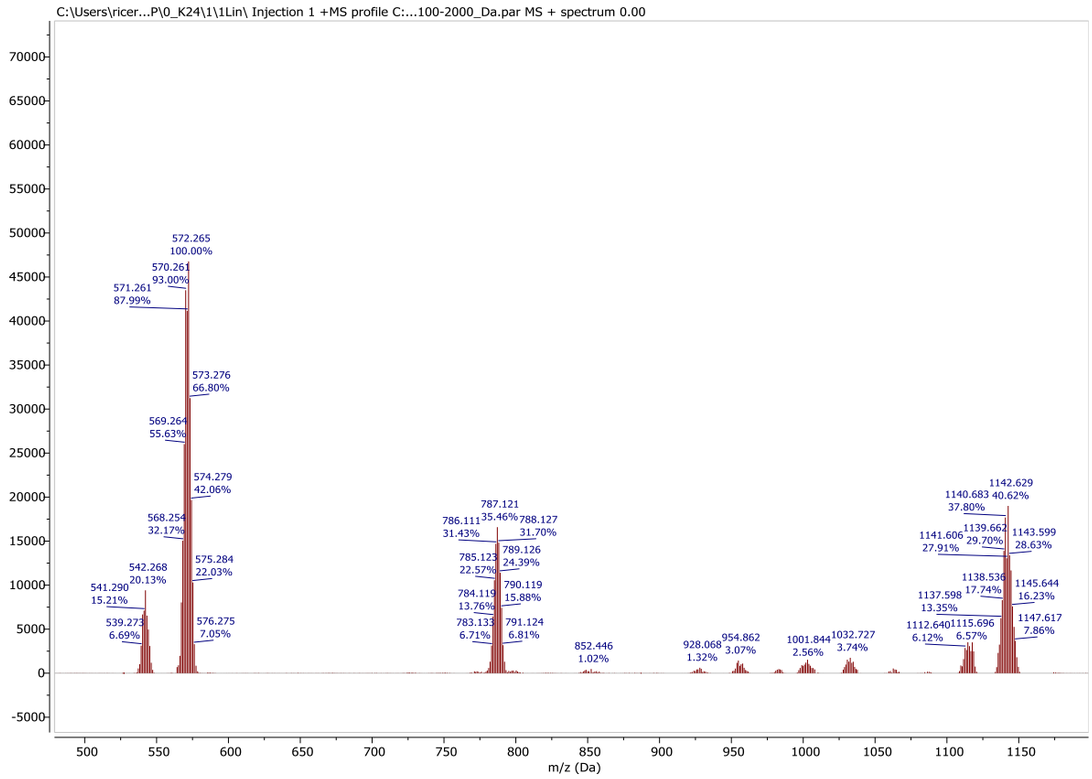

Figure S104: MALDI [M^{+}] spectrum of product mixture. Proposed structures above.[2]

Analysis of Homogeneity for Catalysis for 10

Visual inspection of ambient dehydrogenation reactions with **10** fails to show whether homogenous or heterogenous catalysis is taking place. Upon filtration of the dehydrogenation reaction mixtures (refer to **Large Scale Reactions using catalyst 10**), the color of the solution remains yellow. Upon recharging these solutions with more ethanol and potassium hydroxide, they remain catalytically active for ethanol dehydrogenation.

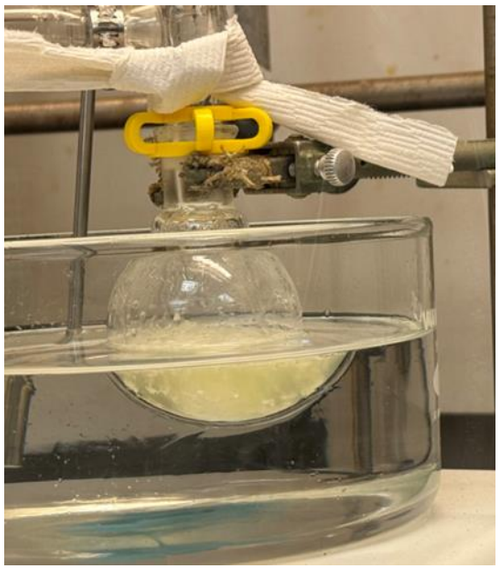

Figure S105: Reaction involving **10**.

Mercury Drop Test

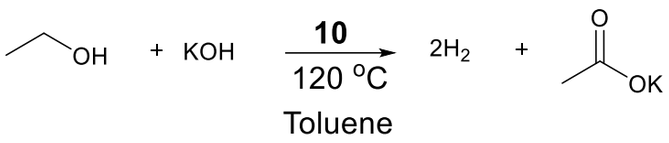

In a nitrogen filled glovebox, ground potassium hydroxide (561 mg, 8.60 mmol), **10** (0.1 mol% with respect to ethanol, 11.7 mg, 20 μmol), and ethanol (200 proof, 0.92 g, 20 mmol) were added to the round bottom flask with toluene (10 mL, distilled from benzophenone ketyl). Outside the glovebox, the flask was sealed with a condenser and septa connected via needle and tubing to a water eudiometer to determine the approximate progress of each reaction. The flask was then lowered into an oil bath at 120 °C and allowed to reflux. After 17 minutes, the reaction was paused, flask sealed, and returned to the glovebox where mercury (40 mg, 200 μmol) was added. The flask was brought out of the box and restarted. No change in catalysis under vigorous stirring was observed. The reaction passes the mercury drop test for homogenous catalysis.[3]

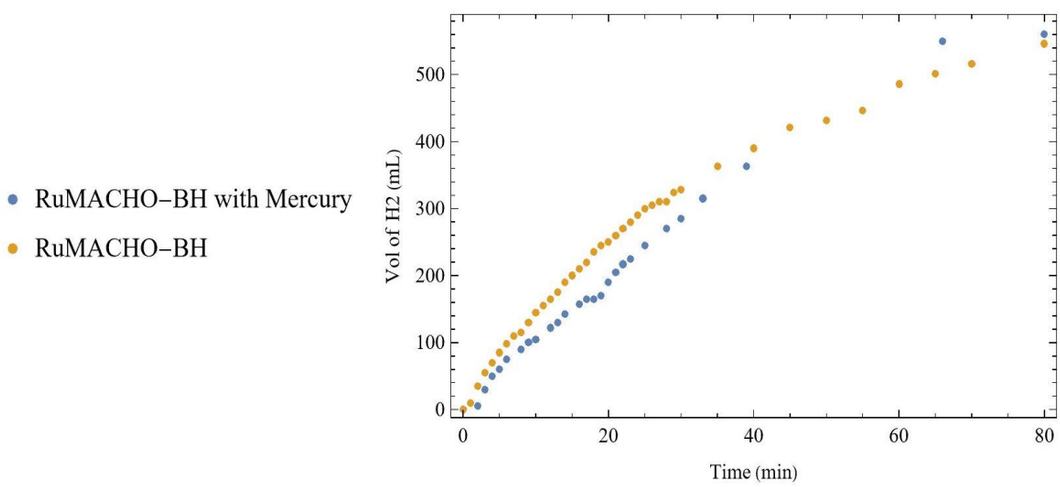

Figure S106: Volume of hydrogen produced over time for **10** with (orange trace) and without mercury (blue trace).

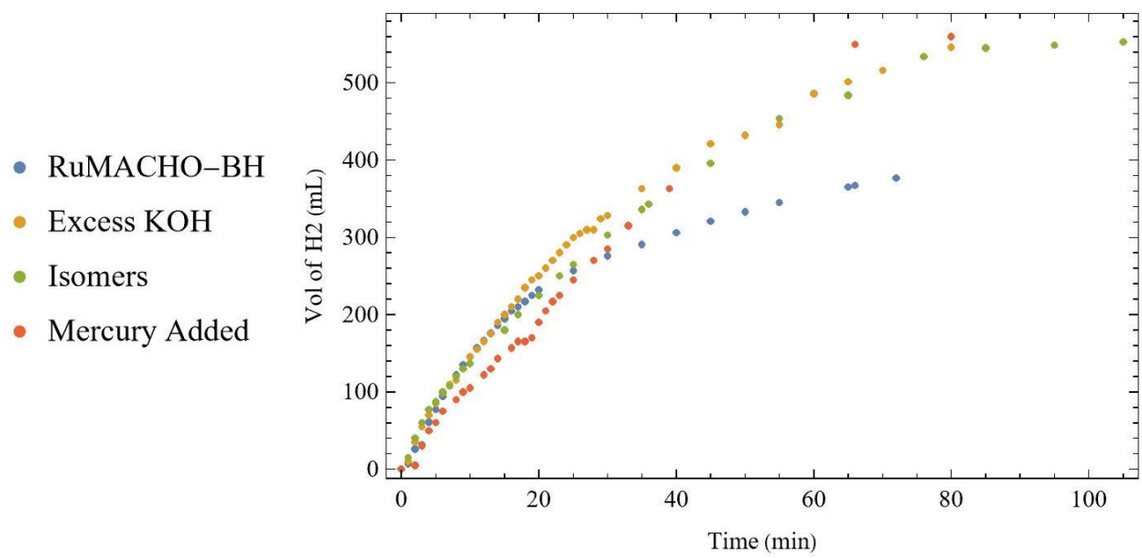

Figure S107: Reproducibility of reaction kinetics with **10**.

Preparative procedure for complex 5

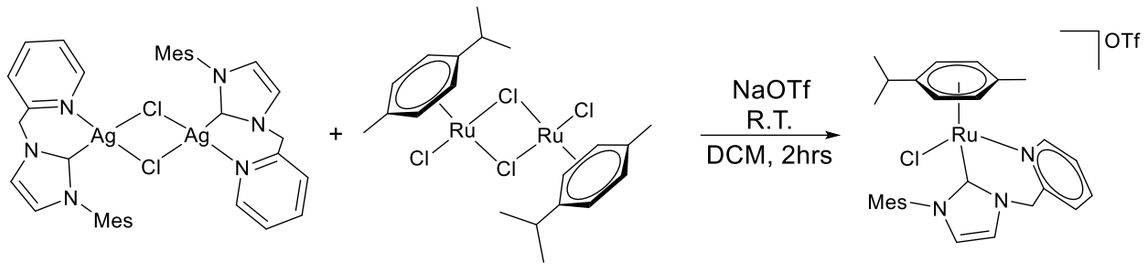

In a nitrogen filled glovebox, dichloro-di(1-(2,4,6-trimethylphenyl)-3-(2-picolyl)-imidazol-2-ylidene)-disilver(I) (125 mg, 0.150 mmol, Catapower Inc.), in dichloromethane (5 mL, dried by JC Meyer solvent purification system). This was added dropwise to a stirring solution of dichloro(p-cymene) ruthenium (II) dimer (91.9 mg, 0.15 mmol, Strem) in dichloromethane (20 mL) in a 100 mL Schlenk flask. After 1 hour, sodium trifluoromethanesulfonate (51.6 mg, 0.300 mmol, Strem) was also added to the mixture. After 30 more minutes of stirring, the solution was filtered through a dry pad of celite to remove solid products. The solvent was evaporated under reduced pressure to yield a yellow, glassy solid. This solid was dissolved in dichloromethane (5 mL), and hexanes (20 mL, dried by JC Meyer solvent purification system) was added to the solution. A deep yellow-orange crystalline solid was acquired (182 mg, 87%).

m. p. 179.3-196 °C (decomposition).

^{1}H NMR (400 MHz, acetone) δ: 9.47 (d, *J* = 5.8 Hz, 1H), 8.07 (t, *J* = 7.6 Hz, 1H), 7.89 (d, *J* = 2.1 Hz, 1H), 7.82 (d, *J* = 7.8 Hz, 1H), 7.52 (t, *J* = 6.8 Hz, 1H), 7.34 (d, *J* = 2.1 Hz, 1H), 7.16 (s, 1H), 6.98 (s, 1H), 5.96 (d, *J* = 6.3 Hz, 1H), 5.92 – 5.84 (m, 2H), 5.79 (d, *J* = 5.9 Hz, 0H), 5.55 (dd, *J* = 19.1, 6.3 Hz, 2H), 5.27 (d, *J* = 15.9 Hz, 1H), 2.35 (d, *J* = 2.0 Hz, 3H), 2.29 (d, *J* = 2.0 Hz, 3H), 1.72 (d, *J* = 2.1 Hz, 3H), 1.35 – 1.24 (m, 1H), 1.15 (dd, *J* = 6.9, 2.1 Hz, 3H), 0.61 (dd, *J* = 6.9, 2.1 Hz, 3H).

^{13}C NMR (151 MHz, CD_2Cl_2) δ: 175.22, 159.37, 156.57, 140.16, 140.00, 138.65, 135.86, 135.59, 130.13, 128.64, 125.76, 125.57, 124.88, 124.28, 109.54, 97.05, 90.27, 89.10, 87.85, 84.27, 55.28, 31.74, 23.97, 21.10, 20.36, 19.71, 18.52.

^{19}F NMR (564 MHz, CD_2Cl_2) δ: -78.87.

Elemental Analysis: Calculated: C 49.89%, H 4.91%, N 6.02%, S 4.59%, found: N 5.704%, C 49.780%, H 4.768%, S 4.705%

FTIR (KBr, cm^{-1}): 1263, 1159, 1031, 638.

MALDI MS for $C_{29}H_{34}ClN_3Ru$ calc'd 549.1640 g/mol; found m/z = 548.509 $[M]^+$.

Characterization Spectra of Complex 5

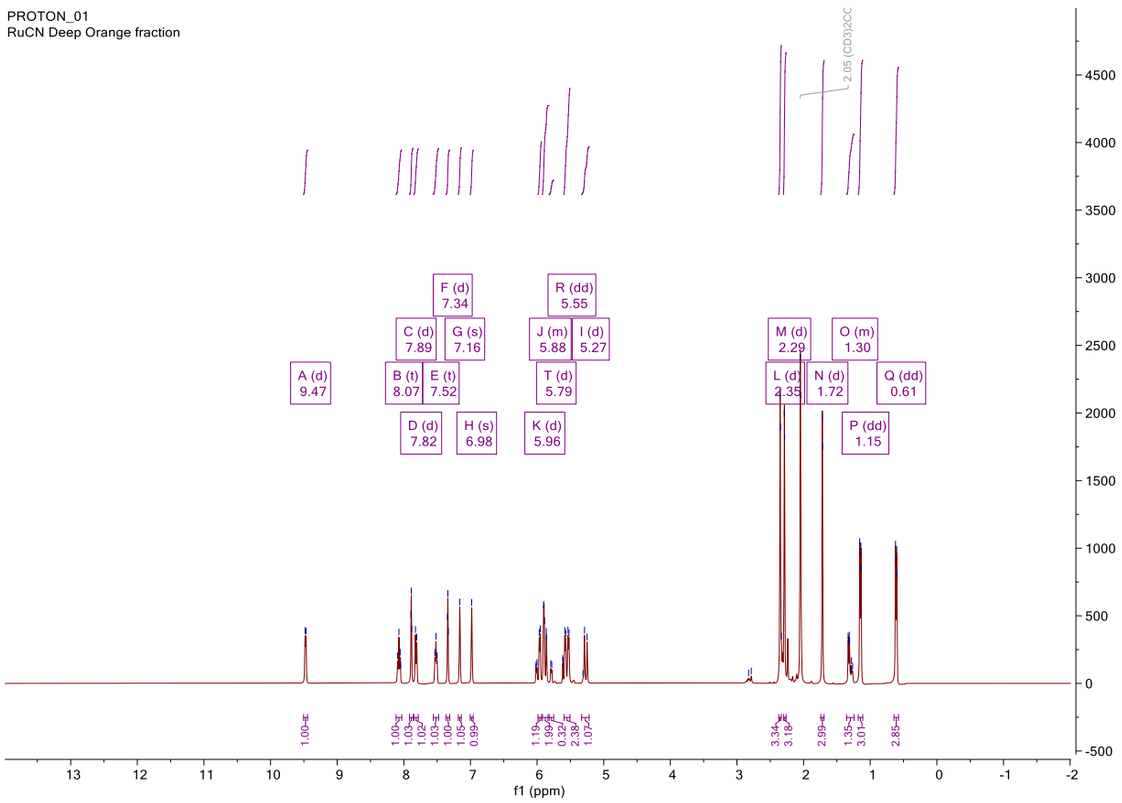

Figure S108: ^{1}H spectrum of complex **5** in acetone-d_6.

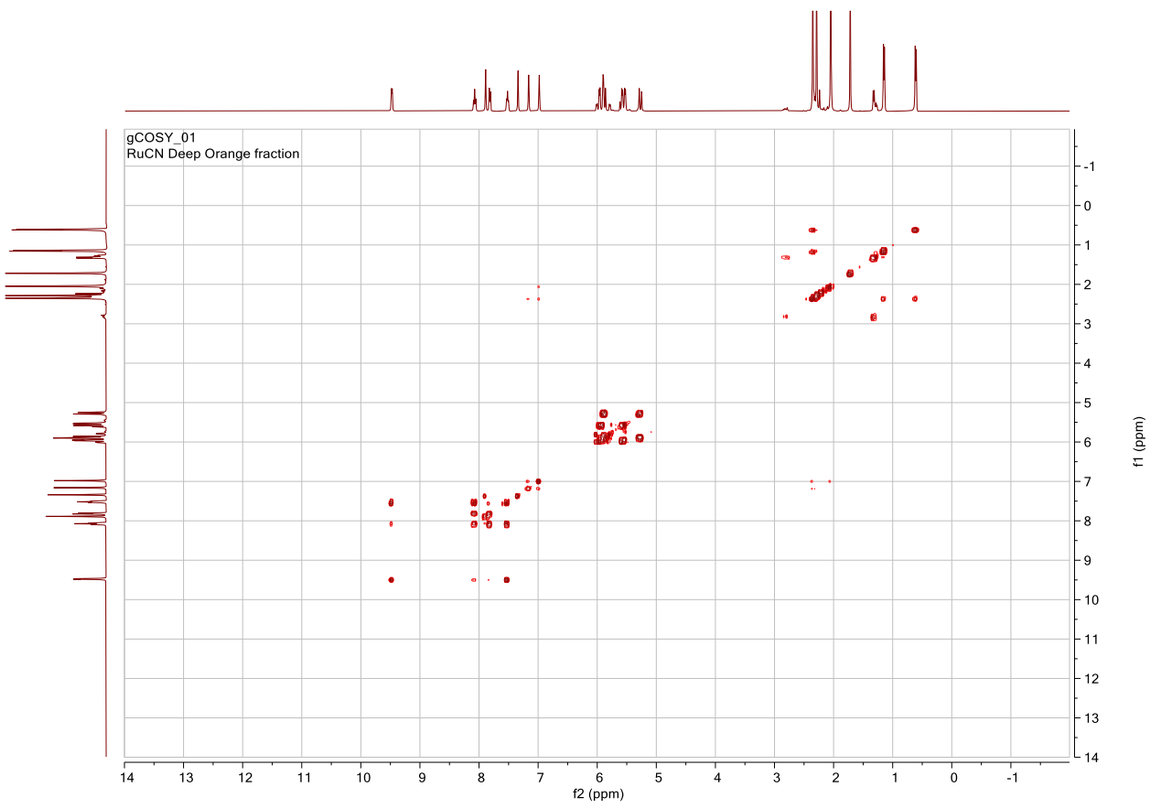

Figure S109: ^{1}H-^{1}H COSY spectrum of complex **5** in methylene dichloromethane d_2.

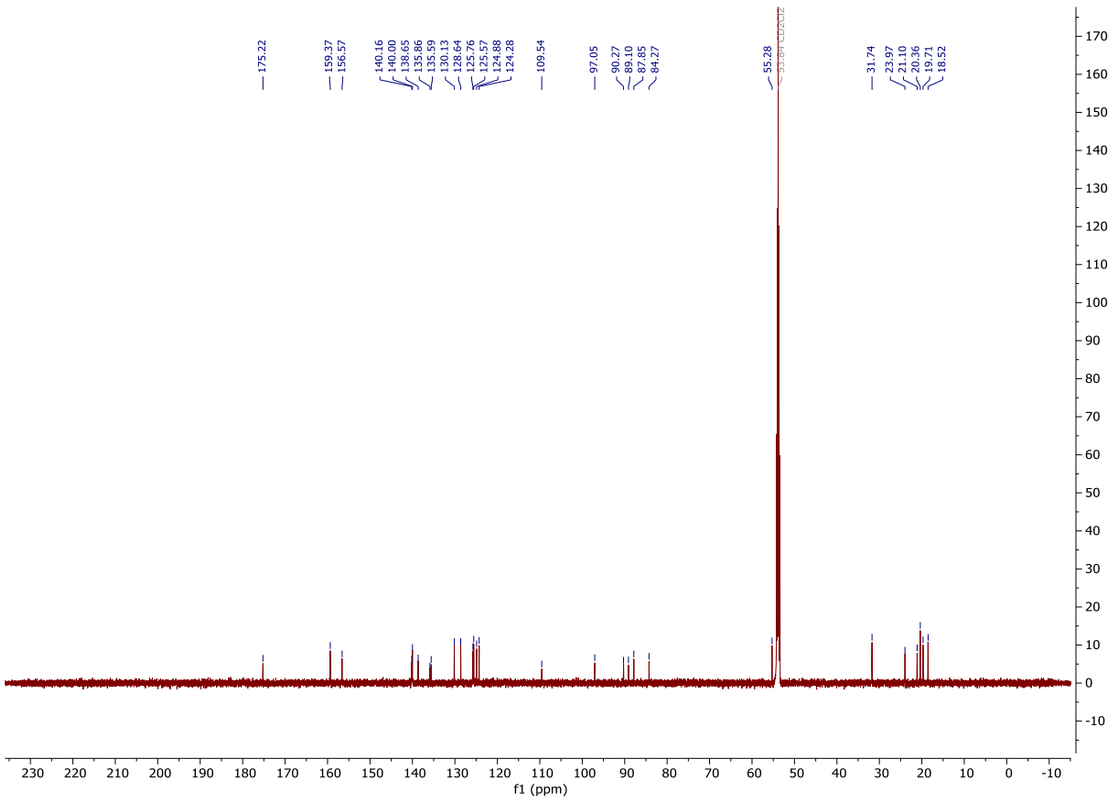

Figure S110: ^{13}C spectrum of complex **5** in dichloromethane d_2.

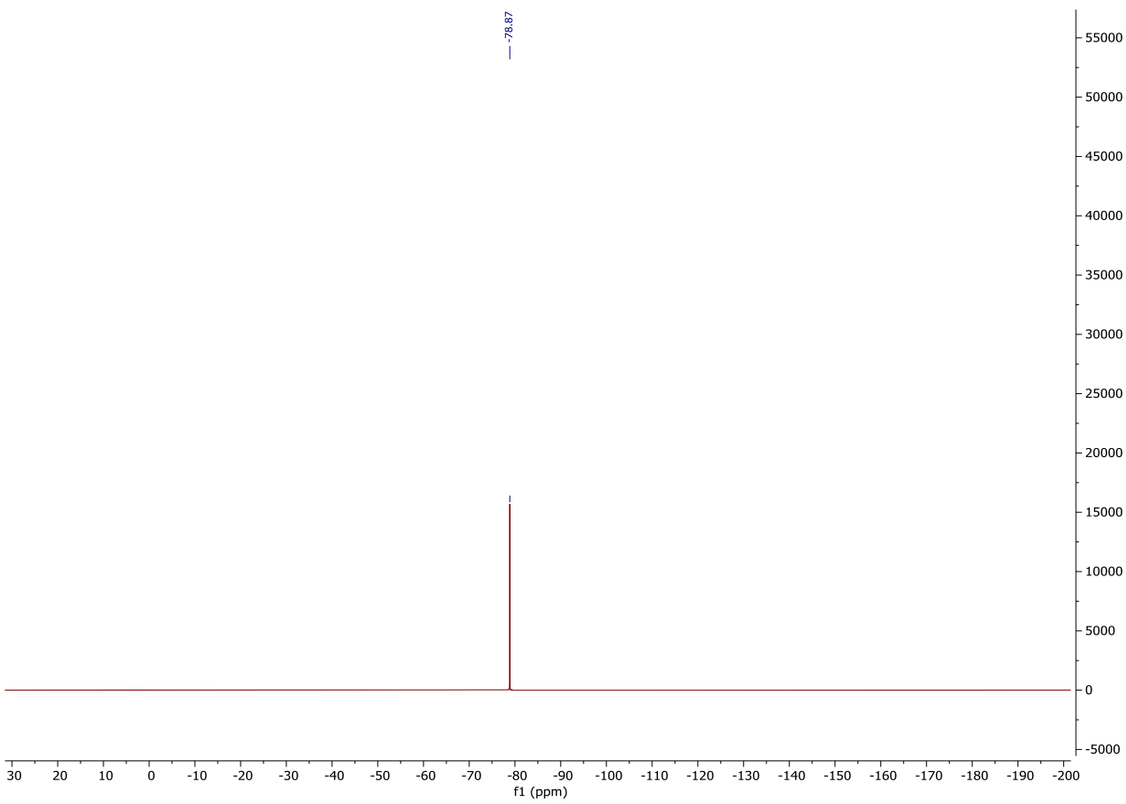

Figure S111: ^{19}F spectrum of complex **5** in dichloromethane d_2.

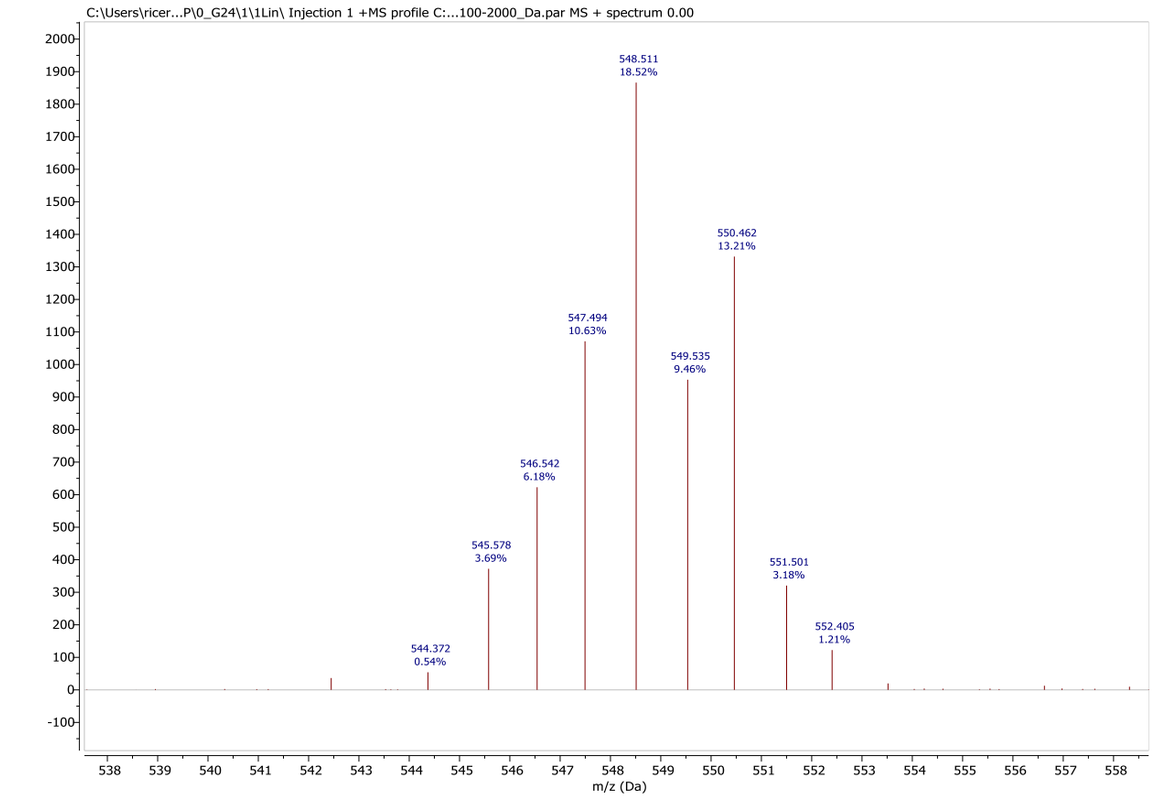

Figure S112: MALDI [M^+] spectrum of complex **5**.

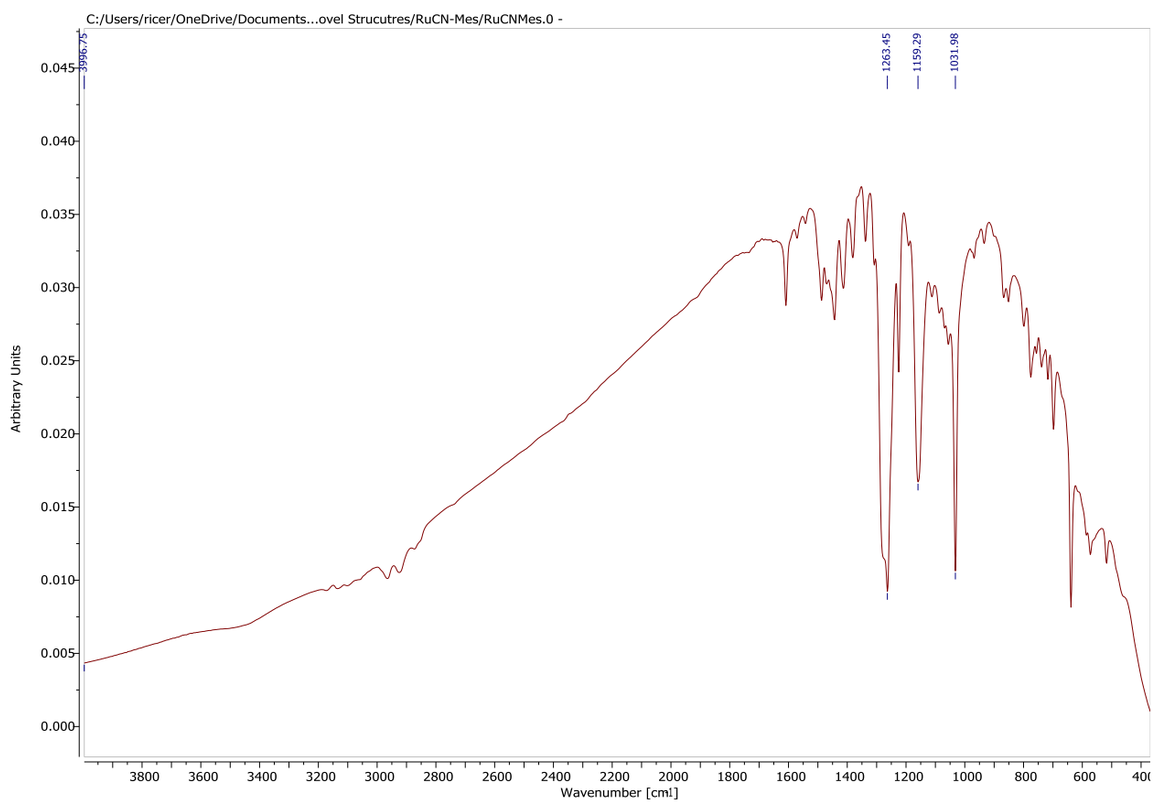

Figure S113: FTIR spectrum of complex **5**.

Preparative Procedure for complex 2

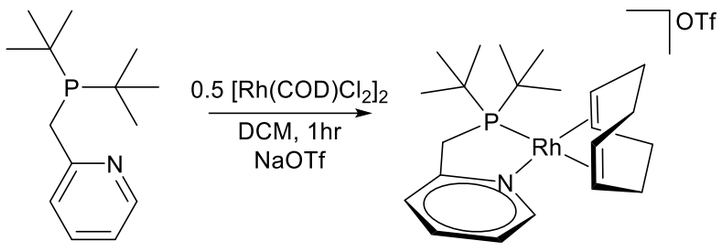

L **2**

The (pyridyl)phosphine-ligand (**L**) was synthesized using previously reported methods from our lab.[1] The ligand (245 mg, 1.03 mmol) was diluted in dichloromethane (2 mL, dried by JC Meyer solvent purification system) in a 25 mL Schlenk flask and in vial 0.5 equivalents of cyclooctadiene rhodium dimer (235 mg, 480 mmol, Strem) was suspended with one equivalent of sodium triflate (250 mg, 1.4 mmol, Aldrich) in dichloromethane (5 mL, dried by JC Meyer solvent purification system). The ligand was added slowly dropwise to the dimer and silver triflate. The resulting suspension was allowed to stir for one hour at room temperature after which the solution was evaporated to dryness under reduced pressure, filtered, and recrystallized from dichloromethane and hexanes resulting in a light yellow-orange solid (400 mg, 66.8% yield).

Melting Point: 199-199.5 °C (decomposition)

^{1}H NMR (600 MHz, CD_2Cl_2) δ 7.97 (at, J = 7.6, 1.3 Hz, 1H), 7.92 (ad, J = 5.8 Hz, 1H), 7.80 (ad, J = 8.0 Hz, 1H), 7.41 (at, J = 13.1, 6.7 Hz, 1H), 5.24 (as, 2H), 4.76 (dp, J = 4.7, 2.2 Hz, 2H), 3.56 (d, J = 9.5 Hz, 2H), 2.50 (dm, 4H), 2.38 – 2.30 (m, 2H), 2.19 (tq, J = 11.8, 4.0 Hz, 2H), 1.31 (d, J = 13.5 Hz, 18H).

^{13}C NMR (151 MHz, CD_2Cl_2) δ 164.45 (d, J = 5.8 Hz), 149.26, 141.14, 125.19 (d, J = 9.2 Hz), 124.28, 122.56 (q, J = 321.5 Hz), 120.43 (q, J = 321.5 Hz), 102.76 (dd, J = 17.0, 8.4 Hz), 76.80 (d, J = 11.8 Hz), 36.91 (d, J = 14.1 Hz), 34.19 (d, J = 19.0 Hz), 32.83 (d, J = 2.7 Hz), 30.22 (d, J = 4.1 Hz), 28.17.

^{31}P NMR (243 MHz, CD_2Cl_2) δ 64.97 (d, *J* = 144.3 Hz).

^{19}F NMR (564 MHz, CD_2Cl_2) δ -78.90 (at, *J* = 321.8, 88.6 Hz).

Elemental Analysis: Calculated: C 46.24%, H 6.07%, N 2.34%, S 5.37%; found C 46.379%, H 5.919%, N 2.468%, S 5.213%

FTIR (KBr, cm^{-1}): 2953, 1602, 1479, 1259, 1149, 1031, 833, 781, 636, 516.

MALDI MS for $C_{22}H_{35}NPRh$: Calc'd: 448.1640 g/mol; found: m/z = 448.568 $[M]^+$.

Characterization Spectra of Complex 2

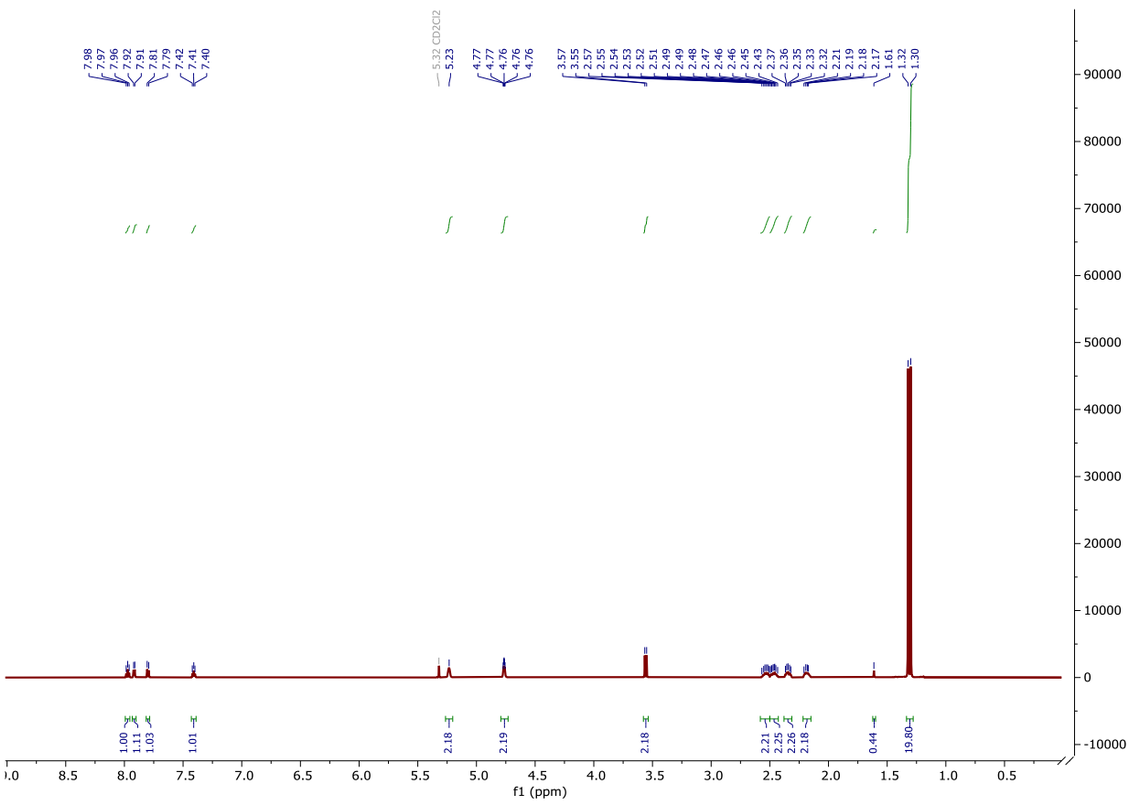

Figure S114: ^{1}H NMR spectrum of complex **2** in dichloromethane-d_2.

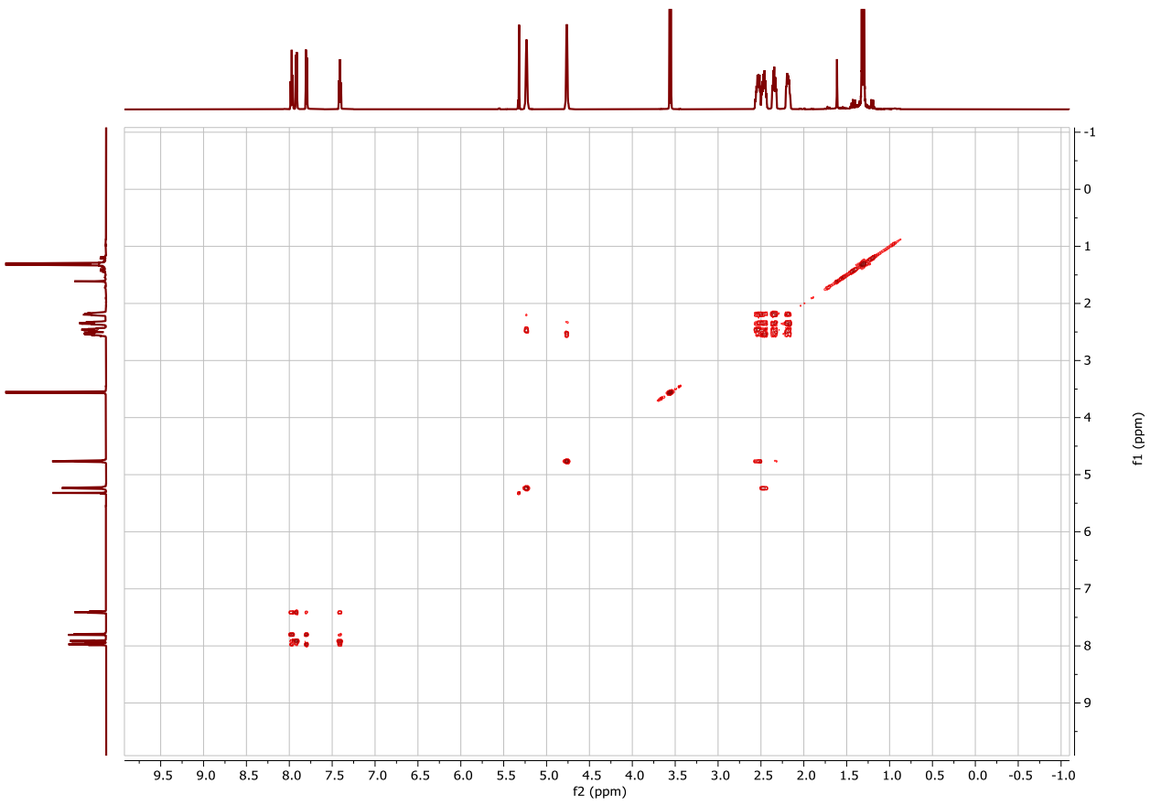

Figure S115: ^{1}H-^{1}H COSY spectrum of complex **2** in dichloromethane-d_2.

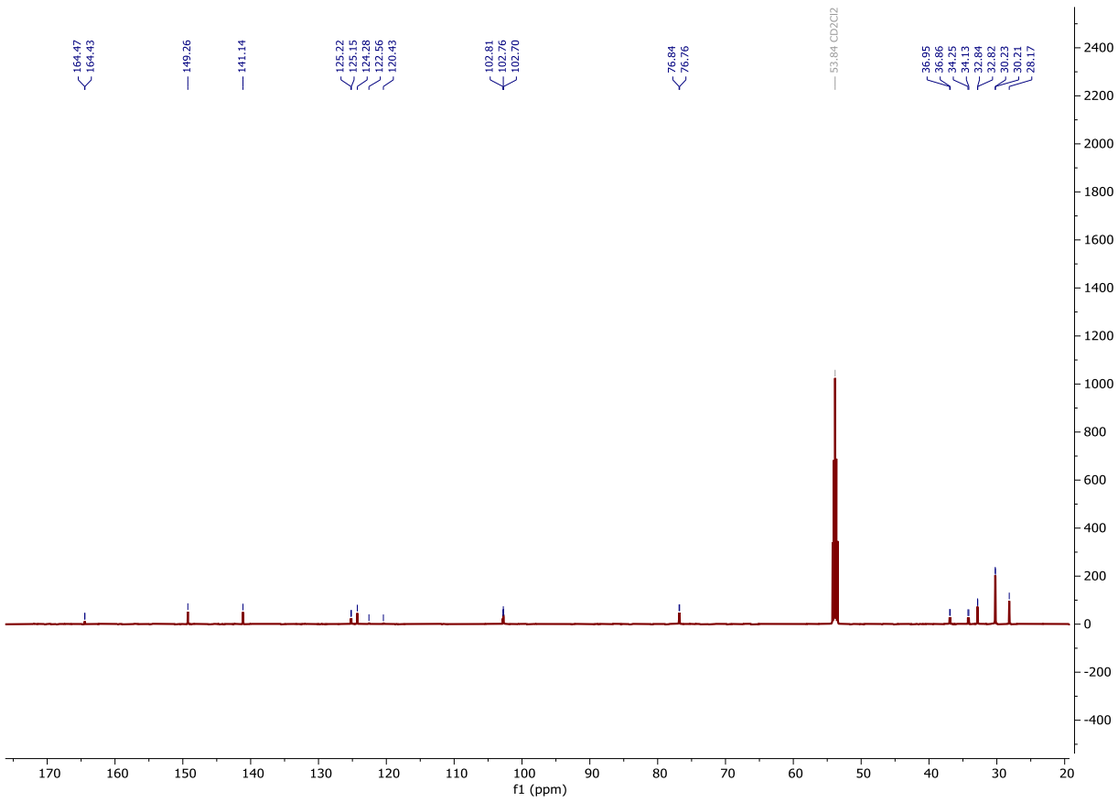

Figure S116: ^{13}C NMR spectrum of complex **2** in dichloromethane-d_2.

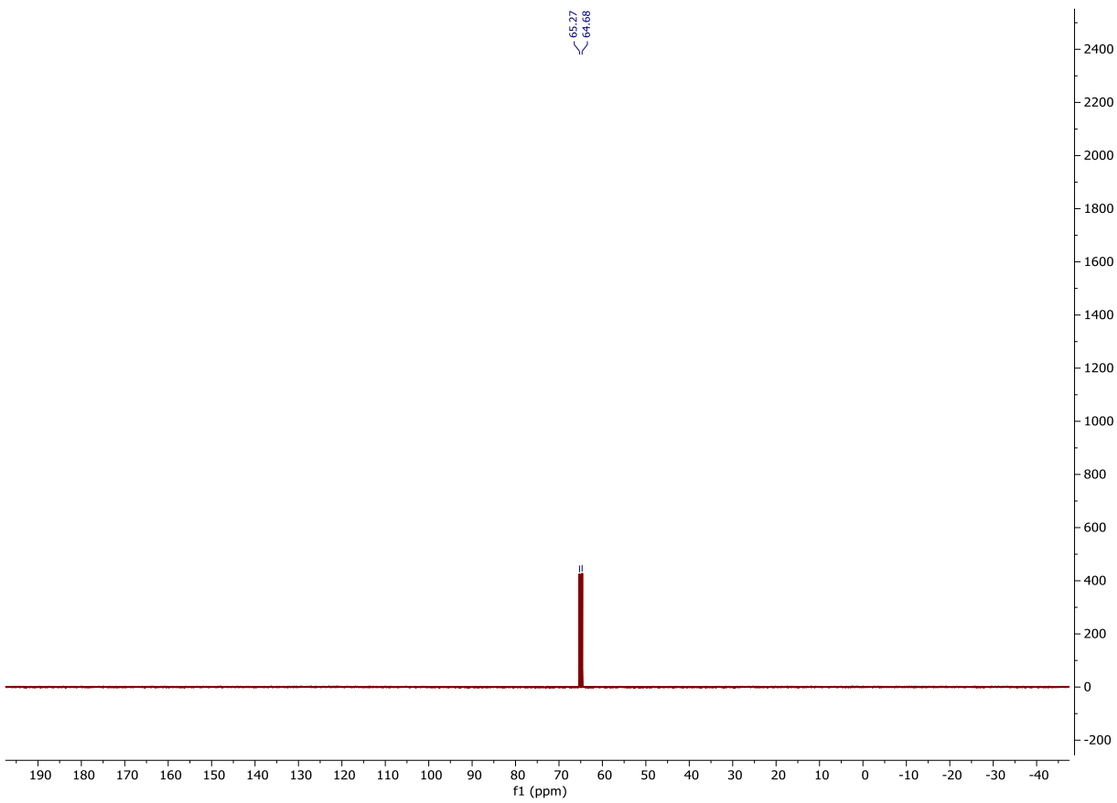

Figure S117: ^{31}P NMR spectrum of complex **2** in dichloromethane-d_2.

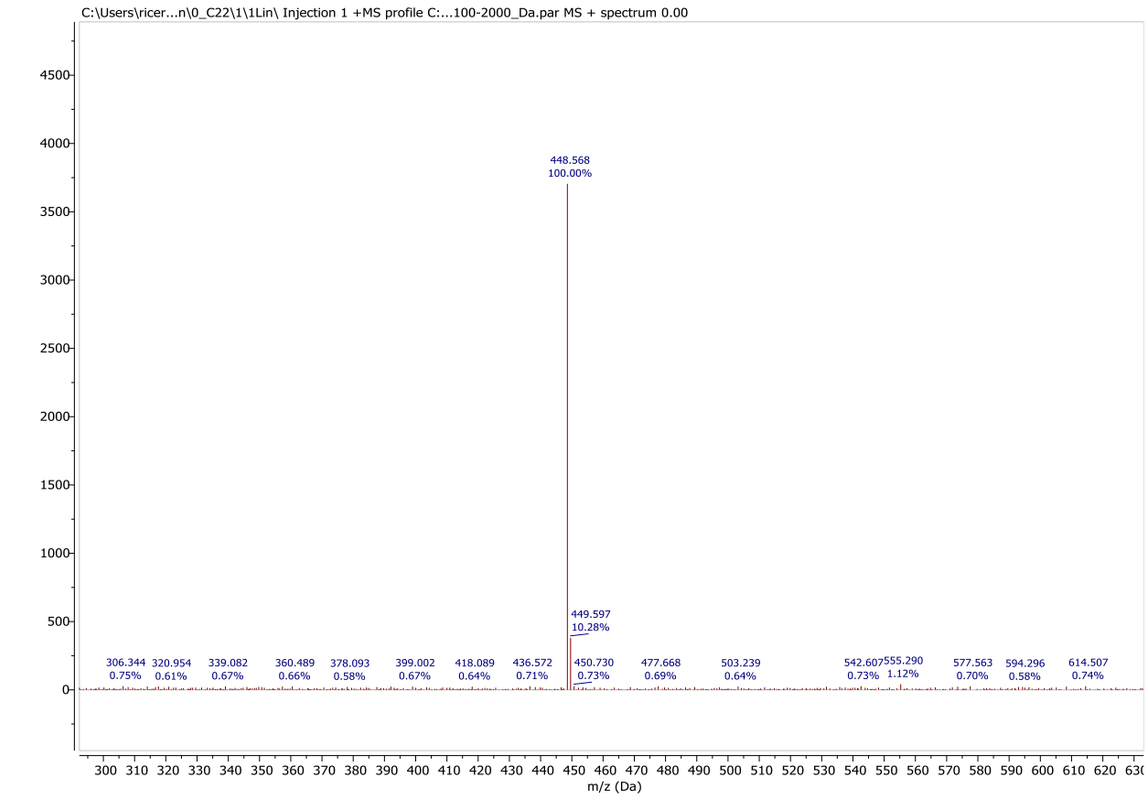

Figure S118: MALDI MS [M⁺] spectrum of complex **2**.

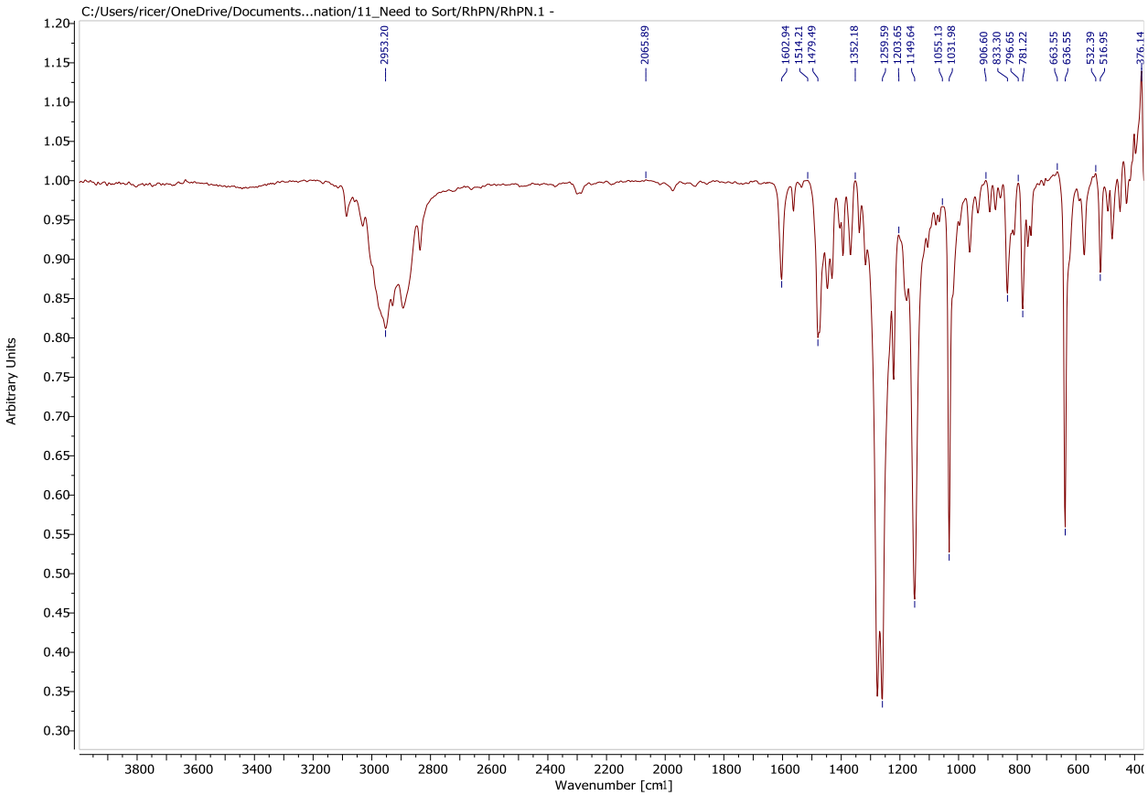

Figure S119: FTIR spectrum of complex **2**.

Preparative procedure for complex 4

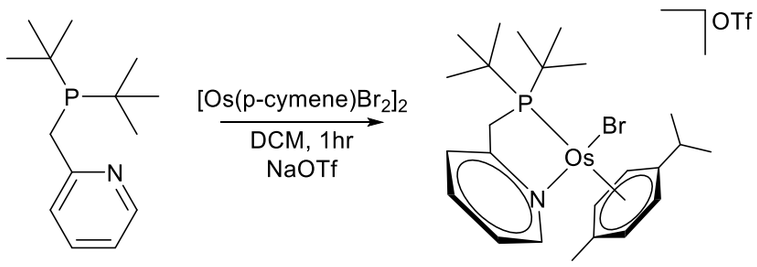

L **4**

The (pyridyl)phosphine-ligand was synthesized using previously reported methods from our lab.[1] The ligand (98 mg, 0.41 mmol) was diluted in dichloromethane (2 mL, dried by JC Meyer solvent purification system) in a 25 mL Schlenk flask and in a vial 0.5 equivalents of p-cymene osmium bromide dimer (200 mg, .207 mmol) was suspended with one equivalent of sodium triflate (142 mg, 0.826 mmol) in dichloromethane (5 mL, dried by JC Meyer solvent purification system). The ligand was added slowly dropwise to the dimer and triflate. This was allowed to stir for one hour after which the solution was evacuated to dryness, filtered, and recrystallized from dichloromethane and hexanes giving vibrant orange crystals (290 mg, 89% yield).

m. p. 215.5-239.7 °C (decomposition)

^{1}H NMR (500 MHz, CD_2Cl_2) δ 9.17 (d, *J* = 6.0 Hz, 1H), 7.84 (t, *J* = 7.7 Hz, 1H), 7.61 (d, *J* = 7.8 Hz, 1H), 7.34 (t, *J* = 6.8 Hz, 1H), 6.35 (d, *J* = 6.2 Hz, 1H), 6.29 (t, *J* = 5.0 Hz, 2H), 6.01 (d, *J* = 5.6 Hz, 1H), 3.90 – 3.76 (m, 2H), 2.85 (hept, *J* = 7.0 Hz, 1H), 2.27 (s, 3H), 1.53 (d, *J* = 14.4 Hz, 10H), 1.34 (dd, *J* = 15.7, 6.9 Hz, 7H), 1.18 (d, *J* = 13.3 Hz, 10H).

^{13}C NMR (151 MHz, CD_2Cl_2) δ 159.50, 140.57, 126.08, 124.22, 89.05, 85.48, 79.93, 77.06, 36.73, 36.56, 31.54, 31.53, 30.11, 30.09, 30.04, 24.47, 22.02, 18.17.

^{31}P NMR (202 MHz, CD_2Cl_2) δ 44.36.

^{19}F NMR (564 MHz, CD_2Cl_2) δ -78.79.

Elemental Analysis: Calculated: C 37.97%, H 4.84%, N 1.77%, S 4.05%; Found: C 38.065%, H 4.755%, N 1.772%, S 3.949%.

MALDI MS for $C_{24}H_{38}BrNOsP$: calc'd 642.1540 g/mol; found m/z = 642.384 $[M]^+$.

FTIR (KBr, cm^{-1}): 2968, 1608, 1471, 1276, 1221, 1147, 1030, 835, 636, 516.

Characterization Spectra of Complex 4

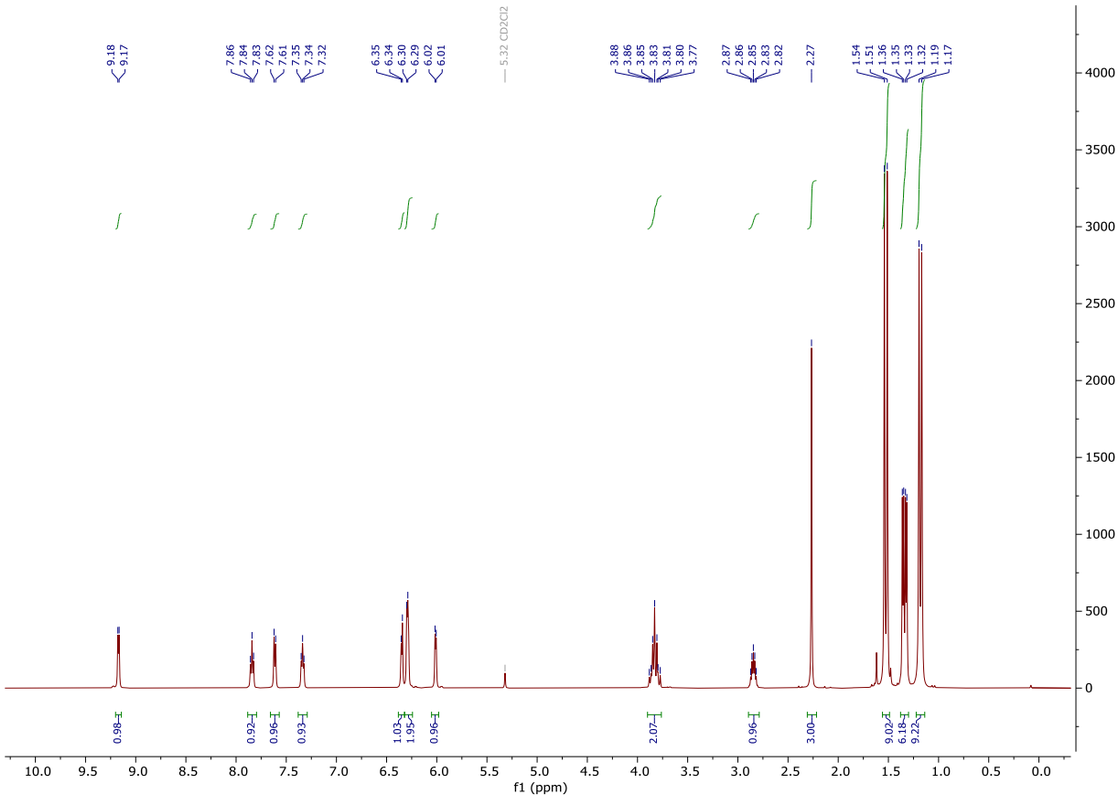

Figure S120: ^{1}H NMR spectrum of complex **4** in d_2-methylene chloride.

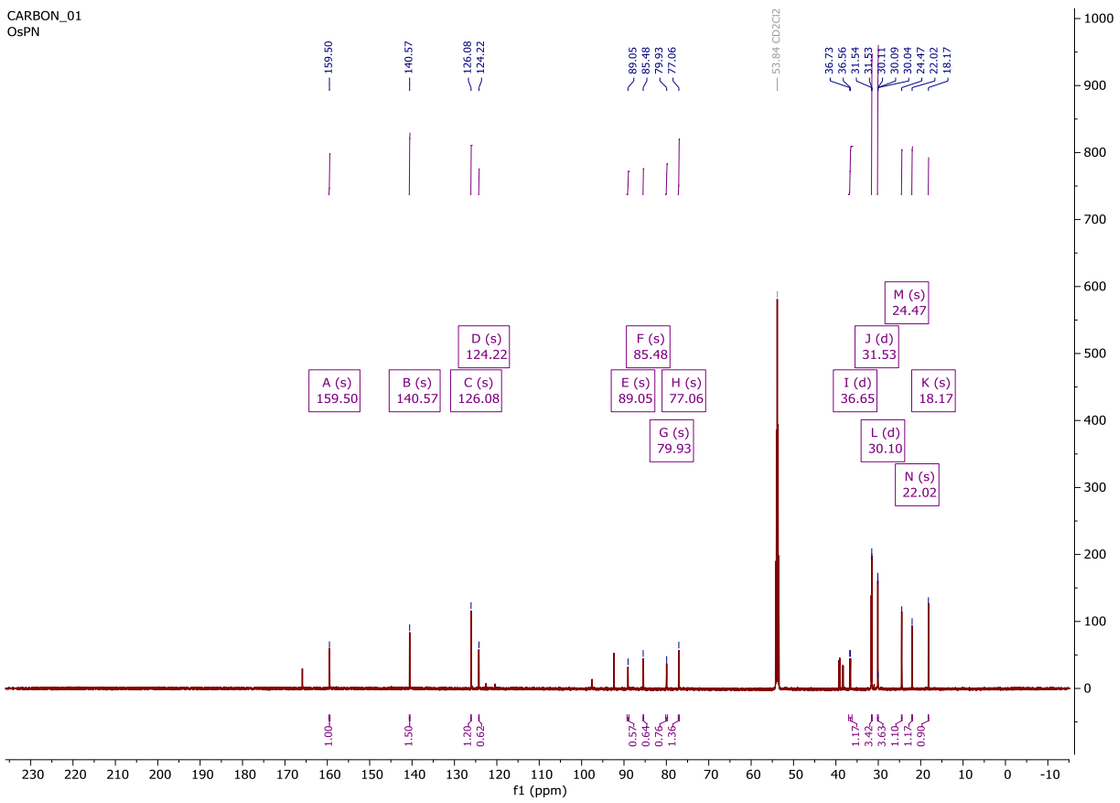

Figure S121: ^{13}C NMR spectrum of complex **4** in d_2-methylene chloride.

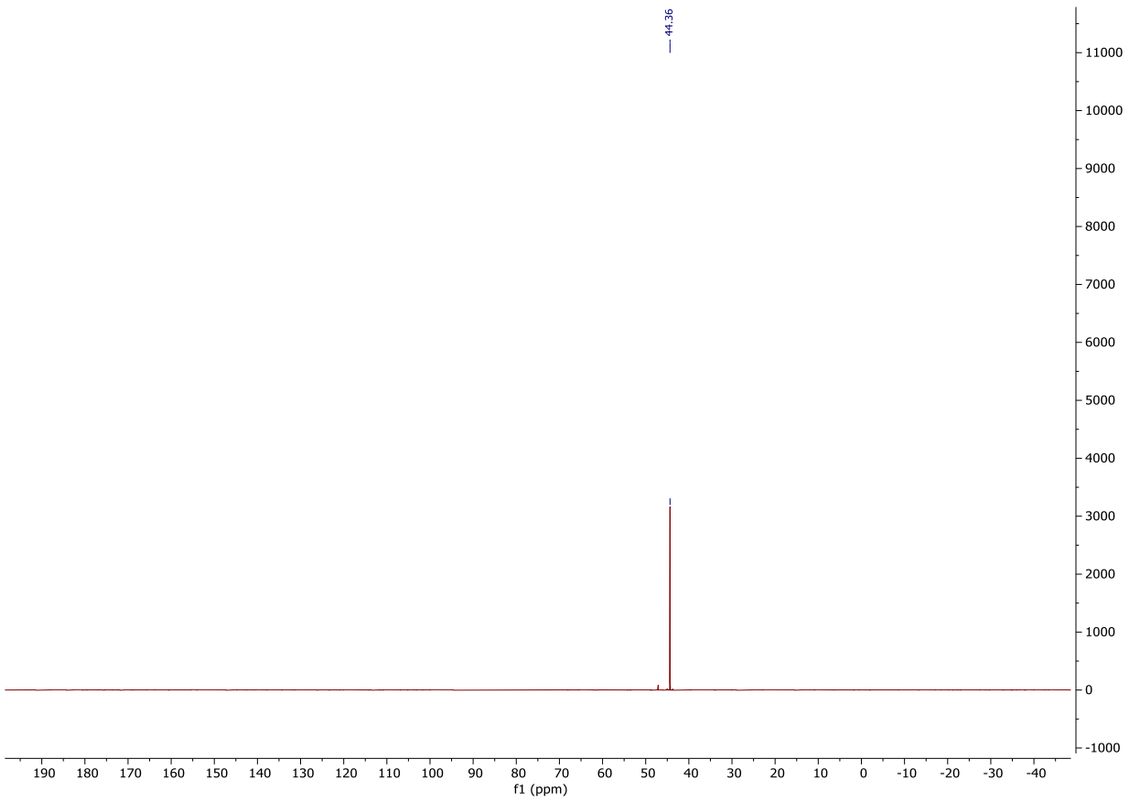

Figure S122: ^{31}P NMR spectrum of complex **4** in d_2-methylene chloride.

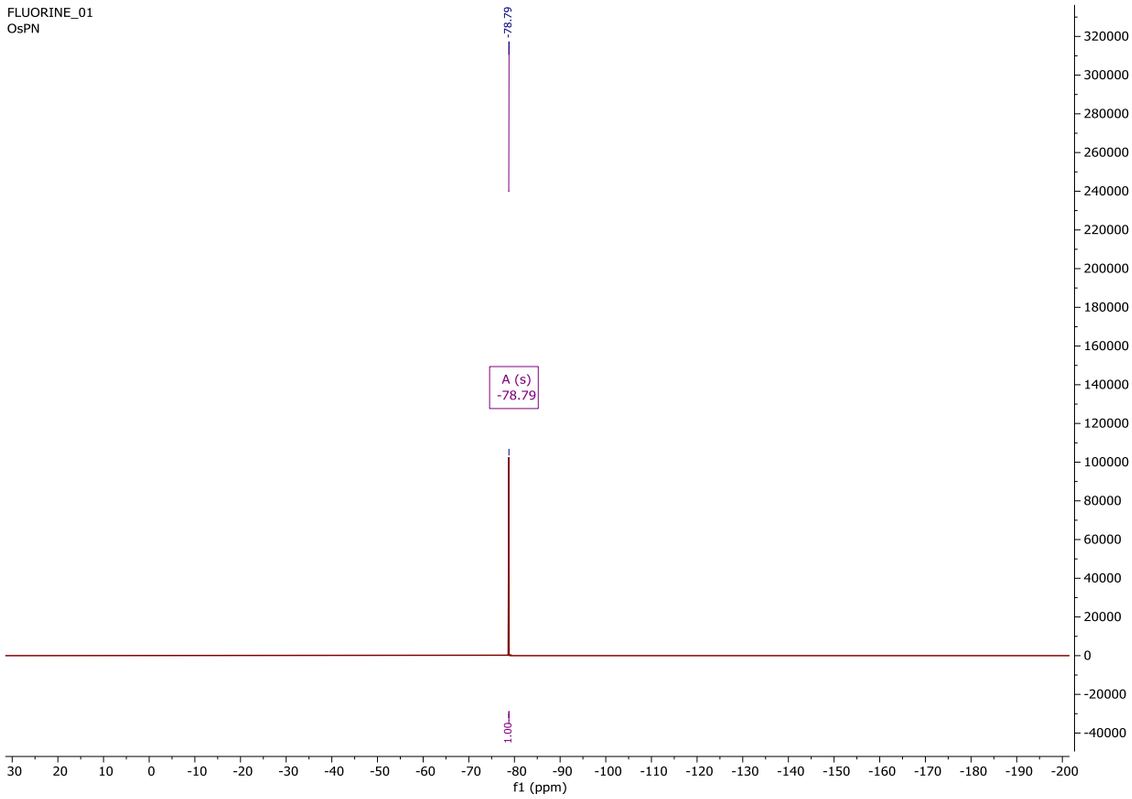

Figure S123: ^{19}F NMR spectrum of complex **4** in methylene chloride-d_2.

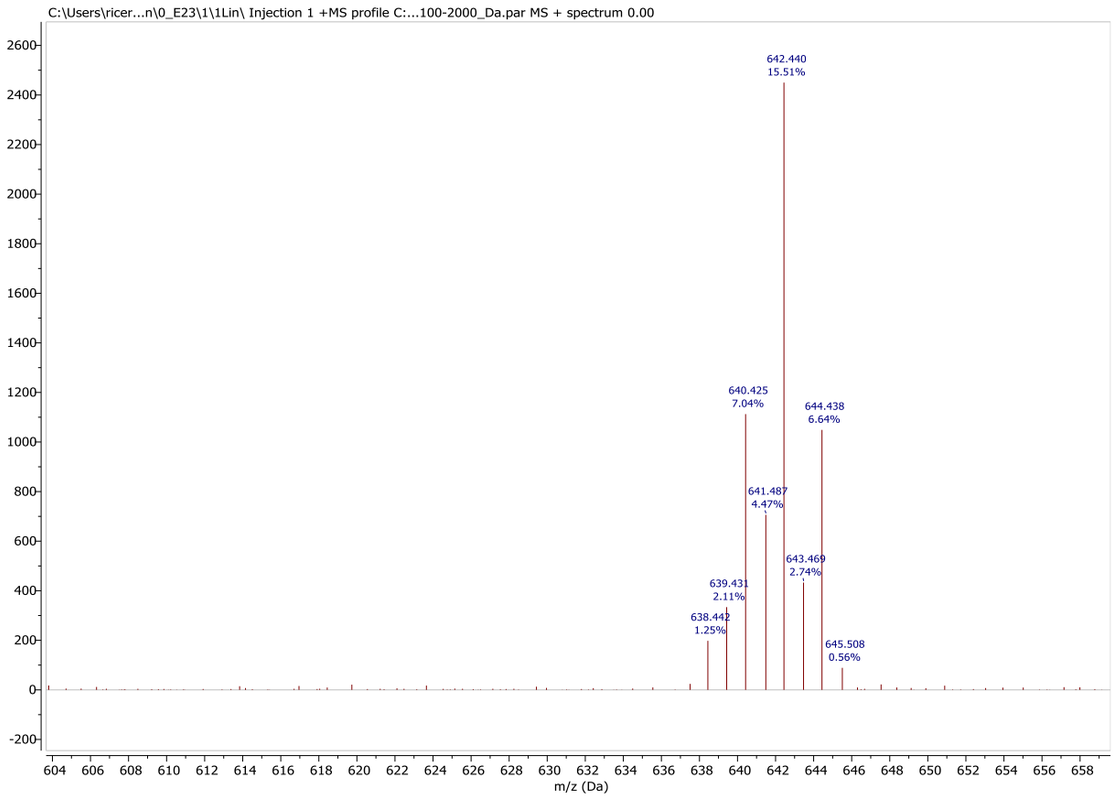

Figure S124: MALDI [M⁺] spectrum of complex **4**.

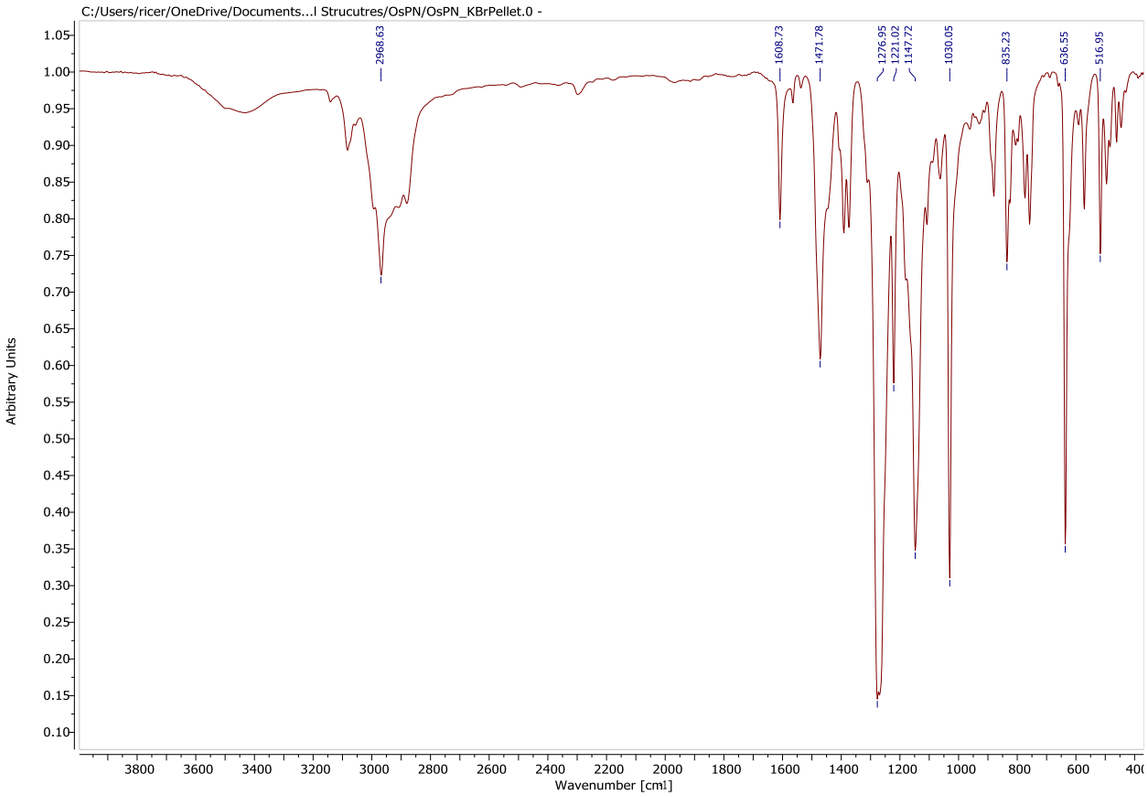

Figure S125: FTIR spectrum of complex **4**.

Crystal Structure of 5

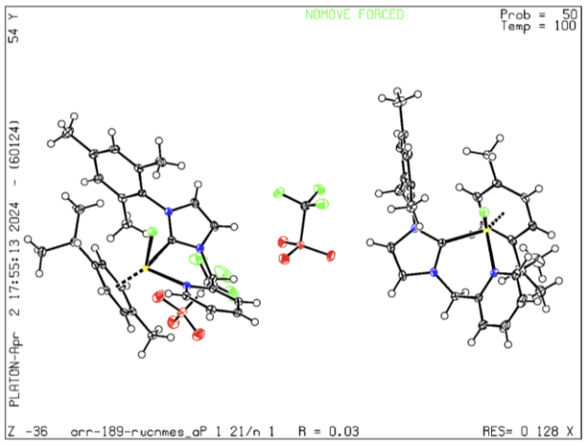

Figure S126: Molecular structure of **5** shown with 50% probability ellipsoids.

A clear yellowish prism- like crystal of $C_{58}H_{66}Cl_2F_6N_6O_6Ru_2S_2$, approximate dimensions 0.471 mm x 0.16 mm x 0.139 mm was used for X-ray crystallographic analysis grown from slow diffusion of hexanes and dichloromethane. The X-ray intensity data was collected on a XtaLAB Synergy, Dualflex, HyPix diffractometer using a Mo Kα fine-focus tube (λ = 0.71073) and kept at 100.00(10) K during data acquisition. The crystal was mounted on a MiTiGen 50um.

A total of 1248 frames were collected; the total exposure time was 3 hours and 37 minutes. The frames were integrated using Rigaku CrysAlisPro software. The integration of the data using a monoclinic crystal system resulted in 134659 reflections to a maximum θ angle of 32.472° (0.75 Å resolution), of which 18833 were independent (completeness = 88.5 % , R_{int} = 0.0493, R_{sigma} = 0.0326) and used in all calculations. The final cell constants are a = 14.4987(2) Å, b = 13.8436(2) Å, c = 29.3646(3) Å, b = 90.5070(10) °, γ = α = 90°, volume = 5893.66(13) Å^3, are based upon the refinement. Data was corrected for absorption effects using the multi -scan method. The ration of minimum to maximum apparent transmission was 0.64389.

The structure was solved using olex2.solve[4] structure solution program using Charge Flipping, and refined with the SHELXL[5] refinement package using Least Squares minimization. The space group $P2_1/n$ was used with Z = 4 for the formula unit, $C_{58}H_{66}Cl_2F_6N_6O_6Ru_2S_2$. The final R_1 = 2.70% and wR_2 = 6.01% (I>2σ(I)) while for all data R_1 = 3.65% and wR_2 = 6.35%. The goodness-of-fit was 1.038. The largest peak in the final difference electron density synthesis was 1.16 e$^-$/ Å^3 and the largest hole was -0.73 e$^-$/ Å^3. On the basis of the final model, the calculated density was 1.571 g/cm^3 and F(000), 2848.0.

Table S11: Crystal data and structure refinement for Ruthenium CN-Mesityl.

Identification code	Ruthenium CN-Mesityl
Empirical formula	$C_{58}H_{66}Cl_2F_6N_6O_6Ru_2S_2$
Formula weight	1394.32
Temperature/K	100.00(10)
Crystal system	monoclinic
Space group	$P2_1/n$
a/Å	14.4987(2)
b/Å	13.8436(2)
c/Å	29.3646(3)
α/°	90
β/°	90.5070(10)
γ/°	90
Volume/Å^3	5893.66(13)
Z	4
ρ_{calc}g/cm^3	1.571
μ/mm^{-1}	0.749
F(000)	2848.0
Crystal size/mm^3	0.471 × 0.16 × 0.139
Radiation	Mo Kα (λ = 0.71073)
2Θ range for data collection/°	4.29 to 64.944
Index ranges	-18 ≤ h ≤ 21, -20 ≤ k ≤ 20, -43 ≤ l ≤ 42
Reflections collected	134659
Independent reflections	18833 [R_{int} = 0.0493, R_{sigma} = 0.0326]
Data/restraints/parameters	18833/0/751
Goodness-of-fit on F^2	1.038
Final R indexes [I>=2σ (I)]	R_1 = 0.0270, wR_2 = 0.0601
Final R indexes [all data]	R_1 = 0.0365, wR_2 = 0.0635
Largest diff. peak/hole / e Å^{-3}	1.16/-0.73

Table S12: Fractional Atomic Coordinates (×10^4) and Equivalent Isotropic Displacement Parameters (Å^2×10^3) for Ruthenium CN-Mesityl. U_{eq} is defined as 1/3 of the trace of the orthogonalised U_{IJ} tensor.

Atom	*x*	*y*	*z*	U(eq)
Ru1	2978.9(2)	-989.8(2)	3259.3(2)	9.23(3)
Cl1	4454.7(2)	-1525.9(3)	3541.3(2)	15.31(7)
N1	3796.5(8)	2.9(9)	2887.7(4)	11.8(2)
N2	3082.9(8)	984.6(9)	3682.1(4)	12.2(2)
N3	2937.3(8)	-4.8(9)	4237.2(4)	12.2(2)
C1	4379.4(10)	-1034.0(12)	4724.5(6)	20.2(3)
C2	3374.3(10)	-1259.2(11)	4787.2(5)	14.9(3)
C3	3100.9(11)	-1951.0(11)	5102.4(5)	18.1(3)
C4	2178.1(11)	-2170.9(12)	5175.4(5)	19.3(3)
C5	1902.0(13)	-2920.0(14)	5522.0(6)	29.5(4)
C6	1512.6(10)	-1667.5(12)	4926.7(5)	18.3(3)
C7	1748.6(10)	-963.6(11)	4607.2(5)	14.5(3)
C8	991.4(10)	-409.8(12)	4366.4(5)	17.2(3)
C9	2684.8(9)	-789.9(10)	4533.1(5)	12.2(2)
C10	3027.6(10)	918.7(11)	4421.8(5)	15.7(3)
C11	3117.9(10)	1540.8(11)	4073.9(5)	15.5(3)
C12	2976.6(9)	29.0(10)	3772.1(5)	10.9(2)
C13	3047.0(10)	1405.8(10)	3227.3(5)	13.7(3)
C14	3746.9(9)	973.8(10)	2912.5(5)	12.3(2)
C15	4291.5(10)	1573.9(11)	2645.6(5)	14.4(3)
C16	4889.4(10)	1165.7(11)	2332.5(5)	16.6(3)
C17	4941.3(10)	167.3(11)	2306.9(5)	16.0(3)
C18	4397.6(9)	-389.7(11)	2589.2(5)	14.0(3)
C19	1522.8(11)	-14.1(11)	2495.1(5)	18.1(3)
C20	1812.9(9)	-873.0(10)	2775.5(5)	13.5(3)
C21	2456.6(10)	-1558.1(11)	2596.1(5)	14.2(3)
C22	2758.0(9)	-2343.3(10)	2853.0(5)	13.0(3)
C23	1473.8(9)	-1033.9(10)	3218.7(5)	12.6(3)
C24	1768.8(9)	-1847.5(10)	3481.0(5)	12.1(2)
C25	2419.2(9)	-2501.7(10)	3306.5(5)	12.6(2)
C26	2725.2(10)	-3396.9(10)	3562.5(5)	14.6(3)
C27	1986.1(11)	-4175.7(11)	3483.4(6)	19.4(3)
C28	2902.5(11)	-3246.5(12)	4069.6(5)	20.3(3)
Ru2	7834.7(2)	8724.6(2)	3634.6(2)	9.91(3)
Cl2	9263.8(2)	7840.8(3)	3605.0(2)	16.30(7)
N4	8004.7(8)	8835.2(9)	2920.7(4)	13.0(2)
N5	6516.2(8)	7480.5(9)	3109.4(4)	12.5(2)
N6	6924.5(8)	6652.5(9)	3691.2(4)	13.7(2)
C29	8579.9(13)	5380.9(15)	5363.4(6)	29.6(4)
C30	8133.3(11)	5693.8(12)	4921.7(5)	20.1(3)
C31	8576.0(11)	5548.0(11)	4509.3(5)	19.2(3)
C32	8186.4(10)	5833.0(11)	4095.9(5)	15.8(3)
C33	8641.5(11)	5555.5(12)	3656.8(5)	20.6(3)
C34	7341.1(10)	6313.6(11)	4109.1(5)	14.5(3)
C35	6843.4(10)	6420.1(11)	4512.3(5)	16.6(3)
C36	5871.1(11)	6810.9(13)	4512.3(6)	22.0(3)
C37	7260.4(11)	6112.8(12)	4916.7(5)	19.7(3)
C38	6247.6(10)	6126.5(11)	3461.6(5)	18.4(3)
C39	5991.8(10)	6646.1(11)	3097.3(5)	17.6(3)
C40	7084.3(9)	7508.4(10)	3477.7(5)	11.3(2)
C41	6425.7(10)	8276.3(11)	2790.0(5)	13.9(3)
C42	7348.3(10)	8579.9(10)	2614.5(5)	13.7(3)
C43	7509.3(12)	8600.0(11)	2148.6(5)	19.9(3)
C44	8361.6(13)	8893.7(13)	1992.2(6)	26.8(4)
C45	9023.6(12)	9182.9(13)	2305.1(6)	25.4(3)
C46	8826.0(10)	9146.7(12)	2764.3(6)	18.9(3)
C47	8677.2(11)	8453.7(12)	4686.4(5)	19.2(3)
C48	8113.0(10)	9048.6(11)	4360.3(5)	15.5(3)
C49	7165.0(10)	8869.0(11)	4295.5(5)	16.0(3)

Table S12: Fractional Atomic Coordinates (×10^4) and Equivalent Isotropic Displacement Parameters (Å^2×10^3) for Ruthenium CN-Mesityl. U_{eq} is defined as 1/3 of the trace of the orthogonalised U_{IJ} tensor.

Atom	*x*	*y*	*z*	U(eq)
C50	6641.0(10)	9388.6(11)	3961.5(5)	15.8(3)
C51	8525.0(10)	9805.3(11)	4097.0(5)	15.8(3)
C52	8017.8(10)	10321.5(11)	3773.3(5)	15.6(3)
C53	7059.3(10)	10106.5(11)	3693.2(5)	15.3(3)
C54	6477.5(11)	10705.5(11)	3367.3(6)	20.6(3)
C55	6078.3(14)	11546.4(15)	3643.7(7)	36.4(5)
C56	6992.2(12)	11079.9(12)	2950.6(6)	26.0(4)
S1	69.4(3)	1970.1(3)	3258.3(2)	17.07(7)
F1	337.6(9)	3676.0(9)	3620.5(5)	44.6(3)
F2	1501.8(8)	2729.2(12)	3667.3(5)	54.5(4)
F3	341.9(10)	2516.4(11)	4102.7(4)	47.7(3)
O1	313.8(10)	1014.8(9)	3410.8(4)	32.1(3)
O2	497.4(9)	2274.9(10)	2840.7(4)	28.7(3)
O3	-897.7(8)	2200.2(10)	3286.2(5)	28.4(3)
C58	590.1(12)	2764.7(14)	3685.3(6)	26.6(4)
S2	4201.6(2)	4012.4(3)	3731.2(2)	12.34(6)
F4	4890.0(7)	2930.2(7)	4386.4(3)	22.8(2)
F5	5875.3(6)	3909.9(8)	4090.6(3)	25.8(2)
F6	4838.2(7)	4448.7(8)	4546.4(3)	25.3(2)
O4	4440.5(8)	4968.9(8)	3579.7(4)	19.4(2)
O5	3307.7(7)	3908.5(8)	3937.8(4)	19.3(2)
O6	4438.4(8)	3248.8(8)	3417.7(4)	20.0(2)
C57	4990.1(10)	3818.1(11)	4213.1(5)	16.3(3)

Table S13: Anisotropic Displacement Parameters (Å^2×10^3) for Ruthenium CN-Mesityl. The Anisotropic displacement factor exponent takes the form: $-2\pi^2[h^2a^{*2}U_{11}+2hka^*b^*U_{12}+\ldots]$.

Atom	U_{11}	U_{22}	U_{33}	U_{23}	U_{13}	U_{12}
Ru1	8.55(5)	9.41(5)	9.75(5)	-1.05(4)	0.66(4)	-0.75(4)
Cl1	10.70(14)	17.46(16)	17.75(16)	0.68(12)	-1.04(11)	1.23(12)
N1	11.3(5)	12.8(5)	11.3(5)	-0.7(4)	0.4(4)	-1.3(4)
N2	13.8(5)	10.8(5)	12.0(5)	-1.3(4)	2.1(4)	-0.4(4)
N3	13.7(5)	11.7(5)	11.1(5)	-1.1(4)	0.3(4)	-0.8(4)
C1	14.6(7)	25.0(8)	20.9(7)	0.3(6)	-3.5(5)	-0.6(6)
C2	15.5(6)	16.6(7)	12.6(6)	-2.5(5)	-1.8(5)	0.8(5)
C3	20.7(7)	18.4(7)	15.1(7)	1.2(5)	-3.3(5)	3.1(6)
C4	24.1(7)	19.2(7)	14.5(7)	2.8(6)	0.6(6)	-1.4(6)
C5	32.0(9)	30.2(9)	26.1(9)	13.2(7)	0.2(7)	-4.0(7)
C6	16.0(7)	21.1(7)	17.9(7)	2.6(6)	2.3(5)	-2.3(6)
C7	13.7(6)	16.5(7)	13.4(6)	-1.0(5)	-0.3(5)	1.0(5)
C8	13.1(6)	20.5(7)	18.0(7)	1.6(6)	1.0(5)	2.7(5)
C9	14.3(6)	12.8(6)	9.6(6)	-0.6(5)	0.6(5)	0.1(5)
C10	19.1(7)	14.0(7)	13.9(6)	-4.8(5)	1.2(5)	-1.6(5)
C11	18.4(7)	12.6(6)	15.5(7)	-4.2(5)	2.1(5)	-2.0(5)
C12	8.0(5)	13.3(6)	11.4(6)	0.0(5)	0.3(4)	-0.1(5)
C13	16.3(6)	11.7(6)	13.2(6)	1.1(5)	2.2(5)	1.0(5)
C14	12.1(6)	13.3(6)	11.4(6)	-0.5(5)	-0.6(5)	-1.0(5)
C15	14.8(6)	14.6(6)	13.8(6)	1.4(5)	-1.3(5)	-3.0(5)
C16	14.7(6)	21.2(7)	13.9(6)	3.7(5)	0.7(5)	-3.2(5)
C17	13.7(6)	20.9(7)	13.4(6)	-0.2(5)	2.0(5)	0.3(5)
C18	12.5(6)	15.7(7)	13.7(6)	-1.1(5)	0.5(5)	-0.1(5)
C19	20.2(7)	18.8(7)	15.1(7)	4.0(6)	-3.7(5)	0.1(6)
C20	12.3(6)	14.0(6)	14.1(6)	-0.5(5)	-2.8(5)	-3.0(5)
C21	14.8(6)	17.1(7)	10.6(6)	-2.4(5)	-0.5(5)	-3.2(5)
C22	13.1(6)	12.5(6)	13.5(6)	-4.6(5)	0.2(5)	-2.3(5)
C23	9.0(6)	14.2(6)	14.7(6)	-1.8(5)	-0.3(5)	-1.4(5)
C24	9.8(6)	12.5(6)	14.2(6)	0.1(5)	0.8(5)	-2.8(5)
C25	12.1(6)	11.7(6)	14.1(6)	-1.5(5)	-1.7(5)	-2.4(5)
C26	15.4(6)	11.1(6)	17.1(7)	0.9(5)	-0.7(5)	0.7(5)
C27	20.7(7)	13.7(7)	23.7(8)	2.1(6)	-2.0(6)	-2.1(6)
C28	27.3(8)	15.9(7)	17.7(7)	1.4(6)	-4.7(6)	1.5(6)

Table S13: Anisotropic Displacement Parameters ($Å^2 \times 10^3$) for Ruthenium CN-Mesityl. The Anisotropic displacement factor exponent takes the form: $-2\pi^2[h^2a^{*2}U_{11}+2hka^*b^*U_{12}+\ldots]$.

Atom	U_{11}	U_{22}	U_{33}	U_{23}	U_{13}	U_{12}
Ru2	8.41(5)	9.94(5)	11.38(5)	-0.84(4)	0.65(4)	-0.56(4)
Cl2	12.03(14)	16.89(16)	20.00(16)	-0.69(13)	1.08(12)	3.18(12)
N4	12.9(5)	12.9(6)	13.2(5)	2.1(4)	2.1(4)	0.3(4)
N5	11.8(5)	12.0(5)	13.7(5)	-0.4(4)	-0.3(4)	-1.7(4)
N6	14.1(5)	13.0(6)	14.0(5)	1.3(4)	2.2(4)	-1.9(4)
C29	31.9(9)	36.7(10)	20.3(8)	8.0(7)	-1.0(7)	5.1(8)
C30	22.4(7)	20.2(7)	17.8(7)	5.3(6)	1.1(6)	0.1(6)
C31	19.5(7)	17.4(7)	20.6(7)	3.2(6)	2.0(6)	3.1(6)
C32	17.4(7)	14.2(7)	16.0(7)	1.4(5)	4.0(5)	-0.1(5)
C33	23.1(7)	18.7(7)	20.0(7)	-1.5(6)	7.1(6)	3.1(6)
C34	16.7(6)	13.1(6)	13.9(6)	2.7(5)	2.3(5)	-1.9(5)
C35	17.0(7)	14.4(7)	18.6(7)	2.6(5)	5.8(5)	-0.6(5)
C36	18.4(7)	24.0(8)	23.8(8)	5.3(6)	7.9(6)	2.4(6)
C37	23.1(7)	20.7(8)	15.4(7)	1.8(6)	6.6(6)	-0.4(6)
C38	18.5(7)	15.3(7)	21.4(7)	-0.3(6)	1.2(6)	-7.0(5)
C39	16.5(7)	15.2(7)	21.1(7)	-1.4(6)	-0.4(5)	-5.7(5)
C40	10.2(6)	12.5(6)	11.3(6)	-0.3(5)	2.7(5)	0.2(5)
C41	15.0(6)	13.9(6)	12.9(6)	0.8(5)	-1.2(5)	-0.1(5)
C42	18.0(7)	10.3(6)	12.9(6)	0.1(5)	1.9(5)	1.3(5)
C43	30.9(8)	15.4(7)	13.6(7)	0.5(5)	1.8(6)	-1.7(6)
C44	39.8(10)	23.2(8)	17.5(8)	2.4(6)	12.0(7)	-4.6(7)
C45	25.8(8)	24.4(8)	26.2(8)	3.8(7)	13.0(7)	-3.2(6)
C46	15.3(7)	18.7(7)	22.7(7)	3.7(6)	4.5(6)	-1.5(5)
C47	21.5(7)	21.1(8)	14.9(7)	-0.1(6)	-2.6(5)	-0.9(6)
C48	16.7(7)	16.1(7)	13.5(6)	-4.5(5)	-0.8(5)	1.3(5)
C49	15.5(6)	19.3(7)	13.3(6)	-6.1(5)	3.8(5)	-1.4(5)
C50	11.3(6)	18.0(7)	18.2(7)	-8.2(6)	1.7(5)	0.0(5)
C51	13.4(6)	14.9(7)	19.0(7)	-4.6(5)	-3.1(5)	-1.5(5)
C52	14.3(6)	11.3(6)	21.2(7)	-2.8(5)	-1.4(5)	0.5(5)
C53	12.9(6)	12.8(6)	20.3(7)	-6.8(5)	-2.9(5)	2.6(5)
C54	17.8(7)	14.3(7)	29.7(8)	-5.0(6)	-9.3(6)	4.3(5)
C55	37.9(10)	27.6(10)	43.3(11)	-14.6(8)	-16.5(9)	19.2(8)
C56	26.4(8)	17.0(8)	34.4(9)	4.8(7)	-11.3(7)	0.5(6)
S1	17.94(17)	17.15(17)	16.13(17)	2.94(13)	0.67(13)	1.59(13)
F1	51.0(8)	25.8(6)	56.7(8)	-12.0(6)	-14.3(6)	4.4(5)
F2	18.4(5)	76.6(11)	68.3(9)	-27.0(8)	-13.4(6)	4.0(6)
F3	62.0(8)	60.1(9)	20.8(6)	-7.2(6)	-2.6(5)	7.8(7)
O1	48.4(8)	20.8(6)	27.2(7)	5.3(5)	2.1(6)	10.0(6)
O2	35.0(7)	30.4(7)	21.0(6)	4.4(5)	8.7(5)	-0.9(5)
O3	15.9(5)	32.3(7)	37.0(7)	4.6(6)	-2.5(5)	-1.7(5)
C58	21.8(8)	30.5(9)	27.5(9)	-5.4(7)	-3.6(6)	6.0(7)
S2	11.89(15)	11.65(15)	13.48(15)	1.16(12)	0.76(12)	-0.40(11)
F4	26.4(5)	21.5(5)	20.5(5)	8.8(4)	-0.7(4)	2.7(4)
F5	12.7(4)	43.5(6)	21.3(5)	5.9(4)	0.3(3)	-1.6(4)
F6	31.9(5)	28.1(5)	15.9(4)	-5.9(4)	-0.1(4)	-2.8(4)
O4	20.7(5)	14.8(5)	22.8(6)	5.6(4)	-1.4(4)	-3.5(4)
O5	12.4(5)	21.3(6)	24.4(6)	3.8(4)	3.8(4)	0.2(4)
O6	23.1(5)	19.6(6)	17.3(5)	-4.3(4)	0.3(4)	1.4(4)
C57	15.7(7)	19.0(7)	14.2(6)	2.1(5)	2.4(5)	-0.3(5)

Table S14: Bond Lengths for Ruthenium CN-Mesityl.

Atom	Atom	Length/Å	Atom	Atom	Length/Å
Ru1	Cl1	2.4048(3)	Ru2	C52	2.2631(15)
Ru1	N1	2.1230(12)	Ru2	C53	2.2264(14)
Ru1	C12	2.0632(14)	N4	C42	1.3505(19)
Ru1	C20	2.2044(14)	N4	C46	1.3508(18)
Ru1	C21	2.2268(14)	N5	C39	1.3832(18)
Ru1	C22	2.2429(14)	N5	C40	1.3542(18)
Ru1	C23	2.1852(13)	N5	C41	1.4520(18)
Ru1	C24	2.2208(13)	N6	C34	1.4415(19)
Ru1	C25	2.2495(14)	N6	C38	1.3914(19)

Table S14: Bond Lengths for Ruthenium CN-Mesityl.

Atom	Atom	Length/Å	Atom	Atom	Length/Å
N1	C14	1.3480(18)	N6	C40	1.3613(18)
N1	C18	1.3553(18)	C29	C30	1.508(2)
N2	C11	1.3848(18)	C30	C31	1.390(2)
N2	C12	1.3581(18)	C30	C37	1.392(2)
N2	C13	1.4577(18)	C31	C32	1.392(2)
N3	C9	1.4408(18)	C32	C33	1.503(2)
N3	C10	1.3945(18)	C32	C34	1.395(2)
N3	C12	1.3681(18)	C34	C35	1.400(2)
C1	C2	1.503(2)	C35	C36	1.510(2)
C2	C3	1.392(2)	C35	C37	1.394(2)
C2	C9	1.402(2)	C38	C39	1.339(2)
C3	C4	1.391(2)	C41	C42	1.498(2)
C4	C5	1.510(2)	C42	C43	1.390(2)
C4	C6	1.392(2)	C43	C44	1.383(2)
C6	C7	1.397(2)	C44	C45	1.382(3)
C7	C8	1.510(2)	C45	C46	1.382(2)
C7	C9	1.3974(19)	C47	C48	1.500(2)
C10	C11	1.344(2)	C48	C49	1.408(2)
C13	C14	1.5030(19)	C48	C51	1.435(2)
C14	C15	1.3924(19)	C49	C50	1.429(2)
C15	C16	1.389(2)	C50	C53	1.409(2)
C16	C17	1.386(2)	C51	C52	1.394(2)
C17	C18	1.384(2)	C52	C53	1.438(2)
C19	C20	1.504(2)	C53	C54	1.517(2)
C20	C21	1.434(2)	C54	C55	1.535(2)
C20	C23	1.413(2)	C54	C56	1.530(3)
C21	C22	1.391(2)	S1	O1	1.4395(13)
C22	C25	1.4403(19)	S1	O2	1.4425(12)
C23	C24	1.428(2)	S1	O3	1.4409(12)
C24	C25	1.4074(19)	S1	C58	1.8263(18)
C25	C26	1.514(2)	F1	C58	1.327(2)
C26	C27	1.536(2)	F2	C58	1.324(2)
C26	C28	1.523(2)	F3	C58	1.326(2)
Ru2	Cl2	2.4085(3)	S2	O4	1.4403(11)
Ru2	N4	2.1185(12)	S2	O5	1.4430(11)
Ru2	C40	2.0547(14)	S2	O6	1.4450(11)
Ru2	C48	2.2114(14)	S2	C57	1.8313(15)
Ru2	C49	2.1868(14)	F4	C57	1.3387(18)
Ru2	C50	2.1888(14)	F5	C57	1.3420(17)
Ru2	C51	2.2493(14)	F6	C57	1.3312(18)

Table S15: Bond Angles for Ruthenium CN-Mesityl.

Atom	Atom	Atom	Angle/˚	Atom	Atom	Atom	Angle/˚
N1	Ru1	Cl1	82.97(3)	C40	Ru2	C51	155.82(5)
N1	Ru1	C20	92.85(5)	C40	Ru2	C52	154.40(5)
N1	Ru1	C21	88.07(5)	C40	Ru2	C53	117.05(5)
N1	Ru1	C22	110.19(5)	C48	Ru2	Cl2	89.32(4)
N1	Ru1	C23	123.49(5)	C48	Ru2	C51	37.53(6)
N1	Ru1	C24	160.54(5)	C48	Ru2	C52	66.94(6)
N1	Ru1	C25	146.85(5)	C48	Ru2	C53	80.74(5)
C12	Ru1	Cl1	88.10(4)	C49	Ru2	Cl2	117.86(4)
C12	Ru1	N1	86.40(5)	C49	Ru2	C48	37.34(5)
C12	Ru1	C20	114.46(5)	C49	Ru2	C50	38.14(6)
C12	Ru1	C21	151.29(5)	C49	Ru2	C51	66.56(5)
C12	Ru1	C22	163.38(5)	C49	Ru2	C52	78.66(6)
C12	Ru1	C23	92.92(5)	C49	Ru2	C53	67.94(6)
C12	Ru1	C24	98.35(5)	C50	Ru2	Cl2	155.92(4)
C12	Ru1	C25	126.03(5)	C50	Ru2	C48	68.32(5)
C20	Ru1	Cl1	156.84(4)	C50	Ru2	C51	78.77(5)
C20	Ru1	C21	37.76(5)	C50	Ru2	C52	66.60(5)
C20	Ru1	C22	67.26(5)	C50	Ru2	C53	37.20(6)

Table S15: Bond Angles for Ruthenium CN-Mesityl.

Atom	Atom	Atom	Angle/˚	Atom	Atom	Atom	Angle/˚
C20	Ru1	C24	67.97(5)	C51	Ru2	Cl2	88.93(4)
C20	Ru1	C25	80.39(5)	C51	Ru2	C52	35.98(5)
C21	Ru1	Cl1	119.12(4)	C52	Ru2	Cl2	113.77(4)
C21	Ru1	C22	36.27(5)	C53	Ru2	Cl2	150.98(4)
C21	Ru1	C25	66.74(5)	C53	Ru2	C51	66.68(5)
C22	Ru1	Cl1	92.74(4)	C53	Ru2	C52	37.36(5)
C22	Ru1	C25	37.40(5)	C42	N4	Ru2	123.54(9)
C23	Ru1	Cl1	153.54(4)	C42	N4	C46	118.37(13)
C23	Ru1	C20	37.55(5)	C46	N4	Ru2	118.05(10)
C23	Ru1	C21	67.09(5)	C39	N5	C41	124.78(12)
C23	Ru1	C22	79.03(5)	C40	N5	C39	112.01(12)
C23	Ru1	C24	37.81(5)	C40	N5	C41	123.03(12)
C23	Ru1	C25	67.47(5)	C38	N6	C34	122.05(12)
C24	Ru1	Cl1	115.91(4)	C40	N6	C34	127.12(12)
C24	Ru1	C21	78.70(5)	C40	N6	C38	110.77(12)
C24	Ru1	C22	66.41(5)	C31	C30	C29	120.62(15)
C24	Ru1	C25	36.69(5)	C31	C30	C37	118.55(14)
C25	Ru1	Cl1	90.69(4)	C37	C30	C29	120.81(15)
C14	N1	Ru1	125.97(9)	C30	C31	C32	122.12(14)
C14	N1	C18	118.01(12)	C31	C32	C33	119.86(14)
C18	N1	Ru1	115.98(10)	C31	C32	C34	117.44(14)
C11	N2	C13	122.64(12)	C34	C32	C33	122.54(14)
C12	N2	C11	112.54(12)	C32	C34	N6	119.54(13)
C12	N2	C13	124.38(12)	C32	C34	C35	122.22(14)
C10	N3	C9	118.72(12)	C35	C34	N6	118.07(13)
C12	N3	C9	129.86(12)	C34	C35	C36	121.73(14)
C12	N3	C10	110.62(12)	C37	C35	C34	117.73(14)
C3	C2	C1	120.42(13)	C37	C35	C36	120.48(13)
C3	C2	C9	117.83(13)	C30	C37	C35	121.57(14)
C9	C2	C1	121.76(14)	C39	C38	N6	107.18(13)
C4	C3	C2	122.22(14)	C38	C39	N5	106.24(13)
C3	C4	C5	121.04(15)	N5	C40	Ru2	121.30(10)
C3	C4	C6	118.23(14)	N5	C40	N6	103.77(12)
C6	C4	C5	120.72(15)	N6	C40	Ru2	134.59(10)
C4	C6	C7	121.91(14)	N5	C41	C42	111.05(12)
C6	C7	C8	119.15(13)	N4	C42	C41	118.06(12)
C6	C7	C9	117.95(13)	N4	C42	C43	121.77(14)
C9	C7	C8	122.89(13)	C43	C42	C41	120.17(13)
C2	C9	N3	119.13(12)	C44	C43	C42	119.41(15)
C7	C9	N3	118.43(12)	C45	C44	C43	118.78(15)
C7	C9	C2	121.77(13)	C46	C45	C44	119.29(15)
C11	C10	N3	107.54(13)	N4	C46	C45	122.31(15)
C10	C11	N2	105.80(13)	C47	C48	Ru2	126.70(10)
N2	C12	Ru1	121.53(10)	C49	C48	Ru2	70.38(8)
N2	C12	N3	103.49(12)	C49	C48	C47	121.03(14)
N3	C12	Ru1	134.87(10)	C49	C48	C51	117.80(14)
N2	C13	C14	112.68(12)	C51	C48	Ru2	72.67(8)
N1	C14	C13	117.81(12)	C51	C48	C47	121.16(13)
N1	C14	C15	122.26(13)	C48	C49	Ru2	72.28(8)
C15	C14	C13	119.88(13)	C48	C49	C50	121.07(14)
C16	C15	C14	119.35(14)	C50	C49	Ru2	71.01(8)
C17	C16	C15	118.42(14)	C49	C50	Ru2	70.85(8)
C18	C17	C16	119.44(14)	C53	C50	Ru2	72.85(8)
N1	C18	C17	122.49(14)	C53	C50	C49	120.65(13)
C19	C20	Ru1	128.31(10)	C48	C51	Ru2	69.80(8)
C21	C20	Ru1	71.97(8)	C52	C51	Ru2	72.54(8)
C21	C20	C19	120.09(13)	C52	C51	C48	121.47(13)
C23	C20	Ru1	70.49(8)	C51	C52	Ru2	71.47(9)
C23	C20	C19	122.07(13)	C51	C52	C53	120.56(14)
C23	C20	C21	117.83(13)	C53	C52	Ru2	69.93(8)
C20	C21	Ru1	70.27(8)	C50	C53	Ru2	69.95(8)
C22	C21	Ru1	72.49(8)	C50	C53	C52	118.34(13)
C22	C21	C20	121.32(13)	C50	C53	C54	119.91(13)

Table S15: Bond Angles for Ruthenium CN-Mesityl.

Atom	Atom	Atom	Angle/˚	Atom	Atom	Atom	Angle/˚
C21	C22	Ru1	71.24(8)	C52	C53	Ru2	72.70(8)
C21	C22	C25	120.81(13)	C52	C53	C54	121.40(14)
C25	C22	Ru1	71.55(8)	C54	C53	Ru2	134.37(10)
C20	C23	Ru1	71.96(8)	C53	C54	C55	106.92(14)
C20	C23	C24	121.08(13)	C53	C54	C56	114.68(13)
C24	C23	Ru1	72.45(8)	C56	C54	C55	110.78(15)
C23	C24	Ru1	69.74(8)	O1	S1	O2	115.25(8)
C25	C24	Ru1	72.76(8)	O1	S1	O3	114.98(8)
C25	C24	C23	120.63(13)	O1	S1	C58	103.93(8)
C22	C25	Ru1	71.05(8)	O2	S1	C58	103.25(8)
C22	C25	C26	118.87(12)	O3	S1	O2	114.20(8)
C24	C25	Ru1	70.55(8)	O3	S1	C58	102.97(8)
C24	C25	C22	118.28(13)	F1	C58	S1	111.24(12)
C24	C25	C26	122.71(13)	F2	C58	S1	110.91(12)
C26	C25	Ru1	133.47(10)	F2	C58	F1	107.68(17)
C25	C26	C27	107.36(12)	F2	C58	F3	107.86(15)
C25	C26	C28	114.81(12)	F3	C58	S1	111.38(14)
C28	C26	C27	110.81(13)	F3	C58	F1	107.60(15)
N4	Ru2	Cl2	83.87(3)	O4	S2	O5	116.16(7)
N4	Ru2	C48	156.50(5)	O4	S2	O6	114.62(7)
N4	Ru2	C49	158.13(5)	O4	S2	C57	102.92(7)
N4	Ru2	C50	120.20(5)	O5	S2	O6	114.48(7)
N4	Ru2	C51	119.62(5)	O5	S2	C57	102.55(7)
N4	Ru2	C52	95.33(5)	O6	S2	C57	103.57(7)
N4	Ru2	C53	94.45(5)	F4	C57	S2	111.07(10)
C40	Ru2	Cl2	91.70(4)	F4	C57	F5	107.22(12)
C40	Ru2	N4	84.46(5)	F5	C57	S2	111.77(10)
C40	Ru2	C48	118.30(6)	F6	C57	S2	111.44(10)
C40	Ru2	C49	92.03(5)	F6	C57	F4	107.68(12)
C40	Ru2	C50	91.34(5)	F6	C57	F5	107.45(12)

Table S16: Torsion Angles for Ruthenium CN-Mesityl.

A	B	C	D	Angle/˚	A	B	C	D	Angle/˚
Ru1	N1	C14	C13	-0.56(18)	Ru2	C52	C53	C50	54.84(12)
Ru1	N1	C14	C15	-177.99(10)	Ru2	C52	C53	C54	-131.91(14)
Ru1	N1	C18	C17	176.62(11)	Ru2	C53	C54	C55	175.57(13)
Ru1	C20	C21	C22	53.68(12)	Ru2	C53	C54	C56	-61.2(2)
Ru1	C20	C23	C24	-55.48(12)	N4	C42	C43	C44	-0.4(2)
Ru1	C21	C22	C25	53.72(12)	N5	C41	C42	N4	-56.07(17)
Ru1	C22	C25	C24	54.22(11)	N5	C41	C42	C43	124.36(14)
Ru1	C22	C25	C26	-129.89(12)	N6	C34	C35	C36	4.3(2)
Ru1	C23	C24	C25	-54.15(12)	N6	C34	C35	C37	-178.43(14)
Ru1	C24	C25	C22	-54.47(11)	N6	C38	C39	N5	0.05(17)
Ru1	C24	C25	C26	129.81(13)	C29	C30	C31	C32	-179.61(16)
Ru1	C25	C26	C27	174.79(11)	C29	C30	C37	C35	178.97(16)
Ru1	C25	C26	C28	51.11(18)	C30	C31	C32	C33	-172.88(15)
N1	C14	C15	C16	1.9(2)	C30	C31	C32	C34	2.6(2)
N2	C13	C14	N1	49.43(17)	C31	C30	C37	C35	-2.6(2)
N2	C13	C14	C15	-133.07(14)	C31	C32	C34	N6	177.90(13)
N3	C10	C11	N2	-0.12(16)	C31	C32	C34	C35	-6.9(2)
C1	C2	C3	C4	179.06(15)	C32	C34	C35	C36	-170.99(15)
C1	C2	C9	N3	-6.3(2)	C32	C34	C35	C37	6.3(2)
C1	C2	C9	C7	-176.73(14)	C33	C32	C34	N6	-6.7(2)
C2	C3	C4	C5	-179.57(16)	C33	C32	C34	C35	168.53(15)
C2	C3	C4	C6	-0.8(2)	C34	N6	C38	C39	178.44(13)
C3	C2	C9	N3	173.93(13)	C34	N6	C40	Ru2	-5.9(2)
C3	C2	C9	C7	3.5(2)	C34	N6	C40	N5	-178.93(13)
C3	C4	C6	C7	0.6(2)	C34	C35	C37	C30	-1.4(2)
C4	C6	C7	C8	-176.95(15)	C36	C35	C37	C30	175.90(15)
C4	C6	C7	C9	1.6(2)	C37	C30	C31	C32	1.9(2)
C5	C4	C6	C7	179.33(16)	C38	N6	C34	C32	97.11(17)

Table S16: Torsion Angles for Ruthenium CN-Mesityl.

A	B	C	D	Angle/˚	A	B	C	D	Angle/˚
C6	C7	C9	N3	-174.22(13)	C38	N6	C34	C35	-78.33(18)
C6	C7	C9	C2	-3.7(2)	C38	N6	C40	Ru2	171.32(11)
C8	C7	C9	N3	4.3(2)	C38	N6	C40	N5	-1.74(15)
C8	C7	C9	C2	174.80(14)	C39	N5	C40	Ru2	-172.42(10)
C9	N3	C10	C11	-170.33(12)	C39	N5	C40	N6	1.80(15)
C9	N3	C12	Ru1	-15.0(2)	C39	N5	C41	C42	-131.99(14)
C9	N3	C12	N2	168.89(13)	C40	N5	C39	C38	-1.20(17)
C9	C2	C3	C4	-1.1(2)	C40	N5	C41	C42	53.29(17)
C10	N3	C9	C2	-84.00(17)	C40	N6	C34	C32	-85.99(19)
C10	N3	C9	C7	86.77(16)	C40	N6	C34	C35	98.57(17)
C10	N3	C12	Ru1	175.57(11)	C40	N6	C38	C39	1.09(17)
C10	N3	C12	N2	-0.54(15)	C41	N5	C39	C38	-176.43(13)
C11	N2	C12	Ru1	-176.29(9)	C41	N5	C40	Ru2	2.91(18)
C11	N2	C12	N3	0.47(15)	C41	N5	C40	N6	177.13(12)
C11	N2	C13	C14	130.47(14)	C41	C42	C43	C44	179.19(15)
C12	N2	C11	C10	-0.23(17)	C42	N4	C46	C45	-2.1(2)
C12	N2	C13	C14	-57.67(18)	C42	C43	C44	C45	-1.6(3)
C12	N3	C9	C2	107.29(17)	C43	C44	C45	C46	1.7(3)
C12	N3	C9	C7	-81.93(18)	C44	C45	C46	N4	0.1(3)
C12	N3	C10	C11	0.42(16)	C46	N4	C42	C41	-177.39(13)
C13	N2	C11	C10	172.50(13)	C46	N4	C42	C43	2.2(2)
C13	N2	C12	Ru1	11.12(18)	C47	C48	C49	Ru2	-121.73(14)
C13	N2	C12	N3	-172.11(12)	C47	C48	C49	C50	-175.47(13)
C13	C14	C15	C16	-175.46(13)	C47	C48	C51	Ru2	122.88(14)
C14	N1	C18	C17	-1.3(2)	C47	C48	C51	C52	176.01(14)
C14	C15	C16	C17	-1.9(2)	C48	C49	C50	Ru2	54.32(13)
C15	C16	C17	C18	0.4(2)	C48	C49	C50	C53	-1.0(2)
C16	C17	C18	N1	1.2(2)	C48	C51	C52	Ru2	-51.91(13)
C18	N1	C14	C13	177.09(12)	C48	C51	C52	C53	-0.1(2)
C18	N1	C14	C15	-0.3(2)	C49	C48	C51	Ru2	-55.80(12)
C19	C20	C21	Ru1	124.39(13)	C49	C48	C51	C52	-2.7(2)
C19	C20	C21	C22	178.07(13)	C49	C50	C53	Ru2	54.42(12)
C19	C20	C23	Ru1	-123.65(13)	C49	C50	C53	C52	-1.8(2)
C19	C20	C23	C24	-179.13(13)	C49	C50	C53	C54	-175.13(13)
C20	C21	C22	Ru1	-52.68(12)	C50	C53	C54	C55	85.02(18)
C20	C21	C22	C25	1.0(2)	C50	C53	C54	C56	-151.75(14)
C20	C23	C24	Ru1	55.26(12)	C51	C48	C49	Ru2	56.95(12)
C20	C23	C24	C25	1.1(2)	C51	C48	C49	C50	3.2(2)
C21	C20	C23	Ru1	56.05(11)	C51	C52	C53	Ru2	-52.52(13)
C21	C20	C23	C24	0.6(2)	C51	C52	C53	C50	2.3(2)
C21	C22	C25	Ru1	-53.58(12)	C51	C52	C53	C54	175.57(14)
C21	C22	C25	C24	0.6(2)	C52	C53	C54	C55	-88.12(18)
C21	C22	C25	C26	176.53(12)	C52	C53	C54	C56	35.1(2)
C22	C25	C26	C27	-94.53(15)	O1	S1	C58	F1	-172.92(13)
C22	C25	C26	C28	141.78(13)	O1	S1	C58	F2	67.25(16)
C23	C20	C21	Ru1	-55.31(11)	O1	S1	C58	F3	-52.88(14)
C23	C20	C21	C22	-1.6(2)	O2	S1	C58	F1	66.42(15)
C23	C24	C25	Ru1	52.77(11)	O2	S1	C58	F2	-53.40(16)
C23	C24	C25	C22	-1.70(19)	O2	S1	C58	F3	-173.54(12)
C23	C24	C25	C26	-177.42(12)	O3	S1	C58	F1	-52.68(15)
C24	C25	C26	C27	81.16(16)	O3	S1	C58	F2	-172.50(14)
C24	C25	C26	C28	-42.52(19)	O3	S1	C58	F3	67.36(14)
Ru2	N4	C42	C41	4.99(18)	O4	S2	C57	F4	-177.22(10)
Ru2	N4	C42	C43	-175.45(11)	O4	S2	C57	F5	-57.52(12)
Ru2	N4	C46	C45	175.69(13)	O4	S2	C57	F6	62.72(12)
Ru2	C48	C49	C50	-53.74(12)	O5	S2	C57	F4	61.82(11)
Ru2	C48	C51	C52	53.13(13)	O5	S2	C57	F5	-178.48(11)
Ru2	C49	C50	C53	-55.34(12)	O5	S2	C57	F6	-58.24(12)
Ru2	C50	C53	C52	-56.19(12)	O6	S2	C57	F4	-57.55(11)
Ru2	C50	C53	C54	130.46(13)	O6	S2	C57	F5	62.15(12)
Ru2	C51	C52	C53	51.82(13)	O6	S2	C57	F6	-177.60(10)

Table S17: Hydrogen Atom Coordinates (Å×10⁴) and Isotropic Displacement Parameters (Å²×10³) for Ruthenium CN-Mesityl.

Atom	*x*	*y*	*z*	U(eq)
H1A	4730.98	-1264.01	4989.58	30
H1B	4460.24	-334.31	4693.37	30
H1C	4602.19	-1356.74	4449.52	30
H3	3560.2	-2284.19	5273.37	22
H5A	2382.79	-3415.65	5544.29	44
H5B	1318.91	-3220.17	5427.34	44
H5C	1824.9	-2610.36	5819.36	44
H6	879.48	-1806.66	4975.5	22
H8A	655.15	-844.21	4160.31	26
H8B	1261.96	119.63	4190.86	26
H8C	565.57	-145.34	4591.78	26
H10	3025.69	1078.87	4736.41	19
H11	3190.78	2221.62	4092.7	19
H13A	3155.53	2110.17	3250.57	16
H13B	2422.47	1307.86	3096.28	16
H15	4254.55	2255.68	2677.24	17
H16	5253.97	1561.4	2140.56	20
H17	5346.73	-131.97	2097.26	19
H18	4447.6	-1073.03	2573.16	17
H19A	1162.26	428.68	2683.53	27
H19B	1145.64	-231.61	2236.19	27
H19C	2071.64	320.06	2382.87	27
H21	2681.69	-1474.16	2295.89	17
H22	3192.54	-2780.39	2727.73	16
H23	1042.42	-593.7	3344.15	15
H24	1523.61	-1948.16	3776.2	15
H26	3311.73	-3629.36	3423.26	17
H27A	1415.6	-3986.14	3636.03	29
H27B	2203.75	-4792.68	3607.77	29
H27C	1867.35	-4245.14	3155.97	29
H28A	3383.19	-2756.23	4112.26	30
H28B	3105.27	-3856.17	4207.41	30
H28C	2333.27	-3030.28	4215.4	30
H29A	8676.37	4680.29	5359.02	44
H29B	8178.27	5550.79	5617.83	44
H29C	9175.18	5708.2	5400.28	44
H31	9163.48	5244.09	4509.78	23
H33A	9307.73	5664.79	3682.87	31
H33B	8389.27	5949.56	3408.01	31
H33C	8524.25	4871.22	3593.35	31
H36A	5780.98	7236.45	4248.9	33
H36B	5768.71	7176.63	4793.07	33
H36C	5432.45	6273.3	4494.81	33
H37	6941.25	6191.08	5195.4	24
H38	6011.3	5513.51	3547.28	22
H39	5540.42	6475.81	2874.92	21
H41A	6128.11	8830.76	2942.88	17
H41B	6026.16	8076.9	2531.53	17
H43	7038.25	8413.67	1939.59	24
H44	8489.47	8896.62	1675.42	32
H45	9608.38	9404.33	2205.51	30
H46	9283.77	9347.83	2977.39	23
H47A	8328.91	7876.14	4772.56	29
H47B	8817.48	8835.98	4959.26	29
H47C	9253.75	8260.18	4540.53	29
H49	6868.81	8394.7	4476.64	19
H50	6004.34	9248.41	3920.01	19
H51	9157.43	9957.66	4144.45	19
H52	8307.62	10819.48	3604.01	19
H54	5952.42	10295.88	3257.85	25
H55A	5711.29	11290.18	3894.98	55
H55B	5685.38	11944.82	3445.87	55
H55C	6583.48	11940.9	3766.64	55

Table S17: Hydrogen Atom Coordinates (Å×10⁴) and Isotropic Displacement Parameters (Å²×10³) for Ruthenium CN-Mesityl.

Atom	*x*	*y*	*z*	U(eq)
H56A	7527.41	11459.73	3050.34	39
H56B	6578.92	11487.82	2767.74	39
H56C	7200.03	10532.21	2766.63	39

Crystal Structure of 2

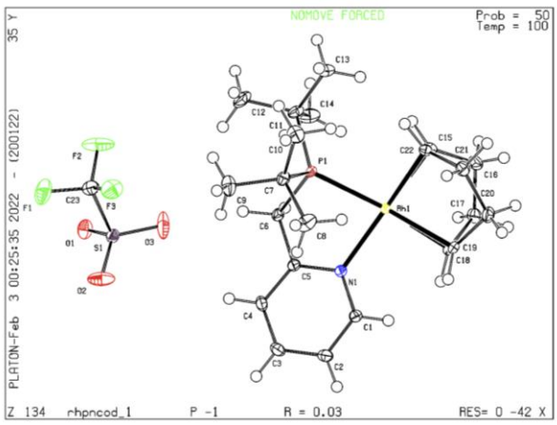

Figure S127: Molecular structure of **2** shown with 50% probability ellipsoids.

A clear yellowish prism- like crystal of, $C_{23}H_{36}F_3NO_3PRhS$. approximate dimensions 0.329 mm x 0.188 mm x 0.138 mm was used for X-ray crystallographic analysis grown from layering dichloromethane and toluene. The X-ray intensity data was collected on a XtaLAB Synergy, Dualflex, HyPix diffractometer using a Mo Kα fine-focus tube (λ = 0.71073) and kept at 100.00(10) K during data acquisition. The crystal was mounted on a MiTiGen 50um.

Frames were integrated using Rigaku CrysAlisPro software. The integration of the data using a monoclinic crystal system resulted in 41340 reflections to a maximum θ angle of 33.241° (0.75 Å resolution), of which 8380 were independent (completeness = 87.4 % , Rint = 0.0735, Rsigma = 0.0437). The final cell constants are a = 8.8927(3) Å, b = 10.3448(3) Å, c = 14.8521 Å, α = 109.951°, β = 100.254(2)°, γ = 94.693(2)°, volume = 1248.68(3) Å^3, are based upon the refinement of the. Data was corrected for absorption effects using the multi -scan method. The ration of minimum to maximum apparent transmission was 0.392.

The structure was solved using olex2.solve[4] structure solution program using Charge Flipping and refined with the SHELXL[5] refinement package using Least Squares minimization. The space group P-1 was used with Z = 2 for the formula unit, $C_{23}H_{36}F_3NO_3PRhS$. The final R_1 = 3.24% and wR_2 = 8.66% R(I>2σ(I)) and for all data R_1 = 3.53% wR_2 = 8.84%. The goodness-of-fit was 1.083. The largest peak in the final difference electron density synthesis was 0.78 e-/ Å3 and the largest hole was -1.04 e-/ Å3. Based on the final model, the calculated density was 1.589 g/cm3 and F (000), 616.0.

Table S18: Crystal data and structure refinement for RhPNCOD_1.

Identification code	RhPNCOD_1
Empirical formula	$C_{23}H_{36}F_3NO_3PRhS$
Formula weight	597.47
Temperature/K	100.00(10)
Crystal system	triclinic
Space group	P-1
a/Å	8.8927(3)
b/Å	10.3448(3)
c/Å	14.8521(3)
α/°	109.951(2)
β/°	100.254(2)
γ/°	94.693(2)
Volume/Å^3	1248.68(6)
Z	2
ρ_{calc}g/cm^3	1.589
μ/mm^{-1}	0.879
F(000)	616.0
Crystal size/mm^3	0.329 × 0.188 × 0.138
Radiation	Mo Kα (λ = 0.71073)
2Θ range for data collection/°	4.994 to 66.482
Index ranges	-12 ≤ h ≤ 13, -14 ≤ k ≤ 15, -22 ≤ l ≤ 21
Reflections collected	41340
Independent reflections	8380 [R_{int} = 0.0735, R_{sigma} = 0.0437]
Data/restraints/parameters	8380/0/304
Goodness-of-fit on F^2	1.083
Final R indexes [I>=2σ (I)]	R_1 = 0.0324, wR_2 = 0.0866
Final R indexes [all data]	R_1 = 0.0353, wR_2 = 0.0884
Largest diff. peak/hole / e Å^{-3}	0.78/-1.04

Table S19: Fractional Atomic Coordinates (×10⁴) and Equivalent Isotropic Displacement Parameters (Å²×10³) for RhPNCOD_1. U_{eq} is defined as 1/3 of the trace of the orthogonalised U_{IJ} tensor.

Atom	*x*	*y*	*z*	U(eq)
Rh1	4686.0(2)	8477.9(2)	6871.0(2)	9.28(5)
P1	5564.5(5)	7182.7(4)	7798.9(3)	10.32(8)
N1	6108.1(15)	7317.4(13)	5964.9(9)	11.6(2)
C20	4133(2)	11471.0(17)	6958.4(12)	17.0(3)
C9	8603(2)	6858(2)	8665.9(14)	24.7(4)
C14	2908(2)	5493.7(19)	7658.3(13)	23.2(4)
C10	7488(2)	8925.3(19)	9603.8(12)	21.9(3)
C11	4337(2)	6383.2(16)	8441.1(11)	15.6(3)
C18	3480.2(18)	9013.1(16)	5626.5(11)	12.9(3)
C15	2629.2(18)	9019.3(16)	7386.4(11)	13.6(3)
C13	3772(2)	7500.6(18)	9242.7(12)	19.4(3)
C22	3917.4(18)	9997.0(16)	8008.9(11)	13.7(3)
C16	1412.8(19)	9288.3(18)	6639.6(12)	17.4(3)
C6	5815.1(19)	5649.7(15)	6776.0(11)	13.2(3)
C17	1767.1(18)	8823.9(18)	5608.5(12)	16.7(3)
C4	7574.4(19)	5418.4(17)	5591.3(12)	16.4(3)
C3	8227.7(19)	5926.0(19)	4970.8(12)	17.8(3)
C8	8359(2)	8839(2)	8088.8(13)	23.7(4)
C1	6763.0(18)	7792.7(16)	5358.1(11)	13.4(3)
C21	4359(2)	11434.6(16)	8005.0(12)	17.3(3)
C12	5174(3)	5441.5(19)	8895.8(14)	25.6(4)
C2	7821.8(18)	7134.5(18)	4856.8(11)	15.8(3)
C19	4535.4(18)	10167.8(16)	6245.8(11)	13.3(3)
C5	6525.7(18)	6140.0(16)	6081.4(10)	12.6(3)
C7	7581.4(19)	7951.5(16)	8575.1(11)	14.5(3)
S1	8949.9(5)	2415.6(4)	7109.0(3)	14.64(8)
F1	10631.1(17)	2134.3(14)	8656.2(9)	37.7(3)
F2	8432.5(17)	2734.4(18)	8860.1(9)	46.1(4)
F3	10270.1(15)	4242.0(12)	8874.6(8)	30.3(3)
O1	8315.2(15)	964.3(13)	6780.8(9)	21.0(2)
O2	10371.4(17)	2694.2(16)	6820.5(10)	30.9(3)
O3	7830(2)	3313.6(16)	7013.6(12)	36.8(4)
C23	9601(2)	2911.5(19)	8440.2(13)	20.3(3)

Table S20: Anisotropic Displacement Parameters (Å²×10³) for RhPNCOD_1. The Anisotropic displacement factor exponent takes the form: $-2\pi^2[h^2a^{*2}U_{11}+2hka^*b^*U_{12}+\ldots]$.

Atom	U_{11}	U_{22}	U_{33}	U_{23}	U_{13}	U_{12}
Rh1	10.52(7)	9.76(7)	9.07(7)	4.53(4)	3.09(4)	2.89(4)
P1	13.81(18)	8.89(16)	9.02(17)	4.33(13)	2.36(13)	1.47(13)
N1	12.9(6)	12.5(6)	10.1(6)	4.5(4)	2.8(4)	3.3(4)
C20	20.8(8)	13.3(7)	18.8(7)	7.8(6)	3.7(6)	5.2(6)
C9	23.0(9)	22.2(8)	25.8(9)	7.4(7)	-1.2(7)	7.5(7)
C14	25.8(9)	20.8(8)	18.9(8)	3.8(6)	7.3(6)	-8.1(7)
C10	21.8(8)	22.1(8)	15.5(7)	1.4(6)	-0.6(6)	2.9(6)
C11	22.2(8)	12.6(6)	12.8(7)	5.7(5)	5.2(5)	-1.4(6)
C18	14.2(7)	15.3(7)	11.6(6)	7.5(5)	2.9(5)	4.5(5)
C15	13.4(7)	15.4(7)	13.7(7)	5.1(5)	6.3(5)	4.3(5)
C13	24.6(8)	19.8(8)	13.8(7)	5.0(6)	8.2(6)	0.1(6)
C22	16.9(7)	14.6(7)	10.7(6)	4.0(5)	5.2(5)	5.5(5)
C16	12.4(7)	23.6(8)	16.7(7)	6.9(6)	3.9(5)	5.6(6)
C6	18.8(7)	9.8(6)	12.0(6)	4.3(5)	4.3(5)	3.2(5)
C17	11.9(7)	22.0(8)	15.9(7)	7.2(6)	0.8(5)	4.2(6)
C4	18.0(7)	16.4(7)	15.4(7)	5.2(5)	3.4(5)	9.1(6)
C3	15.5(7)	24.8(8)	13.4(7)	5.2(6)	5.1(5)	8.6(6)
C8	18.9(8)	29.1(9)	21.4(8)	12.5(7)	-2.1(6)	-6.8(7)
C1	13.2(7)	15.9(7)	12.5(7)	6.4(5)	3.4(5)	3.2(5)
C21	22.1(8)	12.7(7)	16.3(7)	3.6(5)	4.7(6)	4.3(6)
C12	43.3(11)	17.9(8)	22.2(8)	13.6(7)	10.9(7)	3.8(7)
C2	12.2(7)	23.3(8)	12.2(7)	6.3(6)	3.7(5)	3.1(6)
C19	15.8(7)	14.6(7)	13.7(7)	9.2(5)	4.3(5)	5.1(5)
C5	14.2(7)	14.0(7)	9.4(6)	4.3(5)	1.8(5)	3.3(5)

Table S20: Anisotropic Displacement Parameters ($Å^2 \times 10^3$) for RhPNCOD_1. The Anisotropic displacement factor exponent takes the form: $-2\pi^2[h^2a^{*2}U_{11}+2hka^*b^*U_{12}+\ldots]$.

Atom	U_{11}	U_{22}	U_{33}	U_{23}	U_{13}	U_{12}
C7	15.2(7)	14.5(7)	12.1(7)	5.0(5)	-0.5(5)	1.3(5)
S1	16.70(18)	13.14(17)	15.36(18)	6.57(13)	3.73(13)	2.65(13)
F1	43.2(8)	36.9(7)	30.6(7)	16.1(5)	-8.1(5)	11.9(6)
F2	36.1(7)	73.6(11)	25.9(6)	13.7(6)	16.8(5)	-9.7(7)
F3	41.2(7)	22.3(5)	20.3(5)	1.2(4)	4.7(5)	-0.6(5)
O1	18.9(6)	15.4(5)	26.5(6)	8.3(5)	-0.3(5)	-0.2(4)
O2	30.3(7)	35.0(8)	20.8(6)	2.9(5)	11.7(5)	-13.0(6)
O3	45.3(9)	25.3(7)	35.8(8)	9.6(6)	-5.2(7)	20.8(7)
C23	21.1(8)	23.3(8)	18.5(8)	9.4(6)	6.0(6)	2.5(6)

Table S21: Bond Lengths for RhPNCOD_1.

Atom	Atom	Length/Å	Atom	Atom	Length/Å
Rh1	P1	2.3136(4)	C18	C19	1.383(2)
Rh1	N1	2.1456(13)	C15	C22	1.409(2)
Rh1	C18	2.2277(15)	C15	C16	1.520(2)
Rh1	C15	2.1490(15)	C22	C21	1.509(2)
Rh1	C22	2.1371(15)	C16	C17	1.539(2)
Rh1	C19	2.2445(15)	C6	C5	1.503(2)
P1	C11	1.8830(16)	C4	C3	1.390(2)
P1	C6	1.8458(15)	C4	C5	1.393(2)
P1	C7	1.8930(16)	C3	C2	1.385(2)
N1	C1	1.3548(19)	C8	C7	1.539(2)
N1	C5	1.359(2)	C1	C2	1.383(2)
C20	C21	1.545(2)	S1	O1	1.4402(13)
C20	C19	1.519(2)	S1	O2	1.4429(14)
C9	C7	1.533(2)	S1	O3	1.4373(15)
C14	C11	1.538(2)	S1	C23	1.8327(18)
C10	C7	1.538(2)	F1	C23	1.334(2)
C11	C13	1.541(2)	F2	C23	1.334(2)
C11	C12	1.532(3)	F3	C23	1.337(2)
C18	C17	1.514(2)			

Table S22: Bond Angles for RhPNCOD_1.

Atom	Atom	Atom	Angle/˚	Atom	Atom	Atom	Angle/˚
N1	Rh1	P1	80.92(4)	C16	C15	Rh1	113.50(10)
N1	Rh1	C18	90.48(5)	C15	C22	Rh1	71.27(9)
N1	Rh1	C15	158.59(6)	C15	C22	C21	125.89(14)
N1	Rh1	C19	97.32(5)	C21	C22	Rh1	110.28(10)
C18	Rh1	P1	160.72(4)	C15	C16	C17	112.75(13)
C18	Rh1	C19	36.03(6)	C5	C6	P1	108.78(10)
C15	Rh1	P1	100.80(4)	C18	C17	C16	113.26(13)
C15	Rh1	C18	81.09(6)	C3	C4	C5	119.03(15)
C15	Rh1	C19	87.41(6)	C2	C3	C4	119.24(15)
C22	Rh1	P1	96.03(4)	N1	C1	C2	123.08(15)
C22	Rh1	N1	163.01(6)	C22	C21	C20	112.87(13)
C22	Rh1	C18	97.03(6)	C1	C2	C3	118.79(15)
C22	Rh1	C15	38.38(6)	C20	C19	Rh1	111.51(10)
C22	Rh1	C19	80.38(6)	C18	C19	Rh1	71.32(9)
C19	Rh1	P1	161.96(4)	C18	C19	C20	125.07(14)
C11	P1	Rh1	124.44(6)	N1	C5	C6	116.91(13)
C11	P1	C7	112.03(7)	N1	C5	C4	122.10(14)
C6	P1	Rh1	97.25(5)	C4	C5	C6	120.99(14)
C6	P1	C11	102.50(7)	C9	C7	P1	113.80(12)
C6	P1	C7	105.26(7)	C9	C7	C10	109.65(14)
C7	P1	Rh1	111.75(5)	C9	C7	C8	108.07(15)
C1	N1	Rh1	122.56(10)	C10	C7	P1	109.89(12)
C1	N1	C5	117.76(13)	C10	C7	C8	107.61(14)
C5	N1	Rh1	119.22(10)	C8	C7	P1	107.61(11)
C19	C20	C21	111.46(13)	O1	S1	O2	114.86(9)

Table S22: Bond Angles for RhPNCOD_1.

Atom	Atom	Atom	Angle/˚	Atom	Atom	Atom	Angle/˚
C14	C11	P1	106.70(11)	O1	S1	C23	103.57(8)
C14	C11	C13	107.89(15)	O2	S1	C23	102.09(8)
C13	C11	P1	111.72(11)	O3	S1	O1	114.60(9)
C12	C11	P1	112.72(13)	O3	S1	O2	115.63(11)
C12	C11	C14	108.48(14)	O3	S1	C23	103.60(9)
C12	C11	C13	109.15(13)	F1	C23	S1	111.16(13)
C17	C18	Rh1	107.27(10)	F1	C23	F2	106.66(16)
C19	C18	Rh1	72.65(9)	F1	C23	F3	107.34(15)
C19	C18	C17	124.88(14)	F2	C23	S1	111.73(13)
C22	C15	Rh1	70.35(9)	F2	C23	F3	107.66(15)
C22	C15	C16	124.74(15)	F3	C23	S1	112.02(12)

Table S23: Torsion Angles for RhPNCOD_1.

A	B	C	D	Angle/˚	A	B	C	D	Angle/˚
Rh1	P1	C11	C14	54.16(13)	C6	P1	C7	C9	-38.42(14)
Rh1	P1	C11	C13	-63.53(13)	C6	P1	C7	C10	-161.82(11)
Rh1	P1	C11	C12	173.14(10)	C6	P1	C7	C8	81.29(13)
Rh1	P1	C6	C5	41.80(11)	C17	C18	C19	Rh1	99.29(14)
Rh1	P1	C7	C9	-142.88(11)	C17	C18	C19	C20	-4.3(2)
Rh1	P1	C7	C10	93.72(11)	C4	C3	C2	C1	-0.7(2)
Rh1	P1	C7	C8	-23.17(13)	C3	C4	C5	N1	0.7(2)
Rh1	N1	C1	C2	172.31(11)	C3	C4	C5	C6	-178.68(15)
Rh1	N1	C5	C6	6.20(18)	C1	N1	C5	C6	178.58(13)
Rh1	N1	C5	C4	-173.20(12)	C1	N1	C5	C4	-0.8(2)
Rh1	C18	C17	C16	38.02(16)	C21	C20	C19	Rh1	15.09(16)
Rh1	C18	C19	C20	-103.63(14)	C21	C20	C19	C18	96.82(18)
Rh1	C15	C22	C21	101.91(15)	C19	C20	C21	C22	-36.70(19)
Rh1	C15	C16	C17	11.92(17)	C19	C18	C17	C16	-42.5(2)
Rh1	C22	C21	C20	40.70(17)	C5	N1	C1	C2	0.2(2)
P1	C6	C5	N1	-34.59(17)	C5	C4	C3	C2	0.1(2)
P1	C6	C5	C4	144.82(13)	C7	P1	C11	C14	-166.19(12)
N1	C1	C2	C3	0.5(2)	C7	P1	C11	C13	76.12(13)
C11	P1	C6	C5	169.55(11)	C7	P1	C11	C12	-47.22(14)
C11	P1	C7	C9	72.21(14)	C7	P1	C6	C5	-73.15(12)
C11	P1	C7	C10	-51.18(13)	O1	S1	C23	F1	58.35(14)
C11	P1	C7	C8	-168.07(12)	O1	S1	C23	F2	-60.68(16)
C15	C22	C21	C20	-40.4(2)	O1	S1	C23	F3	178.44(12)
C15	C16	C17	C18	-34.1(2)	O2	S1	C23	F1	-61.26(15)
C22	C15	C16	C17	93.60(18)	O2	S1	C23	F2	179.72(15)
C16	C15	C22	Rh1	-105.52(14)	O2	S1	C23	F3	58.83(15)
C16	C15	C22	C21	-3.6(2)	O3	S1	C23	F1	178.28(14)
C6	P1	C11	C14	-53.83(13)	O3	S1	C23	F2	59.26(17)
C6	P1	C11	C13	-171.52(12)	O3	S1	C23	F3	-61.63(15)
C6	P1	C11	C12	65.15(13)					

Table S24: Hydrogen Atom Coordinates (Å×10⁴) and Isotropic Displacement Parameters (Å²×10³) for RhPNCOD_1.

Atom	*x*	*y*	*z*	U(eq)
H20A	3043.08	11555.22	6727.33	20
H20B	4796.73	12298.31	6974.34	20
H9A	9640.48	7325.53	9048.45	37
H9B	8672.09	6247.5	8009.71	37
H9C	8149.73	6303.77	8997.69	37
H14A	3198.11	4631.72	7243.48	35
H14B	2506.8	6015.17	7251.62	35
H14C	2108.97	5267.39	7981.12	35
H10A	7093.25	8374.8	9957.28	33
H10B	6791.08	9591.68	9542.82	33
H10C	8521.38	9430.14	9966.86	33
H18	3752.17	8521.48	4983.52	15

Table S24: Hydrogen Atom Coordinates (Å×10⁴) and Isotropic Displacement Parameters (Å²×10³) for RhPNCOD_1.

Atom	*x*	*y*	*z*	U(eq)
H15	2209.26	8381.24	7689.44	16
H13A	4665.29	8111.54	9734.43	29
H13B	3135.74	7048.22	9558.71	29
H13C	3154.78	8052.44	8944.49	29
H22	4226.68	9922.38	8668.31	16
H16A	1346.43	10295.45	6865.33	21
H16B	393.64	8785.36	6601.99	21
H6A	6494.2	5084.45	7032.86	16
H6B	4800.25	5063.21	6427.71	16
H17A	1327.22	7829.82	5250.79	20
H17B	1250.82	9365.2	5242.9	20
H4	7839.15	4591.77	5679.7	20
H3	8944.13	5449.37	4629	21
H8A	9363.03	9332.75	8512.38	36
H8B	7698.2	9514.69	7992.6	36
H8C	8510.34	8233.02	7451.81	36
H1	6481.73	8616.77	5272.94	16
H21A	5457.16	11777.13	8346.16	21
H21B	3725.29	12072.46	8375.85	21
H12A	5610.2	4777.72	8402.5	38
H12B	4438.5	4932.79	9122.26	38
H12C	6007.85	6011.57	9453.59	38
H2	8262.7	7504.56	4441.91	19
H19	5446.48	10347.33	5972.27	16

References

(1) Celaje, J. J. A.; Lu, Z.; Kedzie, E. A.; Terrile, N. J.; Lo, J. N.; Williams, T. J.. *Nat Commun* **2016**, *7* (1), 11308.
(2) Anaby, A.; Schelwies, M.; Schwaben, J.; Rominger, F.; Hashmi, A. S. K.; Schaub, T. *Organometallics* **2018**, *37* (13), 2193–2201.
(3) Sharninghausen, L. S.; Crabtree, R. H. *Israel Journal of Chemistry* **2017**, *57* (10–11), 937–944.
(4) Bourhis, L. J.; Dolomanov, O. V.; Gildea, R. J.; Howard, J. A. K.; Puschmann, H. *Acta Crystallogr A Found Adv* **2015**, *71* (Pt 1), 59–75.
(5) Sheldrick, G. M. *Acta Cryst C* **2015**, *71* (1), 3–8.